A NUCLEAR MAGNETIC RESONANCE INVESTIGATION INTO THE EFFECT OF THE SYN CONFORMATION OF THE N-GLYCOSYL BOND ON THE OVERALL CONFORMATION OF SOME PYRIMIDINE NUCLEOSIDES, NUCLEOTIDES, AND DINUCLEOSIDE MONOPHOSPHATES

A Thesis
Submitted to
The Faculty of Graduate Studies and Research
at the University of Manitoba
in Partial Fulfillment
of the Requirements for the Degree of
DOCTOR OF PHILOSOPHY

by

WALTER P. NIEMCZURA

Winnipeg, Manitoba

October, 1979

A NUCLEAR MAGNETIC RESONANCE INVESTIGATION INTO THE EFFECT OF THE SYN CONFORMATION OF THE N-GLYCOSYL BOND ON THE OVERALL CONFORMATION OF SOME PYRIMIDINE NUCLEOSIDES, NUCLEOTIDES, AND DINUCLEOSIDE MONOPHOSPHATES

BY

WALTER PAUL NIEMCZURA

A thesis submitted to the Faculty of Graduate Studies of the University of Manitoba in partial fulfillment of the requirements of the degree of

DOCTOR OF PHILOSOPHY

ACKNOWLEDGEMENTS

I would like to express my appreciation to Dr. Ted Schaefer for the guidance, encouragement, and opportunities he has extended to me over the past five years.

I would also like to thank Dr. Frank Hruska for sharing his expertise and for the trust he has placed in me.

I am indebted to Dr. Krish Sadana who taught me the art of nucleotide synthesis and to Dr. Peter Loewen and the staff and students of the Department of Microbiology who provided me with a place to practice this art and the encouragement to make it through many frustrating days.

I am also grateful to my colleagues in the NMR group - Dr. Leonard Kruczynski, Dr. Salman R. Salman, Werner Danchura, Tim Wildman, Rudy Sebastian, Wayne Blonski, and Kirk Marat for their friendship and encouragement.

I am grateful to Drs. John Markley and Jerry Dallas and the members of the Purdue Biological Magnetic Resonance Laboratory for the opportunity to use the NT-360 and the time they took helping me to learn how to operate it.

I would also like to thank Dr. M Sundaralingam for the informative discussion we had concerning nucleotide conformation.

And last, but not least, I am very grateful to my wife, Margo, for her encouragement over the past five years and her invaluable help in correcting and typing this manuscript.

ACKNOWLEDGEMENTS (CONTINUED)

I am also grateful to the Department of Chemistry and Graduate Studies at the University of Manitoba for financial support.

ABSTRACT

A series of nucleic acid model compounds, m^6dU, 3'-m^6dUMP, 5'-m^6dUMP, 3',5'-m^6dUDP, d(Tpm^6U), d(m^6UpT) and d(m^6Upm^6U), were synthesized and compared to a similar series of dT derivatives to investigate the effect of the syn conformation of the N-glycosyl bond on the overall conformation of pyrimidine nucleosides, nucleotides, and nucleotidyl fragments of dinucleoside monophosphates in solution. Proton chemical shifts (δ) and coupling constants were determined at 360 MHz for 3',5'-dTDP and 3',5'-m^6dUDP at two pH values and compared with respect to the conformational information they contained. In addition, the proton chemical shifts and coupling constants (also at 360 MHz) were determined for the dinucleoside monophosphates, d(TpT), d(Tpm^6U), d(m^6UpT), and d(m^6Upm^6U), and compared with the reported chemical shifts and coupling constants for the dT and m^6dU nucleotides available in the literature. The carbon chemical shifts at 22.63 MHz and carbon-phosphorus coupling constants for the entire series of dT and m^6dU nucleosides, nucleotides, nucleoside diphosphates, and dinucleoside monophosphates (including the mixed dinucleoside monophosphates of dT and m^6dU) are reported and discussed in light of the conformational information available from the ^1H NMR data. Also, the proton-carbon vicinal coupling constants between the anomeric proton, $H_{1'}$, and C_2 and C_6 of the pyrimidine ring of the nucleosides and nucleotides are reported. An attempt was made to use the observed ^3J(H1'-C2) and ^3J(H1'-C6) in the m^6dU series to make a quantitative estimate of the syn and anti conformer populations in dT.

ABSTRACT (Continued)

The effect of pH and temperature changes on the proton and ^{13}C NMR was examined. The data provide information about the conformation of the 2'-deoxyfuranose ring and the orientation of nucleotide units about the exocyclic $C_{4'}—C_{5'}$, $C_{5'}—O_{5'}$, and $C_{3'}—O_{3'}$ bonds for the molecules listed above. It was found that the syn base, in general, has shifted the normal 2'-endo-3'-endo equilibrium normally found in anti pyrimidine deoxyribose derivatives. In addition, destabilization of the g_+ ($C_{4'}—C_{5'}$) conformer and, to a lesser extent, the t ($C_{5'}—O_{5'}$) conformer which are assumed by the units in helical DNA is apparent. Finally, stabilization of the t ($C_{3'}—O_{3'}$) conformer, particularly at the 3',5'-diphosphate level in basic solution in which the phosphates are doubly ionized is indicated.

This study also provides information about correlations between the sugar pucker and the $C_{4'}—C_{5'}$ and $C_{3'}—O_{3'}$ conformations and the conformational requirements for, and consequences of, UV-induced photodimer formation in the d(TpT) fragment.

TABLE OF CONTENTS

		Page
I.	INTRODUCTION	1
II.	EXPERIMENTAL CONSIDERATIONS	7
	A. Nomenclature	8
	1. Chemical Nomenclature	8
	2. Conformational Nomenclature	8
	B. Proton NMR Approach to Nucleic Acid Conformation	13
	1. N-Glycosyl Bond Conformation	13
	a. Chemical Shifts	13
	b. Spin-Spin Coupling Constants	15
	c. Relaxation Measurements	16
	2. Sugar Ring Conformation	18
	a. Pseudorotational Analysis	21
	3. Sugar-Phosphate Backbone Conformation	26
	a. The $C_{5'}$—$C_{4'}$ Bond, Ψ	30
	b. The $O_{5'}$—$C_{5'}$ Bond, Φ	32
	i. Vicinal Coupling Constants, $^{3}J(H-P)$	32
	ii. Long-Range Coupling Constants, $^{4}J(H4'-P5')$	34
	c. The $C_{3'}$—$O_{3'}$ Bond, Φ'	34
	C. Carbon-13 Approach to Nucleic Acid Conformation	37
	1. N-Glycosyl Bond Conformation	37
	a. ^{13}C Chemical Shifrs	37
	b. Vicinal Proton-Carbon Coupling Constants, $^{3}J(H-C)$	38

TABLE OF CONTENTS (Continued)

	Page
2. Sugar-Phosphate Backbone Conformation	39
a. The $O_{5'}$—$C_{5'}$ Bond, Φ	40
b. The $C_{3'}$—$O_{3'}$ Bond, Φ'	40
3. Determination of Overall and Internal Mobility of Nucleic Acid Constituents	41
D. Phosphorus-31 NMR Approach to Nucleic Acid Conformation	44
1. Sugar-Phosphate Backbone Conformation	44
a. The $O_{5'}$—$C_{5'}$ and $C_{3'}$—$O_{3'}$ Bonds, Φ and Φ' . .	44
b. The P—$O_{5'}$ and the $O_{3'}$—P Bonds, ω and ω' . .	45
III. EXPERIMENTAL METHOD	47
A. Materials	48
1. Nucleoside Synthesis	49
a. Discussion	49
b. Procedures	51
2. Protected Nucleoside and Nucleotide Synthesis . .	52
a. Discussion	52
b. Procedures	54
3. Dinucleoside Monophosphate Synthesis	58
a. Discussion	58
b. Procedures	62
4. Photodimer Synthesis	65
B. NMR Method	68
1. Samples	68

TABLE OF CONTENTS (Continued)

	Page
2. Spectra	69
a. ^{1}H NMR Spectra	69
b. ^{13}C NMR Spectra	69
c. ^{31}P NMR Spectra	70
IV. DATA AND RESULTS	72
A. ^{1}H NMR Data	72
B. ^{13}C NMR Data	97
V. DISCUSSION	124
A. N-Glycosyl Bond Conformation	124
1. Chemical Shifts	124
a. Proton Chemical Shifts	124
b. Carbon-13 Chemical Shifts	125
2. Spin-Spin Coupling Constants	128
a. Long-Range Proton-Proton Coupling Constants	128
b. Proton-Carbon Vicinal Spin-Spin Coupling Constants	129
i. Qualitative Evaluation	129
ii. Quantitative Evaluation	131
B. Deoxyribose Ring Conformation	136
1. Pseudorotational Analysis	136
a. Standard Pseudorotational Analysis	136
b. Modified Pseudorotational Analysis	142
2. Qualitative Analysis	145
3. Summary	150

TABLE OF CONTENTS (Continued)

Page

C. Backbone Conformation 151

1. The $C_{5'}$—$C_{4'}$ Bond, Ψ 151

a. Vicinal Proton-Proton Spin-Spin Coupling Constants 151

i. Nucleosides and Mononucleotides 151

ii. Nucleoside Diphosphates 154

iii. Dinucleoside Monophosphates 155

b. Correlation Between the Sugar Pucker and the $C_{5'}$—$C_{4'}$ Bond Conformation 161

2. The $O_{5'}$—$C_{5'}$ Bond, Φ 163

a. Proton-Phosphorus Vicinal Spin-Spin Coupling Constants 163

b. Correlation Between Ψ and Φ 165

c. Long-Range Proton-Phosphorus Coupling Constants, ^4J(H4'-P5') 165

d. Carbon-Phosphorus Vicinal Spin-Spin Coupling Constants 166

i. Nucleotides and Nucleoside Diphosphates . 166

ii. Dinucleoside Monophosphates 170

e. Correlation of Σ' With ^3J(C4'-P5') 172

3. The $C_{3'}$—$O_{3'}$ Bond, Φ' 174

a. Nucleotides and Nucleoside Diphosphates . . . 178

b. Dinucleoside Monophosphates 185

c. The Sum (^3J(C4'-P3') + ^3J(C2'-P3')) 188

TABLE OF CONTENTS (Continued)

		Page
	D. Genimal Carbon-Phosphorus Coupling Constants	193
	E. Carbon Chemical Shifts	196
	1. Nucleotides and Nucleoside Diphosphates	196
	2. Dinucleoside Monophosphates	203
	F. A Comparison of the Carbon-13 Relaxation Times (T_1's) of d(TpT) and the Internal Cyclobutane Photodimer, d(T(p)T)	205
VI.	CONCLUSIONS	211
VII.	RECOMMENDATIONS FOR FUTURE RESEARCH	215
	BIBLIOGRAPHY	217

LIST OF FIGURES

FIGURE NUMBER	PAGE
2.1	9
2.2	10
2.3	14
2.4	20
2.5	23
2.6	27
2.7	28
2.8	29
3.1	50
3.2	53
3.3	60
3.4	66
4.1	74
4.2	75
4.3	81
4.4	88
4.5	93
4.6	96
4.7	101
4.8	103
4.9	107
4.10	113
4.11	116
4.12	123
5.1	162
5.2	168
5.3	173
5.4	179
5.5	189
5.6	194
5.7	200
5.8	201
5.9	202

LIST OF TABLES

TABLE NUMBER	PAGE	TABLE NUMBER	PAGE
4.1	77	5.1	126
4.2	79	5.2	127
4.3	82	5.3	130
4.4	84	5.4	137
4.5	86	5.5	143
4.6	89	5.6	147
4.7	91	5.7	152
4.8	94	5.8	164
4.9	99	5.9	171
4.10	100	5.10	177
4.11	102	5.11	191
4.12	104	5.12	197
4.13	105	5.13	198
4.14	108	5.14	207
4.15	109		
4.16	110		
4.17	111		
4.18	114		
4.19	117		
4.20	119		
4.21	121		

FOR FERNANDO

CHAPTER I

INTRODUCTION

Nuclear magnetic resonance spectroscopy (NMR) has been established as a definitive method for the study of the conformation and dynamics of molecules in solution. NMR was first used for organic structure determination and for physical studies of the nature of molecular environments and interactions. As confidence in the technique grew, researchers in the field began to investigate the complicated problems of biochemical processes with the aid of NMR spectroscopy. These applications have grown in number over the past twenty-five years and have made substantial contributions to the understanding of life processes. Recent reviews have summarized the role of magnetic resonance in the study of peptides[1], proteins and enzymes[2,3], lipids and membranes[4], carbohydrates and polysaccharides[5], and of nucleosides, nucleotides, and nucleic acids[6,7].

The use of NMR spectroscopy for the conformational analysis of nucleic acids and their components in solution has been particularly extensive, as can be seen in the reviews of Davies[6] and Kearns[7]. Early proton NMR studies of nucleoside conformation were reported by C. D. Jardetzky[8-10]. These investigations were hampered by the low resolving power of the available magnetic fields ($B \leq 1.4T$ or 60 MHz for ^1H), and were confined to discussions of sugar ring pucker based on spin couplings measured from the splittings of isolated resonances. A similar study of thymidine by Lemieux[11] showed that some proton-proton couplings could be determined for the deoxyribose ring at these fields. For the most part, the early work on nucleosides was confined to the interpretation of the dependence of base ring proton

shifts and resolvable proton-proton couplings in terms of the conformational changes induced by perturbations from the medium (i.e., pH, concentration, temperature, solvent composition, etc.)[12-18]. These perturbations were discussed primarily with respect to changes in base stacking and internal hydrogen bonds.

The conformational analysis of nucleosides and nucleotides by ^1H NMR was aided by the development of high resolution, high field spectrometers operating at 100 MHz and above for protons[19-25]. Hruska, Smith, and co-workers[19-22] combined high resolution spectra with computer calculated and simulated spectra to extract all the chemical shifts and coupling constants from the tightly coupled six-spin system of the sugar ring of uridine and α- and β-pseudouridine. These studies were the first to demonstrate the application of high resolution NMR spectra to the complete conformational analysis of the ribofuranose ring and the backbone of nucleosides and, later, nucleotides[23-25].

Instrumental advances further expanded the range of commercially available spectrometers. Today, facilities are available to record routinely 360 MHz and 400 MHz proton spectra, while members of the Department of Chemistry at the Carnegie-Mellon Institute in Pittsburgh have built a spectrometer operating at 600 MHz - ten times the field strength used in the original work on nucleosides in the early 1960's.

The early work on nucleosides and nucleotides has already been extended to many dinucleoside phosphates[26-36], a dinucleotide[36], trinucleoside diphosphates[37-39], and to polynucleotides[37,40].

Danyluk and co-workers[34,35,41,42] have shown that synthesis of an oligonucleotide in which one or more residues are selectively deuterated allows the proton analysis of the monomer components in an oligomer. Recently, Altona and co-workers[28,38] have shown that high field spectra (360 MHz), combined with extensive homonuclear and heteronuclear (i.e., ^{31}P) decoupling experiments and aided by computer simulation of the observed spectrum, yields an unambiguous assignment of resonances up to the trimer level. With the development of the 600 MHz machine, this limit might be extended to the tetramer or pentamer level, but the complete proton analysis of larger oligonucleotides is restricted by the extensive peak overlap accompanying the increased number of resonances.

Aside from the use of the conventional proton chemical shift and coupling constant analysis, there has been an increase in the use of other spectral parameters for structure determination. Applications of the proton spin-lattice relaxation time, T_1[43-45], and nuclear Overhauser effect (NOE)[44,45] measurements have attempted to answer questions concerning the dynamics of nucleosides in addition to supplementing the information on their conformation obtained from other methods. These studies have focused primarily on the N-glycosyl bond conformation and on the dynamics of the ribofuranose ring, but a recent application[46] has demonstrated the utility of these methods in determining exocyclic or backbone conformations.

The use of other nuclei in the magnetic resonance studies of nucleic acids has grown in recent years. With the introduction of

pulsed Fourier transform techniques, carbon-13 NMR has been employed in the conformational analysis of these molecules. Although not as extensively used as proton NMR, ^{13}C studies have the advantage of a wider chemical shift dispersion of the resonances. In addition, the low natural abundance, combined with proton noise decoupling, yields a spectrum in which each distinct carbon gives rise to only one line, in the case of nucleosides. Early studies by Jones et al.[47-50] on nucleosides and Dorman and Roberts[51] on nucleotides hinted at the utility of ^{13}C shifts in conformational work although no effects due to base stacking, as detected from proton work, could be observed. Reports published by Lemeiux and co-workers[52] and Davies[53] have described the utility of proton-carbon couplings for conformational studies. The ribose carbons were found to give rise to broad resonances from unresolved long-range couplings. Only the large one-bond coupling was measurable. The base carbons, however, are better resolved, and the three-bond ^{1}H-^{13}C coupling from the anomeric proton into the base ring carbons could be used to determine the conformation about the N-glycosyl bond. For nucleotides and larger oligomers, the carbon-phosphorus spin-spin couplings can be measured directly under conditions of proton noise decoupling and serve as another conformational probe[54-56]. Carbon-13 relaxation measurements[57-59] can be used to study the overall motion of nucleic acids in solution and can detect the presence of internal motion in a molecule.

Nuclei, such as phosphorus and nitrogen-15, have not been used as extensively as protons or carbon-13. ^{31}P NMR[34,35,60,61] has been utilized primarily as an aid in proton analysis, while the low sensitivity and natural abundance of ^{15}N has limited the widespread use of this nucleus[62-64].

The major emphasis of the afore-mentioned studies has been placed on conventional nucleic acid derivatives, i.e., the naturally occurring purine and pyrimidine nucleosidyl units. In these molecules, the orientation about the N-glycosyl bond is believed to be predominantly anti (for the pyrimidine base) or in equilibrium between the syn and anti conformations (as is the case for the purine base). To date, there have been few studies which investigate the effect of the syn conformation on the overall conformation of nucleic acid derivatives.

This thesis presents a systematic comparison between two pyrimidine nucleosides - thymidine and 6-methyldeoxyuridine. The former molecule is believed to exist predominantly in the anti conformation while the latter is expected to exist predominantly in the syn conformation. Proton and carbon-13 high-resolution nuclear magnetic resonance data will be used to determine quantitative conformational properties for a selected series of nucleosides, nucleotides, nucleoside diphosphates, and dinucleoside monophosphates containing the 5-methyluracil and 6-methyluracil bases. The information, in turn, will be compared in order to determine the conformational preferences for model nucleic acid compounds which contain a pyrimidine ring in the syn or anti conformation about the N-glycosyl

bond. The data will also be examined to see what effect phosphorylation or incorporation into a dinucleoside monophosphate has on the N-glycosyl bond.

The results presented should further our knowledge of nucleic acid structure and function.

CHAPTER II

EXPERIMENTAL CONSIDERATIONS

The purpose of the conformational analysis of a molecule is to determine the position of an atom or group of atoms relative to the other members of the molecule. In this thesis, an attempt will be made to determine the conformation of a related group of nucleosides, nucleotides, and dinucleoside phosphates in solution. In this chapter, the state of the art of the conformational analysis of nucleic acid derivatives is reviewed. The more common techniques are discussed, divided according to the magnetic nucleus used, and further subdivided according to what portion of the molecule the information probes.

A. NOMENCLATURE

1. CHEMICAL NOMENCLATURE

The nomenclature and symbols used in this chapter and throughout the rest of this work follow from the IUPAC-IUB recommendations[65]. For example, thymidine is hereafter referred to as 2'-deoxythymidine and symbolized as dT while the 6-methyl analogue will be called 6-methyl-2'-deoxyuridine and symbolized as m^6dU. Figure 2.1 illustrates the structure of these two nucleosides along with the accepted numbering scheme. Nucleotides will be designated as 3'-dTMP, 5'-dTMP and 3',5'-dTDP for the 3'- and 5'-monophosphates and 3',5'-diphosphate derivatives of 2'-deoxythymidine, respectively. Similarly, the nucleotides of 6-methyl-2'-deoxyuridine will be symbolized as 3'-m^6dUMP, 5'-m^6dUMP and 3',5'-m^6dUDP.

The designation of dinucleoside phosphates follows along similar lines. For example, the molecule 2'-deoxythymidyl-(3'-5')-2'-deoxythymidine will be written as d(TpT) while 2'-deoxythymidyl-(3'-5')-6-methyl-2'-deoxyuridine will be abbreviated as d(Tpm^{6}U). All dinucleoside phosphates studied are 3',5'-linked.

2. CONFORMATIONAL NOMENCLATURE

The conformational nomenclature follows that recommended at the 5th Jerusalem Symposium[66] and used in Davies' review[6]. Figure 2.2 shows a dinucleoside phosphate fragment where all the major bonds have been designated by their standard labels. The nucleotide

FIGURE 2.1 contains the structural formulas for a) dT and b) m^6dU with the numbering scheme used for the pyrimidine and deoxyribose rings.

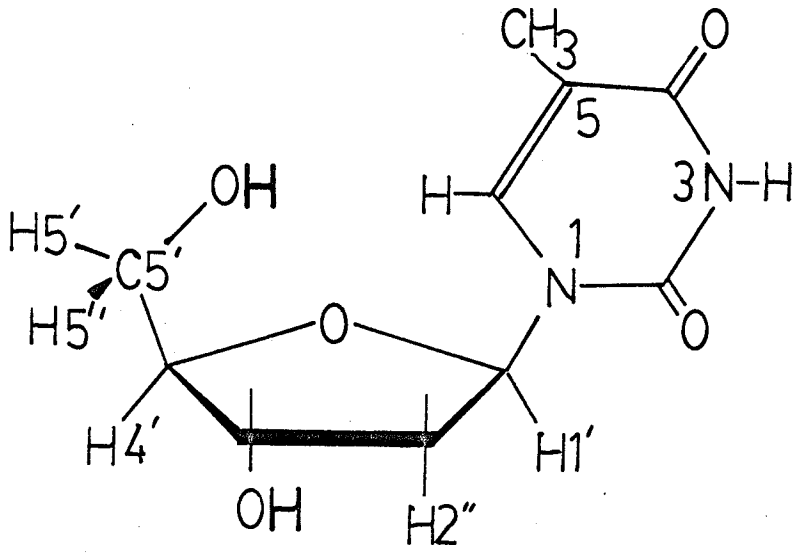
CH3
O
5
H
3N-H
OH
H5′
C5′
H5″
1
N
O
O
H4′
H1′
OH
H2″

a

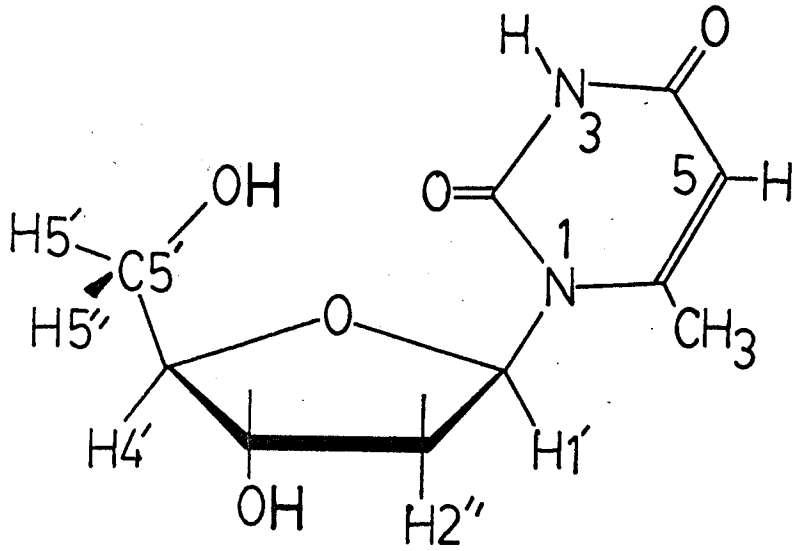
H
N
O
3
5
H
OH
H5′
C5′
O
1
H5″
N
CH3
O
H4′
H1′
OH
H2″

b

FIGURE 2.2 shows the structural formula for d(TpT). Superimposed on the figure are the labels for the bonds discussed in this thesis.

d(TpT)

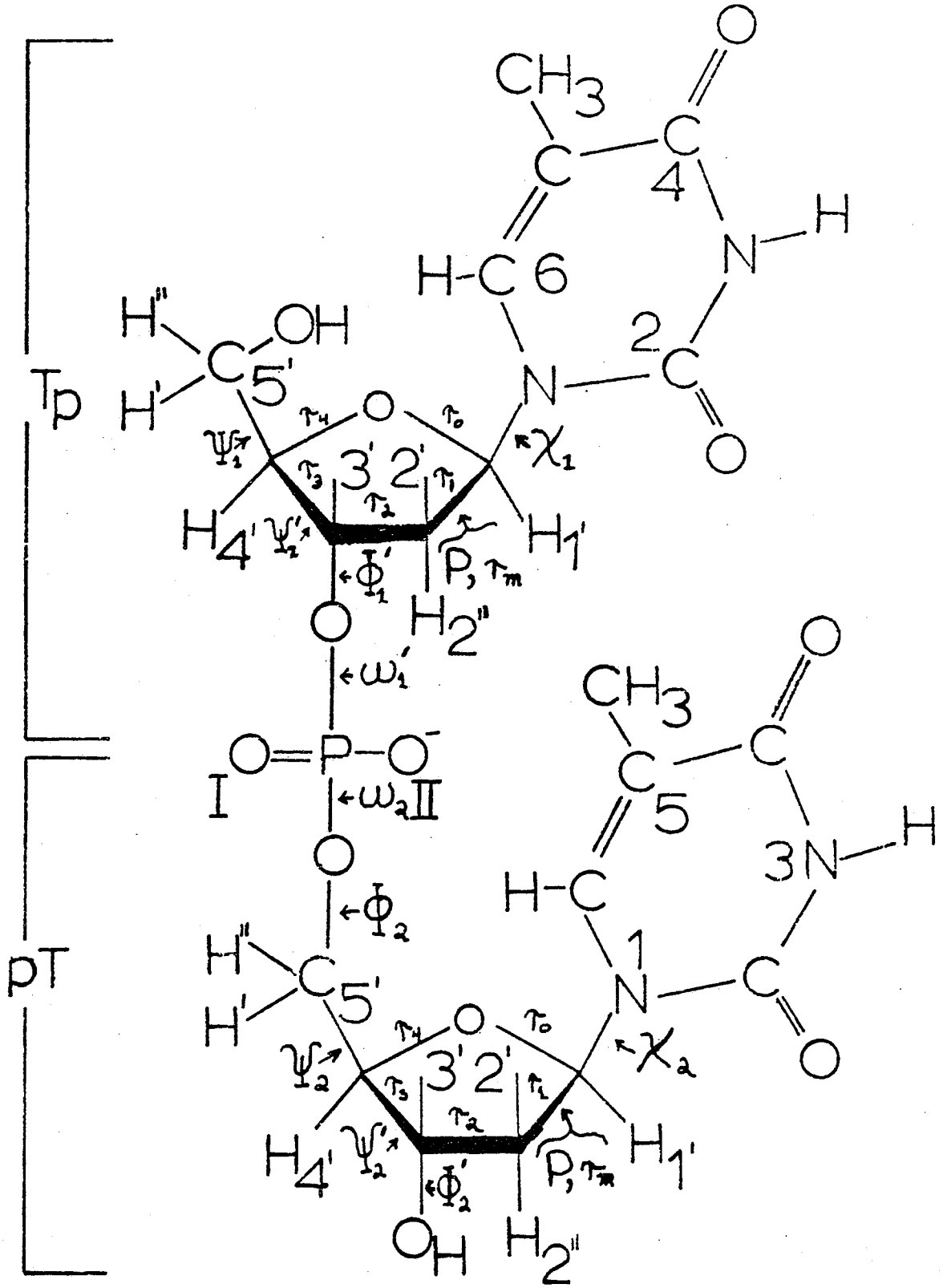
Tp
pT
CH3
C
C
4
N
H
H-C 6
2
C
O
H''
OH
H'
C 5'
N
O
χ1
Ψ1
τ4
τ0
τ3
3' 2'
τ1
τ2
H4'
Ψ2'
H1'
Φ1'
P, τm
H2''
ω1'
O=P-O⁻
I
ω2 II
Φ2
CH3
C
C
5
3N
H
H-C
1
N
C
O
χ2
Ψ2
τ4
τ0
τ3
3' 2'
τ1
τ2
H4'
Ψ2'
H1'
Φ2'
P, τm
OH
H2''

fragment can be conveniently dissected into three segments for conformational discussions. These are the N-glycosyl bond conformations, the sugar conformation or ring pucker of the deoxyribose ring, and the backbone conformation.

In the discussions that follow, the pyrimidine ring is assumed to be planar, as shown by X-ray studies[67,68]. The N-glycosyl bond conformation is then defined by a rotational angle about $C_{1'}$ of the deoxyribose ring and N_1 of the pyrimidine ring. (The definition of these and other conformational angles will be presented in the next section.)

There are two methods used to describe the conformation of the deoxyribose ring currently in use. One uses the twenty envelope (E) and twist (T) conformations which were developed into a cycle of pseudorotation by Hall and co-workers[201]. The other uses the pseudorotational concept developed by Altona and Sundaralingam[67] in which each point on the pseudorotational cycle is defined by two parameters: P and τ_m. P is the phase angle of pseudorotation, and τ_m is the degree of pucker. The two methods are similar, but the method of Hall et al. does not include a parameter describing the amplitude of pucker (i.e., τ_m). In this thesis, the pseudorotational analysis of Altona and Sundaralingam will be used, supplemented by the envelope and twist notation to aid in visualizing the various conformations.

Finally, the backbone conformational angles are discussed according to the classical staggered rotamers for the backbone bonds

ω, ϕ, ψ, ψ', ϕ', ω'. The nomenclature used by NMR spectroscopists to differentiate these rotamers (g_+, t, g_-, etc.) will be employed[6].

The torsion angle (or dihedral angle) about the bond B—C in a fragment composed of the atoms A—B—C—D is defined as the angle of rotation of the far bond C—D relative to the near bond A—B from the eclipsed position of the bonds A—B and C—D. The eclipsed position of the bonds A—B and C—D defines the 0° torsion angle. The angle of rotation is defined as positive for a clockwise rotation of the C—D bond from the A—B bond when viewed along B—C.

B. PROTON NMR APPROACH TO NUCLEIC ACID CONFORMATION

1. N-GLYCOSYL BOND CONFORMATION

The N-glycosyl bond of a nucleoside is represented by the Newman projection in Figure 2.3. The conformation is defined by the rotational angle of the pyrimidine ring relative to the ribofuranose ring about the bond between $C_{1'}$ and N_1 and is symbolized by χ. The zero point is defined as the eclipsed orientation of the $C_{1'}—O_{4'}$ and $N_1—C_2$ bonds with the positive direction defined as an anticlockwise rotation of the pyrimidine ring.

Pyrimidine nucleosides and nucleotides are found to exist in two broad conformational ranges, syn ($\chi = 90^{\circ} \pm 90^{\circ}$) and anti ($\chi = 270^{\circ} \pm 90^{\circ}$). The large majority of pyrimidine derivatives studied, both in the solid state[67,68] and in solution[69,73], prefer the anti conformation or exist as an equilibrium mixture (in solution) of the two conformers[74,75]. A bulky substituent at C_6 of the pyrimidine ring favors the syn position[72,73,76].

In general, there are three methods for determining the N-glycosyl bond conformation using proton NMR. They are chemical shift, coupling constant, and relaxation studies.

a. CHEMICAL SHIFTS

The first use of chemical shifts for the study of the N-glycosyl bonds monitored the effect of phosphorylation at the 5'-ribose position on the proton chemical shifts of the pyrimidine ring[12,16]. The 5'-mononucleotides were compared with the nucleosides and the

FIGURE 2.3 is a Newman projection depicting the rotation about the N-glycosyl bond. The direction of rotations shown in the figure is positive.

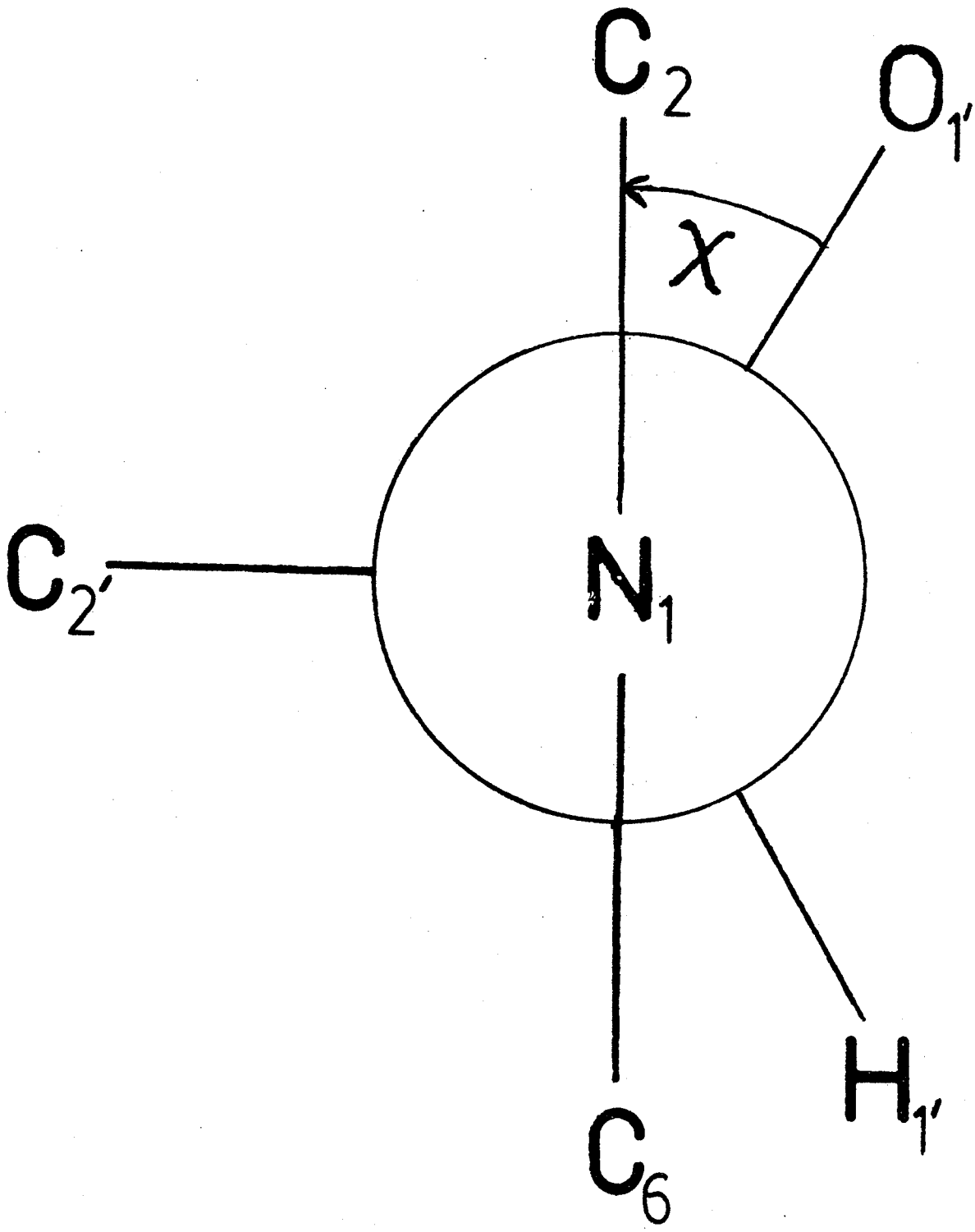
C2
O1'
χ
C2'
N1
C6
H1'

2'- and 3'-mononucleotides for a complete set of ribo- and deoxyribonucleotides. The data indicated that the pyrimidine derivatives studied exist primarily in the anti conformation[77].

Other studies monitored the effect of the 2-keto group on the chemical shifts of the ribose protons[72]. In these studies[72], a series of 5- and 6-substituted pyrimidine nucleosides were compared with the parent nucleosides. The results show that while there is little change in the ribose chemical shifts upon 5-substitution, 6-substitution results in substantial shifts in H_2, (+0.50 ppm downfield), H_3, (+0.15 ppm), and H_4, (-0.15 ppm upfield) as a result of the shielding anisotropy of the keto group. Theoretical calculations support the direction and relative magnitudes of these shifts[78].

b. SPIN-SPIN COUPLING CONSTANTS

Studies using spin-spin coupling constants provide more reliable conformational information than that based on chemical shift measurements. The proton coupling constants used in N-glycosyl bond conformation are the four- and five-bond couplings between the anomeric proton H_1, and H_6 or H_5 (i.e., ^4J(H1'-H6) and ^5J(H1'-H5)[79,80]). Variations of ^4J(H1'-H6) and ^5J(H1'-H5) with glycosidic torsion angle χ have been calculated by Giessner-Prettre and Pullman using finite perturbation methods at either the CNDO[81] or INDO[82] level of approximation. These studies show that ^5J(H1'-H5') is extremely sensitive to this rotation, and the results are in qualitative agreement with the observed coupling assuming an anti conformation for uridine and some of its derivatives. For the syn conformation,

the calculated values predict a small coupling (^5J(H1'-H5) ≃ 0.1 Hz). The calculations also indicate that ^4J(H1'-H6) varies with χ, but the computed values are small, especially for the anti conformation.

c. RELAXATION MEASUREMENTS

Recently, applications of proton T_1 [83-85] and nuclear Overhauser enhancement (NOE) [44,74,75] measurements have been applied to the problem of glycosidic conformation. The NOE is the fractional increase in intensity of the resonance of a nucleus, i, when another nucleus, j, in the vicinity, is irradiated with a second r.f. field, i.e.,

$$f_i(j) = \frac{\text{area of i when j is saturated} - \text{equilibrium area of i}}{\text{equilibrium area of i}} \qquad \text{- 2.1 -}$$

These quantities are a measure of the dipolar coupling between magnetic nuclei at both the intra- and intermolecular level. They are sensitive to the distance between the coupled nuclei and to the overall and internal motions of the molecule[44]. It is difficult to disentangle the different interactions that contribute to the observed proton T_1's and NOE's. For example, what proportion of an observed T_1 arises from the dipolar interaction of a given nucleus; by what amount do mechanisms other than the dipolar mechanism contribute to a given relaxation time; or what effect do other degrees of freedom have on these quantities? For the rigid molecule 2',3'-O-isopropylidene-3,5'-cycloguanosine, the theory for the quantitative interpretation of multispin NOE measurements has yielded reliable

estimates of the various interproton distances[44].

In studies of pyrimidine derivatives, for an anti conformation, significant NOE measurements would be expected for H_6 when $H_{1'}$, $H_{3'}$, and $H_{5'}$ are irradiated, while a syn conformation would result in an enhancement of H_6 upon irradiating $H_{1'}$. Experimentally, all four enhancements were observed, providing strong evidence that both syn and anti forms exist in equilibrium[74,75]. A later NOE study on β-pseudouridine in D_2O by Smith and co-workers[83] concluded that it was not possible to interpret NOE results by assuming a two-state model where only the more dominant syn and anti conformers provide the dominant relaxation mechanism..

T_1 measurements have had limited applicability in the study of N-glycosyl bond conformation. Initial proton relaxation studies[84] indicated that the ratio of proton T_1's for purine derivatives $T_1(H_8):T_1(H_{1'})$ should be sensitive to the base orientation (i.e., $(T_1)_8/(T_1)_{1'} > 1$ for syn and $(T_1)_8/(T_1)_{1'} < 1$ for anti). The reasoning behind this assumption is that in the syn conformation, H_8 is relaxed by only $H_{1'}$ while $H_{1'}$ is relaxed by $H_{2'}$ and $H_{3'}$ in addition to H_8 resulting in a shorter T_1 for $H_{1'}$. In the anti conformation, H_8 would be relaxed by all the ribose protons except $H_{1'}$ resulting, therefore, in a shorter relaxation time for H_8 than $H_{1'}$. These studies were in qualitative agreement with other available data[84].

Another method measures the effect on the T_1 of a given proton when a neighboring proton is replaced by deuterium. The deuterium

substitution effect on relaxation time (DESERT method)[85], combined with the overall tumbling correlation time τ_c from ^{13}C studies, yields the reciprocal sixth-power average interproton distance between the substituted and observed protons and can be interpreted in terms of molecular conformation. The method was tested on the rigid 2'3'-O-isopropylidene-3,5'-cycloguanosine with encouraging results. Extension to flexible purine nucleosides and nucleotides showed that they exist as an equilibrium mixture of syn and anti forms.

The above data indicate that pyrimidine nucleosides and nucleotides substituted at other than the 2- or 6-positions exist predominantly in the anti conformation. Although this conformation is favored, NOE and relaxation studies suggest that the molecule is equilibrating between the syn and anti forms[74,75,83]. The dominance of the anti conformer is increased by 2-substitution while 6-substitution shifts the dominance to the syn conformer.

2. SUGAR RING CONFORMATION

Proton NMR spectroscopy provides the most detailed information about the ribofuranose ring conformation in solution. The strength of the method lies in the dependence of the three-bond spin coupling constant, $^3J(H-H)$, on the dihedral angle[86,87]. This angular dependence, often called the Karplus equation[86,87], can be expressed as

$$^3J(H-H) = A \cos^2 \theta_{H,H} - B \cos \theta_{H,H} + C \qquad \text{- 2.2 -}$$

This relationship has been investigated both experimentally and theoretically. The vicinal coupling has been found to depend on bond length, bond angles, and the electronegativity and orientation of substituents in addition to the dependence on dihedral angles. For this reason, the coefficients A, B, and C are normally evaluated empirically for a given series of related model compounds (e.g., 3'5'-O-cyclic nucleotides[88,89] or 2',O^2-anhydroarabinonucleosides)[88,90]. Other methods adapt theoretical values of A, B, and C to fit the observed values in a series of compounds.

In principal, this relationship could be applied to the ribose ring to determine the dihedral angles for the bonds $C_{1'}$—$C_{2'}$, $C_{2'}$—$C_{3'}$, and $C_{3'}$—$C_{4'}$. It is currently accepted[67,91] that the furanose ring does not exist in a unique rigid form in solution but is in dynamic equilibrium between at least two different puckered forms separated by a small barrier to interconversion (∿12 to 20 kJ $mole^{-1}$)[58,92]. If the interconversion rate is rapid enough, the observed couplings represent a weighted average of the coupling from each contributing conformer. From the numerous X-ray structure determinations of nucleosides and nucleotides[67], the ribose and deoxyribose rings are found to exist in either of two narrow conformational ranges - one near the $^2T_3$($C_{2'}$ endo - $C_{3'}$ exo) conformation and the other near the $^3T_2$($C_{3'}$ endo - $C_{2'}$ exo) conformation shown in Figure 2.4a. Later, the envelope (i.e., ^2E and ^3E) conformations were taken as the basis for the two conformational regions (Figure 2.4b). Both experimental[58] and theoretical[93-97] attempts have been made to

FIGURE 2.4 contains the two twist (a) and two envelope (b) conformers used to denote the equilibrium conformations in the pseudorotational analysis of the deoxyribose ring.

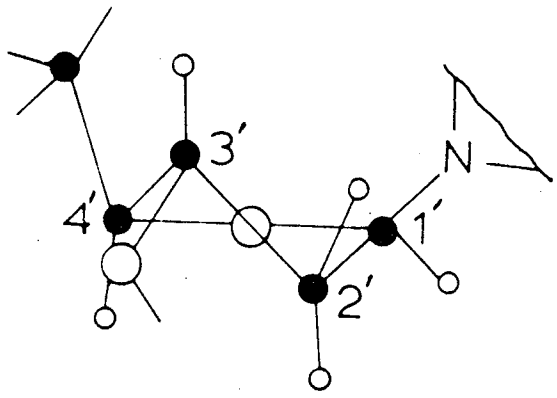

$(^3T_2)$

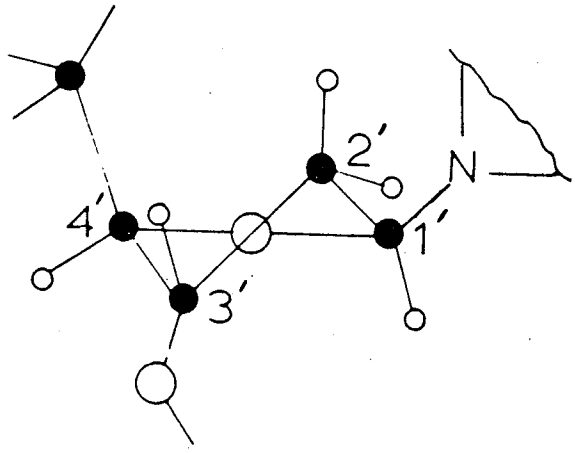

$(^2T_3)$

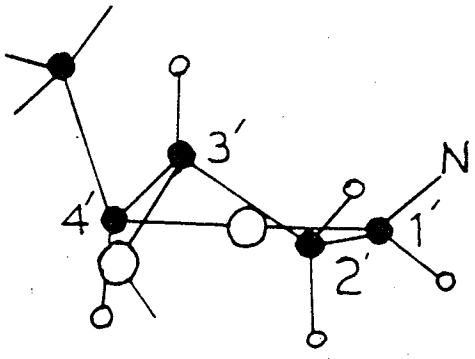

^3E

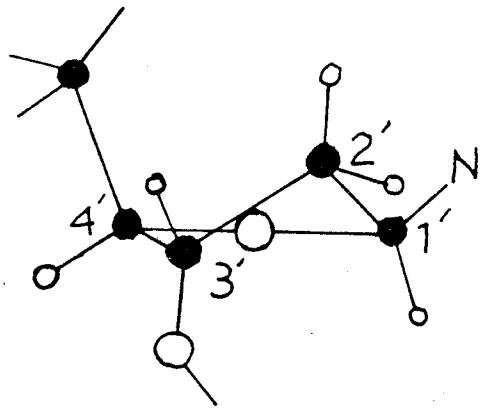

^2E

estimate the energy barriers between these two states. A relaxation study of ribonucleosides in liquid deuterio-ammonia arrived at an average activation energy for pseudorotation of 20 $\pm$ 2 kJ mole^{-1} for purine derivatives while indicating that the pyrimidines studied must be higher since the E_a was not determinable in the temperature range studied[58]. Theoretical estimates vary wildly, ranging from 16 kJ mole^{-1} using quantum mechanical calculations[93,94] to 10-12 kJ mole^{-1} for ribose and about 8 kJ mole^{-1} for deoxyribose[95], using classical potential energy calculations. A recent study[97] employing consistent force field calculations, has placed the barrier at 1.5 kJ mole^{-1} for both the ribose and deoxyribose rings. As can be seen, the exact magnitude of the barrier is not known with great certainty. The averaging procedure is sensitive to the magnitude of the barriers within the limits stated above. If the barrier is in the upper end of the range, the currently used weighted average is appropriate. If, however, the lower range is the case, a more complicated sum over states method must be used.

a. PSEUDOROTATIONAL ANALYSIS

A number of attempts have been made to derive conformational information about the ribose ring from the vicinal coupling constants observed in nucleosides and nucleotides in solution based on the above observations. Work by Altona and Sundaralingam[98] describes a method for deducing the major components in the ribofuranose interconversion in solution and their relative proportion in a two-state equilibrium. This method[98], derived from X-ray data on nucleosides

and nucleotides, brings out the salient features concerning the ring dynamics and will be the subject of the rest of this section.

In the Altona-Sundaralingam notation, N denotes the northern hemisphere of the pseudorotational cycle (see Figure 2.5), while the southern half is denoted by S. If the equilibrium is exclusively a two-site blend between N and S states, then the following equations can be written.

$$- 2.3 - \qquad {}^3J(H1'\text{-}H2') = {}^N X J_{89^o} + (1 - {}^N X) J_{158^o}$$

$$- 2.4 - \qquad {}^3J(H1'\text{-}H2'') = {}^N X J_{-32^o} + (1 - {}^N X) J_{39^o}$$

$$- 2.5 - \qquad {}^3J(H2'\text{-}H3') = {}^N X J_{43^o} + (1 - {}^N X) J_{-39^o}$$

$$- 2.6 - \qquad {}^3J(H2'',H3') = {}^N X J_{166^o} + (1 - {}^N X) J_{80^o}$$

$$- 2.7 - \qquad {}^3J(H3'\text{-}H4') = {}^N X J_{-158^o} + (1 - {}^N X) J_{-96^o}$$

where ${}^N X$ is the mole fraction of the N conformer. Since $J_{43^o} \simeq J_{-39^o}$ and $J_{89^o} \simeq J_{96^o} \simeq 0$, inspection of the above equations reveals that $({}^3J(H1'\text{-}H2') + {}^3J(H3'\text{-}H4'))$ and ${}^3J(H2'\text{-}H3')$ should remain constant. This invariance was observed in the limited data available at the time, and the data acquired since then more or less conform to these observations[6]. Indeed, a molecule must display this invariance in $({}^3J(H1'\text{-}H2') + {}^3J(H3'\text{-}H4'))$ and ${}^3J(H2'\text{-}H3')$ in order to be accessible to this method of analysis. Substantial deviations in $({}^3J(H1'\text{-}H2') + {}^3J(H3'\text{-}H4'))$ from $10.6 \pm .2$ Hz and ${}^3J(H2'\text{-}H3')$ from $5.6 \pm .2$ Hz for

FIGURE 2.5 shows the pseudorotational cycle used by Altona and Sundaralingam to analyze the conformer interconversion in the ribofuranose ring of nucleic acid derivatives.

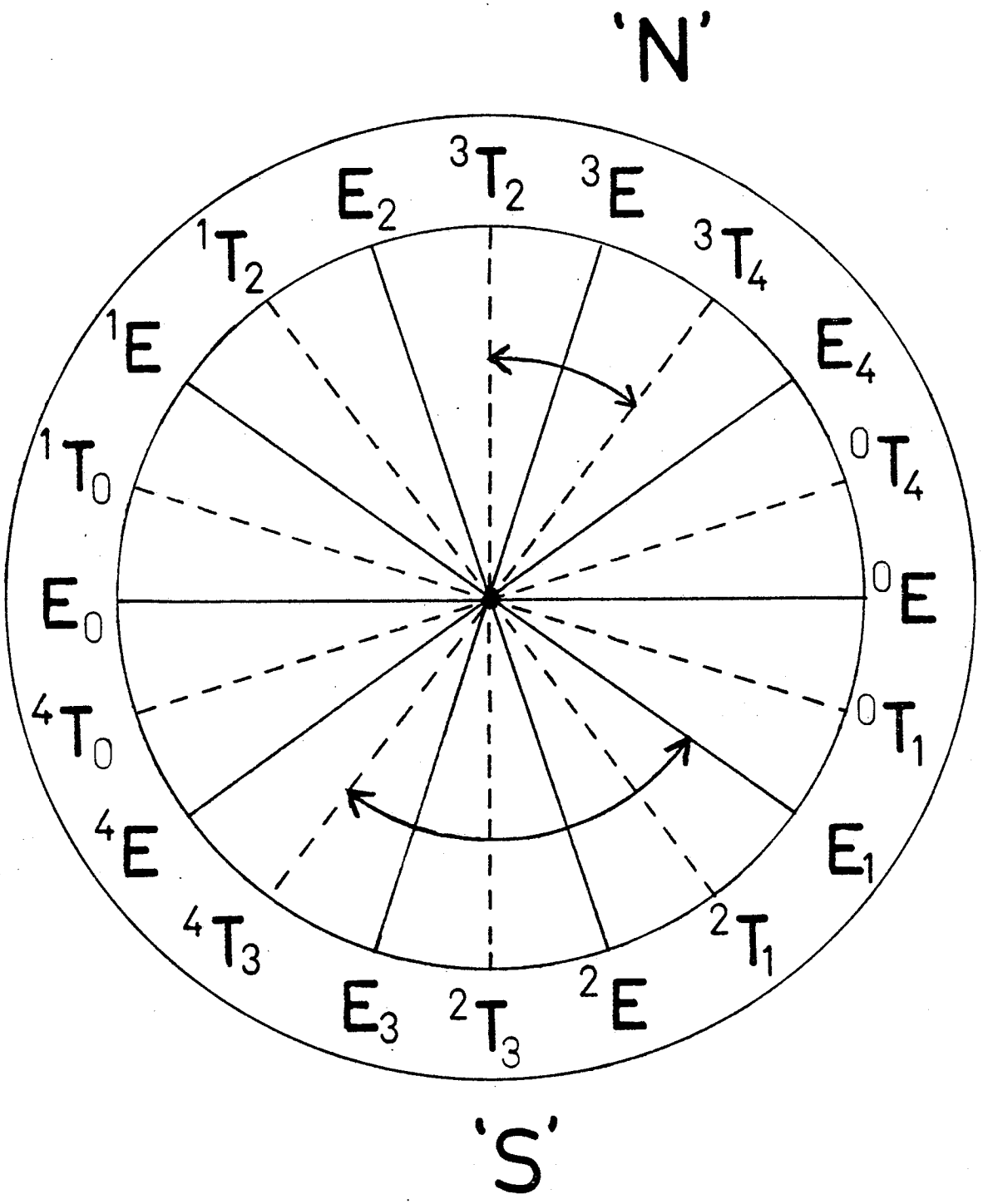
'N'
$^3T_2$
^3E
$^3T_4$
E_2
E_4
$^1T_2$
^1E
$^0T_4$
$^1T_0$
^0E
E_0
$^0T_1$
$^4T_0$
E_1
^4E
$^2T_1$
$^4T_3$
^2E
E_3
$^2T_3$
'S'

ribofuranose derivatives indicate that either the equilibrium is no longer between N and S states or that other conformers are making substantial contributions to the equilibrium. It should be noted that changes in the constants in the Karplus equation can also lead to deviations in these quantities.

To facilitate the analysis, a plot has been published[6,99] which relates the observed (^3J(H1'-H2') + ^3J(H3'-H4')) and ^3J(H2'-H3') magnitudes to the parameters P and τ_m. Another graph relates the P and τ_m values to static estimates of ^3J(H1'-H2') in N (or S) and to ^3J(H3'-H4') in N (or S). These are obtained and substituted into Equation 2.8 to find the mole fraction of the N or S conformer.

$$- 2.8 - \qquad J_{OBS} = {}^{S}_{X}J + (1 - {}^{S}_{X})^{N}J$$

A similar method developed by Davies and Danyluk[77b] relies on essentially the same expressions except that ^N_J and ^S_J values are estimated from models and the magnitudes vary from procedure to procedure. The equilibrium constant can be determined from the full pseudorotational analysis, but an approximate method relates K_{eq} directly to the observed couplings.

$$- 2.9 - \qquad K_{eq} = \frac{S_X}{N_X} = \frac{^3J(H1'-H2')}{^3J(H3'-H4')}$$

Numbers obtained for K_{eq} from any of the above methods agree well.

For deoxy derivatives, the situation is more complex. In their original work[68], Altona and Sundaralingam noted a wider spread for the

ring conformers in the deoxy series than observed for the ribose derivatives. These workers concluded that a flatter potential minimum exists for the deoxyribose sugars because this broad range of conformers could not be accounted for by crystal packing forces alone. Also, the observed (^3J(H1'-H2') + ^3J(H3'-H4')) and ^3J(H2'-H3') magnitudes are larger in the deoxy series. This, in part, is due to the change in electronegativity due to the removal of the 2'-hydroxyl group, but other causes of this increase are possible. Sarma noted[100] that if the conformational blend was supplemented by contributions from the $_4E$ and $_1E$ states to the ^3E and ^2E states, respectively, an increase in (^3J(H1'-H2') + ^3J(H3'-H4')) would result. Instead of disentangling the countering effects of electronegativity and additional conformers, Sarma chose to analyze the data, ignoring the electronegativity effect, assuming an equilibrium between states of the type (see Figure 2.5)

$$|E_1 \rightleftharpoons {}^2E \rightleftharpoons E_3| \rightleftharpoons |E_2 \rightleftharpoons {}^3E \rightleftharpoons E_4|$$

The symbolism implies a minor equilibrium between neighboring states in each of the two conformational domains while retaining the major N $\rightleftharpoons$ S conformational blend. Under conditions where the populations of the added states are nearly equal (i.e., $_1E \simeq {}_3E$ and $_2E \simeq {}_4E$), no appreciable change will occur in the sum of the couplings (^3J(H1'-H2') + ^3J(H3'-H4')) or in ^3J(H2'-H3'). Although this method appears reasonable, some correction for electronegativity must be made before comparing the deoxyribose data with the ribose data,

especially K_{eq}. In this work, the 1.1 Hz electronegativity correction determined by Davies[6] will be subtracted from $^3J(H1'-H2')$ and $^3J(H2'-H3')$ before any comparison is made.

The use of the information obtained from the pseudorotational analysis (the effect of the base, point of phosphorylation and/or dimerization on ring pucker conformation) will be taken up in the Discussion.

3. SUGAR-PHOSPHATE BACKBONE CONFORMATION

The last major conformational unit needed to describe totally the conformation of a nucleoside or nucleotide unit is the sugar-phosphate backbone. Figure 2.2 shows the atoms involved and the symbols used to denote the various torsion angles about the bonds. Ψ' is identical to τ_3 and was included above in the discussion of the sugar pucker. Of the five remaining angles, three (ϕ, ψ, and ϕ') are accessible to the vicinal coupling analysis. ω and ω' involve no magnetic nuclei which readily yield coupling information to use as conformational probes, so information concerning these angles is inferred from base stacking studies or from the temperature dependence of ^{31}P shifts. Figures 2.6, 2.7, and 2.8 show the Newman projections of the substituents attached to the $C_{5'}—C_{4'}(\psi)$, $C_{5'}—O_{5'}(\phi)$ and $C_{3'}—O_{3'}(\phi')$ bonds, respectively. Overwhelming evidence[6] indicates that the ψ and ϕ angles can be discussed in terms of the (classical) staggered forms. X-ray studies[101] show that ψ is observed in the three distinct conformational ranges of 35^o-65^o (ψ_+),

FIGURE 2.6 contains the three staggered conformations about the $C_{5'}$—$C_{4'}$ bond along with their conformational labels.

$C_{4'}$—$C_{5'}$ CONFORMERS, Ψ

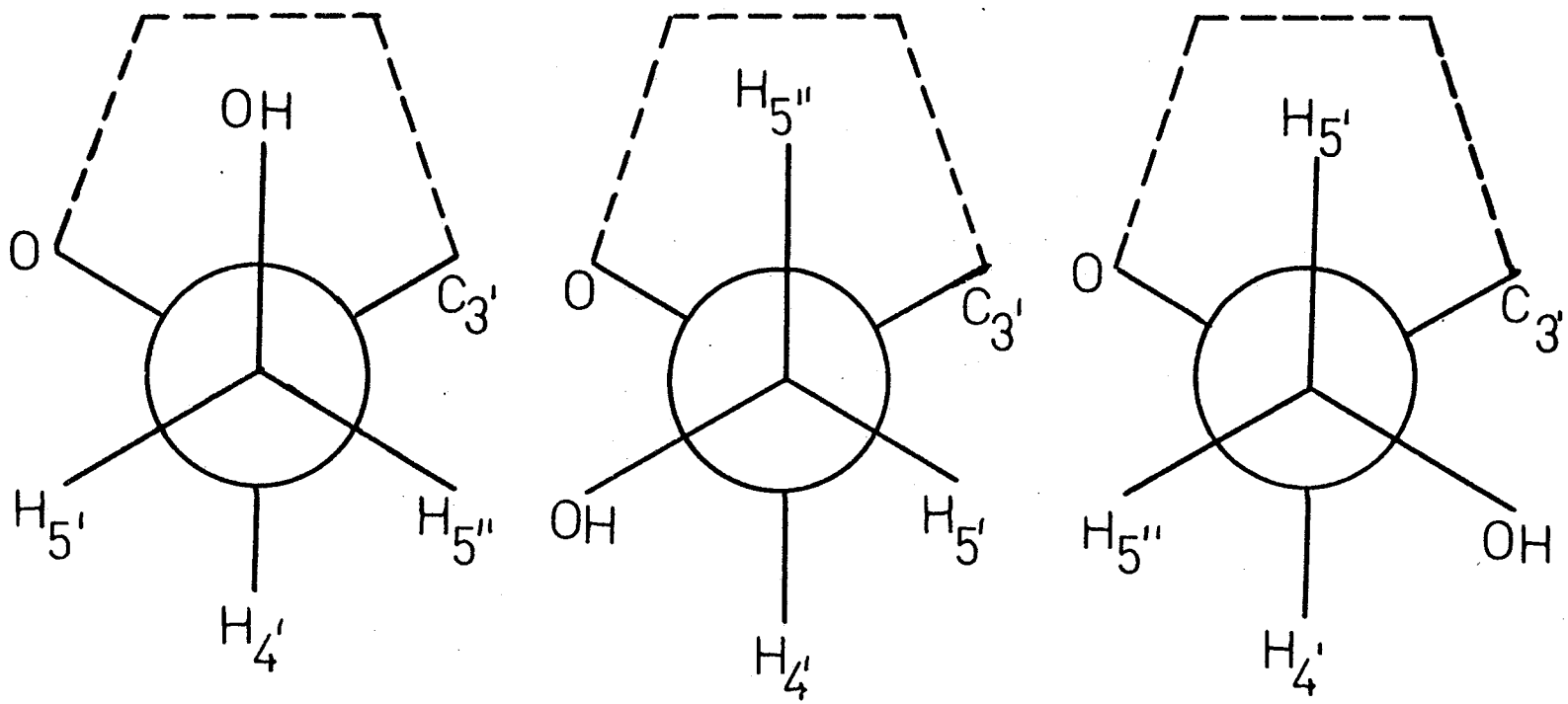

g_+ t g_-

FIGURE 2.7 contains the three staggered conformations about the $O_{5'}$—$C_{5'}$ bond along with their conformational labels.

$C_{5'}$–$O_{5'}$ Bond Conformers, Φ

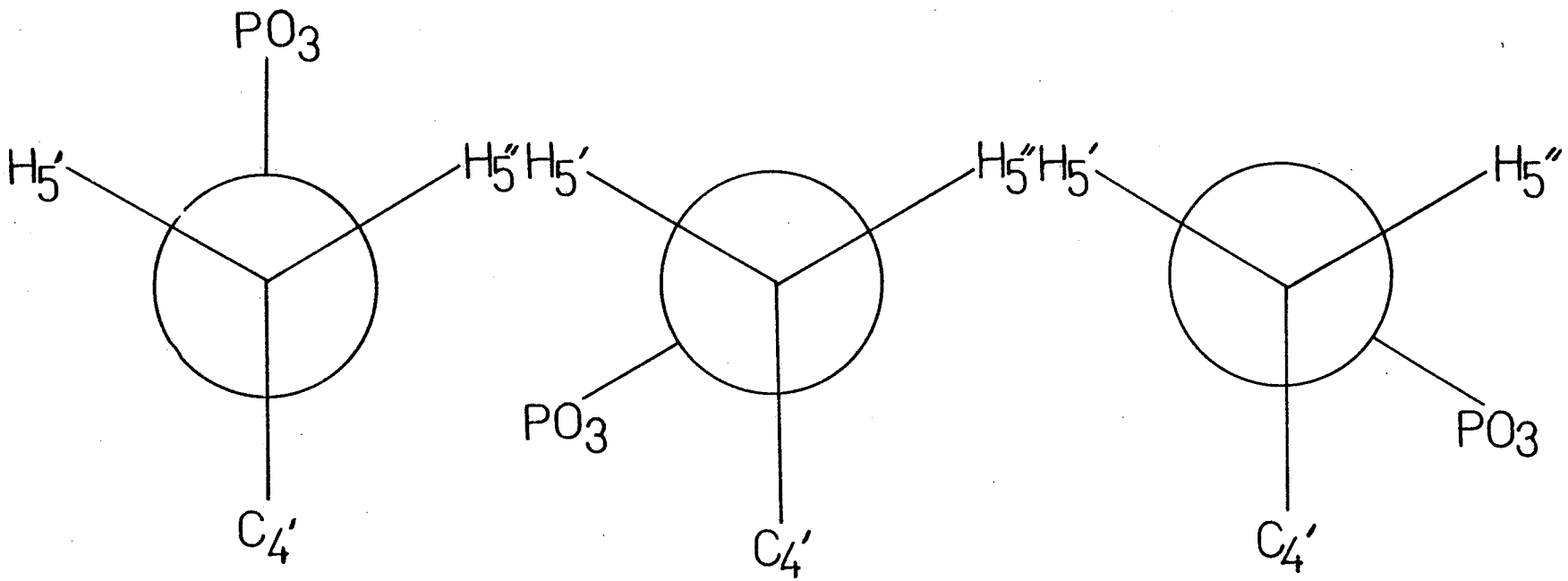

t **g_+** **g_-**

FIGURE 2.8 contains the three staggered conformations about the $C_{3'}$—$O_{3'}$ bond along with their conformational labels.

$C_{3'}$-$O_{3'}$ CONFORMERS, Φ'

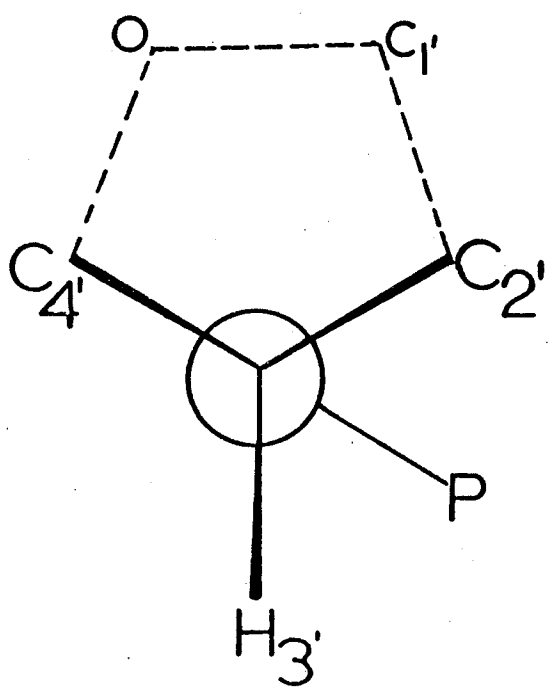

t

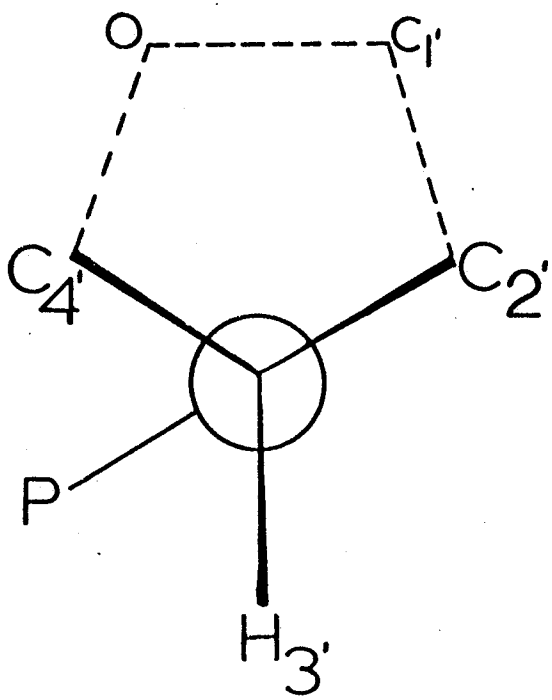

g_-

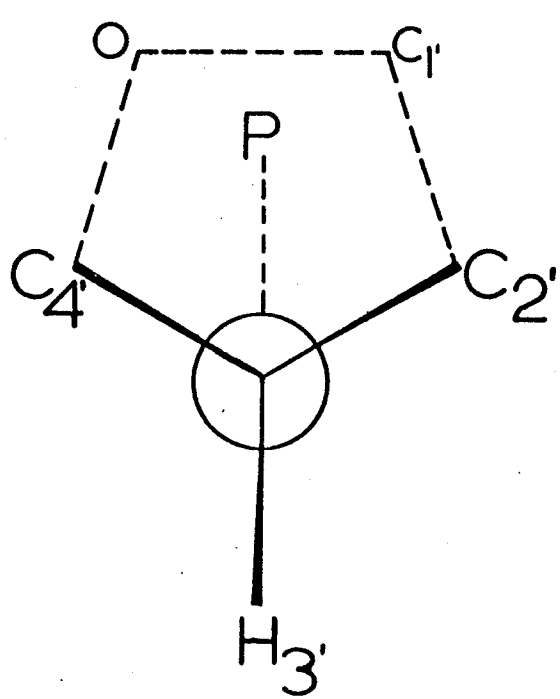

g_+

160^{o}-190^{o} (ψ_t), and 295^{o}-325^{o} (ψ_-), as shown in Figure 2.6. For the ϕ and ϕ' angles, the former is observed as only one value (ϕ_t in Figure 2.7) in the solid state studies of 5'-nucleosides, dinucleoside monophosphates, and polynucleotides[6]. On the other hand, ϕ' varies over values between ϕ'_t and ϕ'_- in Figure 2.8[102].

a. THE $C_{5'}$—$C_{4'}$ BOND, Ψ

The conformational analysis of this angle is based on the interpretation of the two vicinal coupling constants, ^3J(H4'-H5') and ^3J(H4'-H5"), in terms of a rapid interconversion between the three rotamer states in Figure 2.6. A complete analysis of these couplings, in terms of the three-state model, depends on the correct assignment of the $H_{5'}$ and $H_{5''}$ signals. Both assignments have been proposed based on experimental observations. The assignment shown in Figure 2.6 is that of Remin and Shugar[103] based on a comparison of the chemical shifts of $H_{5'}$ and $H_{5''}$ in uridine, β-pseudouridine, and their 3'-nucleotides[104]. Other independent studies have confirmed this assignment for nucleosides and both 2'- and 3'-nucleotides[105,106]. The assignment for the common 5'-nucleotides and corresponding nucleotide fragments has not been proven, but considerations of the spectra and conformational models for dinucleoside phosphates suggest that the Remin-Shugar assignment still holds[34,35]. Given that this assignment is correct, then each conformer population about the $C_{5'}$—$C_{4'}$ bond can be calculated from the following expressions:

- 2.10 - $$^3J(H4'\text{-}H5') = p_+ {}^3J_+(H4'\text{-}H5') + p_t {}^3J_t(H4'\text{-}H5') + p_- {}^3J_-(H4'\text{-}H5')$$

- 2.11 - $$^3J(H4'-H5'') = p_+ {}^3J_+(H4'-H5'') + p_t {}^3J_t(H4'-H5'') + p_- {}^3J_-(H4'-H5'')$$

- 2.12 - $$1 = p_+ + p_t + p_-$$

Inspection of Figure 2.6 suggests that only two values of the vicinal coupling constant are needed if the effect from the different orientations of the substituents can be ignored. Generally, this is done since it is not known if the magnitude of the change would be detectable considering the resolution of the resonances involved ($\nu_{\frac{1}{2}} \geq 0.7$ Hz in nucleosides and nucleotides and $\nu_{\frac{1}{2}} > 1.0$ Hz in dinucleoside phosphates). For this reason, conformational trends rather than absolute populations have been emphasized. The values used are those of Hruska and Sarma[107-109] ($J_g = {}^3J_+(H4'-H5') = {}^3J_+(H4'-H5'') = {}^3J_t(H4'-H5') = {}^3J_-(H4'-H5'') = 1.5$ Hz and $J_t = {}^3J_t(H4'-H5'') = {}^3J_-(H4'-H5') = 11.5$ Hz). These numbers have been widely used in the analysis of the $C_{5'}$—$C_{4'}$ bond and are able to account for the full range of observed $^3J(H4'-H5')$ and $^3J(H4'-H5'')$ couplings[6].

Upon rearranging Equations 2.10 to 2.12, expressions for the populations of the three rotamers are obtained as Equations 2.13 to 2.15.

- 2.13 - $$p(\psi_+) = \frac{\left[{}^3J_t + {}^3J_g\right] - \left[{}^3J(H4'-H5') + {}^3J(H4'-H5'')\right]}{{}^3J_t - {}^3J_g} = \frac{13 - \Sigma}{10}$$

$$- 2.14 - \qquad p(\psi_t) = \frac{^3J(H4'-H5'') - J_g}{^3J_t - ^3J_g} = \frac{^3J(H4'-H5'') - 1.5}{10}$$

$$- 2.15 - \qquad p(\psi_-) = \frac{^3J(H4'-H5') - J_g}{^3J_t - ^3J_g} = \frac{^3J(H4'-H5') - 1.5}{10}$$

where $\Sigma = {}^3J(H4'-H5') + {}^3J(H4'-H5'')$ and the values of $J_t = 11.5$ Hz and $J_g = 1.5$ Hz have been substituted where appropriate. Notice that the g_+ conformer depends only on the sum of the observed couplings and is independent of the assignment. Differences of 5% are considered as within experimental accuracy of the measurements ($\pm$0.2 Hz). It has been noted[6] that the uncertainty of the analysis increases as $^3J(H4'-H5')$ increases to 4 or 5 Hz.

b. THE $O_{5'}$—$C_{5'}$ BOND, Φ

i. Vicinal Coupling Constants, $^3J(^1H-^{31}P)$

The determination of the conformational properties of the ϕ bond depends upon whether the fragment under consideration is a nucleoside or nucleotide. In the former instance, the vicinal proton-proton couplings are used, while the latter circumstance requires the analysis of proton-phosphorus couplings. Since only the nucleotidyl unit will be considered in this work, only the $^1H-^{31}P$ analysis will be discussed.

As mentioned earlier, the rotamer population is discussed in terms of a rapid interconversion between the three staggered forms in Figure 2.7. Solid state and solution studies have indicated a strong preference for the ϕ_t rotamer in nucleotides, dinucleoside mono-

phosphates, polynucleotides and in t-RNA's[101]. Again the approximation is used that the individual gauche and trans coupling constants, $^3J_g(H\text{-}P)$ and $^3J_t(H\text{-}P)$, are independent of the orientation of substituents. A number of estimates have been made for the magnitude of $^3J_g(H\text{-}P)$ and $^3J_t(H\text{-}P)$ from studies of model compounds, and the values suggested by Sarma and co-workers[88] (^3J_t = 22.9 Hz and ^3J_g = 2.1 Hz) will be used in this work. Starting with identical expressions (Equations 2.13 to 2.15) and using $^3J_t(H\text{-}P)$ and $^3J_g(H\text{-}P)$ instead of the proton-proton coupling, the following equations can be written[109]

$$p(\phi_t) = \frac{\left[{}^3J_t(H\text{-}P) + {}^3J_g(H\text{-}P)\right] - \left[{}^3J(H5'\text{-}P) + {}^3J(H5''\text{-}P)\right]}{{}^3J_t(H\text{-}P) - {}^3J_g(H\text{-}P)} \qquad \text{- 2.16 -}$$

$$= \frac{25 - {}^3J(H5'\text{-}P) + {}^3J(H5''\text{-}P)}{21} = \frac{25 - \Sigma'}{21}$$

$$p(\phi_+) = \frac{{}^3J(H5''\text{-}P) - {}^3J_g(H\text{-}P)}{{}^3J_t(H\text{-}P) - {}^3J_g(H\text{-}P)} = \frac{{}^3J(H5''\text{-}P) - 2.1}{21} \qquad \text{- 2.17 -}$$

$$p(\phi_-) = \frac{{}^3J(H5'\text{-}P) - {}^3J_g(H\text{-}P)}{{}^3J_t(H\text{-}P) - {}^3J_g(H\text{-}P)} = \frac{{}^3J(H5'\text{-}P) - 2.1}{21} \qquad \text{- 2.18 -}$$

Again, one of the populations, $p_t(\phi)$, is independent of the assignment of the $H_{5'}$ and $H_{5''}$ signals. The same accuracy (between ± 5 and $\pm 10\%$, as noted in the expressions for the ψ angle) is expected for populations extracted from these equations.

ii. Long-Range Coupling Constants, ^4J(H4'-P5')

Although it is difficult to quantify the dependence of ^4J(H4'-P5') on the intervening angles, the magnitude of ^4J(H4'-P5') does give some information concerning the angular relationship of ψ and ϕ. Hall and co-workers[110-112] showed that the magnitude of ^4J(H-P) exhibits a maximum of ~2.7 Hz for the planar "W" conformation and drops to zero for other conformations[107]. Sarma, Hruska, and co-workers[107] have demonstrated a linear correlation between ^4J(H4'-P5') and both Σ and Σ'. These workers showed that ^4J(H4'-P5') increased with the correlated increase of ψ_+ and ϕ_t.

c. THE $C_{3'}$—$O_{3'}$ BOND, Φ'

The conformational discussion of the ϕ' bond will be restricted to 3'-nucleotides and the corresponding nucleotidyl fragment in dinucleoside monophosphates. In principle, all three of the staggered conformers in Figure 2.8 are accessible to ϕ'. Initial analysis of this bond[104] employed the proton-phosphorus vicinal coupling constant and used the three-state model. Following this approach, little correspondence was found between the ^1H NMR and ^{13}C NMR work[77b]. Additional solid state studies[101] and energy calculations[182,183] suggested that the $O_{3'}$—P bond was restricted to the two gauche domains (i.e., conformers ϕ'_t and ϕ'_- in Figure 2.8). These energy calculations indicate that, in the ϕ'_+ domain, steric interactions between the non-ester oxygens and the substituents at $C_{4'}$ and $C_{2'}$ would repress any significant population of this conformer.

Complications in the interpretation of the observed proton-phosphorus couplings based on the two-state model still exist. ^1H NMR analysis predicts a small magnitude for the observed vicinal coupling ($J \simeq 2.5$ Hz) while values in the range of 6.0 to 8.5 Hz are observed. Some workers have attempted to determine conformational angles by using the $\cos^2 \theta$ Karplus dependence of $^3J(H-P)$. Angles of $\pm 36^\circ$ and $\pm 123^\circ$ from the eclipsed conformation are obtained from the observed couplings. The $\pm 123^\circ$ values are ruled out on the basis of the energy calculations above. This leaves the $\pm 36^\circ$ value, or $\phi' = 204^\circ$ to 276° range. These ranges can then be correlated with X-ray analysis which shows that $N(^3E)$ sugars prefer the lower ϕ' range while $S(^2E)$ sugars prefer the higher ϕ' range. With this information, the equilibrium was presented in the form[34,35]

- 2.19 - $$N\phi'_{205} \rightleftharpoons S\phi'_{275}$$

Further support for this type of equilibrium can be obtained from long-range $^4J(H2'-P)$ coupling constants in 3'-ribonucleotides[77a].

Although a two-state model is currently being used for the ϕ' bond analysis, new X-ray data[102] suggest that there may, in fact, be no barrier to interconversion between the two gauche domains and that a single broad continuum exists encompassing $\phi' = 195^\circ$ to $\phi' = 268^\circ$. Indeed, in the crystal structure of 3'-AMP $\cdot$ $2H_2O$, ϕ' is 237°, just 3° from the eclipsed conformation of the $C_{3'}—H_{3'}$ and the $O_{3'}—P$ bonds, indicating that the barrier to rotation about the eclipsed form is small.

Due to the above inconsistencies, no attempt will be made to resolve rotamer populations from the observed couplings. Instead, only a qualitative discussion of the conformational preferences implied from the observed couplings will be presented. If future evidence indicates the applicability of a two-site model, the data reported can be used in such an analysis. It seems unwarranted at the present time, in light of the data on 3'-nucleotides, to attempt any quantitative discussion of rotamer populations.

C. CARBON-13 APPROACH TO NUCLEIC ACID CONFORMATION

As mentioned in the Introduction, ^{13}C NMR has been shown to be an invaluable aid in the conformational analysis of nucleic acids and derivatives. In the studies reported so far, ^{13}C results have been interpreted on the basis of information obtained from the proton studies of corresponding molecules. In general, the information obtained from the two methods is in agreement. In some cases, the ^{13}C results offer data which are easier to interpret than the proton data (e.g., determination of N-glycosyl bond conformation by the vicinal proton-carbon coupling constants rather than proton chemical shifts or proton-proton NOE measurements). This section will discuss what information from the observed ^{13}C spectrum can be used for the conformational analysis of nucleosides and nucleotides.

1. N-GLYCOSYL BOND CONFORMATION

Of the two parameters which possess information concerning N-glycosyl bond conformation, (ribose carbon chemical shifts and $^{3}J(H-C)$ coupling constants), the former generally yields only qualitative information while the latter, in principle, is capable of yielding the magnitude of χ to within a given conformational range. The ribose carbon chemical shifts will be discussed briefly, followed by a discussion of the proton-carbon vicinal coupling constants.

a. ^{13}C CHEMICAL SHIFTS

As for protons, there are differences in the chemical shifts of the ribose carbons for a pyrimidine base in the anti or syn

conformation. In a comparison of 6-methylcytidine with cytidine, upfield shifts are observed for the $C_{2'}$ and $C_{3'}$ carbons (4.9 and 1.6 ppm, respectively) while downfield shifts are observed for $C_{1'}$, $C_{4'}$, and $C_{5'}$ (3.4, 1.8, and 2.2 ppm)[72]. This trend is observed in the ^{13}C data of Jones et al.[47-50] based on known information from proton data of the corresponding molecules. However, the only clear trend that could be discerned from the data is the 3 ppm upfield shift of $C_{2'}$. The observed shifts in 6-methylcytidine are in the opposite direction to the directly bound protons. This suggests a possible bond polarization, especially for $C_{2'}$—$H_{2'}$ in 6-methylcytidine, due to the electric field effect of the 2-keto group in the base located over the ribose ring.

b. VICINAL PROTON-CARBON COUPLING CONSTANTS, $^3J(H-C)$

Early studies by Lemieux and co-workers[52,115,116] demonstrated the existence of a Karplus-type relationship between $H_{1'}$ and C_2 of the pyrimidine ring in two fixed derivatives of uridine (2,2'-anhydro-β-D-arabinouridine and 2,5'-anhydrouridine). In these studies, the observed coupling constant between C_2 and $H_{1'}$ was related to the dihedral angles determined from X-ray studies[52] using A = 6.7 Hz, B = 1.3 Hz, and C = 0 in Equation 2.2. Lemieux et al.[115] suggested that the observed $^3J(H1'-C2)$ magnitude of 2.4 Hz in uridine is consistent with the anti conformation deduced from $^5J(H5-H1')$. Further studies by Schweizer and Kreishman[117] and Davies[53] showed that a measurement of $^3J(H1'-C2) < 5$ Hz cannot differentiate between the syn and anti conformation. In the Davies work[53], natural abundance

spectra were recorded for a series of pyrimidine nucleosides and nucleotides. Vicinal couplings were observed from $H_{1'}$ to both C_2 and C_6 and assigned by selective decoupling of the $H_{1'}$ and H_6 resonances (where appropriate) in the proton spectrum. Although the data could differentiate between the syn and anti conformation, the $\cos^2 \theta$ nature of the Karplus relation prohibits differentiation between the two syn or two anti conformers. The above observations[53] assumed that ^3J(H1'-C6) followed the same relation as ^3J(H1'-C2). Further studies[6] on methylated bases of uracil and cytosine, however, indicate that ^3J(H1'-C6) > ^3J(H1'-C2) due to the electronegativity difference between the 2-keto group and the 6-substituent. The minor differences preclude an exact analysis, but it is predicted that ^3J(H1'-C6) > ^3J(H1'-C2) for a predominant anti conformer while ^3J(H1'-C2) > ^3J(H1'-C6) for a predominant syn conformer.

2. SUGAR-PHOSPHATE BACKBONE CONFORMATION

In addition to the information obtained from proton-proton and proton-phosphorus vicinal coupling constants, carbon-phosphorus vicinal couplings can be used to further quantify the backbone conformers about ϕ ($O_{5'}$—$C_{5'}$) with ^3J(C4'-P5') and about ϕ' ($C_{3'}$—$O_{3'}$) with ^3J(C4'-P3') and ^3J(C2'-P3'). Pioneering studies by Mantsch and Smith[54], followed by others[56,118,119], demonstrate the existence of a Karplus relationship which, when suitably parameterized, can supply an independent means of determining ϕ and ϕ' rotamer populations. Although the current parameters have not been refined through

extensive comparison with fixed model compounds, the populations predicted from $^3J(C4'-P5')$ are in agreement with those determined from the proton-phosphorus results. Agreement with the ϕ' bond is worse, but this is probably due to the uncertainty in the analysis, as mentioned above.

a. THE $O_{5'}-C_{5'}$ BOND, Φ

In a manner analogous to that used for the proton-phosphorus couplings, the observed vicinal carbon-phosphorus coupling can be described as a weighted average between the three states shown in Figure 2.7. The appropriate expression can be written as

$$^3J(C4'-P5') = p_+J_+ + p_tJ_t + p_-J_- \qquad \text{- 2.20 -}$$

$$= p_tJ_t + (p_+ + p_-)J_g \qquad \text{- 2.21 -}$$

$$= 8p_t + 2(p_+ + p_-) \qquad \text{- 2.22 -}$$

where the J_t and J_g values of Govil and Smith[119] have been used. As seen from the above expression, p_t and the sum $(p_+ + p_-)$ can be determined from the observed $^3J(C4'-P5')$, i.e.,

$$p(\phi_t) = \frac{^3J(C4'-P5') - 2.0}{8} \qquad \text{- 2.23 -}$$

Agreement between the $^1H-^{31}P$ and $^{13}C-^{31}P$ results depends upon the system under investigation. A reasonable agreement is obtained for 5'-nucleotides and homo dinucleoside monophosphates, while conclusions

for hetero dinucleoside monophosphates are in conflict. More data are needed to remove the discrepancies.

b. THE $C_{3'}$—$O_{3'}$ BOND, Φ'

As mentioned above, in view of the uncertainty about the exact nature of conformational equilibrium, an exact analysis of the rotamer populations is unjustified at this time. However, certain qualitative conclusions can be proposed on the basis of the observed ^3J(C4'-P3') and ^3J(C2'-P3') magnitudes. Examination of Figure 2,8 reveals that, for a pure ϕ_t' conformer, ^3J(C4'-P3') ≃ 10 Hz and ^3J(C2'-P3') ≃ 2.5 Hz, while the magnitudes are reversed for the ϕ_-' conformer. Therefore, large magnitudes for ^3J(C4'-P3') would imply a large contribution from the ϕ_t' state. As $p(\phi_t')$ decreases and $p(\phi_-')$ increases, a concomitant decrease in ^3J(C4'-P3') and increase in ^3J(C2'-P3') is expected. In addition, Davies and Danyluk[77] and Chen and Sarma[100] have discussed a correlation between sugar ring pucker and ϕ' bond conformation (i.e., Equation 2.19). This would imply a dependence of ^3J(C-P) on the sugar pucker. The proposed model predicts that for a predominant N sugar conformation, ^3J(C4'-P3') > ^3J(C2'-P3'). For the S conformation, the above inequality is reversed. The model also predicts the consistency of ^3J(C4'-P3') + ^3J(C2'-P3'). The present data will be examined for this correlation.

3. DETERMINATION OF OVERALL AND INTERNAL MOBILITY OF NUCLEIC ACID CONSTITUENTS

NMR relaxation time measurements (T_1's) can be used for the determination of the overall mobility of molecules in solution[57,120-122].

^{13}C relaxation times are particularly sensitive to the motions of a molecule. Since the ^{13}C relaxation time for a carbon with a directly bound proton is dominated by the direct ^{1}H-^{13}C dipolar interaction from that proton, T_1 measurements can be related to the correlation time for molecular tumbling in solution by[119]

$$- 2.24 - \qquad \frac{1}{T_1} = \frac{N\gamma^2_{^{13}C}\gamma^2_{^{1}H}\hbar^2\tau_c}{r^6}$$

where N is the number of directly bonded protons, $\gamma_{^{13}C}$ and $\gamma_{^{1}H}$ are the magnetogyric ratios for ^{13}C and ^{1}H respectively, r is the internuclear distance, and τ_c is the correlation time for overall molecular tumbling. This expression is a valid approximation as long as the extreme narrowing condition is met (i.e., $\omega_H^2\tau_c^2 << 1$ where ω_H is the proton resonance frequency in radians/sec). The equation also assumes that the molecular tumbling is isotropic.

Correlation times thus calculated can be compared with the expected correlation time of an isotropically reorientating sphere determined from the Stokes-Einstein equation[120].

$$- 2.25 - \qquad \tau_c = \frac{\eta V}{kT}$$

where V, the molecular volume, is approximated by summing the appropriate van der Waals volumes of the atomic constituents[123].

Both of the above equations invoke serious approximations, the most serious of which is that the molecule undergoes isotropic reorientation. Therefore, exact agreement between the two τ_c's is

not expected. What is obtained is a qualitative estimate of the spherical nature of the molecule and/or an idea as to the molecule's departure from isotropic reorientation.

^{13}C relaxation times are also sensitive to internal motion in the molecule[121]. In this case, the observed T_1's are modulated relative to "fixed" carbons. The effect is normally manifested as a lengthening of the T_1 for the carbon in question. This effect has been quantified for a tetrahedral carbon with one attached hydrogen[121]. Although these results cannot be used in the molecules under consideration here, a qualitative estimate can be obtained of the degree of internal flexibility for some of the molecules studied in this work.

D. PHOSPHORUS-31 NMR APPROACH TO NUCLEIC ACID CONFORMATION

The primary use of ^{31}P NMR in the conformational analysis of nucleotides[60,61], dinucleoside monophosphates[31,32,34,35,37], and polynucleotides[7] has been to aid in the analysis of proton-phosphorus coupling constants. Due to its location, this nucleus is capable of supplying information concerning the sugar-phosphate backbone. The magnetic nucleus is 100% abundant, but the strong affinity for metal ions (in particular, paramagnetic metal ions) imparts a special difficulty to the observation of small coupling constants. In addition, second order effects resulting from tightly coupled proton spin systems (usually involving $H_{4'}$, $H_{5'}$, and $H_{5''}$) preclude, in most cases, the direct measurement of proton-phosphorus couplings from the observed splittings.

1. SUGAR-PHOSPHATE BACKBONE CONFORMATION

a. THE $O_{5'}$—$C_{5'}$ AND $C_{3'}$—$O_{3'}$ BONDS, Φ AND Φ'

If rigorous methods are used to remove paramagnetic impurities[60,61], the proton coupled ^{31}P spectra can increase the certainty of the determined $^{3}J(H3'-P)$ couplings observed from the proton spectra. Due to the tightly coupled nature of the proton spectrum, care must be used in order to avoid errors arising from the assumption of a first order spectra. Exact magnitudes can only be extracted by computer simulation and an iterative analysis of the observed multiplet.

The additional observation of proton coupled ^{31}P spectra is sometimes essential to complete the proton analysis. In many cases, the

$H_{3'}$ resonance of the 3'-nucleotidyl fragment is obscured by the residual HDO signal in the proton spectrum. In this case, ^{31}P NMR is the easiest way of obtaining the magnitude of $^{3}J(H3'-P3')$.

b. THE P—$O_{5'}$ AND THE $O_{3'}$—P BONDS, ω AND ω'

To date, NMR has not been able to supply any direct information concerning the ω and ω' bonds. Recently, however, experimental studies[124-126] and theoretical calculations[127-130] have indicated that the ^{31}P chemical shift is sensitive to the ω—ω' bond conformation. Studies by Gorenstein et al.[124,127] have proposed a chemical shift dependence for both the O—P—O bond angle and the ω—ω' conformer angles. Given that the O—P—O angle is relatively independent of the nature of the nucleotidyl unit involved, the observed temperature dependence of the chemical shifts[124] was interpreted as reflecting the conformational change of the ω—ω' torsion angles. Hence, the theoretical and experimental studies agree, at least qualitatively, with a downfield shift of the ^{31}P resonance when going from a predominant gg'* conformer (i.e., base stacked form) to a mixture of the gg' and gt conformers (i.e., random coil form).

To reiterate, these results are of a purely qualitative nature in that no distinction can be made between the g_+ or g_- states. The

---

* This notation should not be confused with the old gg, gt, tg notation used by NMR spectroscopists to describe the backbone bond conformations. In this context, and throughout the thesis, the gg' or gt notation will be used to denote the gauche or trans conformers about the ω and ω' bond. Since NMR methods cannot differentiate between g_+g_+, g_+g_-, g_-g_+ or g_-g_- and g_+t, g_-t, tg_+, tg_-, etc., these subscripts are dropped when discussing ω and ω'.

studies do show, however, that at least the qualitative information is available. More accurate theoretical calculations[130] have refined the agreement, but the results still indicate the tenuous nature of obtaining quantitative information from experimental observations.

CHAPTER III

EXPERIMENTAL METHODS

This chapter is divided into two sections - materials and NMR method. The first section is primarily concerned with the synthesis and purification of the molecules used in this study. In the second section, the actual NMR sample preparation and a description of how the spectra were recorded are outlined.

A. MATERIALS

Some of the compounds used in this study were commercially available. dT, 3'-dTMP, 5'-dTMP, and some of the d(TpT) were purchased from Sigma Chemical Company (St. Louis, Missouri, U.S.A.). 3'-O-Acetyldeoxythymidine (3'-O'AcdT), used for some parts of the dinucleoside monophosphate synthesis, was also purchased from Sigma. All other compounds, i.e., m^6dU; blocked nucleosides of dT and m^6dU; mixed dinucleoside monophosphates d(TpT), d(Tpm^6U), d(m^6UpT), and d(m^6Upm^6U); and the nucleoside diphosphates d(pTp) and d(pm^6Up) were synthesized by the procedures outlined below.

The origin of the common reagents and solvents used in the following synthetic procedures are not specified. The commercial source of specialty reagents will, however, be identified.

The chromatographic procedures for the separation of the various intermediates and products were performed using MN-Kieselgel P/UV_{254} (Macherey Nagel and Co., Germany, distributed by Brinkman Instruments, Ontario, Canada) for the preparative thin layer chromatography and Brinkman Polygram Sil G/UV_{254} sheets (Macherey Nagel and Co.) for monitoring the progress of reactions and the analytical determination of R_f values. Whatman 3MM paper was used exclusively for the preparative separation of the deblocked nucleotides and dinucleoside monophosphates using the solvent systems specified below. The composition of all chromatographic solvents used is reported as volume ratios (i.e., v/v).

1. NUCLEOSIDE SYNTHESIS

a. DISCUSSION

Holy[131-134] has described two approaches to the synthesis of m^6dU. These are illustrated in Figure 3.1. The methods are essentially the same except for the condensing reagents used to form the pyrimidine ring.

In both procedures, the first step is to condense β-arabinose (Sigma Chemical Co.) with cyanamide (Sigma Chemical Co.) to form the starting 2-amino-β-D-arabinofuro{1',2':4,5}oxazoline (I). At this point, the two methods digress momentarily. In the original procedure[131-133], the oxazoline (I) was condensed with ethyltetrolate (ethyl-2-butynoate) (II) (ICN Pharmaceuticals Inc., Quebec, Canada) in dry DMF with catalytic amounts of triethylamine. Although the reported yields were high (∿70-80%)[131,132], difficulty was encountered in obtaining yields greater than 20%. A variation of the above procedure[133] is more convenient. The oxazoline (I) is condensed with ethyl-β-chlorocrotonate (ethyl-3-chloro-2-butenoate, cis or trans) (III) under identical conditions. Yields of $O^{2,2'}$-anhydro-6-methyl-arabinouridine (IV) by this method correspond to those reported (60-70%), and this procedure was used for the bulk of the m^6dU synthesis.

For the remainder of the synthesis, the two methods are identical. The anhydronucleoside (IV) was reacted with benzoyl cyanide (ICN Pharmaceuticals, Inc.) in dry acetonitrile and triethylamine to produce the 3',5'-di-O-benzoyl-$O^{2,2'}$-anhydro-6-methylarabinouridine (V). This

FIGURE 3.1 traces the reaction sequence used to synthesize m^6dU. Refer to the written text for details.

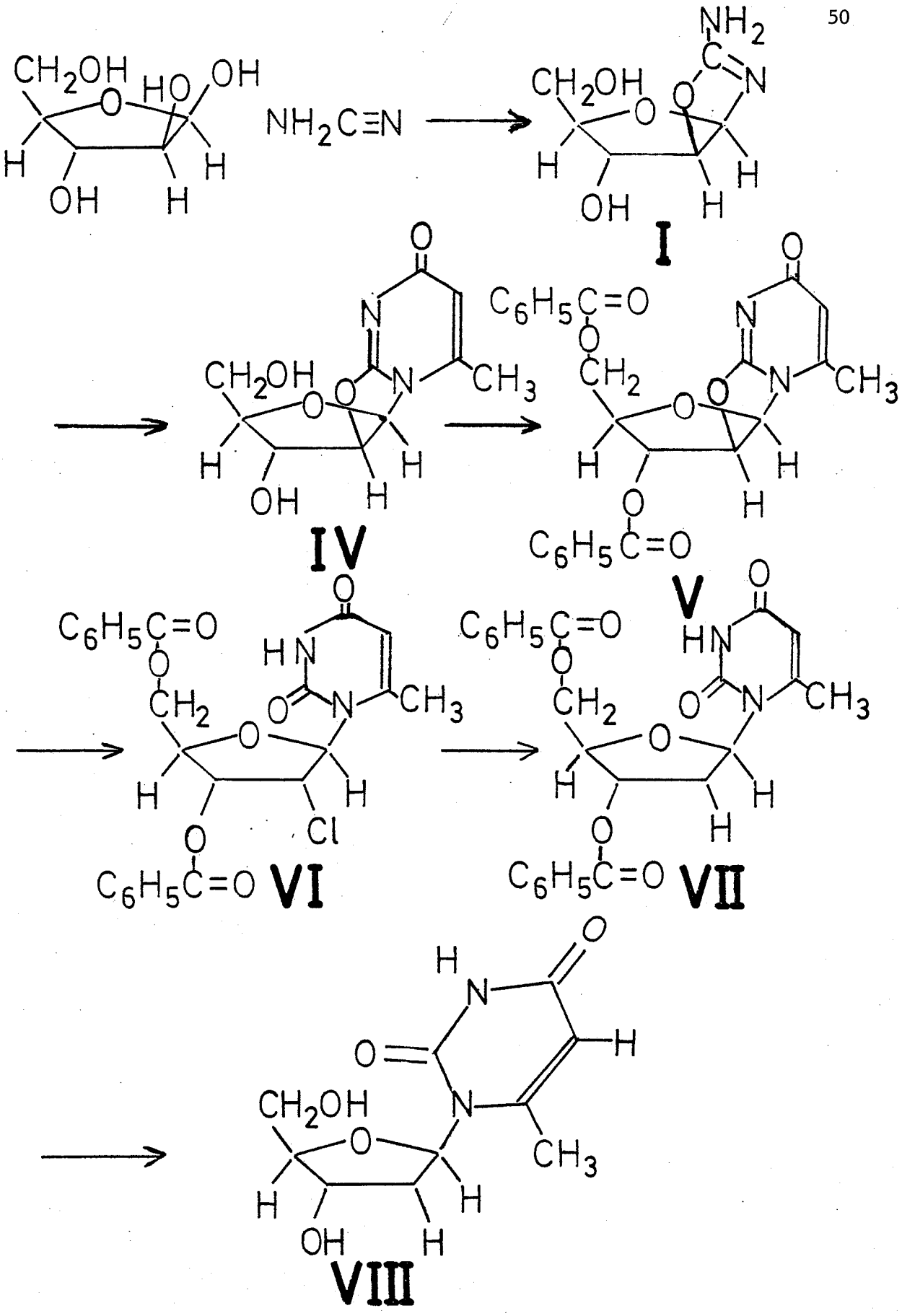
NH2C≡N
I
IV
V
VI
VII
VIII

product (V), in turn, was treated with 3M HCl in dry DMF to afford 3',5'-di-O-benzoyl-2'-chloro-2'-deoxy-6-methyluridine (VI). Subsequent refluxing of (VI) with tri-n-butyltinhydride (Alfa-Ventron, Inc., Massachusetts, U.S.A.) and catalytic amounts of 2,2'-azo-bis-isobutyronitrile (ICN Pharmaceuticals, Inc.) in benzene produced the 3',5'-di-O-benzoyl-2'-deoxy-6-methyluridine (VII). Finally, overnight hydrolysis of (VII) in methanolic-NaOMe resulted in 2'-deoxy-6-methyluridine, m^6dU (VIII).

b. PROCEDURES

Only minor modifications were made to the reported procedures[131-134]. These are noted below.

Due to the marginal difference in reaction yield of the anhydropyrimidine (IV) for the cis or trans ethyl-β-crotonate, no attempt was made to separate the two isomers. Instead, the reaction mixture was distilled under reduced pressure to remove the products from the starting material.

Instead of the recommended one hour reaction time for the benzoylation of (IV)[132], the reaction was monitored until no appreciable decrease of the starting material was noted (2.5 hours). The observed yield was marginally higher (∿5%) than that reported[132].

Again, an increase in the reaction time (1 hour reported)[132] for the acid hydrolysis of the anhydro linkage to 3 hours, concomitant with a slight decrease in reaction temperature, resulted in a substantial increase in the yield of (VI) from 58 to 95%. The product was checked chromatographically and found to be pure (no trace of the starting

material or by-products).

All products were purified, where necessary, using the reported procedures, checked spectroscopically using NMR, and compared with the reported chemical shifts and splittings. Exact agreement was noted in all cases. Purified samples were also checked on analytical TLC strips in the reported solvents[131,132], and the R_f values were comparable. A sample of the final product, m^6dU, was crystallized, and its structure was determined and confirmed by X-ray analysis[135].

2. PROTECTED NUCLEOSIDE AND NUCLEOTIDE SYNTHESIS

a. DISCUSSION

The synthesis of nucleotides of dT or m^6dU is straightforward in that only one hydroxyl function need be protected while the other is phosphorylated. In the case of 3',5'-nucleoside diphosphates, the nucleoside is phosphorylated directly without any intervening protection reactions. The general procedure for mononucleotide synthesis is outlined in Figure 3.2.

The starting nucleoside is first protected at the 5'-hydroxyl by reacting with monomethoxytrityl chloride (MMTrCl) in the case of dT or trityl chloride (TrCl) for m^6dU. The use of the less reactive trityl group for m^6dU was found to be necessary since the corresponding 5'-O-MMTrm^6dU derivative was unstable and would decompose on work-up due to unknown reasons. The purified 5'-blocked nucleoside can then be phosphorylated with β-cyanoethylphosphate in the presence of 2,4,6-tri-isopropylbenzenesulfonylchloride (TPS) to yield, after

FIGURE 3.2 illustrates the reaction sequence used to synthesize either a 3'- or 5'-mononucleotide.

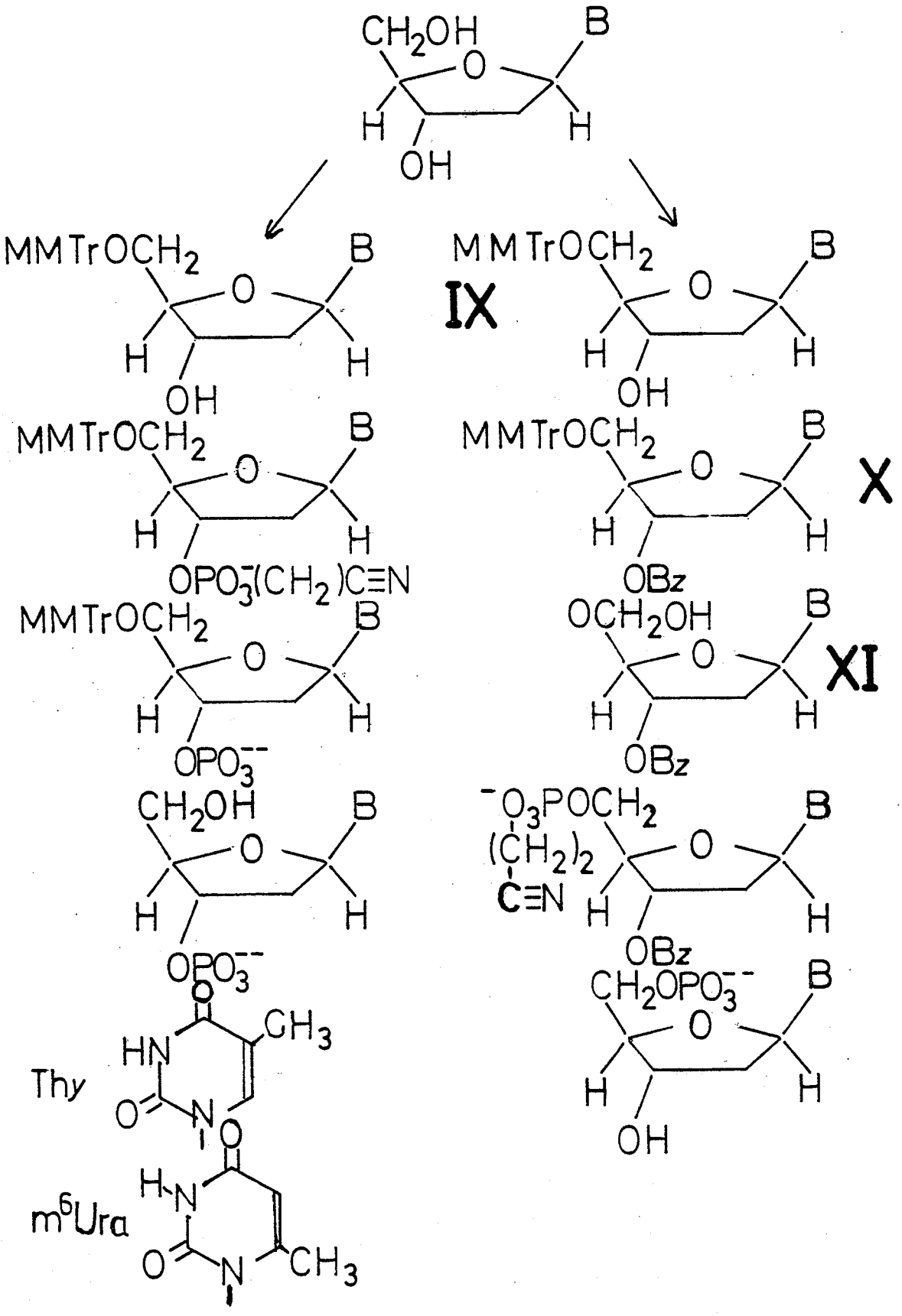
CH2OH
B
O
H
H
OH
MMTrOCH2
B
O
H
H
OH
IX
MMTrOCH2
B
O
H
H
OH
MMTrOCH2
B
O
H
H
OPO3-(CH2)CEN
MMTrOCH2
B
O
H
H
OPO3--
X
OBz
OCH2OH
B
O
H
H
OBz
XI
CH2OH
B
O
H
H
OPO3--
-O3POCH2
(CH2)2
CEN
B
O
H
H
OBz
CH2OPO3--
B
O
H
H
OH
Thy
CH3
HN
O
N
O
m6Ura
H-N
O
N
CH3

deprotection, the 3'-nucleotide. Alternately, the 5'-blocked nucleoside can be further protected at the 3'-hydroxyl group by reacting with benzoyl chloride. Removal of the acid labile trityl or monomethoxytrityl group, followed by phosphorylation, as described above, and subsequent deprotection, results in the 5'-nucleotide. This approach is standard and follows the procedure outlined by George et al.[73].

b. PROCEDURES

i. 5'-O-Monomethoxytrityldeoxythymidine (5'-O-MMTrdT) (IX) (B = Thy)[136]

Typically, one equivalent of dT was dried by co-evaporating with three 5 ml portions of dry pyridine. The dT was dissolved in dry pyridine (12 ml/mM dT), and 1.1 equivalents of p-monomethoxytrityl-chloride were added. The mixture was stirred overnight (~14 hours) and checked by TLC for starting material. When completed, the reaction was quenched by adding absolute ethanol (1 ml/mM dT) with ice cooling and stirring for an additional 15 minutes. The solvents were removed under reduced pressure. The residue was dissolved in $CHCl_3$, washed with three 5 ml portions of water, concentrated, and applied to preparative silica TLC plates (20 x 20 x 1 mm, 2 plates/mM dT). The plates were developed in $CHCl_3$-ethanol (12:1). The product was scraped from the plates (R_f 0.35 in above solvent) and eluted with $CHCl_3$-ethanol (1:1). The product was compared with a known sample of 5'-O-MMTrdT for purity. Typical yields were >90%.

ii. 3'-O-Benzoyl-5'-O-Monomethoxytrityldeoxythymidine (3'-O-Bz-5'-O-MMTrdT) (X) (B = Thy)[137]

Typically, one equivalent of 5'-O-MMTrdT was dried as described above and dissolved in dry pyridine (5 ml/mM 5'-O-MMTrdT). Next, 1.2 equivalents of benzoyl chloride were added dropwise with stirring and ice cooling over about ½ hour. When the reaction was complete, as determined by TLC (2-4 hours), the mixture was cooled with ice. Crushed ice was added to quench the reaction, and stirring continued for an additional 30 minutes. The pyridine was removed under reduced pressure, the residue dissolved in $CHCl_3$ and extracted with water. The $CHCl_3$ layer was concentrated and freed from residual pyridine before applying to TLC plates (2 plates/mM 5'-O-MMTrdT), and developed in $CHCl_3$-ethanol (15:1). The product was removed and eluted with $CHCl_3$-ethanol (1:1). Typical yields lay between 65 and 75%.

iii. 3'-O-Benzoyldeoxythymidine (3'-O-BzdT) (XI) (B = Thy)[137]

The product from above (X) was dissolved in 80% acetic acid and stirred overnight at room temperature or for 1 hour at 70° C. The acetic acid was removed in vacuo followed by co-distillation with toluene. The residue was suspended in diethyl ether, stirred for ½ hour, filtered, and suspended again. The product, 3'-O-BzdT, was obtained in >95% purity. The yields were ∿90%, with less than 3% product in the ether extract.

iv. 5'-O-Trityl-6-Methyl-2'-Deoxyuridine (5'-O-Trm^{6}dU) (IX) (B = m^6Ura)[73]

The procedure, reaction conditions, and work-up of this compound were identical to those described for (IX). Reaction times were

longer (∿18 hours) but the yields were similar (>90%). The sample was compared with the properties reported by George et al.[73].

v. 3'-O-Benzoyl-5'-O-Trityl-6-Methyl-2'-Deoxyuridine (3'-O-Bz-5'-O-Trm^{6}dU) (X) (B = m^{6}Ura)

The procedure, reaction conditions, and work-up of this compound were identical to those described for (X). Reaction times and yields were comparable.

vi. 3'-O-Benzoyl-6-Methyl-2'-Deoxyuridine (3'-O-Bzm^{6}dU) (XI) (B = m^{6}Ura)

The procedure, reaction conditions, and work-up of this compound were identical to those described for (XI). Reaction times and yields were comparable.

vii. 5'-dTMP or 5'-m^{6}dUMP

One equivalent of the 3'-O-benzoyl derivative of dT or m^{6}dU was dried by three co-evaporations with 5 ml portions of pyridine. Two equivalents of β-cyanoethylphosphate (pyridinium salt, a 0.8 mM/ml solution in pyridine) were added and dried an additional two times. The mixture was dissolved in dry pyridine (10 ml/mM nucleoside), and 4 equivalents of TPS were added. The reaction was stirred until complete (∿4 hours). The flask was cooled in ice, 10 g of crushed ice were added to quench the reaction, and the mixture was then stirred an additional ½ hour. The solvents were removed under reduced pressure, and the residue was dissolved in $CHCl_3$ and extracted with 3-5 ml portions of water. The $CHCl_3$ was removed, and the mixture was dissolved in 50:50 concentrated ammonia:pyridine and allowed to stir for 18 hours at room temperature. The solvents were then removed, and

the residue was dissolved in water (20 ml/mM nucleotide) and extracted with 3-10 ml portions of $CHCl_3$ to remove the non-nucleotidyl material. The aqueous solution was concentrated, applied to Whatmann 3MM sheets (9" x 22", 30 mg per sheet), developed in solvent F (55:35:10 - n-propanol - water - conc. NH_3), and the appropriate portion of the papers was eluted with water (R_f = 0.47). Samples were checked by electrophoresis (referenced against 3'-UMP) and by ^1H and ^{13}C NMR. Yields were ∿80%.

viii.3'-dTMP or 3'-m^6dUMP

The phosphorylation and work-up for these compounds were performed identically to the procedure for the 5'-nucleotides described above. The de-protection was performed in two steps. In the first step, the cyanoethanol group was removed, as outlined previously. The residue was dissolved in 80% acetic acid (20 ml/mM nucleotide) and stirred overnight for both the 5'-O-MMTr-3'-dTMP and the 5'-O-Tr-3'-m^6dUMP. The solvent was removed, and the residue was dissolved in water and extracted with 3-10 ml portions of diethylether. The aqueous solution was concentrated, applied to chromatography papers, and developed in solvent F (R_f^F = 0.45). Yields were ∿80%.

ix. 3',5'-dTDP or 3',5'-m^6dUDP

The unprotected deoxynucleosides were dried in an analogous manner to the protected nucleosides. The appropriate phosphorylating reagents were added (2 equivalents β-cyanoethylphosphate and 3 equivalents TPS for each hydroxyl), and the reaction mixture was allowed to stir for two days. The reaction was quenched with water,

the solvents were completely removed, and the residue was dissolved in water (50 ml/mM nucleoside diphosphate). The solution was extracted with 3-10 ml portions of $CHCl_3$, the water was removed, and the residue was dissolved in 50:50 conc. NH_3:pyridine (1:1, v/v) and stirred for 24 hours. The solvents were again removed. The residue was dissolved in water, applied to chromatography papers, and developed in solvent F. The product was eluted with water (R_f^F = 0.26) and lyophilized. The yield was ∿85%.

3. DINUCLEOSIDE MONOPHOSPHATE SYNTHESIS

The area of oligonucleotide synthesis encompasses a large branch of organic chemistry, as can be seen in the review by Amarnath and Broom[136]. Pioneering work by Khorana and others has resulted in the total synthesis of a gene. The advantage of applying polynucleotides of a known sequence to the study of life processes is obvious. In this work, only the coupling of two nucleosides by a phosphate group was performed. The procedures used, however, are the same for dinucleoside monophosphates and larger oligomers. The aforementioned review[136] is complete to September, 1975, and the interested reader is referred to this work. In the discussion that follows, only those aspects which are directly relevant to the present work will be covered.

a. DISCUSSION

The synthesis of dinucleoside monophosphates (referred to as dimers for the remainder of this section) is just an extension of the nucleotide synthesis described above. Essentially, an appropriately

blocked nucleotide is reacted with a protected nucleoside in the presence of a condensing agent. The procedure described in this section follows what is known as the triester approach (i.e., the nucleotide possesses a protecting group on the phosphate). In its current form, the method has advantages such as quicker reaction times, more efficient use of reagents, and ease in purification of the protected dimers from the reaction mixture[137-139]. The arylsulfonamide condensing reagents have been shown to be far superior to other condensing reagents used in nucleotide synthesis[138,139] (e.g., TPS has been the commonly used reagent to date).

Two general approaches have been used in the condensation of constituent nucleosides and nucleotides to resultant dimers. The type-1 condensation links a protected 5'-nucleotide to the free 3'-hydroxyl function of a protected nucleoside. In the type-2 condensation, the reverse is followed (i.e., a 3'-nucleotide is joined to the free 5'-hydroxyl function of the desired nucleoside). Figure 3.3 illustrates both these schemes. The former approach is mainly used in deoxypolynucleotide synthesis, while the latter method is used for the ribose series. In this work, both methods were used. The nature of the constituent nucleosidyl units in the product dimer determined the use of a type-1 or type-2 condensation. This was the preferred route as m^6dU is scarce relative to dT, the former being synthesized while the latter was commercially available. As an example, the synthesis of d(Tpm^{6}U) will be described, starting with the appropriately blocked nucleosides.

FIGURE 3.3 illustrates the difference between a type-1 and a type-2 condensation.

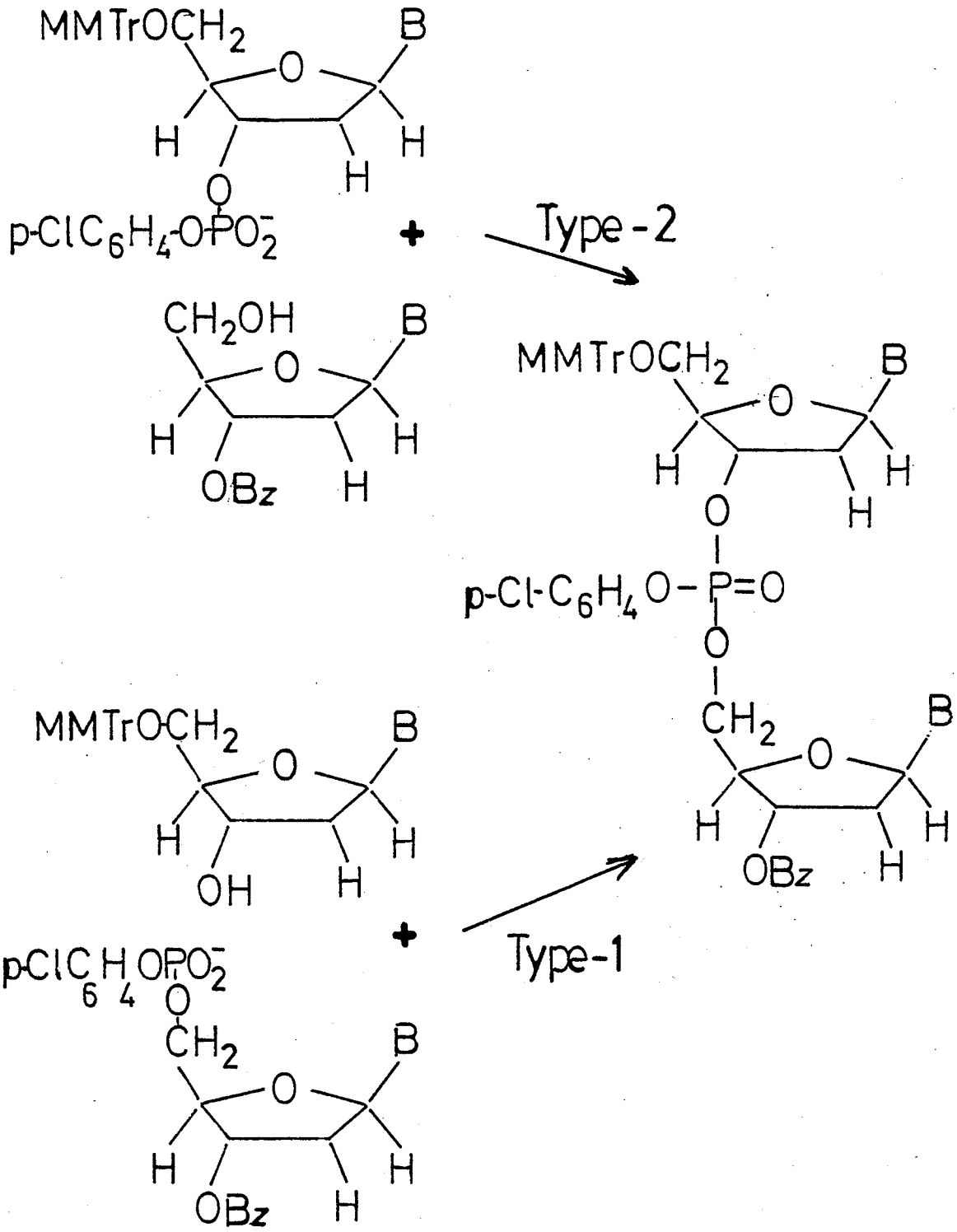
MMTrOCH2
B
O
H
H
H
p-ClC6H4-OPO2-
+
Type-2
CH2OH
B
O
H
H
OBz
H
MMTrOCH2
B
O
H
H
O
p-Cl-C6H4O-P=O
O
CH2
B
O
H
H
OBz
H
MMTrOCH2
B
O
H
H
OH
H
+
Type-1
p-ClC6H4OPO2-
O
CH2
B
O
H
H
OBz
H

Since the m^6dU unit will form the 5'-nucleotide in the product dimer, the 3'-O-benzoyl-2'-deoxy-6-methyluridine (3'-O-Bzm^6dU) is phosphorylated. This is accomplished by reacting 3'-O-Bzm^6dU with p-chlorophenylphosphate in dry pyridine in the presence of TPS. The reaction is allowed to go to completion (as determined by TLC). The reaction is then quenched, the TPS and pyridine hydrochloride are removed by extraction, and the substrate is dried in preparation for the condensation. Since this is a type-2 condensation, an excess of 5'-O-MMTrdT is added, dried once again, dissolved in pyridine, and the condensing reagent, 1-{2,4,6-trimethylbenzenesulfanoyl}tetrazole (1-Ms Tetrazole), is added. After about two hours, the reaction is quenched and the reagents are removed by extraction. The product is isolated on preparative TLC plates, developed in the appropriate solvents, and isolated. The base labile groups are first removed in 50:50 concentrated ammonia:pyridine followed by the removal of the acid labile group. The order of deprotection has been found to be important[140,141]. If the reverse sequence is used, unwanted side products of the dinucleoside monophosphate are formed, probably involving the free 5'-hydroxymethyl group of the 3'-nucleotidyl fragment[141]. Purification of the deprotected dimer is performed on papers in a suitable solvent.

For the other dimers, d(m^6UpT) uses a type-1 condensation, d(m^6Upm^6U) uses a type-2 condensation, and d(TpT) uses a type-1 condensation.

As noted in the previous section, there are slight differences in reactivity between the dT and m^6dU nucleosides towards phosphorylation and condensation. In the phosphorylation step, the 3'-protected m^6dU phosphorylates slower than the corresponding dT nucleoside, while no difference in phosphorylation rates is apparent for 3'-phosphorylation. Analogously, the condensation of a 5'-nucleotide proceeds 1.5 to 2 times slower for the m^6dU unit than the dT unit with, again, no difference noted for the 3'-nucleotides, except in the case of $d(m^6Upm^6U)$.

b. PROCEDURES

The procedures outlined in this section start with the protected nucleosides and nucleotides which are described above. The exact synthetic steps reported are those developed from adjusting experimental conditions to optimize the yields. Typically, the condensation yield for a given dimer increased from ∿20% at a first attempt to about 70 to 80% at the last two attempts.

The protected nucleosides used in this section follow from those synthesized in the previous section. In the condensations that follow, the appropriate nucleoside is first phosphorylated using p-chlorophenylphosphate instead of β-cyanoethylphosphate. The phosphorylation reaction is worked-up, as described above, except that the pyridine solvent is not removed prior to the extraction of the reagents.

i. 1-{2,4,6-Trimethylbenzenesulfonyl}Tetrazole, 1-Ms Tetrazole[138]

1.1 equivalents of triethylamine in ethylacetate (1 ml/mM tetrazole) were added dropwise over 40 minutes to a suspension of

mesitylenesulfonylchloride and 1-H tetrazole (Aldrich Chemical Company, Wisconsin, U.S.A.) in ethylacetate (20 ml/mM tetrazole) with ice cooling. The mixture was allowed to stir an additional two hours. The precipitated amine hydrochloride was filtered, and the ethylacetate was removed under reduced pressure with no heating. The crystalline residue was dissolved in $CHCl_3$ (1 ml/mM tetrazole) and washed with water (2 x 0.2 ml/mM tetrazole). The $CHCl_3$ layer was dried by stirring over Na_2SO_4 for two hours. The $CHCl_3$ was then filtered and the Na_2SO_4 washed with a little ethylacetate. The solvents were removed, again with no heating, and the flask was placed on the vacuum pump for about 5 to 10 minutes. The product, 1-Ms tetrazole, was used without further purification.

ii. Condensation of 5'-O-MMTrdT With 3'-O-Bz-5'-p-Chlorophenyl-5'-m^6dUMP

Typically, 1 equivalent of 3'-O-Bzm^6dUMP was phosphorylated with 2 equivalents of p-chlorophenylphosphate and worked-up as described above (except for the removal of the solvent) until after the extraction. The residual pyridine was removed under vacuum, and the residue was dried again three times with dry pyridine. The nucleoside 5'-O-MMTrdT (1.5 equivalents) was added, and two more co-evaporations with pyridine were performed. The mixture was dissolved in pyridine (15 ml/mM) and 3 equivalents of 1-Ms tetrazole were added with stirring. After 1 hour, the reaction was checked via TLC and monitored every 30 minutes until no further reduction of the starting nucleotide was detected. The reaction was quenched by the addition of ice with

stirring for 30 minutes. The mixture was dissolved in $CHCl_3$ and washed with three 20 ml portions of triethylamine·H_2CO_3 buffer (pH = 7.6) and two 20 ml portions of water. The mixture was concentrated, and the product was isolated using preparative TLC (2 plates/.5 mM) in $CHCl_3$-ethanol (15:1) and eluted with $CHCl_3$-ethanol (1:1) (R_f = 0.24). Typical yields were 70 to 85%.

iii. Condensation of 5'-O-Tr-3'-p-Chlorophenyl-3'-m^6dUMP With 3'-O-BzdT

The condensation was performed as described above. One equivalent of 5'-O-Trm^{6}dU was phosphorylated, condensed with 1.5 equivalents of 3'-O-BzdT, worked-up, and separated on TLC plates in $CHCl_3$-ethanol (15:1) (R_f = 0.24). Typical yields were 75 to 85%.

iv. Condensation of 3'-O-Bz-5'-p-Chlorophenyl-5'-m^6dUMP With 5'-O-Trm^{6}dU

One equivalent of 3'-O-Bzm^{6}dU was phosphorylated and condensed with 1.5 equivalents of 5'-O-Trm^{6}dU. The reaction was worked-up and the product separated in $CHCl_3$-ethanol (15:1) (R_f = 0.24). Typical yields were 50 to 65%.

v. Condensation of 3'-O-Bz-5'-p-Chlorophenyl-5'-dTMP With 5'-O-MMTrdT

One equivalent of 3'-O-BzdT was phosphorylated and condensed with 1.5 equivalents of 5'-O-MMTrdT. The reaction was worked-up and the product separated in $CHCl_3$-ethanol (15:1) (R_f = 0.25). The yield was 92%.

vi. Deprotection of Product Dinucleoside Monophosphates

The procedure for deprotection was identical for all four molecules. The base labile groups were removed first in order to prevent side

reaction at the free 5'-hydroxyl[140,141]. The acid labile group was then removed.

vii. Base Hydrolysis of the p-Chlorophenyl- and 3'-O-Benzyl Groups

The product, dinucleoside monophosphate, was dissolved in 50:50 concentrated ammonia:pyridine and stirred at room temperature until the reaction was completed (18 to 24 hours). The solvents were removed under reduced pressure and the residue was used directly for the acid hydrolysis.

viii.Acid Hydrolysis of the MMTrityl and Trityl Groups

The residue from the base hydrolysis was dissolved in 80% acetic acid and stirred until the reaction was completed. The solvents were removed, and the residue was dissolved in 10 ml water. The solution was extracted with three 10 ml portions of diethyl ether. The water solution was concentrated, and the resulting liquid was applied to chromatography paper and developed in solvent A (70:10:20 isopropanol: concentrated ammonia:water). The four dimers have near identical R_f^A values in solvent A: d(TpT), $R_f^A = 0.28$; d(Tpm^{6}U), $R_f^A = 0.25$; d(m^{6}UpT), $R_f^A = 0.28$; d(m^{6}Upm^{6}U), $R_f^A = 0.28$.

4. PHOTODIMER SYNTHESIS

The in-vitro synthesis of the d(TpT) internal cyclobutane type photodimer (The proposed structural formula is shown in Figure 3.4, and this molecule will hereafter be symbolized by d(T(p)T).) follows the procedure outlined by Liu and Yang[142]. Their method of performing a photosensitized reaction of d(TpT) in the presence of acetophenone

FIGURE 3.4 contains the proposed structure of the internal cyclobutane type photodimer of d(TpT).

d(T[p]T)

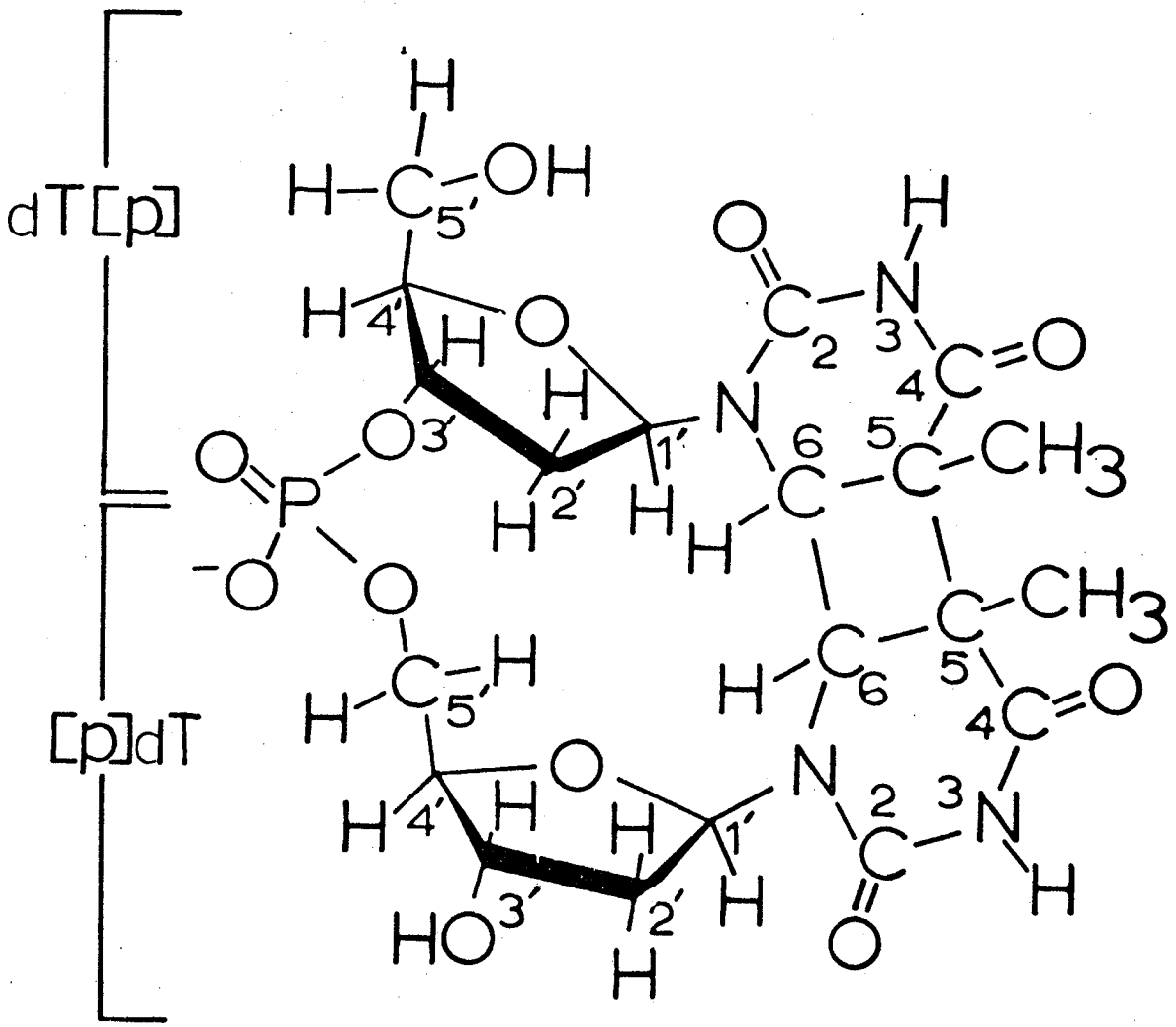

was used due to the reduced reaction time and because it yielded the same products in the same ratios as the previously reported direct irradiation[143]. The procedures are exactly the same as those reported[142], except that the products were isolated by paper chromatography[144] rather than by TLC[142].

B. NMR METHOD

1. SAMPLES

All samples of nucleotides, nucleoside diphosphates, and dinucleoside monophosphates were treated for the removal of paramagnetic metal ions according to the procedure of Cozzone and Jardetzky[60,61]. Typically, a solution of the respective molecule in 2 ml deionized and distilled water was passed through a Chelex 100 disposable column (Biorad Laboratories (Canada) Ltd., Ontario). The solution was adjusted to pH = 6.5 and extracted three times with 0.1% dithiazone (BDH Chemicals Ltd., England) in spectrograde CCl_4 and once with pure CCl_4. The sample was lyophilized and dissolved in 1.0 ml metal ion free D_2O (Aldrich Chemical Company, Wisconsin, U.S.A.). In the case of nucleoside diphosphates, a small amount (total concentration 2.0 mM) of EDTA was added to provide for the additional removal of the effect of the paramagnetic impurities from the spectrum. All ^{31}P spectra were recorded with the addition of EDTA. All glassware, teflon vortex plugs, NMR tubes, sample vials, and glass syringes were soaked for at least 24 hours in 10 mM EDTA @ pH $\simeq$ 9 and rinsed with distilled and triply deionized water. Sample concentrations and temperatures were as noted in the tables in the next chapter. The pH adjustments for the titration data were made using dilute solutions ($\sim$.5 M) of NaOD and DCl (Merck, Sharpe, and Dome, Quebec, Canada). pH measurements were made on a Beckman Expandomatic Model SS-2 pH meter (Beckman Instruments, Ltd., Ontario, Canada) at 25^{o} C using a Beckman combination

standard glass electrode and calibrated with standard buffers at pH = 4.01, 7.00, and 9.18, depending on the pH range desired. Probe temperatures reported in the next chapter are accurate to better than $\pm 1^{o}$ as determined by calibrating against a standard iron-constantan thermocouple.

2. SPECTRA

a. ^{1}H NMR SPECTRA

Proton spectra were recorded on a Nicolet NT-360 Fourier transform spectrometer (Nicolet Technology Corporation, Mountain View, California, U.S.A.) using an Oxford Instrument superconducting solenoid operating at 8.4555 T at the Purdue Biological Magnetic Resonance Lab (Purdue University, West Lafayette, Indiana). The proton frequency was 360.061 MHz. Spectral widths were typically 2400 Hz, acquired with quadrature detection into 32 K of data memory. The free induction decay (FID) was apodized by exponential multiplication using a line broadening equal to the digital resolution (ca 0.15 Hz). Frequencies were referenced to internal TSP.

b. ^{13}C NMR SPECTRA

All carbon spectra were recorded on a Bruker WH-90 DS spectrometer at the University of Manitoba operating at 22.628 MHz for ^{13}C at a magnetic field strength of 2.114 T. The spectrometer is interfaced with a Nicolet 1180 computer and Nicolet 293 A pulse programmer (Nicolet Instruments Corporation, Madison, Wisconsin, U.S.A.) operating with the NTCFT-1180 software package (Nicolet Technology Corporation,

Mountain View, California, U.S.A.). Spectral widths were typically 3800 Hz, acquired with quadrature detection and under conditions of broad-band proton decoupling (where appropriate) into 16 K data points and zero filled to 32 K data points. FID's were apodized by exponential multiplication with a line broadening equal to the digital resolution (ca 0.2 Hz). Proton coupled spectra were recorded using the gated decoupled sequence in which the decoupler is gated off during the acquisition and on during the pre-acquisition delay[145-147]. Chemical shifts are reported relative to external tetramethylsilane (TMS) by assigning the internal dioxane peak (∿1%) a shift of 67.859 ppm.

T_1 measurements were made using the inversion recovery pulse sequence $(180^{\circ}-\tau-90^{\circ}-AT-D)_n$ with alternating phases of the 180° and 90° pulses (26 μsec and 13 μsec, respectively). The phase alternation is used to eliminate errors due to small imperfections in the pulse width (i.e., not exactly 180° or 90°) or pulse homogenity[146-148]. The delay between the pulse cycle (AT + D) was set to at least five times the longest T_1 of the sample. T_1's were obtained from the inversion recovery spectra using the least squares analysis of Levy and Peat[149] or Sass and Ziessow[150].

c. ^{31}P NMR SPECTRA

All phosphorus spectra were recorded on the same Bruker WH-90DS spectrometer described above operating at 36.44 MHz. Spectral widths were typically 1000 Hz, acquired with quadrature phase detection into

8 K data points and apodized as above with a line broadening of 0.5 Hz. Chemical shifts are reported relative to external 85% H_3PO_4. All samples were approximately 2 mM in EDTA.

CHAPTER IV

DATA AND RESULTS

A. ^{1}H NMR DATA

Tables 4.1 to 4.8 contain the chemical shift and spin-spin coupling constants for two nucleoside diphosphates and four dinucleoside monophosphates. The proton NMR data for the dT nucleoside and mononucleotides[29,77a] and the m^6dU nucleoside and mononucleotides[73] have been reported in the literature. The ^{1}H NMR spectrum of dinucleoside monophosphate d(TpT) has been re-analyzed because of the tightly coupled nature of the spin system in the original analysis. The assignment of the various resonances in the spectra of the dinucleoside monophosphates is straightforward at 360 MHz[28,38], and the molecule d(m^6UpT) will be used as an example.

Typically, a full spectrum is recorded of a given molecule at ambient temperature. In the case of the thymine or 6-methyluracil bases, the assignment of the shifts for H_6 (of thymine), H_5 (of 6-methyluracil) and the methyl groups follows directly from the nucleosides. In the case of the ribose protons, nuclei from various parts of the molecule resonate in definite portions of the spectrum[6,100]. For example, in pyrimidine deoxyribose nucleotidyl units in dinucleoside monophosphates, the $H_{1'}$ protons appear between 6.34 ppm and 6.05 ppm from internal TSP. The $H_{2'}$ and $H_{2''}$ protons of dT are found in the narrow range of 2.23 ppm to 2.61 ppm, while in m^6dU the $H_{2'}$ proton is shifted downfield to $\sim$2.95 ppm and the $H_{2''}$ remains in the aforementioned range for dT. The $H_{3'}$ protons resonate between 4.53 ppm and 4.85 ppm with $H_{3'}$ peaks from the 3'-nucleotidyl unit occurring at lower field than the corresponding resonance of the 5'-nucleotidyl

unit. The two $H_{4'}$ and four exocyclic protons ($H_{5'}$'s and $H_{5''}$'s) are spread between 3.73 ppm and 4.22 ppm with those from the 3'-nucleotide end at higher field (typically) than the other sets of resonances.

Ambiguities in the assignment of a given resonance to a given deoxy-sugar can be resolved with the aid of spin decoupling experiments[28,38]. Figures 4.1 and 4.2 show the $H_{3'}$, $H_{4'}$, $H_{5'}$, $H_{5''}$ and the $H_{2'}$, $H_{2''}$ regions respectively of d(m^6UpT) at 333 K. Figures 4.1a and 4.2a show the unperturbed spectrum, while 4.1b, 4.2b and 4.1c, 4.2c show the effect of decoupling the lowfield $H_{3'}$ (from the m^6dUp- unit) and highfield $H_{3'}$ (from the -pdT unit), respectively. These spectra clearly locate the resonances coupled to the irradiated nuclei (i.e., $H_{2'}$, $H_{2''}$, and $H_{4'}$) for each part of the molecule. One of the $H_{2'}$ multiplets can be irradiated, in turn, to assign the $H_{1'}$ multiplets (as was done in the case of d(TpT) and d(m^6Upm^{6}U)). This procedure also helps to sort out the magnitudes by which $H_{1'}$ and $H_{3'}$ couple to $H_{2'}$ and $H_{2''}$ in the m^6dU moieties. All proton spectra of dinucleoside monophosphates analyzed in this work were assigned using this technique. The differentiation between $H_{2'}$ and $H_{2''}$ and between $H_{5'}$ and $H_{5''}$ follows the arguments presented in the literature for these nuclei. Unless otherwise stated, those assignments will be used here[29,73,103].

Proton spectral parameters reported in the next eight tables were obtained by computer simulation of each nucleotidyl unit separately, using the program LAME 8 [151,152]. The calculated transitions were then iteratively fit to the observed frequencies, where possible, using the same program. The standard deviations quoted in the tables are those

FIGURE 4.1 illustrates the proton spin-decoupling experiments performed on d(m^6UpT) at 333 K. a) is the unperturbed region showing the two H_3, protons, the two H_4, protons, and the four exocyclic H_5, protons. b) shows the effect of irradiating the highfield H_3, resonance from -pdT. The arrow indicates the location of the coupled H_4,. c) shows the effect of irradiating the lowfield H_3, resonance from m^6dUp-. The arrow indicates the location of the coupled H_4,.

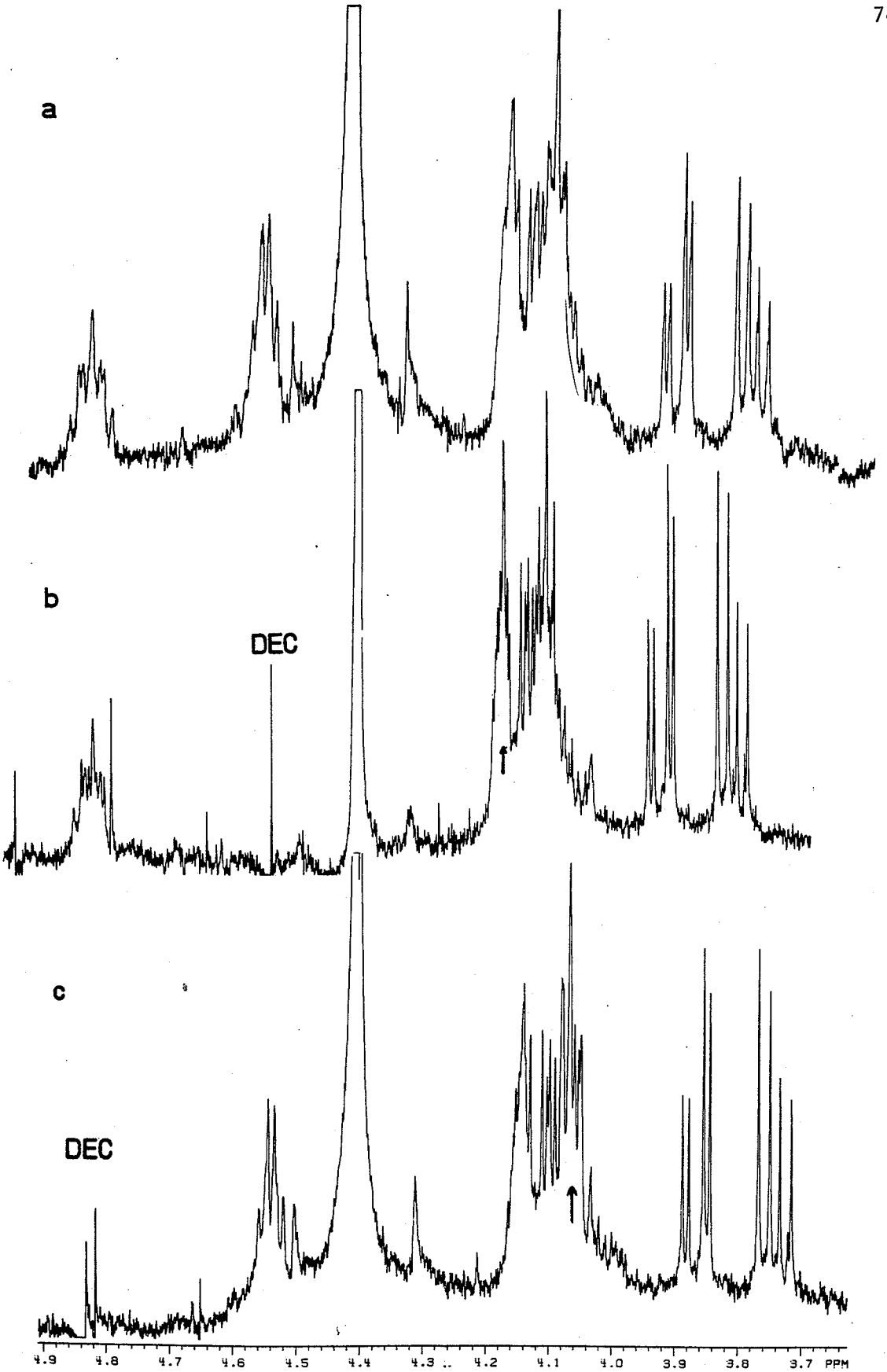
a
b
DEC
f
c
DEC
4.9
4.8
4.7
4.6
4.5
4.4
4.3
4.2
4.1
4.0
3.9
3.8
3.7
PPM

FIGURE 4.2 is a continuation of the proton spin-decoupling experiments performed on d(m^6UpT) at 333 K. a) is the unperturbed region showing the two $H_{2'}$ and the two $H_{2''}$ resonances of d(m^6UpT). b) shows the effect of irradiating the highfield $H_{3'}$ resonance in Figure 4.1b from -pdT. The arrow indicates the coupled $H_{2'}$ and $H_{2''}$ signals. c) shows the effect of irradiating the lowfield $H_{3'}$ resonance in Figure 4.1c from m^6dUp-. The arrows indicate the coupled $H_{2'}$ and $H_{2''}$ signals.


a
b
c
3.0
2.9
2.8
2.7
2.6
2.5
2.4
2.3
2.2
2.1
2.0
1.9
1.8
PP

calculated by the program. A reliable estimate of the error in the parameters is the digital resolution of the spectra (ca 0.12 Hz). In some cases, extensive overlap of resonances resulted in too few observed frequencies relative to the number of calculated transitions. In these cases, the spectrum was simulated (using SPECSIM on the Nicolet 1180) and the parameters were changed until the experimental and calculated spectra agreed. Here the reported errors are the amount by which a given parameter can be changed without affecting the appearance of the spectrum.

The calculated spectra, shown in the representative spectra in Figures 4.3 to 4.6 to follow, were obtained by using the final parameters from the iterative analysis or simulation to generate the theoretical spectrum of the nucleotidyl unit using SPECSIM. The two halves were then added together, using the software available on the spectrometer and were plotted using the spectrometer's digital plotter. Line widths used in the simulated spectra are typically 1.0 to 1.2 Hz, depending on the sample.

TABLE 4.1

PROTON CHEMICAL SHIFTS (ν) AND COUPLING CONSTANTS (J) FOR 3',5'-dTDP [a] AT 293 K

pH = 4.5 [b]			pH = 7.30 [b]		
		Std. Dev.[c]			Std. Dev.[c]
ν(1')	2305.393	0.014	ν(1')	2299.855	0.022
ν(2')	870.755	0.014	ν(2')	865.084	0.023
ν(2")	915.905	0.014	ν(2")	900.879	0.024
ν(3')	1761.813	0.019	ν(3')	1719.290	0.026
ν(4') [d]	1575.837	0.039	ν(4') [f]	1551.72	±0.5
ν(5') [d,e]	1482.32	0.051	ν(5') [f]	1443.04	±0.5
ν(5") [d,e]			ν(5") [f]		
ν(6)	2808.31	±0.1	ν(6)	2829.20	±0.1
ν(CH_3)	696.97	±0.1	ν(CH_3)	698.52	±0.1
J(6-CH_3)	1.2	±0.1	J(6-CH_3)	1.05	±0.1
J(1'-2')	8.172	0.020	J(1'-2')	8.193	0.032
J(1'-2")	6.023	0.020	J(1'-2")	6.079	0.032
J(2'-2")	-14.148	0.019	J(2'-2")	-13.926	0.031
J(2'-3')	6.103	0.023	J(2'-3')	5.918	0.034
J(2"-3')	2.305	0.028	J(2"-3')	2.444	0.035
J(3'-4')	2.392 (2.344) [d]	0.047	J(3'-4')	2.437	0.052
J(4'-5') [d]	2.885	0.063	J(4'-5') [f]	2.8	(±0.5)
J(4'-5") [d]			J(4'-5") [f]		
J(5'-5") [d,e]	———	———	J(5'-5") [e]	———	———
J(3'-P3')	7.910	0.038	J(3'-P3')	8.264	0.049
J(4'-P5') [d]	2.372	0.084	J(4'-P5')	1.0	(±0.5)
J(5'-P5') [d]	4.570	0.103	J(5'-P5') [f]	4.0	(±0.5)
J(5"-P5') [d]			J(5"-P5') [f]		
RMS Error[c]	0.0726 (0.1928) [d]				0.1148
Largest Error[c]	0.151 (0.278) [d]				0.344

FOOTNOTES FOR TABLE 4.1

a) Unless otherwise stated, chemical shifts and coupling constants are in Hz, at 360.061 MHz, as obtained from the iterative analysis. Sample was 4 mgs 3',5'-dTDP in 1 ml D_2O. Chemical shifts are downfield from internal TSP.

b) pH is the meter reading (uncorrected) for the deuterium isotope effect.

c) These parameters are obtained from the output of LAME 8. Estimated accuracy is $\pm$0.12 Hz unless otherwise indicated.

d) Obtained from a separate analysis.

e) $H_{5'}$ and $H_{5''}$ are assumed equivalent. The spectrum is independent of the value of J(5'-5") in this case.

f) These resonances were too broad to assign at this pH. The chemical shifts are the estimated centers of the bands while the coupling constants were derived from the line spacings.

TABLE 4.2

PROTON CHEMICAL SHIFTS (ν) AND COUPLING CONSTANTS (J)

FOR 3',5'-m^6dUDP[a] AT 293 K

	pH = 3.67[b]			pH = 7.45[b]	
		Std. Dev.[c]			Std. Dev.[c]
ν(1')	2255.851	0.020	ν(1')	2251.098	0.018
ν(2')	1093.193	0.018	ν(2')	1083.648	0.018
ν(2")	891.693	0.016	ν(2")	877.163	0.036
ν(3')	——— [d]	———	ν(3')	——— [d]	———
ν(4')	1505.953	0.015	ν(4')	1487.183	0.019
ν(5')	1510.864	0.014	ν(5')	1484.680	0.016
ν(5")	1457.881	0.013	ν(5")	1426.301	0.017
ν(5)	2060.15	±0.1 [e]	ν(5)	2058.90	±0.1 [e]
ν(CH_3)	865.89	±0.1 [e]	ν(CH_3)	869.38	±0.1 [e]
J(5-CH_3)	0.81	±0.1 [e]	J(5-CH_3)	0.83	±0.1 [e]
J(1'-2')	4.948	0.027	J(1'-2')	5.383	0.031
J(1'-2")	8.738	0.025	J(1'-2")	8.531	0.034
J(2'-2")	-14.061	0.024	J(2'-2")	-13.791	0.035
J(2'-3')	8.373	0.035	J(2'-3')	8.317	0.035
J(2"-3')	5.558	0.032	J(2"-3')	5.630	0.063
J(3'-4')	6.140	0.026	J(3'-4')	5.675	0.037
J(4'-5')	3.429	0.016	J(4'-5')	3.285	0.026
J(4'-5")	7.504	0.023	J(4'-5")	7.903	0.030
J(5'-5")	-11.436	0.020	J(5'-5")	-11.584	0.025
J(3'-P3')	7.9	±0.1 [f]	J(3'-P3')	9.8	±0.5 [f]
J(4'-P5')	≈0.0	—— [g]	J(4'-P5')	≈0.0	—— [g]
J(5'-P5')	6.259	0.022	J(5'-P5')	5.760	0.031
J(5"-P5')	6.302	0.027	J(5"-P5')	5.683	0.034
RMS Error [c]		0.0882			0.0952
Largest Error[c]		0.191			0.238

FOOTNOTES FOR TABLE 4.2

a) Unless otherwise stated, chemical shifts and coupling constants are in Hz, at 360.061 MHz, as obtained from the iterative analysis. Sample was 4 mgs 3',5'-m^6dUDP in 1 ml D_2O. Chemical shifts are downfield from internal TSP.

b) pH is the meter reading (uncorrected) for the deuterium isotope effect.

c) These parameters are obtained from the output of LAME 8. Estimated accuracy is $\pm$0.12 Hz unless otherwise indicated.

d) This resonance was not observed.

e) These parameters were not obtained from an iterative analysis but were derived directly from the line positions in the spectrum.

f) This parameter was obtained from the ^{31}P spectrum.

g) The simulated spectrum is sensitive to this value, and any value of J(4'-P5') larger than 0.2 Hz produced noticeable splittings which were not observed.

FIGURE 4.3 shows the observed and calculated transitions for the $H_{4'}$, $H_{5'}$, and $H_{5''}$ protons of 3',5'-m^6dUDP at 293 and pH = 7.45. The sample is 4 mgs in 1 ml D_2O. Chemical shifts are in ppm downfield from internal TSP.

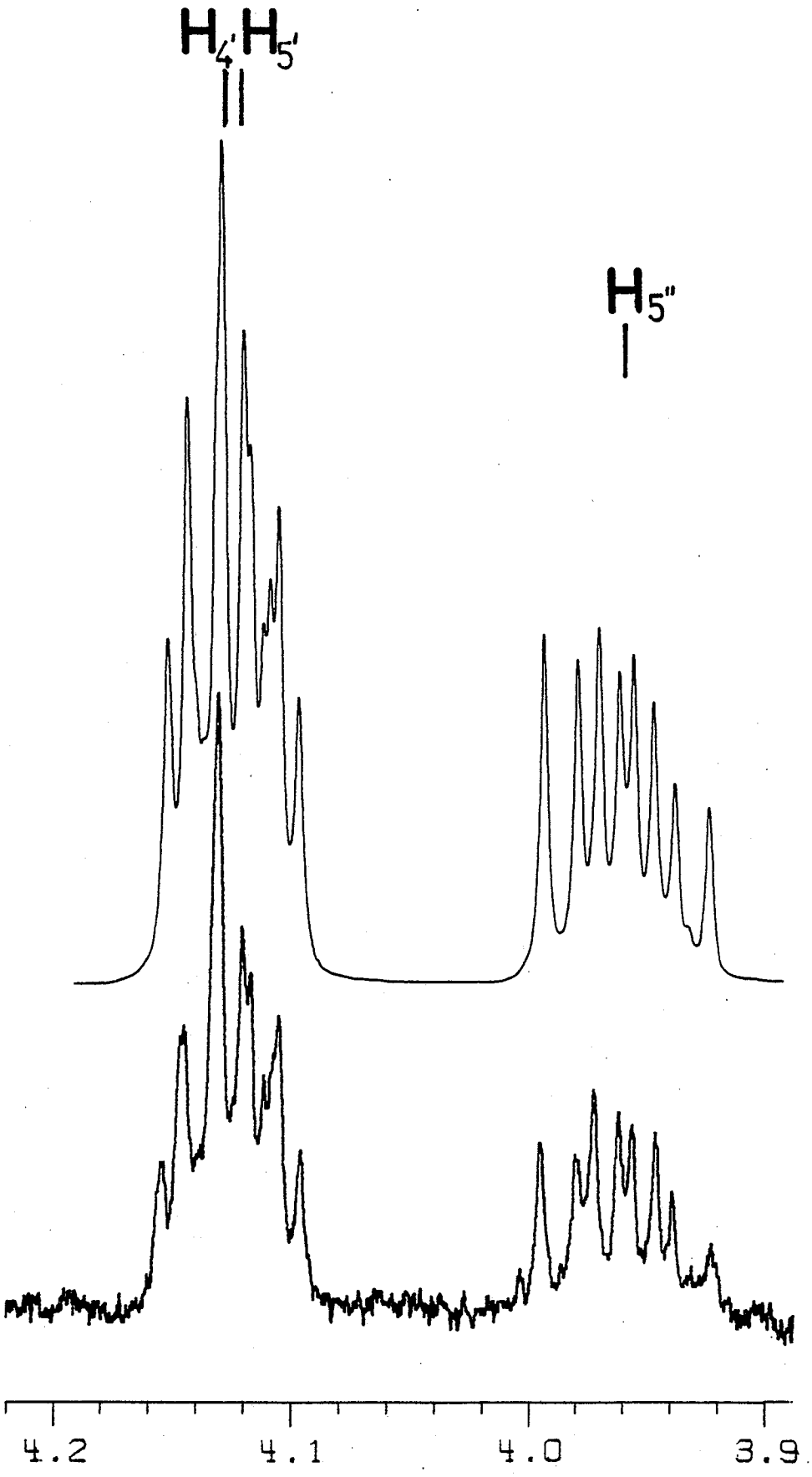
H4' H5'
H5"
4.2
4.1
4.0
3.9

TABLE 4.3

PROTON CHEMICAL SHIFTS (ν) AND COUPLING CONSTANTS (J) FOR d(TpT)[a] AT 293 K

dTp- PART			-pdT PART		
		Std. Dev.[b]			Std. Dev.[b]
ν(1')	2228.206	0.031	ν(1')	2268.550	0.017
ν(2')	839.468	0.025	ν(2')[c]	882.315	———
ν(2")	915.062	0.025	ν(2")	880.315	———
ν(3')	1709.574	0.019	ν(3')	1646.879	0.027
ν(4')	1498.977	0.023	ν(4')	1478.490	0.025
ν(5')	1370.803	0.038	ν(5')	1487.207	0.023
ν(5")	1353.583	0.038	ν(5")	1461.402	0.024
ν(5)[d]	2759.92	±0.1	ν(5)[d]	2752.40	±0.1
$\nu(CH_3)$[d]	672.81	±0.1	$\nu(CH_3)$[d]	669.55	±0.1
$J(5\text{-}CH_3)$[d]	1.1	±0.1	$J(5\text{-}CH_3)$[d]	1.1	±0.1
J(1'-2')	6.926	0.036	J(1'-2')[e]	6.870	0.063
J(1'-2")	6.468	0.036	J(1'-2")	6.870	0.063
J(2'-2")	-14.096	0.031	J(2'-2")[f]	-12.1	———
J(2'-3')	7.034	0.029	J(2'-3')[e]	5.515	0.058
J(2"-3')	3.771	0.031	J(2"-3')	5.515	0.058
J(3'-4')	3.489	0.036	J(3'-4')	3.468	0.038
J(4'-5')	3.661	0.045	J(4'-5')	2.341	0.032
J(4'-5")	4.194	0.047	J(4'-5")	3.714	0.037
J(5'-5")	-12.554	0.045	J(5'-5")	-11.931	0.037
J(3'-P)	6.307	0.043	J(4'-P)	1.493	0.045
			J(5'-P)	4.148	0.036
			J(5"-P)	3.643	0.031
RMS Error[b]		0.1965			0.1151
Largest Error[b]		0.317			0.279

FOOTNOTES FOR TABLE 4.3

a) Unless otherwise stated, chemical shifts and coupling constants are in Hz, at 360.061 MHz, as obtained from the iterative analysis. Sample was 4 mgs d(TpT) in 1 ml D_2O. Chemical shifts are downfield from internal TSP.

b) These parameters are obtained from the output of LAME 8. Estimated accuracy is $\pm$0.12 Hz unless otherwise indicated.

c) $H_{2'}$ and $H_{2''}$ of the -pdT part of the molecule are near equivalent. The chemical shift difference is arbitrary.

d) These parameters were not obtained from an iterative analysis but were derived directly from the line positions in the spectrum.

e) The observed couplings to $H_{1'}$ and $H_{3'}$ are the averages of the actual couplings, i.e., $^{OBS}J(1'-2) = (J(1'-2') + J(1'-2''))/2$..

f) For near equivalence of $H_{2'}$ and $H_{2''}$, the spectrum is independent of J(2'-2'').

TABLE 4.4

PROTON CHEMICAL SHIFTS (ν) AND COUPLING CONSTANTS (J) FOR d(Tpm^{6}U) [a] AT 293 K

dTp- PART			-pm^{6}dU PART		
		Std. Dev.[b]			Std. Dev.[b]
ν(1')	2250.507	0.020	ν(1')	2228.496	0.015
ν(2')	801.941	0.020	ν(2')	1063.531	0.012
ν(2")	869.945	0.019	ν(2")	832.178	0.016
ν(3')	1714.127	0.055	ν(3')	1634.624	0.010
ν(4')	1487.138	0.034	ν(4')	1447.986	0.012
ν(5')	1381.620	0.029	ν(5')	1485.647	0.012
ν(5")	1354.584	0.029	ν(5")	1433.564	0.014
ν(6) [c]	2720.23	±0.1	ν(5) [c]	2002.10	±0.1
ν(CH_3) [c]	681.70	±0.1	ν(CH_3) [c]	846.04	±0.1
J(6-CH_3) [c]	1.19	±0.1	J(6-CH_3) [c]	0.74	±0.1
J(1'-2')	6.967	0.028	J(1'-2')	3.673	0.019
J(1'-2")	6.828	0.028	J(1'-2")	9.200	0.023
J(2'-2")	-14.163	0.027	J(2'-2")	-14.000	0.020
J(2'-3')	7.108	0.038	J(2'-3')	9.015	0.016
J(2"-3')	3.619	0.038	J(2"-3')	6.786	0.018
J(3'-4')	4.210	0.066	J(3'-4')	7.051	0.015
J(4'-5')	2.815	0.043	J(4'-5')	2.560	0.021
J(4'-5")	4.563	0.044	J(4'-5")	8.329	0.013
J(5'-5")	-12.620	0.038	J(5'-5")	-10.879	0.021
J(3'-P)	7.627	0.095	J(4'-P) [d]	∼0	———
			J(5'-P)	3.419	0.021
			J(5"-P)	5.619	0.022
RMS Error [b]		0.1007			0.0716
Largest Error [b]		0.193			0.237

FOOTNOTES FOR TABLE 4.4

a) Unless otherwise stated, chemical shifts and coupling constants are in Hz, at 360.061 MHz, as obtained from the iterative analysis. Sample was 4 mgs d(Tpm^{6}U) in 1 ml D_2O. Chemical shifts are downfield from internal TSP.

b) These parameters are obtained from the output of LAME 8. Estimated accuracy is $\pm$0.12 Hz unless otherwise indicated.

c) These parameters were not obtained from an iterative analysis but were derived directly from the line positions in the spectrum.

d) The simulated spectrum is sensitive to this value, and any value of J(4'-P5') larger than 0.2 Hz produced noticeable splittings which were not observed.

TABLE 4.5

PROTON CHEMICAL SHIFTS (ν) AND COUPLING CONSTANTS (J)

FOR d(Tpm^{6}U) [a] AT 333 K

dTp- PART			-pm^{6}dU PART		
		Std. Dev.[b]			Std. Dev.[b]
ν(1')	2249.262	0.023	ν(1')	2231.377	0.042
ν(2')	835.334	0.019	ν(2')	1053.252	0.034
ν(2")	891.543	0.022	ν(2")	834.766	0.031
ν(3')	1721.282	0.016	ν(3')	1646.494	0.034
ν(4')	1500.091	0.031	ν(4')	1455.824	0.025
ν(5')	1388.130	0.029	ν(5')	1494.468	0.025
ν(5")	1361.845	0.030	ν(5")	1451.198	0.028
ν(6) [c]	2722.06	±0.5	ν(5) [c]	2026.42	±0.5
ν(CH_3) [c]	683.76	±0.5	ν(CH_3) [c]	852.26	±0.5
J(6-CH_3) [c]	1.0	±0.2	J(5-CH_3) [c]	<0.5	
J(1'-2')	7.115	0.032	J(1'-3')	4.328	0.050
J(1'-2")	6.826	0.029	J(1'-2")	8.385	0.050
J(2'-2")	-14.236	0.029	J(2'-2")	-14.145	0.046
J(2'-3')	7.262	0.029	J(2'-3')	8.718	0.048
J(2"-3')	3.740	0.027	J(2"-3')	6.209	0.046
J(3'-4')	3.635	0.032	J(3'-4') [d]	6.50	±0.2
J(4'-5')	3.347	0.057	J(4'-5') [d]	3.0	±0.2
J(4'-5")	4.679	0.057	J(4'-5") [d]	8.0	±0.2
J(5'-5")	-12.571	0.038	J(5'-5") [d]	-10.70	±0.2
J(3'-P)	7.049	0.035	J(4'-P) [d]	∿0	
			J(5'-P) [d]	4.80	±0.2
			J(5"-P) [d]	6.0	±0.2
RMS Error[b]		0.0998			0.1191
Largest Error[b]		0.312			0.277

FOOTNOTES FOR TABLE 4.5

a) Unless otherwise stated, chemical shifts and coupling constants are in Hz, at 360.061 MHz, as obtained from the iterative analysis. Sample was 4 mgs d(Tpm^{6}U) in 1 ml D_2O. Chemical shifts are downfield from internal TSP.

b) These parameters are obtained from the output of LAME 8. Estimated accuracy is $\pm$0.12 Hz unless otherwise indicated.

c) These parameters were not obtained from an iterative analysis but were derived directly from the line positions in the spectrum.

d) The extensive overlap of $H_{4'}$ and $H_{5''}$ from the -pm^{6}dU part of the molecule resulted in fewer observed transitions than were calculated. The spectrum was simulated until it reproduced the experimental region. The quoted errors are the amounts by which the parameters can be changed before the simulated and experimental spectrum no longer agree.

FIGURE 4.4 shows the observed and calculated proton spectrum of d(Tpm^{6}U) at 333 K and pH = 5.9. The sample is 4 mgs d(Tpm^{6}U) in 1 ml D_2O. Shifts are in ppm downfield from internal TSP.

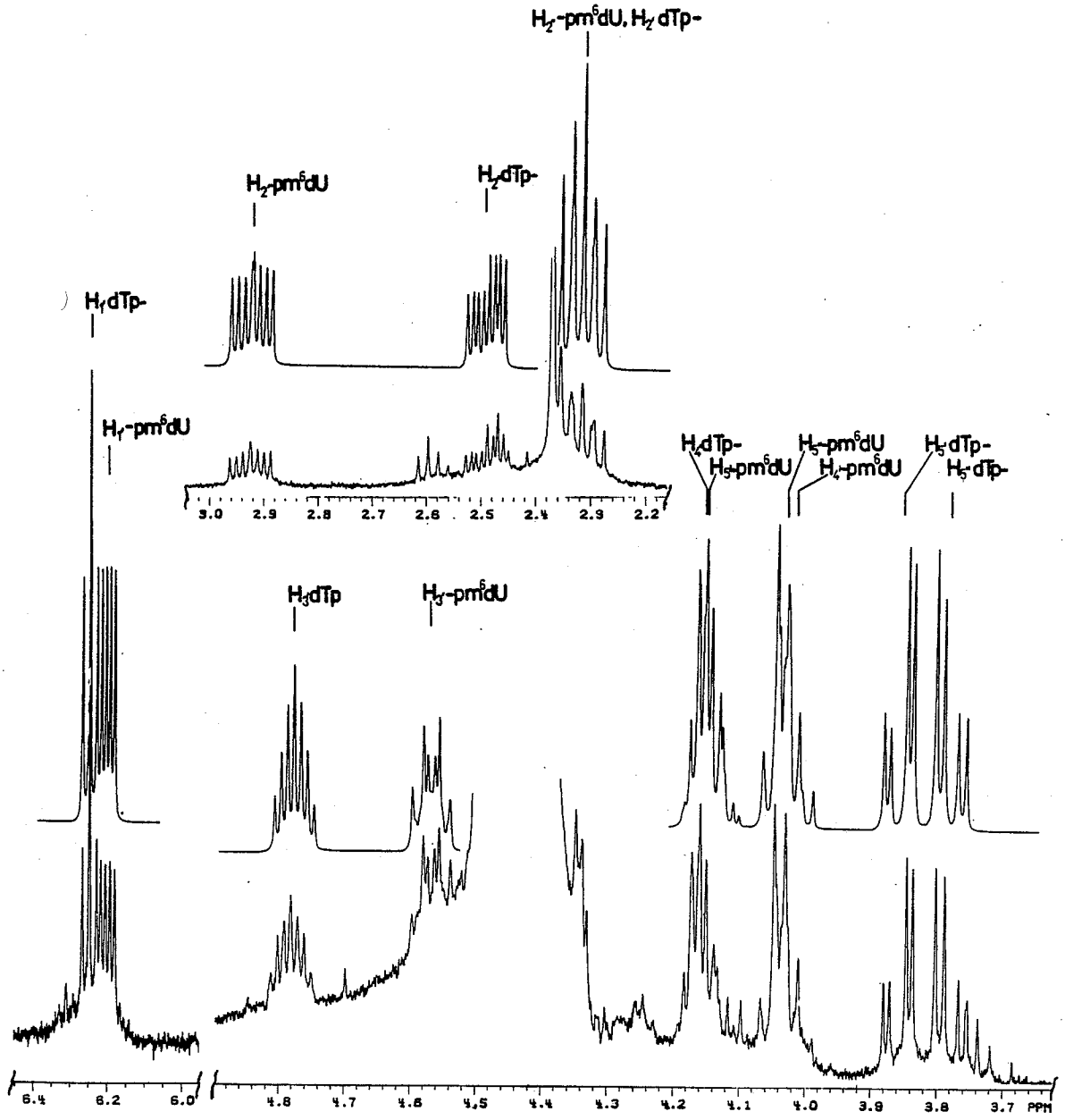
H2'-pm6dU, H2' dTp-
H2-pm6dU
H2-dTp-
H1'dTp-
H1'-pm6dU
H4dTp-
H5-pm6dU
H5-pm6dU
H4-pm6dU
H5'dTp-
H5"-dTp-
H3dTp
H3'-pm6dU
3.0 2.9 2.8 2.7 2.6 2.5 2.4 2.3 2.2
6.4 6.2 6.0
4.8 4.7 4.6 4.5 4.4 4.3 4.2 4.1 4.0 3.9 3.8 3.7 PPM

TABLE 4.6

PROTON CHEMICAL SHIFTS (ν) AND COUPLING CONSTANTS (J) FOR d(m^6UpT) [a] AT 293 K

m^6dUp- PART			-pdT PART		
		Std. Dev.[b]			Std. Dev.[b]
ν(1')	2223.308	0.037	ν(1')	2280.97	0.031
ν(2')	1064.042	0.023	ν(2')	869.800	0.041
ν(2")	877.279	0.031	ν(2")	869.600	0.041
ν(3') [c]	———	———	ν(3')	1644.620	0.031
ν(4')	1460.443	0.031	ν(4')	1496.349	0.041
ν(5')	1396.249	0.031	ν(5')	1484.348	0.021
ν(5")	1344.493	0.031	ν(5")	1459.312	0.027
ν(5) [e]	2053.91	±0.1	ν(6) [e]	2773.94	±0.1
ν(CH_3) [e]	850.88	±0.1	ν(CH_3) [e]	686.70	±0.1
J(5-CH_3) [e]	0.81	±0.1	J(6-CH_3) [e]	1.19	±0.1
J(1'-2')	5.356	0.041	J(1'-2') [d,f]	6.780	0.052
J(1'-2")	8.412	0.047	J(1'-2")	6.780	0.052
J(2'-2")	-13.993	0.040	J(2'-2") [f]	-12.10	———
J(2'-3')	8.485	0.047	J(2'-3') [d,f]	5.515	0.056
J(2"-3')	5.633	0.059	J(2"-3')	5.515	0.056
J(3'-4')	5.521	0.086	J(3'-4')	4.238	0.054
J(4'-5')	3.225	0.044	J(4'-5')	2.905	0.036
J(4'-5")	6.830	0.061	J(4'-5")	4.392	0.041
J(5'-5")	-12.108	0.043	J(5'-5")	-11.520	0.035
J(3'-P)	6.82 [g]	±0.2	J(4'-P)	1.886	0.050
			J(5'-P)	3.904	0.042
			J(5"-P)	4.029	0.046
RMS Error[b]		0.1128			0.1318
Largest Error[b]		0.251			0.416

FOOTNOTES FOR TABLE 4.6

a) Unless otherwise stated, chemical shifts and coupling constants are in Hz, at 360.061 MHz, as obtained from the iterative analysis. Sample was 4 mgs d(m^6UpT) in 1 ml D_2O. Chemical shifts are downfield from internal TSP.

b) These parameters are obtained from the output of LAME 8. Estimated accuracy is $\pm$0.12 Hz unless otherwise indicated.

c) This resonance was not observed.

d) $H_{2'}$ and $H_{2''}$ of the -pdT part of the molecule are near equivalent. The chemical shift difference is arbitrary.

e) These parameters were not obtained from an iterative analysis but were derived directly from the line positions in the spectrum.

f) For near equivalence of $H_{2'}$ and $H_{2''}$, the spectrum is independent of J(2'-2''). The observed couplings to $H_{1'}$ and $H_{3'}$ are the averages of the actual couplings, i.e., $^{OBS}J(1'-2) = (J(1'2') + J(1'-2''))/2$.

g) This parameter was obtained from the ^{31}P spectrum.

TABLE 4.7

PROTON CHEMICAL SHIFTS (ν) AND COUPLING CONSTANTS (J)

FOR d(m^6UpT) [a] AT 333 K

m^6dUp- PART			-pdT PART		
		Std. Dev. [b]			Std. Dev. [b]
ν(1')	2218.052	0.016	ν(1')	2270.731	0.014
ν(2')	1068.337	0.016	ν(2') [c]	862.554	0.348
ν(2")	872.864	0.021	ν(2")	863.031	0.348
ν(3')	1741.036	0.016	ν(3')	1638.465	0.013
ν(4')	1464.110	0.010	ν(4')	1494.151	0.015
ν(5')	1392.096	0.016	ν(5')	1482.028	0.013
ν(5")	1348.919	0.016	ν(5")	1461.169	0.012
ν(5) [d]	2055.70	±0.1	ν(6) [d]	2760.02	±0.1
ν(CH_3) [d]	850.63	±0.1	ν(CH_3) [d]	688.44	±0.1
J(5-CH_3) [d]	0.74	±0.1	J(6-CH_3) [d]	1.37	±0.1
J(1'-2')	5.744	0.022	J(1'-2') [c,e]	6.787	0.016
J(1'-2")	8.349	0.025	J(1'-2")	6.787	0.016
J(2'-2")	-13.787	0.027	J(2'-2") [e]	-12.1	———
J(2'-3')	7.857	0.025	J(2'-3') [c,e]	5.515	0.015
J(2"-3')	5.132	0.025	J(2"-3')	5.515	0.015
J(3'-4')	5.322	0.016	J(3'-4')	3.723	0.022
J(4'-5')	3.544	0.018	J(4'-5')	3.077	0.020
J(4'-5")	6.478	0.017	J(4'-5")	4.747	0.018
J(5'-5")	-12.124	0.022	J(5'-5")	-11.517	0.019
J(3'-P)	7.406	0.022	J(4'-P)	1.392	0.03
			J(5'-P)	4.448	0.025
			J(5"-P)	5.145	0.023
RMS Error		0.0849			0.0967
Largest Error		0.271			0.245

FOOTNOTES FOR TABLE 4.7

a) Unless otherwise stated, chemical shifts and coupling constants are in Hz, at 360.061 MHz, as obtained from the iterative analysis. Sample was 4 mgs d(m^6UpT) in 1 ml D_2O. Chemical shifts are downfield from internal TSP.

b) These parameters are obtained from the output of LAME 8. Estimated accuracy is $\pm$0.12 Hz unless otherwise indicated.

c) $H_{2'}$ and $H_{2''}$ of the -pdT part of the molecule are near equivalent. The chemical shift difference is arbitrary.

d) These parameters were not obtained from an iterative analysis but were derived directly from the line positions in the spectrum.

e) For near equivalence of $H_{2'}$ and $H_{2''}$, the spectrum is independent of J(2'-2''). The observed couplings to $H_{1'}$ and $H_{3'}$ are the averages of the actual couplings, i.e., $^{OBS}J(1'-2) = (J(1'-2) = (J(1'2') + J(1'-2''))/2$.

FIGURE 4.5 contains the observed and calculated proton spectrum of d(m^6UpT) at 333 K and pH = 6.1. The sample is 4 mgs d(m^6UpT) in 1 ml D_2O. Shifts are in ppm downfield from internal TSP.

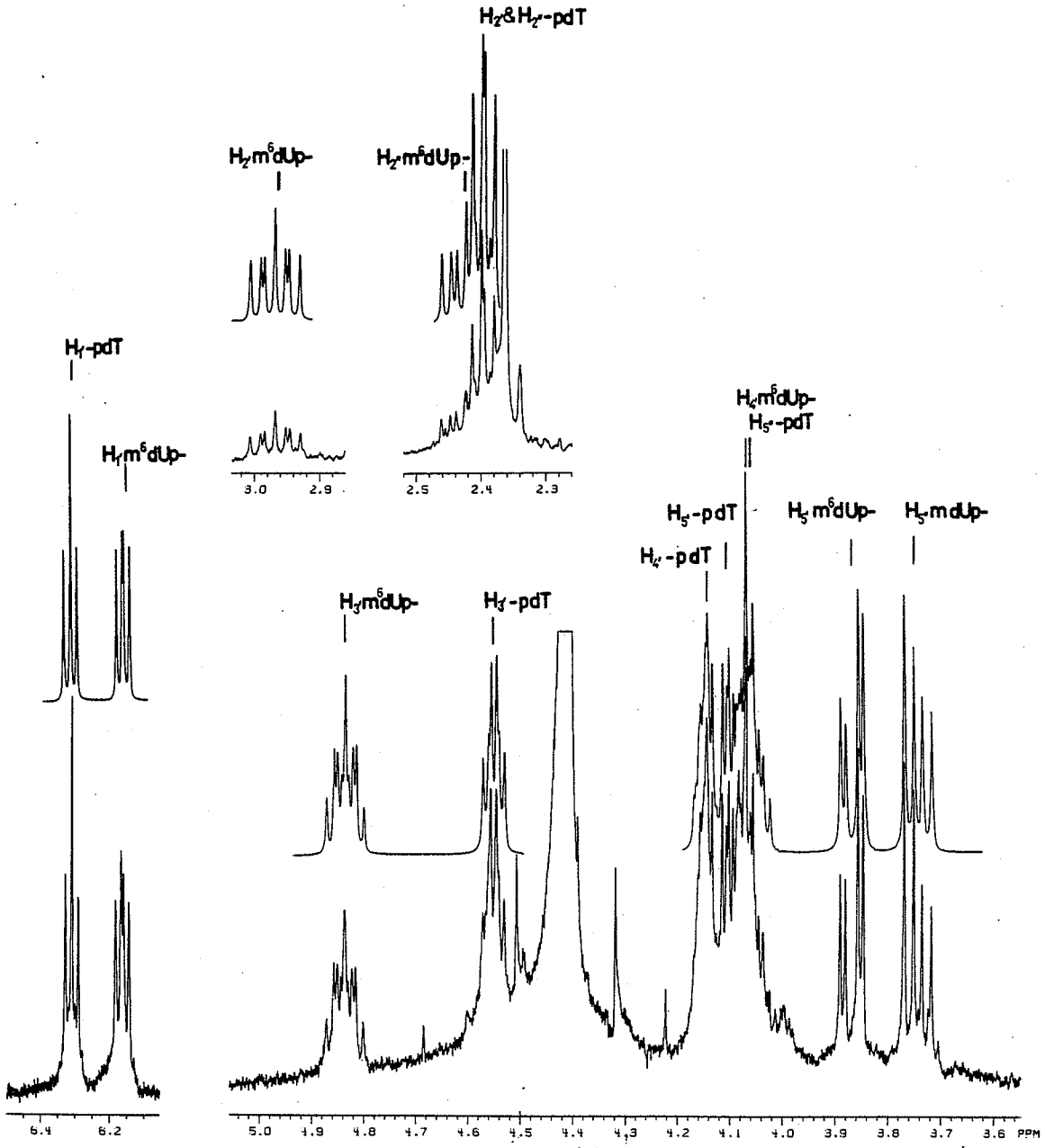
H2&H2'-pdT
H2'm5dUp-
H2'm5dUp-
H1'-pdT
H1'm5dUp-
H4'm5dUp-
H5'-pdT
H5'-pdT
H5'm5dUp-
H5'mdUp-
H4'-pdT
H3'm5dUp-
H3'-pdT
3.0
2.9
2.5
2.4
2.3
6.4
6.2
5.0
4.9
4.8
4.7
4.6
4.5
4.4
4.3
4.2
4.1
4.0
3.9
3.8
3.7
3.6
PPM

TABLE 4.8

PROTON CHEMICAL SHIFTS (ν) AND COUPLING CONSTANTS (J)

FOR d(m^6Upm^6U) [a] AT 293 K

m^6dUp- PART			-pm^6dU PART		
		Std. Dev.[b]			Std. Dev.[b]
ν(1')	2216.542	0.052	ν(1')	2230.110	0.023
ν(2')	1054.837	0.030	ν(2')	1058.994	0.027
ν(2")	886.771	0.034	ν(2")	825.333	0.021
ν(3') [c]	———	———	ν(3')	1676.305	0.017
ν(4')	1471.208	0.033	ν(4')	1434.535	0.021
ν(5')	1379.966	0.046	ν(5')	1495.280	0.013
ν(5")	1343.537	0.046	ν(5")	1452.376	0.017
ν(5) [d]	2059.28	$\pm$0.1	ν(5) [d]	2033.03	$\pm$0.1
$\nu(CH_3)$ [d]	856.43	$\pm$0.1	$\nu(CH_3)$ [d]	852.32	$\pm$0.1
J(5-CH_3) [d]	0.77	$\pm$0.1	J(5-CH_3) [d]	0.78	$\pm$0.1
J(1'-2')	7.502	0.053	J(1'-2')	3.960	0.034
J(1'-2")	6.407	0.058	J(1'-2")	9.084	0.031
J(2'-2")	-13.912	0.045	J(2'-2")	-13.713	0.032
J(2'-3')	6.095	0.060	J(2'-3')	8.879	0.031
J(2"-3')	4.916	0.067	J(2"-3')	6.584	0.027
J(3'-4')	4.839	0.067	J(3'-4')	6.895	0.030
J(4'-5')	3.550	0.054	J(4'-5')	2.742	0.020
J(4'-5")	6.570	0.053	J(4'-5")	6.605	0.026
J(5'-5")	-12.142	0.061	J(5'-5")	-11.305	0.023
J(3'-P) [e]	9.5	$\pm$1.0	J(4'-P) [f]	$\sim$0	———
			J(5'-P)	4.926	0.025
			J(5"-P)	4.811	0.037
RMS Error[b]		0.1632			0.1230
Largest Error[b]		0.415			0.381

FOOTNOTES FOR TABLE 4.8

a) Unless otherwise stated, chemical shifts and coupling constants are in Hz, at 360.061 MHz, as obtained from the iterative analysis. Sample was 4 mgs d(m^6Upm^6U) in 1 ml D_2O. Chemical shifts are downfield from internal TSP.

b) These parameters are obtained from the output of LAME 8. Estimated accuracy is $\pm$ 0.12 Hz unless otherwise indicated.

c) This resonance was not observed.

d) These parameters were not obtained from an iterative analysis but were derived directly from the line positions in the spectrum.

e) This parameter was obtained from the ^{31}P spectrum.

f) The simulated spectrum is sensitive to this value, and any value of J(4'-P5') larger than 0.2 Hz produced noticeable splittings which were not observed.

FIGURE 4.6 is the observed and calculated proton spectrum of d(m^6Upm^{6}U) at 293 K and pH = 6.5. The sample is 4 mgs d(m^6Upm^{6}U) in 1 ml D_2O. Shifts are in ppm downfield from internal TSP.

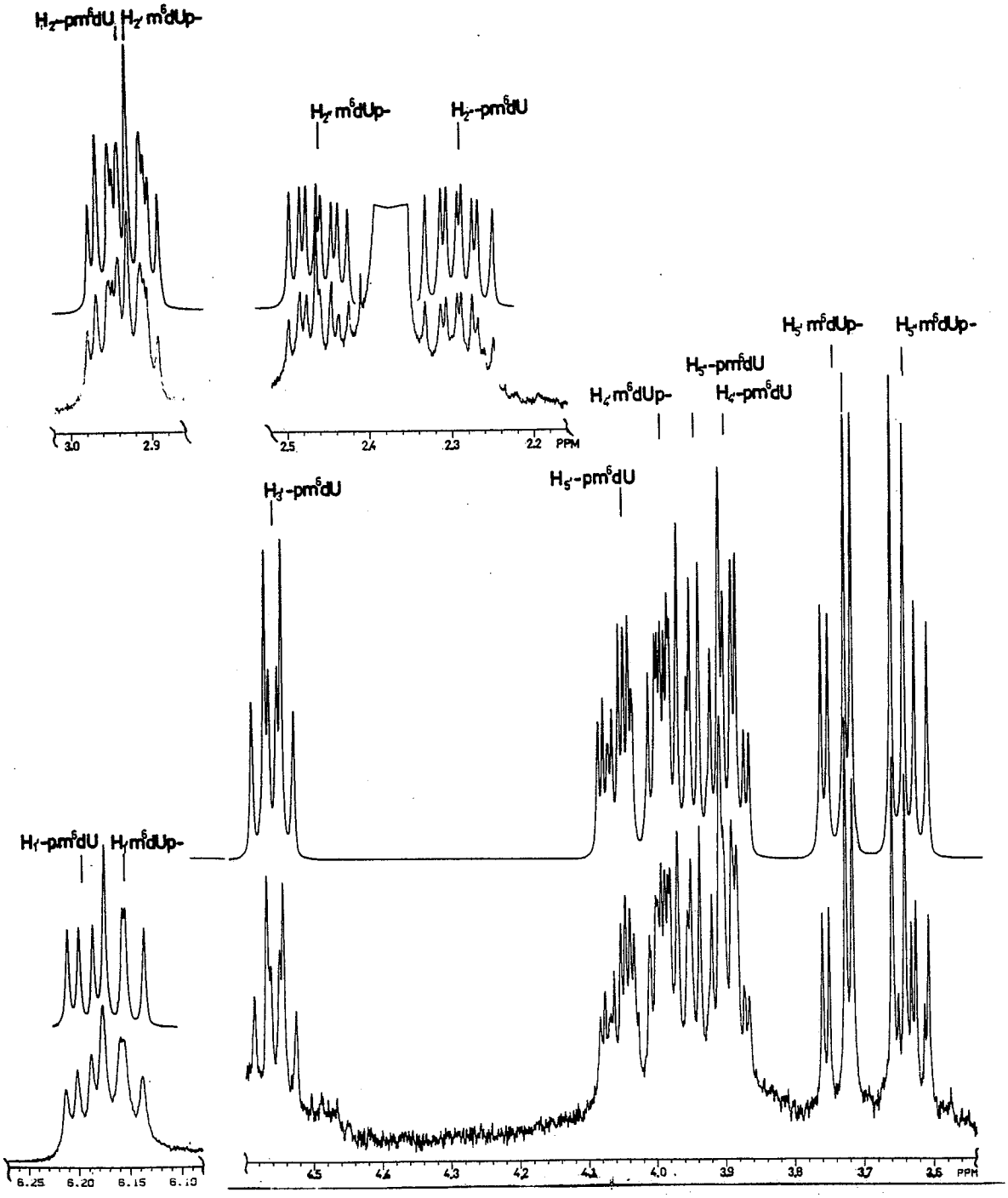
H2'-pm5dU
H2' m5dUp-
H2' m5dUp-
H2'-pm5dU
H5' m5dUp-
H5'-pm5dU
H4' m5dUp-
H4'-pm5dU
H3'-pm5dU
H5'-pm5dU
H1'-pm5dU
H1' m5dUp-
PPM

B. ^{13}C NMR DATA

Tables 4.9 to 4.21 show the ^{13}C chemical shift and spin coupling data for the nucleosides, nucleotides, 3',5'-nucleoside diphosphates and dinucleoside monophosphates studied in this work. The chemical shift data (Table 4.9) and proton-carbon coupling constants for the pyrimidine carbons (Table 4.10) of the two nucleosides are presented first. Chemical shift assignments for specific ribose carbons follow those reported in the literature[47-51]. Specific assignment of the $C_{4'}$ and $C_{1'}$ carbon was based on the magnitude of the one bond proton-carbon coupling constants, $^{1}J(C1'-H1') > {}^{1}J(C4'-H4')$ [53]. Assignment of the base carbons was facilitated by the splittings of these resonances in the gated proton-coupled spectrum of the respective molecules (see Figure 4.7).

The chemical shift assignment for the ribose carbons in the nucleotides and 3',5'-nucleoside diphosphates was facilitated by the appearance of splittings (between 1 to 9 Hz) due to the carbon-phosphorus spin-spin coupling for some of the carbons. In the 5'-nucleotides, $C_{4'}$ and $C_{5'}$ appear as doublets while in the 3'-nucleotides, $C_{2'}$, $C_{3'}$, and $C_{4'}$ are split into doublets (see Figure 4.8). In the 3',5'-nucleoside diphosphates, the $C_{2'}$, $C_{3'}$, and $C_{5'}$ carbons are split while $C_{4'}$ is either a triplet or a doublet of doublets (see Figure 4.9). The pyrimidine carbons undergo only minor chemical shift perturbations upon phosphorylation.

For the dinucleoside monophosphates, the situation is slightly more complicated. The pairs of $C_{2'}$, $C_{3'}$, and $C_{5'}$ resonances can be

differentiated by the carbon-phosphorus spin couplings (see Figures 4.10 to 4.12). In the case of the $C_{4'}$ and $C_{1'}$ pairs, the assignment is not as straightforward. The assignments shown in the tables are based on the observed behavior of these shifts upon phosphorylation and on the dependence of the chemical shifts of these carbons in the nucleotides as a function of pH. The assignments are reasonable in the light of the above information. Conclusive assignments, however, would need either ^{13}C enrichment of one of the carbons in each molecule, or deuterium substitution of the directly bonded proton for two of the carbons.

TABLE 4.9

CARBON CHEMICAL SHIFTS[a] FOR dT AND m^6dU AT 300 K

	dT [b]	dm^6U [b]
$\delta(CH_3)$	12.81	21.03
$\delta(2')$	39.84	37.96
$\delta(5')$	62.51	63.04
$\delta(3')$	71.76	72.09
$\delta(1')$	86.34	86.99
$\delta(4')$	87.81	87.52
$\delta(5)$	112.66	103.59
$\delta(6)$	136.75	157.77
$\delta(2)$	152.91	152.77
$\delta(4)$	167.68	166.79

a) Chemical shifts are in ppm downfield from external TMS by setting the chemical shift of the internal dioxane equal to 67.859 ppm.

b) Samples were 100 mgs dissolved in 1 ml D_2O and contained 1% dioxane as internal reference.

TABLE 4.10

PROTON-CARBON COUPLING CONSTANTS FOR THE THYMINE AND 6-METHYLURACIL MOIETIES IN NUCLEOSIDES AND NUCLEOTIDES AT 300 K [a]

	dT	3'-dTMP	5'-dTMP	m^6dU	3'-m^6dUMP	5'-m^6dUMP
^1J(H6-C6) [b]	179.3	181.8	182.5	———	———	———
^2J(H6-C5)	1.5	1.3	1.3	———	———	———
$^2J(CH_3$-C5)	6.7	6.9	5.9	———	———	———
$^3J(CH_3$-C4)	4.1	4.0	4.0	———	———	———
$^3J(CH_3$-C6)	6.2	5.8	5.9	———	———	———
^3J(H6-C4)	9.8	9.8	10.1	———	———	———
^3J(H6-C2)	7.7	8.1	8.0	———	———	———
^3J(H1'-C2)	2.1	2.4	2.2	———	———	———
^3J(H1'-C6)	3.8	4.4	3.6	———	———	———
^1J(H5-C5)	———	———	———	175.6	176.2	175.5
^2J(H5-C6)	———	———	———	3.0	3.2	3.0
^2J(H5-C4)	———	———	———	1.0	<0.7	<0.7
$^2J(CH_3$-C6)	———	———	———	6.0	6.1	6.0
$^3J(CH_3$-C5)	———	———	———	4.7	4.7	4.6
^3J(H1'-C2)	———	———	———	6.8	6.7	6.2
^3J(H1'-C6)	———	———	———	3.0	3.2	3.0

a) Samples were 100 mgs dissolved in 1 ml D_2O and contained 1% dioxane as internal reference.

b) In Hz. Estimated accuracy $\pm$0.5 Hz.

FIGURE 4.7 is the carbon-13 spectrum of the pyrimidine ring carbons of a) m^6dU and b) dT at 310 K. Both samples are 100 mgs nucleoside dissolved in 1 ml D_2O. The spectra were obtained in the gated-coupled mode to retain the threefold enhancement of the $^{13}C-\{^1H\}$ NOE.

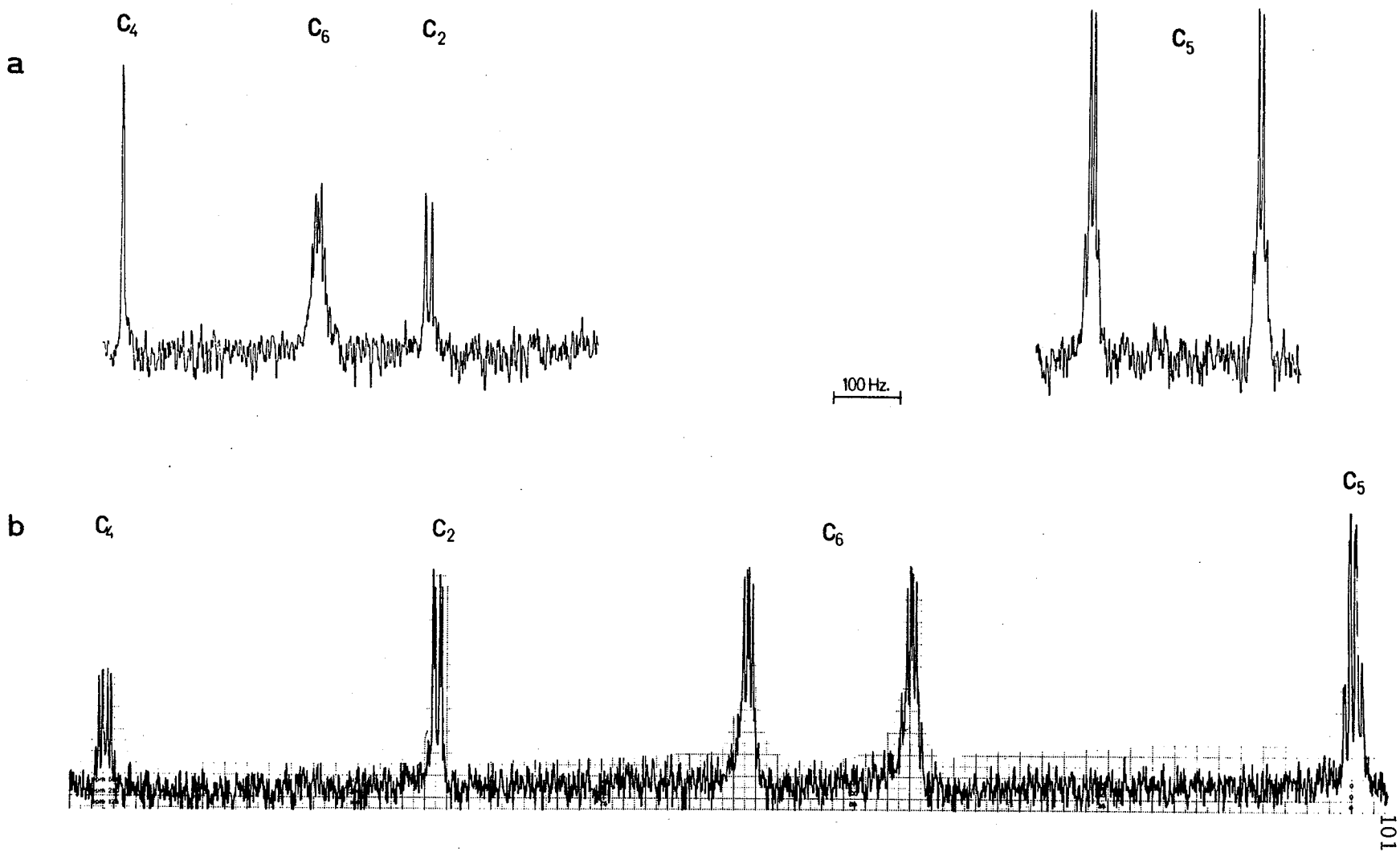
a
C4
C6
C2
C5
100 Hz.
b
C4
C2
C6
C5

TABLE 4.11

CARBON CHEMICAL SHIFTS AND CARBON-PHOSPHORUS COUPLING CONSTANTS FOR 3'-dTMP AT 300 K [a]

δ [c] pH [b]	1.2	2.1	5.6	6.3	7.3	9.4	10.1
$\delta(CH_3)$	12.82	12.84	12.83	12.82	12.82	12.79	13.90
δ(2')	38.85	38.98	39.02	39.15	39.25	39.24	39.36
δ(5')	62.35	62.43	62.50	62.59	62.66	62.63	62.91
δ(3')	76.16	75.82	75.22	74.76	74.32	74.43	74.56
δ(1')	86.33	86.35	86.31	86.30	86.28	86.30	86.46
δ(4')	86.93	87.02	87.10	87.20	87.28	87.26	86.95
δ(5)	112.80	112.76	112.74	112.73	112.71	112.71	113.03
δ(6)	138.80	138.81	138.84	138.90	138.93	138.93	138.00
δ(2)	152.94	152.93	152.95	153.00	153.05	153.02	159.71
δ(4)	167.71	167.69	167.69	167.73	167.78	167.78	176.47
^2J(C3'-P) [d]	4.9	5.1	4.8	4.8	4.6	4.5	4.5
^3J(C2'-P)	3.2	3.4	3.6	3.2	2.9	2.8	3.0
^3J(C4'-P)	6.5	6.3	6.1	5.8	5.8	5.9	5.8

a) Chemical shifts are in ppm downfield from external TMS by setting the chemical shift of the internal dioxane equal to 67.859 ppm.

b) Sample was 100 mgs dissolved in 1 ml D_2O, prepared as described in Chapter III, and contained 1% dioxane as internal reference. pH readings are not corrected for the deuterium isotope effect.

c) Estimated accuracy $\pm$0.01 ppm

d) Estimated accuracy $\pm$0.2 Hz

FIGURE 4.8 contains the observed carbon-13 spectrum of the ribose carbons of 3'-dTMP at 300 K and pH = 7.3. Sample is 100 mgs 3'-dTMP in 1 ml D_2O prepared as described in Chapter III. Shifts are relative to external TMS by setting the dioxane resonance shift equal to 67.859 ppm.

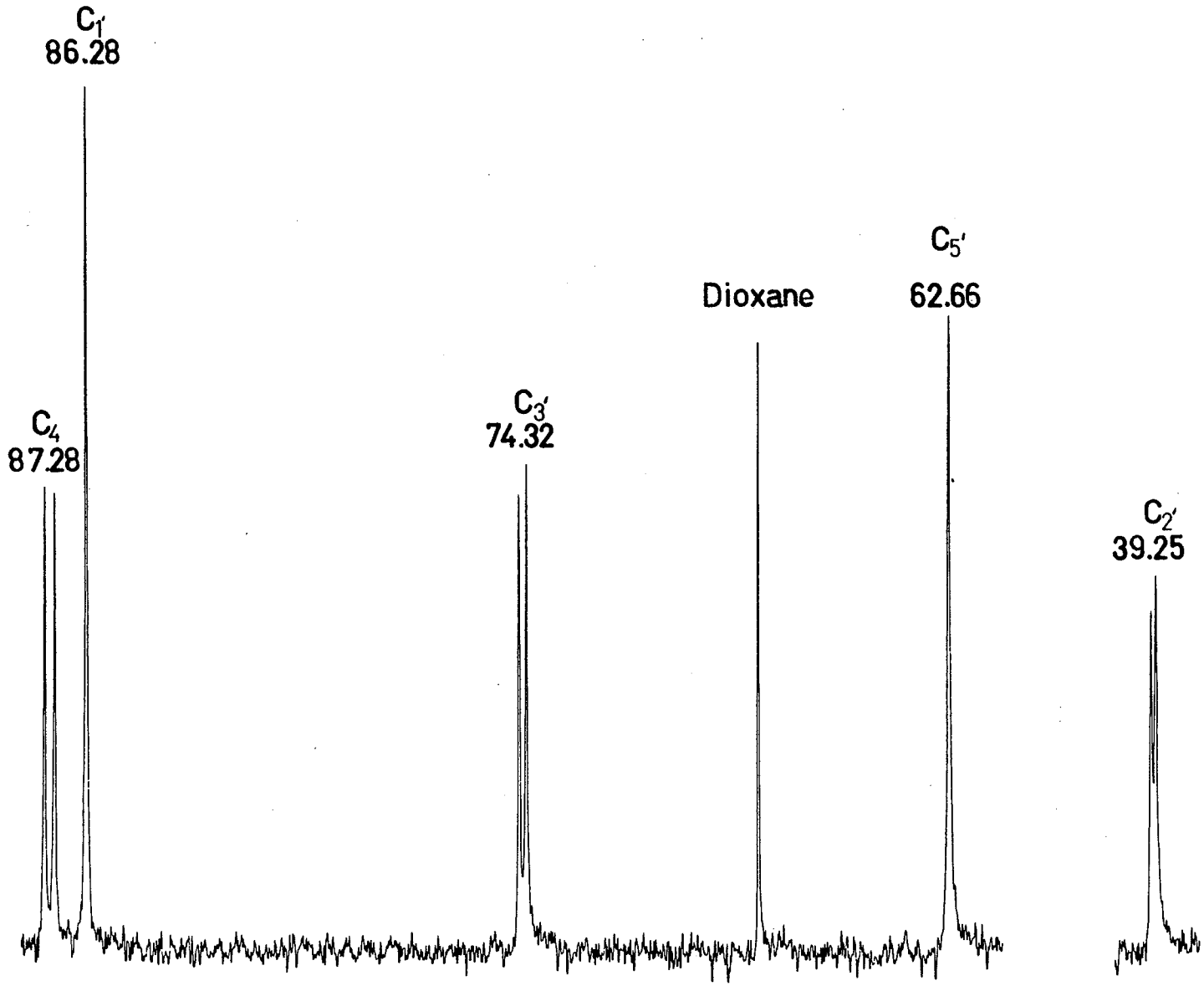
C1'
86.28
C4
87.28
C3'
74.32
Dioxane
C5'
62.66
C2'
39.25

TABLE 4.12

CARBON CHEMICAL SHIFTS AND CARBON-PHOSPHORUS COUPLING CONSTANTS FOR 5'-dTMP AT 300 K [a]

δ [c] pH [b]	1.5	3.4	5.9	6.5	7.1	8.5	10.0	11.5
$\delta(CH_3)$	12.91	12.90	12.91	12.98	12.98	13.00	13.51	14.18
δ(2')	40.09	40.06	39.92	39.75	39.64	39.60	39.51	35.55
δ(5')	66.25	66.05	65.74	65.40	65.12	65.03	65.09	65.18
δ(3')	72.32	72.40	72.42	72.50	72.50	72.48	72.52	72.58
δ(1')	86.39	86.36	86.28	86.16	86.14	86.13	86.14	86.14
δ(4')	86.66	86.81	86.94	87.09	87.18	87.20	86.95	86.61
δ(5)	112.91	112.92	112.93	113.10	113.01	113.01	113.15	113.32
δ(6)	138.63	138.66	138.75	138.97	138.98	138.98	138.46	137.78
δ(2)	152.92	152.95	152.98	153.03	153.06	153.18	156.42	160.73
δ(4)	167.74	167.75	167.78	167.87	167.88	168.03	172.26	177.89
^2J(C5'-P) [d]	5.2	5.1	4.8	4.7	4.6	4.7	4.8	4.7
^3J(C4'-P)	8.9	8.7	8.7	8.7	8.6	8.5	8.4	8.4

---

a) Chemical shifts are in ppm downfield from external TMS by setting the chemical shift of the internal dioxane equal to 67.859 ppm.

b) Sample was 100 mgs dissolved in 1 ml D_2O, prepared as described in Chapter III, and contained 1% dioxane as internal reference. pH readings are not corrected for the deuterium isotope effect.

c) Estimated accuracy $\pm$0.01 ppm

d) Estimated accuracy $\pm$0.2 Hz

TABLE 4.13

CARBON CHEMICAL SHIFTS AND CARBON-PHOSPHORUS COUPLING CONSTANTS FOR 3',5'-dTDP AT 300 K [a]

δ [c] pH [b]	1.3	2.6	4.9	5.9	7.1	9.0	10.1	11.5
$\delta(CH_3)$	12.90	12.92	12.93	12.95	12.93	13.10	14.51	14.21
δ(2')	39.17	39.24	39.24	39.25	39.26	39.25	39.25	39.22
δ(5')	66.32	66.09	65.99	65.72	65.11	65.65	65.73	65.77
δ(3')	76.76	76.58	76.33	75.64	75.48	75.54	75.58	75.57
δ(1')	86.32	86.32	86.31	86.29	86.39	86.44	86.47	86.49
δ(4')	85.63	85.92	85.98	86.27	86.86	86.97	86.65	86.51
δ(5)	113.02	113.06	113.05	113.04	113.04	113.07	113.27	113.26
δ(6)	138.55	138.63	138.68	138.86	139.10	139.00	138.37	137.98
δ(2)	152.96	153.01	153.02	153.07	153.10	154.18	158.39	160.89
δ(4)	167.75	167.79	167.80	167.83	167.88	169.18	174.74	177.96
^2J(C3'-P3') [d]	5.0	5.0	4.9	4.6	4.5	4.5	4.7	4.1
^2J(C5'-P5')	5.0	4.7	5.4	4.8	4.6	4.5	4.7	3.8
^3J(C2'-P3')	3.8	3.5	3.6	3.1	3.0	2.8	2.5	2.4
^3J(C4'-P3')	6.2	6.0	5.8	—— e	5.9	6.0	6.0	—— e
^3J(C4'-P5')	8.8	8.9	8.6	—— e	8.5	8.6	8.8	—— e

a) Chemical shifts are in ppm downfield from external TMS by setting the chemical shift of the internal dioxane equal to 67.859 ppm.

b) Sample was 100 mgs dissolved in 1 ml D_2O, prepared as described in Chapter III, and contained 1% dioxane as internal reference. pH readings are not corrected for the deuterium isotope effect.

CONTINUATION OF FOOTNOTES FOR TABLE 4.13

c) Estimated accuracy $\pm$0.01 ppm

d) Estimated accuracy $\pm$0.2 Hz

e) Not resolvable as the resonance is underneath that from $C_{1'}$

FIGURE 4.9 is a typical carbon-13 spectrum of the ribose carbons of 3',5'-dTDP at 300 K and pH = 1.2. Sample is 100 mgs 3',5'-dTDP in 1 ml D_2O prepared as described in Chapter III. Shifts are relative to external TMP as described for Figure 4.8. The insert shows the $C_{4'}$ and $C_{1'}$ carbons from 3',5'-m^6dUDP.

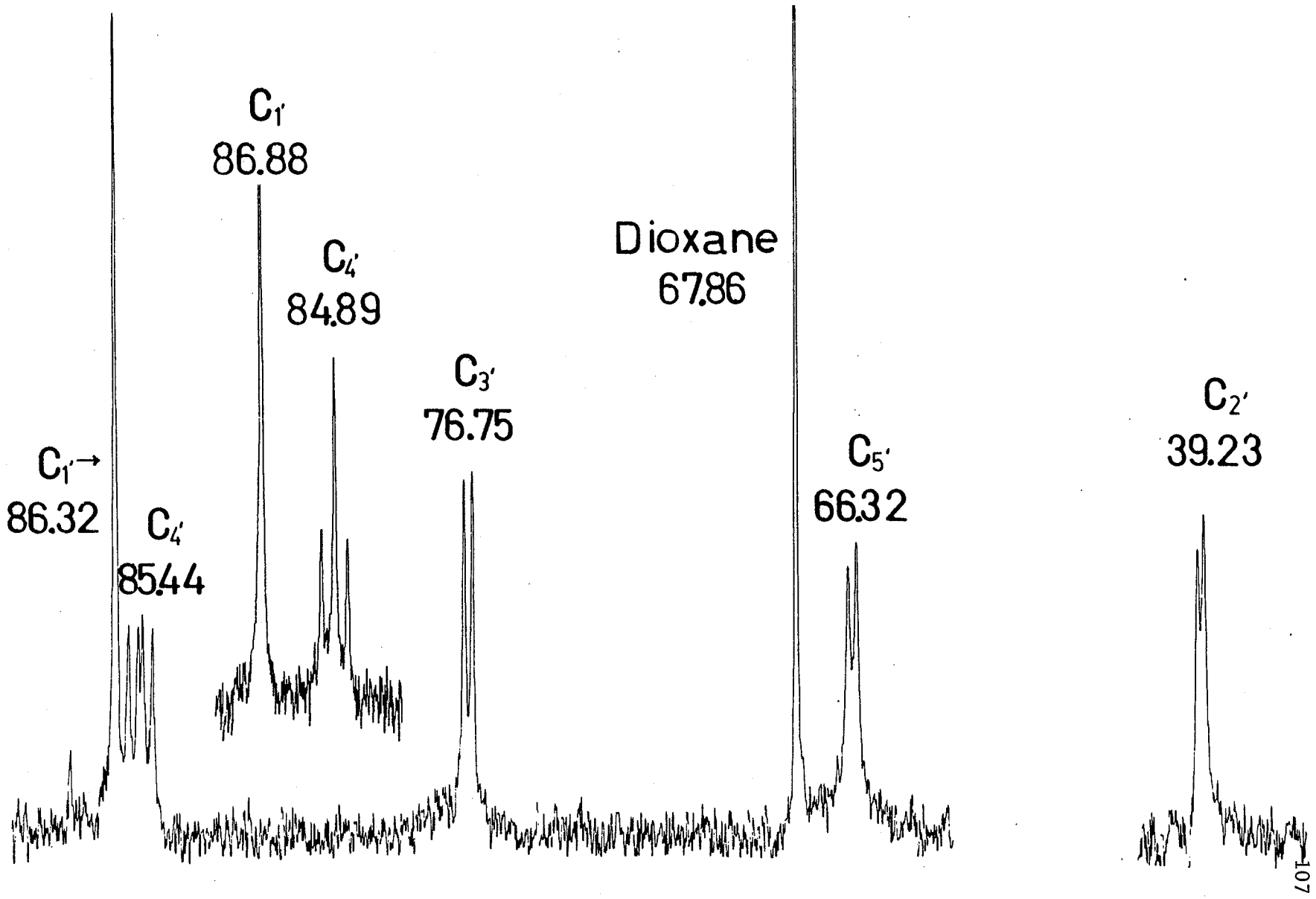
C1'
86.88
C4'
84.89
Dioxane
67.86
C3'
76.75
C1'→
86.32
C4'
85.44
C5'
66.32
C2'
39.23
107

TABLE 4.14

CARBON CHEMICAL SHIFTS AND CARBON-PHOSPHORUS COUPLING CONSTANTS FOR 3'-m^6dUMP [a] AT 300 K

δ [c] pH [b]	2.5	4.5	5.7	6.4	7.8	9.4	10.1	11.6
δ(CH_3)	21.10	21.10	21.13	21.13	21.14	21.06	20.90	20.73
δ(2')	37.17	37.18	37.24	37.34	37.42	37.45	37.49	37.56
δ(5')	62.83	62.88	62.95	63.06	63.16	63.21	63.30	63.38
δ(3')	75.56	75.54	75.32	75.00	74.72	74.85	75.10	75.38
δ(4')	86.56	86.62	86.68	86.79	86.82	86.88	86.88	86.86
δ(1')	86.99	87.02	87.06	87.12	87.18	87.17	87.12	87.06
δ(5)	103.55	103.53	103.54	103.53	103.53	103.70	104.12	104.33
δ(2)	152.81	152.83	152.84	152.86	152.98	154.67	157.71	161.38
δ(6)	157.83	157.84	157.87	157.92	157.94	157.48	156.65	155.66
δ(4)	166.97	167.00	167.01	167.02	167.15	169.29	173.10	177.68
^2J(C3'-P) [d]	4.8	4.6	4.6	4.4	4.4	4.1	4.4	4.6
^3J(C2'-P)	2.7	3.0	2.8	2.8	2.5	3.0	2.7	2.5
^3J(C4'-P)	7.7	7.8	7.3	7.1	6.7	6.4	6.4	6.3

a) Chemical shifts are in ppm downfield from external TMS by setting the chemical shift of the internal dioxane equal to 67.859 ppm.

b) Sample was 100 mgs dissolved in 1 ml D_2O, prepared as described in Chapter III, and contained 1% dioxane as internal reference. pH readings are not corrected for the deuterium isotope effect.

c) Estimated accuracy $\pm$0.01 ppm

d) Estimated accuracy $\pm$0.2 Hz

TABLE 4.15

CARBON CHEMICAL SHIFTS AND CARBON-PHOSPHORUS COUPLING CONSTANTS FOR 5'-m^6dUMP AT 300 K [a]

δ [c] pH [b]	1.3	2.1	4.4	5.4	7.1	8.1	10.1
δ(CH_3)	21.10	21.11	21.11	21.07	21.12	21.07	20.86
δ(2')	37.91	37.82	37.81	37.76	37.70	37.63	37.83
δ(5')	66.95	66.39	66.30	66.18	65.34	65.25	65.35
δ(3')	71.98	72.01	72.02	72.06	72.18	72.22	72.36
δ(4')	85.86	86.00	86.03	86.10	86.37	86.41	86.08
δ(1')	86.91	86.81	86.81	86.78	86.60	86.58	86.25
δ(5)	103.55	103.57	103.60	103.58	103.62	103.58	104.05
δ(2)	152.69	152.72	152.73	152.73	152.78	152.83	157.75
δ(6)	157.77	157.76	157.80	157.78	157.81	157.79	156.43
δ(4)	166.94	166.95	166.93	166.94	166.95	167.06	173.28
^2J(C5'-P) [d]	5.3	5.1	5.2	4.8	4.5	4.6	4.6
^3J(C4'-P)	7.8	8.0	7.9	8.0	8.4	8.3	8.0

a) Chemical shifts are in ppm downfield from external TMS by setting the chemical shift of the internal dioxane equal to 67.859 ppm.

b) Sample was 100 mgs dissolved in 1 ml D_2O, prepared as described in Chapter III, and contained 1% dioxane as internal reference. pH readings are not corrected for the deuterium isotope effect.

c) Estimated accuracy ±0.01 ppm

d) Estimated accuracy ±0.2 Hz

TABLE 4.16

CARBON CHEMICAL SHIFTS AND CARBON-PHOSPHORUS COUPLING CONSTANTS FOR 3',5'-m^6dUDP [a] AT 300 K

δ [c] pH [b]	1.3	2.6	5.7	6.8	7.7	9.4	10.1	11.2
$\delta(CH_3)$	21.11	21.11	21.12	21.17	21.17	21.06	21.00	20.76
δ(2')	37.12	37.10	37.18	37.39	37.34	37.44	37.47	37.63
δ(5')	66.25	66.10	65.70	65.67	65.78	65.83	65.85	65.89
δ(3')	75.50	75.32	74.80	74.44	74.38	74.42	74.44	74.51
δ(4')	84.89	85.08	85.29	85.91	86.18	86.08	86.05	85.71
δ(1')	86.88	86.87	86.86	86.99	87.07	86.91	86.84	86.47
δ(5)	103.58	103.58	103.57	103.56	103.55	103.73	103.80	104.18
δ(2)	152.69	152.71	152.74	152.77	152.86	155.06	155.97	160.48
δ(6)	157.77	157.79	157.85	157.93	157.94	157.33	157.09	155.85
δ(4)	166.90	166.91	166.93	166.93	167.07	169.88	171.05	176.78
^2J(C3'-P) [d]	4.7	4.8	4.5	4.3	4.6	4.3	4.1	4.4
^2J(C5'-P)	5.1	5.1	4.8	4.4	4.2	4.7	4.4	4.6
^3J(C2'-P)	2.2	2.1	1.7	1.0	< .7	< .7	< .7	< .7
^3J(C4'-P)	8.0	8.1	7.9	8.0	8.1	8.3	8.5	8.4

a) Chemical shifts are in ppm downfield from external TMS by setting the chemical shift of the internal dioxane equal to 67.859 ppm.

b) Sample was 100 mgs dissolved in 1 ml D_2O, prepared as described in Chapter III, and contained 1% dioxane as internal reference. pH readings are not corrected for the deuterium isotope effect.

c) Estimated accuracy $\pm$0.01 ppm d) Estimated accuracy $\pm$0.2 Hz

TABLE 4.17

CARBON CHEMICAL SHIFTS AND CARBON-PHOSPHORUS COUPLING CONSTANTS FOR d(TpT) [a] AT pH = 6.7 [b]

δ [d] T [c]	300 K		310 K		320 K		340 K	
	dTp-	-pdT	dTp-	-pdT	dTp-	-pdT	dTp-	-pdT
$\delta(CH_3)$	(13.20 [e]	13.18)	(13.12 [e]	13.08)	(13.06 [e]	13.00)	(12.86 [e]	12.79)
$\delta(2')$	38.91	40.01	38.90	40.00	38.93	40.02	38.93	40.01
$\delta(5')$	62.34	66.19	62.40	66.21	62.49	66.27	62.60	66.31
$\delta(3')$	76.35	71.78	76.32	71.81	76.36	71.88	76.25	71.96
$\delta(1')$	86.48	86.15	86.49	86.18	86.55	86.27	86.63	86.37
$\delta(4')$	86.83	86.26	86.85	86.28	86.89	86.36	86.93	86.43
$\delta(5)$	(112.77 [e]	112.81)	(112.79 [e]	112.75)	(112.78 [e]	112.75)	(112.70 [e]	112.65)
$\delta(6)$	(138.31 [e]	138.38)	(138.32 [e]	138.35)	138.36		138.33	
$\delta(2)$	154.56		154.36		154.19		153.78	
$\delta(4)$	(169.66 [e]	169.93)	(169.63 [e]	169.39)	(169.36 [e]	169.15)	———	———
$^2J(C5'-P)$ [f]	———	5.6	———	5.9	———	5.4	———	5.6
$^2J(C3'-P)$	5.6	———	5.4	———	5.4	———	5.6	———
$^3J(C2'-P)$	2.9	———	3.2	———	3.2	———	3.3	———
$^3J(C4'-P)$	7.1	10.3	7.0	9.5	6.8	8.8	6.8	7.9

a) Sample was 100 mgs dissolved in 1 ml D_2O, prepared as described in Chapter III, and contained 1% dioxane as internal reference.

b) Uncorrected for the deuterium isotope effect and measured at 297 K.

c) Accurate to better than ± 1 K

CONTINUATION OF FOOTNOTES FOR TABLE 4.17

d) In ppm downfield from external TMS by setting the chemical shift of the internal dioxane to 67.859 ppm. Estimated accuracy $\pm$0.01 ppm.

e) It is impossible to definitely assign either of the observed resonances to a specific residue without specific enrichment of one of the nucleotide residues.

f) In Hz. Estimated accuracy $\pm$ 0.2 Hz.

FIGURE 4.10 is the observed carbon-13 spectrum of the ribose carbons of d(TpT) at 320 K and pH = 6.7. Sample is 100 mgs d(TpT) in 1 ml D_2O, prepared as described in Chapter III. Shifts are relative to external TMS as described for Figure 4.8.

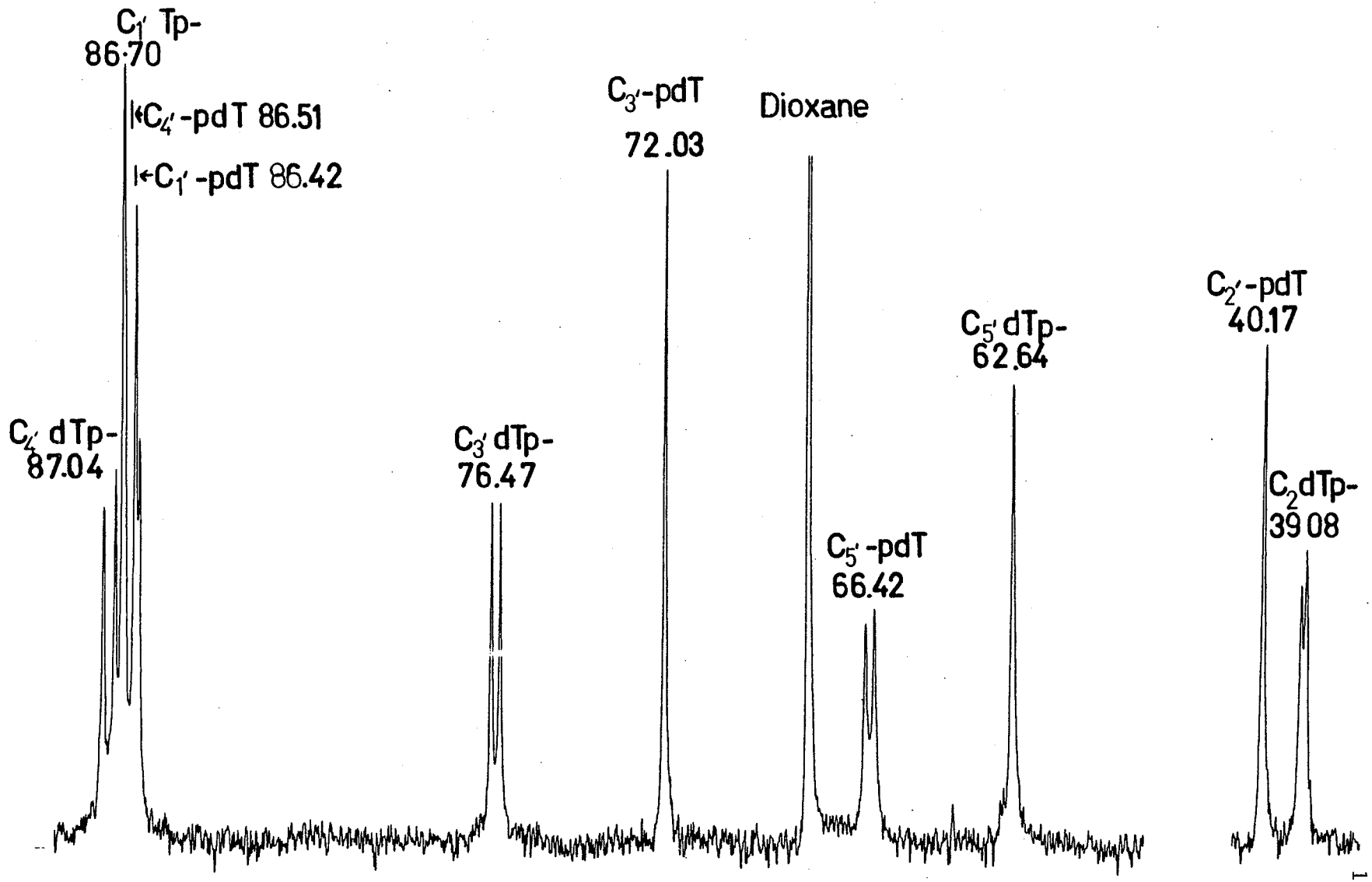
C1' Tp-
86·70
←C4'-pdT 86.51
←C1'-pdT 86.42
C4' dTp-
87.04
C3' dTp-
76.47
C3'-pdT
72.03
Dioxane
C5' dTp-
62.64
C5'-pdT
66.42
C2'-pdT
40.17
C2 dTp-
39 08

TABLE 4.18

CARBON CHEMICAL SHIFTS AND CARBON-PHOSPHORUS COUPLING CONSTANTS FOR d(Tpm^{6}U) [a] AT pH = 6.5 [b]

δ [d] T [c]	297 K		310 K		320 K		340 K	
	dTp-	-pm^{6}dU	dTp-	-pm^{6}dU	dTp-	-pm^{6}dU	dTp-	-pm^{6}dU
$\delta(CH_3)$	12.86	21.05	12.80	21.02	12.76	21.00	12.68	20.94
δ(2')	38.71	38.41	38.71	38.35	38.72	38.31	38.75	38.26
δ(5')	62.31	67.41	62.36	67.33	62.41	67.30	62.51	67.21
δ(3')	75.88	71.88	75.89	71.93	75.91	71.98	75.94	72.09
δ(4')	86.81	86.14	86.86	86.11	86.82	86.17	86.85	86.18
δ(1')	85.93	86.84	86.01	86.85	86.10	86.87	86.26	86.88
δ(5)	113.13	103.09	113.07	103.18	113.03	103.22	112.91	103.38
δ(6)	138.54	157.57	138.55	157.51	138.55	157.57	138.54	157.52
δ(2)	152.42	152.68	152.44	152.69	152.45	152.70	152.63	152.82
δ(4)	166.29	167.55	166.27	167.51	166.26	167.46	166.40	167.51
^2J(C3'-P) [e]	5.3	———	5.3	———	5.4	———	5.4	———
^2J(C5'-P)	———	5.3	———	5.6	———	5.5	———	5.6
^3J(C2'-P)	4.3	———	3.8	———	4.3	———	4.1	———
^3J(C4'-P)	5.0	9.5	5.1	8.4	5.3	8.7	5.6	8.5

———

a) Sample was 100 mgs dissolved in 1 ml D_2O, prepared as described in Chapter III, and contained 1% dioxane as internal reference.

b) Uncorrected for the deuterium isotope effect and measured at 297 K.

c) Accurate to better than $\pm$1 K

CONTINUATION OF FOOTNOTES FOR TABLE 4.18

d) In ppm downfield from external TMS by setting the chemical shift of the internal dioxane to 67.859 ppm. Estimated accuracy $\pm$0.01 ppm.

e) In Hz. Estimated accuracy $\pm$0.2 Hz.

FIGURE 4.11 contains the observed carbon-13 spectrum of the ribose carbons of d(Tpm^{6}U) at 320 K and pH = 6.5. Sample is 100 mgs d(Tpm^{6}U) in 1 ml D_2O, prepared as described in Chapter III. Shifts are relative to external TMS as described for Figure 4.8.

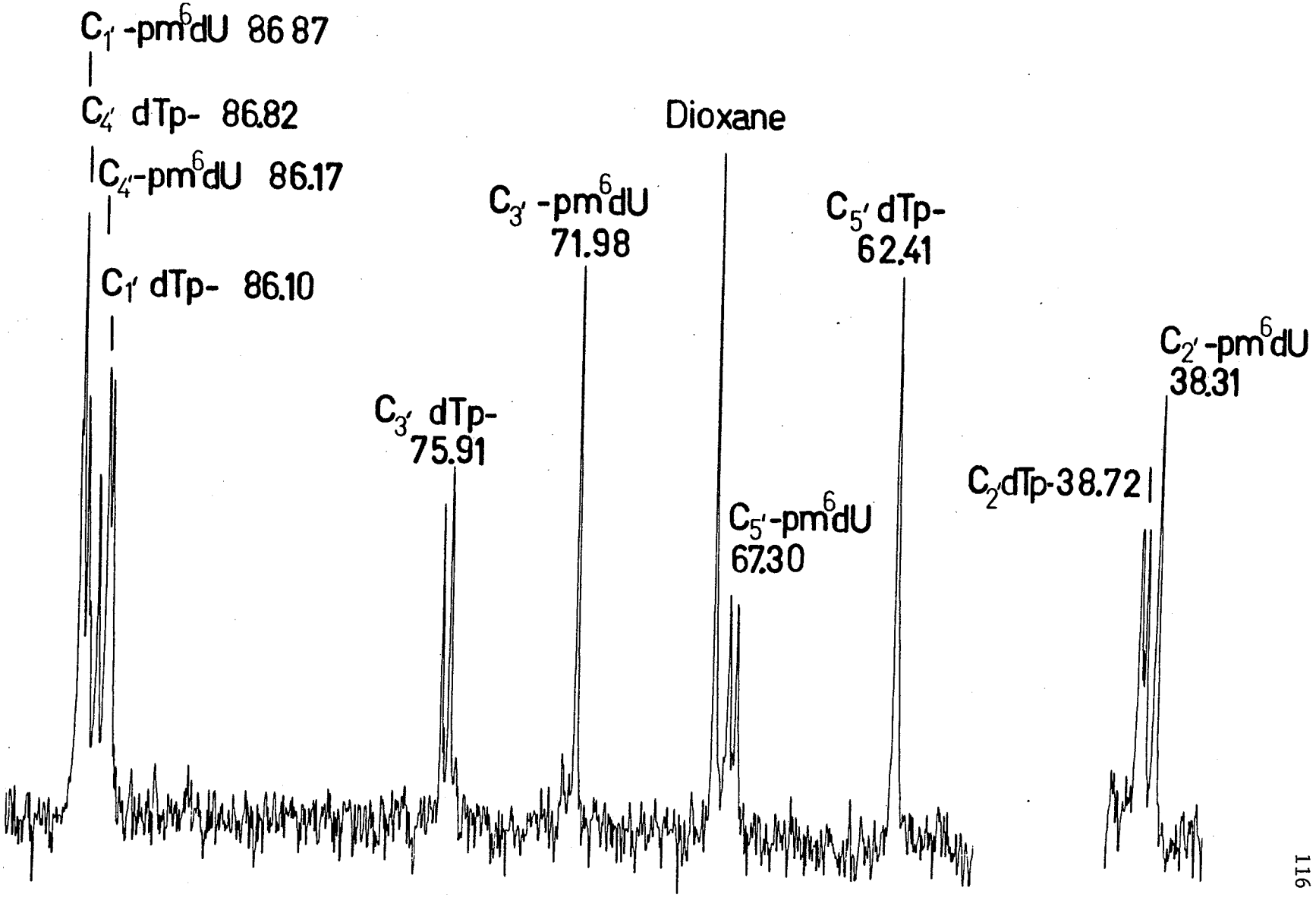
C1′ -pm6dU 86 87
C4′ dTp- 86.82
C4′-pm6dU 86.17
C1′ dTp- 86.10
C3′ dTp- 75.91
C3′ -pm6dU 71.98
Dioxane
C5′-pm6dU 67.30
C5′ dTp- 62.41
C2′dTp-38.72
C2′ -pm6dU 38.31

TABLE 4.19

CARBON CHEMICAL SHIFTS AND CARBON-PHOSPHORUS COUPLING CONSTANTS FOR d(m^6UpT) [a] AT pH = 7.1 [b]

δ [d] T [c]	300 K		320 K		330 K		340 K	
	m^6dUp-	-pdT	m^6dUp-	-pdT	m^6dUp-	-pdT	m^6dUp-	-pdT
$\delta(CH_3)$	20.97	13.11	20.90	13.07	20.86	13.01	20.79	12.99
δ(2')	37.26	39.86	37.25	39.88	37.23	39.92	37.22	39.94
δ(5')	62.86	66.57	62.89	66.53	62.94	66.51	62.97	66.52
δ(3')	76.17	72.01	76.24	72.02	76.33	72.04	76.42	72.07
δ(4')	86.25	86.60	86.29	86.52	86.40	86.58	86.43	86.61
δ(1')	86.79	86.50	86.80	86.50	86.91	86.56	86.95	86.52
δ(5)	103.87	112.75	103.90	112.77	103.91	112.79	103.96	112.77
δ(6)	157.08	138.66	157.10	138.46	156.91	138.43	156.50	138.34
δ(2)	152.51	154.06	152.67	154.31	151.76	154.56	151.64	154.71
δ(4)	169.19	168.97	169.20	168.97	169.18	168.96	169.18	168.94
^2J(C3'-P) [e]	5.3	———	5.3	———	5.2	———	5.1	———
^2J(C5'-P)	———	4.9	———	4.9	———	4.9	———	5.3
^3J(C2'-P)	1.8	———	2.3	———	2.8	———	3.1	———
^3J(C4'-P)	7.2	8.5	8.0	8.2	8.2	8.9	7.8	8.6

———

a) Sample was 100 mgs dissolved in 1 ml D_2O, prepared as described in Chapter III, and contained 1% dioxane as internal reference.

b) Uncorrected for the deuterium isotope effect and measured at 297 K.

c) Accurate to better than $\pm$1 K

CONTINUATION OF FOOTNOTES FOR TABLE 4.19

d) In ppm downfield from external TMS by setting the chemical shift of the internal dioxane to 67.859 ppm. Estimated accuracy $\pm$0.01 ppm.

e) In Hz. Estimated accuracy $\pm$0.2 Hz.

TABLE 4.20

CARBON CHEMICAL SHIFTS AND CARBON-PHOSPHORUS COUPLING CONSTANTS FOR d(m^6Upm^6U) [a] AT pH = 6.6 [b]

δ [d] T [c]	297 K		315 K		330 K		340 K	
	m^6dUp-	-pm^6dU	m^6dUp-	-pm^6dU	m^6dUp-	-pm^6dU	m^6dUp-	-pm^6dU
$\delta(CH_3)$	21.07		21.02		20.99		20.94	
δ(2')	36.54	37.95	36.65	37.96	36.74	38.00	36.79	38.01
δ(5')	62.81	66.24	62.86	66.39	62.90	66.49	62.93	66.55
δ(3')	76.42	71.17	76.53	71.43	76.51	71.63	76.21	71.75
δ(4')	86.89	85.61	86.70	85.72	86.72	85.80	86.73	85.87
δ(1')	87.21	86.53	87.20	86.62	87.20	86.69	87.20	86.71
δ(5)	(103.81 [e]	103.39)	(103.82 [e]	103.47)	(103.82 [e]	103.53)	(103.85 [e]	103.57)
δ(2)	(152.88 [e]	152.66)	(152.95 [e]	152.70)	(152.98 [e]	152.78)	152.90	
δ(6)	(157.62 [e]	157.54)	(157.63 [e]	157.51)	(157.62 [e]	157.49)	(157.56 [e]	157.43)
δ(4)	(167.07 [e]	166.84)	(167.01 [e]	166.79)	166.79		166.76	
^2J(C3'-P) [f]	5.2	———	5.4	———	5.5	———	5.3	———
^2J(C5'-P)	———	5.5	———	5.4	———	5.4	———	5.5
^3J(C2'-P)	2.3	———	2.7	———	2.8	———	3.1	———
^3J(C4'-P)	7.4	8.7	7.5	8.6	7.4	8.6	7.4	8.3

a) Sample was 100 mgs dissolved in 1 ml D_2O, prepared as described in Chapter III, and contained 1% dioxane as internal reference.

b) Uncorrected for the deuterium isotope effect and measured at 297 K.

c) Accurate to better than $\pm$1 K

CONTINUATION OF FOOTNOTES FOR TABLE 4.20

d) In ppm downfield from external TMS by setting the chemical shift of the internal dioxane to 67.859 ppm. Estimated accuracy $\pm$0.01 ppm.

e) It is impossible to definitely assign either of the observed resonances to a specific residue without specific enrichment of one of the nucleotide residues.

f) In Hz. Estimated accuracy $\pm$0.2 Hz.

TABLE 4.21

CARBON CHEMICAL SHIFTS AND CARBON-PHOSPHORUS COUPLING CONSTANTS FOR THE INTERNAL CYCLOBUTANE PHOTODIMER OF d(TpT) [a] AT pH = 6.5 [b]

δ [d] T [c]	300 K		315 K		330 K		345 K	
	dT(p)-	-(p)dT	dT(p)-	-(p)dT	dT(p)-	-(p)dT	dT(p)-	-(p)dT
$\delta(CH_3)$	18.21		(18.75 [e] 18.64)		(18.64 [e] 18.80)		(18.42 [e] 18.62)	
$\delta(2')$	34.64	37.34	35.13	37.93	35.23	38.07	35.10	37.94
$\delta(5')$	62.42	66.73	62.85	67.17	62.85	67.15	62.65	66.94
$\delta(3')$	76.90	70.08	77.09	70.54	76.87	70.56	76.48	70.38
$\delta(4')$	(84.33 [e] 84.19)		(84.80 [e] 84.70)		(84.88 [e] 84.75)		(84.67 [e] 84.58)	
$\delta(1')$	(88.68 [e] 86.54)		(88.90 [e] 86.97)		(88.71 [e] 86.97)		(88.35 [e] 86.75)	
$\delta(5)$	(52.18 [e] 47.57)		(52.56 [e] 48.24)		(52.52 [e] 48.44)		(52.27 [e] 48.42)	
$\delta(6)$	(61.09 [e] 56.59)		(61.39 [e] 57.12)		(61.27 [e] 57.21)		(60.97 [e] 57.07)	
$\delta(2)$	(155.84 [e] 155.17)		(156.30 [e] 155.66)		(156.28 [e] 155.69)		(156.01 [e] 155.47)	
$\delta(4)$	(174.98 [e] 173.95)		(175.39 [e] 174.42)		(175.33 [e] 174.40)		(175.09 [e] 174.16)	
$^2J(C3'-P)$ [f]	5.9	———	5.8	———	5.9	———	5.7	———
$^2J(C5'-P)$	———	5.9	———	5.8	———	6.0	———	5.8
$^3J(C2'-P)$	3.9	———	3.7	———	2.9	———	3.2	———
$^3J(C4'-P)$	(7.71 [e] 8.0)		(7.7 [e] 7.9)		(7.8 [e] 7.9)		(7.7 [e] 7.9)	

———

a) Sample was 100 mgs dissolved in 1 ml D_2O, prepared as described in Chapter III, and contained 1% dioxane as internal reference.

b) Uncorrected for the deuterium isotope effect and measured at 297 K.

c) Accurate to better than ± 1 K

CONTINUATION OF FOOTNOTES FOR TABLE 4.21

d) In ppm downfield from external TMS by setting the chemical shift of the internal dioxane to 67.859 ppm. Estimated accuracy $\pm$0.01 ppm.

e) It is impossible to definitely assign either of the observed resonances to a specific residue without specific enrichment of one of the nucleotide residues.

f) In Hz. Estimated accuracy $\pm$0.2 Hz.

FIGURE 4.12 is the observed carbon-13 spectrum of the ribose carbons and the two C_6 and two C_5 carbons from the pyrimidine ring of the major internal cyclobutane photodimer of d(TpT) at 315 K and pH = 6.5. Sample is 100 mgs of d(T(p)T) in 1 ml D_2O, prepared as described in Chapter III. Shifts are taken from a similar sample containing dioxane and are relative to external TMS as described for Figure 4.8.

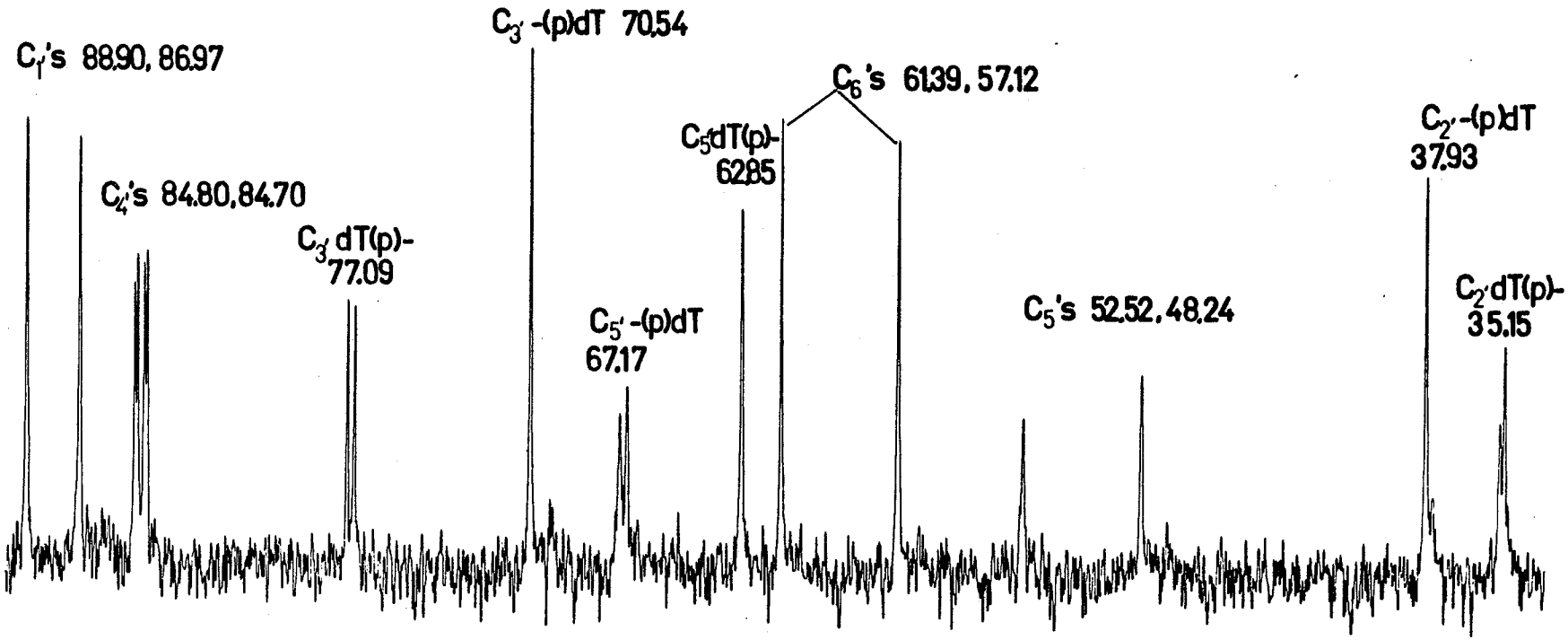
C1's 88.90, 86.97
C4's 84.80, 84.70
C3' dT(p)- 77.09
C3' -(p)dT 70.54
C5' -(p)dT 67.17
C5dT(p)- 62.85
C6's 61.39, 57.12
C5's 52.52, 48.24
C2' -(p)dT 37.93
C2'dT(p)- 35.15

CHAPTER V

DISCUSSION

A. N-GLYCOSYL BOND CONFORMATION

As discussed in Chapter II, pyrimidine nucleosides and nucleotides substituted at other than the 6-position are expected to favor the anti conformation about the N-glycosyl bond[69-73]. Substitution with a bulky group at C-6 of a pyrimidine, however, forces the molecule to adopt a syn conformation[6,126]. This has been verified in the solid state[135] where $\chi = 62.3^{o}$ (see Figure 2.3) was determined. From the structural information obtained[135], it was clear that the anti conformation would bring one of the methyl hydrogens to within < 2Å of either $H_{2'}$ or $O_{1'}$. Since the interatomic distance between $H_{2'}$ and $O_{1'}$ was only 2.3Å, Birnbaum et al.[135] concluded that a syn-anti equilibrium in solution for m^6dU was unlikely. Thus, the m^6dU molecules are good model compounds to study the effect of the syn conformation on the overall conformation of deoxyribo pyrimidine derivatives.

1. CHEMICAL SHIFTS

a. PROTON CHEMICAL SHIFTS

Previous ^1H NMR studies have shown that m^6dU[73,76] and its phosphorylated analogues[73] exhibit the characteristic chemical shift differences, from the corresponding 5-methyl derivatives, imposed by the location of the 2-keto group over the ribose ring[72]. Extending these studies, ^1H NMR data presented here (Tables 4.3 to 4.8) for four dinucleoside monophosphates incorporating dT and/or m^6dU indicate that the N-glycosyl bond conformation in the m^6dU moiety is not affected by incorporation into a dinucleoside monophosphate. Table 5.1

contains the chemical shift differences ($\Delta\delta$) between the ribose protons in m^6dU and dT for the nucleoside[73,76], mononucleotides[73], nucleoside diphosphate, and the dinucleoside monophosphates. The differences, in general, are consistent with the retention of the syn conformation of the m^6dU fragment. For example, an average downfield shift of 0.59 ppm is observed for $H_{2'}$ in a m^6dU fragment relative to a corresponding dT fragment. Shift differences for $H_{1'}$, $H_{2''}$, $H_{3'}$, and $H_{4'}$ are smaller and either positive or negative (averages -0.11, -0.08, +0.03, and -0.14 ppm, respectively) and deviations in these differences may be reflecting other conformational changes (see Section V.C.1.a(iii)). Anomalous differences for $H_{2'}$ between $d(Tpm^6U)$ and d(TpT) of +0.5 ppm and for $H_{2'}$ between $d(m^6Upm^6U)$ and $d(Tpm^6U)$ of +0.7 ppm (see Table 5.1), for example, are probably a reflection of the change in the ribose pucker equilibrium.

As Table 5.1 indicates, only minor variations $\Delta\delta$ for $H_{2'}$ occur in the series of molecules studied. This proton is the best chemical shift indicator for the syn-anti equilibrium since it is on the same side of the deoxyribose ring as the base and is proximate to both the 2-keto group (for a syn conformation) and the C_6-H part of the base (for an anti conformation).

b. CARBON-13 CHEMICAL SHIFTS

Table 5.2 contains an analogous examination of the ribose carbon chemical shifts, as presented above for proton chemical shifts. As can be seen in this table, $C_{2'}$ is shifted upfield by an average of 1.86 ppm when going from a dT fragment to an m^6dU fragment in a

TABLE 5.1

PROTON CHEMICAL SHIFT DIFFERENCES ($\Delta\delta$) [a]
BETWEEN dT and m^6dU FOR A SERIES OF DERIVATIVES

	$\Delta\delta$(H2')	$\Delta\delta$(H2'')	$\Delta\delta$(H3')	$\Delta\delta$(H4')	$\Delta\delta$(H1')
m^6dU - dT	+0.58	-0.12	+0.06	-0.10	-0.10
3'-m^6dUMP - 3'-dTMP	+0.59	-0.13	+0.04	-0.15	-0.10
5'-m^6dUMP - 5'-dTMP	+0.57	-0.11	+0.01	-0.18	-0.13
3',5'-m^6dUDP - 3',5'-dTDP [b]	+0.62	-0.06	——— c	-0.20	-0.14
3',5'-m^6dUDP - 3',5'-dTDP [d]	+0.61	-0.04	——— c	-0.18	-0.14
d(Tpm^6U - d(TpT)	+0.50	-0.14	-0.03	-0.08	-0.11
d(m^6UdT) - d(TpT)	+0.63	-0.10	——— c	-0.10	-0.01
d(m^6Upm^6U) - d(Tpm^6U)	+0.70	+0.04	——— c	-0.04	-0.09
d(m^6Upm^6U) - d(m^6UpT)	+0.53	-0.05	+0.09	-0.26	-0.14

a) Values quoted are ppm. The shift difference is defined as the chemical shift of a given proton in the m^6dU fragment minus the corresponding chemical shift in the dT fragment. A positive value indicates a shift to low field.

b) At pH ≃ 3.6

c) Not available

d) At pH ≃ 7.4

TABLE 5.2

CARBON CHEMICAL SHIFT DIFFERENCES ($\Delta\delta$) [a]
BETWEEN dT AND m^6dU FOR A SERIES OF DERIVATIVES[b]

	$\Delta\delta$(C1')	$\Delta\delta$(C2')	$\Delta\delta$(C3')	$\Delta\delta$(C4')	$\Delta\delta$(C5')
m^6dU - dT	+0.65	-1.88	+0.33	-0.29	+0.53
3'-m^6dUMP - 3'-dTMP	+0.75	-1.78	+0.10	-0.42	+0.45
5'-m^6dUMP - 5'-dTMP	+0.50	-2.16	-0.36	-0.84	+0.44
3',5'-m^6dUDP - 3',5'-dTDP	+0.57	-2.07	-0.84	-0.98	-0.02
d(Tp$\underline{m^6U}$) - d(Tp$\underline{T}$)	+0.69	-1.60	+0.10	-0.12	+1.22
d($\underline{m^6U}$pT) - d($\underline{T}$pT)	+0.31	-1.65	-0.18	-0.58	+0.52
d($\underline{m^6U}$pm^6U) - d($\underline{T}$pm^6U)	+1.28	-2.17	+0.54	+0.08	+0.50
d(m^6Up$\underline{m^6U}$) - d(m^6Up$\underline{T}$)	+0.03	-1.91	-0.84	-0.99	+0.33

a) Values quoted are ppm. The shift difference is defined as the chemical shift of a given carbon in the m^6dU fragment minus the corresponding chemical shift in the dT fragment. A positive value indicates a shift to low field.

b) Data are from Tables 4.11 to 4.20 and are at pH < 6.0 and 300 K for the nucleotides and pH ≃ 6.5 and T = 300 K for the dinucleoside monophosphate.

similar molecular situation. This shift is similar to the observed shift difference of -4.9 ppm [72,117] between m^6C and C. The spectrum of m^6C was recorded in DMSO-d_6 for the ribose analogue, and the shift difference, larger than that observed here for the deoxy series, may reflect a number of changes in the electron environment of $C_{2'}$ in m^6dU and m^6C. The carbon chemical shift changes are in the opposite direction to the proton shift changes observed for the directly bonded proton (comparing Tables 5.1 and 5.2) as was observed by Schweizer et al.[72]. Also, there is no clear trend for the carbons other than $C_{2'}$, as was also observed in other studies[6,47-50]. Generally speaking, the observed carbon chemical shift change appears more sensitive to structural changes than the proton chemical shifts. There appears to be an overall consistency of the deoxyribose shifts resulting from structural changes such as phosphorylation and dimerization similar to carbon chemical shift changes in ribose derivatives[51,119,153-155], independent of the nature of the base (see below). The comparatively minor variations in chemical shift for $C_{1'}$, $C_{3'}$, $C_{4'}$, and $C_{5'}$ are probably monitoring conformational changes in addition to variations in the N-glycosyl bond conformation (see Table 5.2).

2. SPIN-SPIN COUPLING CONSTANTS

a. LONG-RANGE PROTON-PROTON COUPLING CONSTANTS

The molecular structure of the nucleoside and nucleotide derivatives precluded the observation of four- or five-bond long range H-H couplings, as observed for uridine[79,80]. For example, the

coupling analogous to ^5J(H5-H1') in uridine is ^6J(H1'-CH_3) in dT. In m^6dU, the possibility of ^5J(H5-H1') is present, but this coupling is expected to be small or zero for a predominant syn conformation about the N-glycosyl bond[81,82], as is the case in m^6dU. There appears to be some broadening of the $H_{1'}$ and CH_3 lines in the m^6dU derivatives, but no attempt was made to fit this broadening to a small (probably <0.3 Hz) coupling between these protons.

b. PROTON-CARBON VICINAL SPIN-SPIN COUPLING CONSTANTS

i. Qualitative Evaluation

Table 5.3 reproduces the part of Table 4.10 which contains the proton-carbon vicinal coupling constant information relevant to the N-glycosyl bond conformation. Included in this table are the values for cytidine and m^6C [117] for purposes of comparison. (In this work[117], only ^3J(H1'-C2) values were reported.) Technical difficulties including signal overlap, and low signal-to-noise ratio for the available samples, precluded the determination of similar data for the nucleoside diphosphates and dinucleoside monophosphates.

As can be seen, the qualitative relationship of Davies[6,53] (i.e., that ^3J(H1'-C2) > ^3J(H1'-C6) for a molecule predominantly in the syn conformation) is observed for m^6dU and its 3'- and 5'-phosphates. In fact, little variation in the two proton-carbon vicinal coupling constants is seen for the three molecules, consistent with the proposed fixed conformation in solution predicted from the X-ray data[135]. In the dT derivatives presented, however, the appropriate inequality (i.e., ^3J(H1'-C6) > ^3J(H1'-C2), for a predominant anti conformation) is only

TABLE 5.3

PROTON-CARBON VICINAL SPIN-SPIN COUPLING CONSTANTS FOR dT AND m^6dU AND THEIR MONOPHOSPHATES[a]

	^3J(H1'-C2)	^3J(H1'-C6)
dT	2.1	3.8
3'-dTMP	2.4	4.4
5'-dTMP	2.2	3.6
C [b]	3 ± 1	——
m^6dU	6.8	3.0
3'-m^6dUMP	6.7	3.2
5'-m^6dUMP	6.2	3.0
m^6C [b]	6 ± 1	——

a) Data in Hz from Table 4.10 unless otherwise noted.

b) From Reference 115

just observed. The slightly larger magnitude of ^3J(H1'-C6) reflects the conformational equilibrium between the anti and syn forms in which the anti form dominates slightly. The NOE studies of Hart and Davis[74,75] and Nanda et al.[83] support the idea of a conformer interconversion. The data on the pyrimidine nucleosides[74,75], for example, suggested that uridine and cytidine favor the anti conformer more than in the 2',3'-isopropyridine derivatives, which were found to favor the syn conformation[75].

ii. Quantitative Evaluation

A reliable and unambiguous method of estimating the populations of purine or pyrimidine ring conformations about the N-glycosyl bond is still needed. In principle, if the values of the proton-carbon vicinal coupling constants in the pure syn and anti conformations were available, the observed couplings could be used to estimate the conformer populations, as is done for the sugar ring pucker and the backbone conformers.

It would appear that the observed ^3J(H1'-C2) and ^3J(H1'-C6) values in m^6dU are good estimates of the couplings expected in the syn conformation in pyrimidine nucleosides like dT. Lemieux and coworkers[52,115] measured ^3J(H1'-C2) in a series of ^{13}C-2 enriched cyclic nucleosides[52]. For 2,5'-O-anhydro-2',3'-O-isopropylidenecyclouridine, $\chi = 50^o$ and ^3J(H1'-C2) = 6.6 Hz, which is within experimental error of the value observed in m^6dU and m^6C [115] despite the functional change in the C_2 carbon. Starting with the observed vicinal proton-carbon coupling constants in m^6dU, an attempt can be made to fit the observed

vicinal coupling constants in dT to syn and anti conformer populations. If it is assumed that the stable anti conformer in the dT series corresponds to a 180° rotation of the pyrimidine ring in m^6dU, the angle corresponding to $\chi = 242^\circ$ (i.e., χ(Davies) $\simeq 60^\circ$ [53]) is used in Davies' Karplus plots[53]. Approximate ^3J_A(H1'-C2) and ^3J_A(H1'-C6) values for the "pure" anti conformer of 4.6 and 8.0 Hz, respectively, are obtained for this angle. The value for ^3J_A(H1'-C2) is larger than the observed vicinal coupling constant and cannot be used in the conformer population analysis. If, instead, an N-glycosyl torsion angle in the range of the observed angle in the crystal state for anti nucleosides is used (see, for example, the crystal structure of m^5U [156] and the structures for other anti nucleosides[157]), better anti conformer coupling constants can be obtained. Choosing $\chi = 285^\circ$ and using this value in Davies' plots[53], values of 2.0 and 4.0 Hz for ^3J(H1'-C2) and ^3J(H1'-C6) in the "pure" anti are obtained. (It is known that the proton-carbon vicinal coupling constant is smaller in the cis than the trans conformation[158].) Although the choice of the angle (and hence the coupling constants) is arbitrary, and designed to give reasonable results, there is no a priori reason that the syn and anti conformers are separated by 180°. The values of 2.0 and 4.0 Hz for ^3J_A(H1'-C2) and ^3J_A(H1'-C6), respectively, for the "pure" anti conformer coupling constants and the average of the observed couplings in the m^6dU derivatives of 6.5 and 3.0 Hz for ^3J_S(H1'-C2) and ^3J_S(H1'-C6), respectively, for the "pure" syn conformer coupling

constants can be used to see if a rough estimate of the N-glycosyl conformer populations can be obtained. The following standard expressions can be formulated for the two observed proton-carbon vicinal coupling constants in dT.

$$^{3}J(H1'\text{-}C2) = {}^{A}_{X}\ {}^{3}J_{A}(H1'\text{-}C2) + {}^{S}_{X}\ J_{S}(H1'\text{-}C2)$$

$$2.1 = 2.0\ {}^{A}_{X} + 6.5(1 - {}^{A}_{X})$$

$${}^{A}_{X} = 0.98$$

and

$$^{3}J(H1'\text{-}C6) = {}^{A}_{X}\ {}^{3}J_{A}(H1'\text{-}C6) + {}^{S}_{X}\ {}^{3}J_{S}(H1'\text{-}C6)$$

$$3.8 = 4.0\ {}^{A}_{X} + (1 - {}^{A}_{X})3.0$$

$${}^{A}_{X} = 0.8$$

This rough agreement is expected, considering the assumptions needed to arrive at these results. The use of $\chi = 285^{o}$ is arbitrary, and was chosen to give reasonable populations from the observed couplings. (A value of $^{3}J_{A}(H1'\text{-}C2) > 2.1$ would result in a calculated ${}^{A}_{X} > 1$ from the observed $^{3}J(H1'\text{-}C2)$.) It is also important to remember the approximate nature of the angular dependence of the two vicinal coupling constants[53], as pointed out by Davies[6]. In addition, if the syn and anti potential minima are composed of a number of nearly isoenergetic conformations, the observed couplings would be an average of the different conformers within the syn and anti conformational minima. A proper investigation, which parameterizes the two vicinal

couplings, combined with at least a theoretical investigation to determine the shape and width of the conformational wells for the syn and anti conformers, is needed before even a semi-quantitative estimate can be made from these expressions.

Some calculations on the relative syn and anti conformational energies have been made. Early studies by Nanda et al.[83] have used CNDO methods to calculate the energy surface for rotation of the N-glycosyl bond in β-pseudouridine. The calculations were performed for both ^3E and ^2E sugar puckers (keeping ϕ fixed at t and ψ fixed at g_+). The results showed a much lower overall potential energy for the ^3E (type-N) sugar when rotating the N-glycosyl bond. The calculations also found two potential minima at $\chi = 180^\circ$ and $\chi = 60^\circ$ (in type-S or ^2E sugars). The latter angle (corresponding to the syn conformation) was calculated to be 38 kJ mole^{-1} lower in energy than the former angle for a type-S sugar.

Pullman and Saran have recently summarized the energy calculations of purine and pyrimidine nucleosides and nucleotides[159]. Generally, the potential energy and molecular orbital type (i.e., EHT, extended Hückel theory; CNDO, complete neglect of differential overlap; INDO, intermediate neglect of differential overlap; and PCILO, perturbative configuration interaction with localized orbitals) calculations reach the same conclusions. For a type-N (^3E) sugar, the anti form is allowed while for a type-S (^2E) sugar, both anti and syn conformations are permitted. Berthod and Pullman[160] have also calculated the effect of the $O_{5'}$—$C_{5'}$ bond and $C_{2'}$—$O_{2'}$ bond conformations on the syn-anti

conformational energies in nucleotides. In their study[160], stabilizing effects were found for particular conformations of these bonds. The results show that interactions between the $C_{5'}$—$O_{5'}$H bond and the 2-keto group of pyrimidine nucleosides will result in a stabilization of the pyrimidine anti conformer while similar interactions between the $C_{2'}$—$O_{2'}$H bond and the 2-keto group stabilize the syn conformer (The latter case is valid for the ribose series only). The contour of the potential surface for the pyrimidines is not well defined. The conformational energy maps for some of the pyrimidines studied[159] show a broad minimum about either the syn or anti conformers, indicating the possibility of a family of conformations which are nearly isoenergetic.

The problems with deriving expressions similar to those above, relating the syn-anti equilibrium to observed magnitudes of ^3J(H1'-C2) and/or ^3J(H1'-C6), are numerous. For example, characterizing the "minimum" syn or anti conformations in solution, the contour of the potential energy surface near these "minima", and what contribution intermediate conformations make to the observed coupling, are the major unanswered questions inhibiting the formulation of a generally applicable method of determining the syn-anti equilibrium from observed proton-carbon vicinal spin-spin coupling constants. In addition, ^3J(H-C) coupling constants are sensitive to the orientation of substituents, and the contributions from the orientation effects can be sizable[161,162].

B. DEOXYRIBOSE RING CONFORMATION

1. PSEUDOROTATIONAL ANALYSIS

a. STANDARD PSEUDOROTATIONAL ANALYSIS

Table 5.4 shows the vicinal proton-proton coupling constants required for the Altona-Sundaralingam[98] pseudorotational analysis, as described by Guschlbauer and Son[99] and Davies[6], of the deoxyribose ring conformation, together with the parameters derived from this analysis. This table contains the data on the nucleosides[29,73.76], mononucleotides[73], nucleoside diphosphates, and dinucleoside monophosphates of both dT and m^6dU. The coupling constant data in Table 5.4 for this series of deoxy sugars has been corrected for the electronegativity difference of the 2'-substituent (-H vs -OH), as suggested by Davies[6] (i.e., 1.1 Hz has been subtracted from the ^3J(H1'-H2') and ^3J(H2'-H3') values in Table 5.4). No correction has been made for the slight difference in electronegativity of the bases of dT and m^6dU. (This difference is apparent in the small chemical shift differences between $H_{1'}$ and $C_{1'}$ of dT compared with m^6dU, as noted above.) The electronegativity difference is expected to contribute less than 0.2 Hz to the observed coupling constants involving $H_{1'}$ in the pyrimidine to purine transition[77a]. The chemical shift difference in the pyrimidine to purine transition is larger than that observed here, and, therefore, the contribution is probably less.

The first observation that can be made concerning the data in Table 5.4 is that the invariance conditions[6] noted in Section II.B.2

TABLE 5.4

DEOXYRIBOSE RING PROTON-PROTON COUPLING CONSTANTS FOR THE dT AND m^6dU SERIES AND THE CALCULATED PSEUDOROTATIONAL PARAMETERS[a]

	Σ^* [b]	$^3J(2'-3')$	$^3J(3'-4')$	N_P	S_P	τ_m	$N_{X_{PLOT}}$ [c]	$N_{X_{EMP}}$ [d]
dT [e]	—— [f]	——	4.1	——	——	——	——	0.41
3'-dTMP [e]	10.1	5.7	4.0	20^o	160^o	41^o	0.39	0.40
5'-dTMP [g]	9.5	5.5	3.0	13^o	167^o	40^o	0.30	0.29
3',5'-dTDP [h]	9.4	5.0	2.3	6^o	174^o	44^o	0.26	0.24
	(9.5)	(4.8)	(2.4)	(3^o)	(176^o)	(44^o)	(0.26)	(0.25)
d(TpT)	9.3	5.9	3.5	5^o	175^o	43^o	0.38	0.38
d(TpT)	—— [f]	——	3.5	——	——	——	——	0.35
$d(Tpm^6U)$	10.1	6.2	3.6	26^o	154^o	39^o	0.40	0.36
$d(m^6UpT)$	—— [f]	——	4.2	——	——	——	——	0.42
m^6dU [i]	9.1	7.2	5.9	21^o	159^o	31^o	0.54	0.57
$3'-m^6dUMP$ [i]	9.3	7.0	5.8	21^o	159^o	32^o	0.50	0.56
$5'-m^6dUMP$ [i]	9.9	7.4	5.9	33^o	147^o	32^o	0.64	0.54
$3',5'-m^6dUDP$ [h]	10.0	7.3	6.1	33^o	147^o	33^o	0.61	0.55
	(10.0)	(7.2)	(5.7)	(31^o)	(149^o)	(34^o)	(0.55)	(0.51)
$d(m^6Upm^6U)$	11.2	5.0	4.8	32^o	148^o	50^o	0.40	0.39
$d(m^6Upm^6U)$	9.8	7.8	6.9	36^o	144^o	29^o	0.75	0.63
$d(m^6UpT)$ [j]	9.8	7.4	5.5	32^o	148^o	32^o	0.52	0.50
	(9.9)	(6.8)	(5.3)	(27^o)	(153^o)	(35^o)	(0.56)	(0.48)

TABLE 5.4 (CONTINUED)

	Σ^* [b]	$^3J(2'-3')$	$^3J(3'-4')$	N_P	S_P	τ_m	$N_{X_{PLOT}}$ [c]	$N_{X_{EMO}}$ [d]
d(Tpm^{6}U) [j]	9.7	7.9	7.1	36°	144°	28°	0.85	0.66
	(9.6)	(7.6)	(6.5)	(32°)	(148°)	(30°)	(0.74)	(0.61)

---

a) Coupling constants in Hz for samples at pH ∿6.5 and T = 293 K unless otherwise noted.

b) $\Sigma^* = (^3J(H1'-H2') + {}^3J(H3'-H4'))$ in Hz.

c) Calculated from the published plots[6,99] as described in text.

d) Calculated by the empirical expressions as described in the text.

e) From Reference 29

f) Not available

g) From Reference 77a

h) At T = 293 K and pH ∿3.4. Numbers in parenthesis at pH ∿7.4.

i) From Reference 73

j) Numbers in parenthesis for T = 333 K

are not met for the quoted data. In the dT series, the sum of the trans couplings Σ^* (i.e., (^3J(H1'-H2') + ^3J(H3'-H4')) varies between 9.4 and 10.1 Hz, and ^3J(H2'-H3') varies between 4.9 and 6.2 Hz. In the m^6dU series, Σ^* varies between 9.1 and 11.2 Hz while ^3J(H2'-H3') varies between 5.0 and 7.9 Hz. A discussion of the significance of these variations is deferred for the present.

Some interesting features can be seen in the tabulated P and τ_m values in Table 5.4. Upon examining the phase angles of pseudorotation, P, the molecules in the dT series appear to adopt the N⇌S equilibrium normally ascribed to nucleosides[67,77,98] and nucleotidyl fragments[6]. ^N_P values in the range of 5° to 26° and ^S_P values in the range of 154° to 175° are consistent with the ranges observed in the solid state[67] and in solution[77,98]. In addition, the amplitude of pucker, τ_m, observed for the dT derivatives, falls in the narrow range of 39° to 44°, again consistent with previous observations[6,67,77,98]. In the m^6dU derivatives, however, the calculated P and τ_m values differ substantially compared to the dT series and other results[77,98]. ^N_P values between 21° and 36°, coupled with ^S_P values between 144° and 159°, are at the upper and lower limits of the respective ranges in the dT series. Indeed, it would appear that the conformational equilibrium for the deoxyribose sugar in the m^6dU series is now between the $^3T_4$ and $^2T_1$ states (see Figure 2.5) if the P values in Table 5.4 are accurate estimates of the equilibrium conformers. It is interesting to note that the latter conformation for the m^6dU series is that observed in the solid state[135] for m^6dU. The amplitude of pucker, τ_m,

observed in the m^6dU series ranges between 28^o and 35^o (except for the m^6dUp- part of $d(m^6Upm^6U)$ where $\tau_m = 50^o$), significantly lower than those observed in the dT series. The values in solution (average τ_m = 31.6^o), excluding the anomalous value for the m^6dUp- part of $d(m^6Upm^6U)$ for the m^6dU series, compares well to that found in the crystal ($\tau_m = 31.8^o$)[135].

Turning now to the conformer populations calculated for the dT and m^6dU derivatives, Table 5.4 contains the N-state populations (^NX) calculated from the graphs of Guschlbauer and Son[99] and Davies[6] and the populations calculated from empirical expressions[29,77a]. The empirical expressions relate the observed vicinal couplings to the N-state conformer by

$$^NX = \frac{^3J(H3'-H4')}{(^3J(H1'-H2') + ^3J(H3'-H4'))}$$

derived by Davies and Danyluk[77a]. In the case where $^3J(H1'-H2')$ is not available (e.g., dT, 5'-dTMP, and the -pdT parts of d(TpT) and $d(m^6UpT)$), the alternate expression

$$^NX = 9.8(^3J(H3'-H4'))$$

from Davies and Danyluk[77a] can be used. The ^NX values obtained from the plots were obtained by using the (corrected) $^3J(H1'-H2')$ values. An inspection of the ^NX values from the two methods in Table 5.4 shows that the values obtained by either method agree well for the dT series. In the m^6dU series, however, an inspection of the ^NX values shows that

the two methods differ by between .01 to .19 with an average difference of 0.08. The deviation cannot be due to the fact that the plots[6,99] were derived for ribose derivatives, and the electronegativity correction of Davies[6] is inappropriate. Otherwise, both sets of data for the dT and m^6dU series would disagree. Davies and Danyluk[77a] have calculated the pseudorotational parameters for a series of deoxynucleotides using three different parameterizations of the Karplus equation to reflect the electronegativity changes in the deoxyribose ring. Parameters and populations calculated by the three methods agree to within the accuracy of the experimental parameters. The answer to the discrepancies in the populations calculated for the m^6dU series could be related to the spread in observed Σ^* and ^3J(H2'-H3') values noted above. The invariance in these parameters is a result of the assumption that ^3J_N(H2'-H3') = ^3J_S(H2'-H3') or that ϕ_N(H2'-H3') = ϕ_S(H2'-H3') for the two conformational states involved in the equilibrium. This results from the observed conformers in the crystal state. In the pseudorotational analysis[6,98,99], it is assumed that $^N\tau_m \simeq {}^S\tau_m$ and that $^SP \simeq 180^o - {}^NP$, which would preserve the equality of ϕ_N(H2'-H3') and ϕ_S(H2'-H3') (and results in ϕ_S(H1'-H2') = ϕ_N(H3'-H4'), thus requiring Σ^* to be invariant). The 2.1 Hz spread in Σ^* and 2.9 Hz spread in ^3J(H2'-H3') suggests that the aforementioned angular equalities no longer hold. Different values of ϕ(H2'-H3') in the N- and S-states can account for the variation of ^3J(H2'-H3'). A similar inequality of ϕ_S(H1'-H2') and ϕ_N(H3'-H4') will account for the spread in the observed sum Σ^*.

b. MODIFIED PSEUDOROTATIONAL ANALYSIS

Recently, Birnbaum et al.[135,163] have modified the normal pseudorotational analysis to take into account unusual ring puckers observed in the crystal structures of deoxyribonucleosides. In a study of 5-iodo-5'-amino-2',5'-dideoxyuridine, Birnbaum and co-workers[163] found better agreement between observed and calculated coupling constants by assuming a three-state equilibrium between ^3E, ^2E, and ^oE sugar puckers (see Figure 2.5) in the ratio of 25:55:20. The O-endo (^oE) conformation was included because of its presence in the crystal structure of the zwitterionic nucleoside (protonated 5'-amino group and ionized N-3 of the pyrimidine ring). In this molecule, the observed ^3J(H2'-H3') was better estimated by the three-state equilibrium than by the conventional $^3E \rightleftharpoons {}^2E$ (at a ratio of 34:64) equilibrium.

In a re-examination of the ribose coupling constants for m^6dU in DMSO[73], Birnbaum et al.[135] chose to redefine the equilibrium conformers in this molecule. Assuming a 60:40 blend of $_1T^2$ and ^3E conformers, coupling constants were calculated using A = 11.7, B = +0.4, and C = 0 in Equation 2.2. Substituting the proton-proton dihedral angles obtained from the X-ray analysis into this equation, and invoking the usual assumptions used for a two-site equilibrium (see II.B.2), the coupling constants in Table 5.5 were obtained. Included in Table 5.5 are the observed values of m^6dU in DMSO[73] and those predicted for a 50:50 mixture of ^2E and ^3E conformers[77a]. As can be seen, the predicted values for the $_1T^2 \rightleftharpoons {}^3E$ equilibrium are in better agreement with the observed values than those predicted from the $^2E \rightleftharpoons {}^3E$ blend.

TABLE 5.5

OBSERVED AND CALCULATED VICINAL COUPLING CONSTANTS FOR m^6dU IN DMSO

PROTONS	J^{DMSO}_{OBS}	ϕ_{X-RAY}	$^3J(_1T^2:{}^3E)$ [a]	$^3J(^2E:{}^3E)$ [b]
1'-2'	5.7	154	6.0	5.5
1'-2"	8.0	32	8.0	6.8
2'-3'	7.8	26	7.6	5.6
2"-3'	5.3	96	4.6	5.9
3'-4'	5.6	112	5.2	5.3

a) 60:40 for $_1T^2:{}^3E$

b) 50:50 for $^3E:{}^2E$

Again, the worst agreement between the observed and calculated coupling constants from the ^3E-^2E equilibrium is for ^3J(H2'-H3'). The above two examples serve to demonstrate that modified conformer equilibria can better reproduce the observed vicinal coupling constants in the deoxyribose ring. The repeated discrepancy in the observed ^3J(H2'-H3') provides further support that the relation, ϕ_N(H2'-H3') = ϕ_S(H2'-H3'), is not necessarily universal, especially in the deoxysugars. Whether the use of the three-state equilibrium in the former example or different conformers in a two-state equilibrium in the latter example are unambiguous is unknown. It is possible that other combinations can yield similar agreement between the observed and calculated vicinal coupling constants in these two molecules, but more information is needed to clarify the situation.

In the X-ray analysis of the crystal structure of the tetranucleotide d(pApTpApT), Viswamitra et al.[164] concluded that the sugar in the deoxyribose ring is a "soft" parameter reflecting a low energy barrier between different conformations.

Recently, Levitt and Warshell[97] performed consistent force field calculations on ribose and deoxyribose derivatives, mimicking a pyrimidine nucleoside, and concluded that the pseudorotational barrier between N- and S-states is small (ca 1.5 kJ mole^{-1}). The potential surface for the range of conformers between ^3E and $_3E$ in Figure 2.5 is flat (varying by less than 4 kJ mole^{-1} over the entire range). The calculations predicted equal barriers between ^3E and ^2E conformers for the ribose and the deoxyribose sugars, and the C_1, substituent

(an amino group) does not accurately represent the presence of a pyrimidine ring. These calculations imply, however, that the ring puckered modes can easily change to adapt to changes elsewhere in the molecule. The original assumption of a $^3E \rightleftharpoons {}^2E$ equilibrium was not meant to exclude other conformational blends (see footnote 27 in reference 98). The authors[98] used this starting point based on observations of the predominance of these states in the crystal state[63]. The quantitative analysis of the deoxy-syn-nucleosides of the m^6dU series awaits the determination of the crystal structure for a sugar conformation of m^6dU in the N-state. The $^2T_1$ structure above[135] is probably being biased towards this state by the presence of a hydrogen bond between $C_{5'}—O_{5'}H$ and the 2-keto group of the pyrimidine[135]. The crystal structure of the 5'-nucleotide or a 5'-protected nucleoside might yield the desired N-type sugar.

The above observations place some doubt on the accuracy of a quantitative discussion of the deoxyribose conformational equilibrium derived from the observed vicinal coupling constants in the sugar ring. The observed $^3J(H3'-H4')$, however, may still be able to provide a basis for a qualitative discussion of the N-type and/or S-type conformer populations.

2. QUALITATIVE ANALYSIS

In the study of the m^6dU nucleoside and mononucleotides, George et al.[73] approached the ring pucker problem through a discussion of the magnitudes of the observed couplings. For m^6dU, 3'-m^6dUMP, and

5'-m^{6}dUMP, these workers[73] observed an increase in the cis couplings, ^{3}J(H1'-H2") and ^{3}J(H2'-H3'), indicating a bias of the torsion angles τ_1 (about $C_{1'}$—$C_{2'}$) and τ_2 (about $C_{2'}$—$C_{3'}$) towards the eclipsed position ($\tau_1 = \tau_2 = 0$). If this effect is due solely to a reduction in the amplitude of pucker, τ_m, then a concomitant increase in the sum (^{3}J(H1'-H2') + ^{3}J(H3'-H4')) is expected[98]. No appreciable increase was observed, implying a change in the N-type and/or S-type conformers. The authors[73] interpreted these observations as a reduction in the torsion about $C_{1'}$—$C_{2'}$ and $C_{2'}$—$C_{3'}$, implying that the flexibility of these bonds was decreased due to steric interactions between the 2-keto group and the endo ribose substituents, especially $H_{2'}$. A comparison of the data in Tables 4.1 to 4.8 indicates that this trend is continued in the molecules studied here. Table 5.6 contains the (uncorrected) relevant deoxyribose ring couplings from these tables. In the case of the -pm^{6}dU parts of d(m^{6}Upm^{6}U) and d(Tpm^{6}U), a further decrease in the cis couplings is observed. One is tempted to discuss additional flattening of the ring and a further shift of the equilibrium conformations, but the interpretation can be ambiguous. It has been pointed out that changes in τ_m are difficult to disentangle from changes in P [67].

The magnitude of ^{3}J(H3'-H4') is sensitive to the N$\rightleftharpoons$S equilibrium and approximately independent of the substituents on the furanose ring. The magnitude of ^{3}J(H3'-H4') is expected to be large in the N conformer and small in the S conformer[98,100]. In the dT series, ^{3}J(H3'-H4') is consistently less than 4 Hz. In the m^{6}dU series, this

TABLE 5.6

PROTON-PROTON VICINAL COUPLING CONSTANTS IN THE DEOXYRIBOSE RINGS IN A SERIES OF dT AND m^6dU DERIVATIVES[a]

	Σ*	$^3J(1'-2')$	$^3J(1'-2'')$	$^3J(2'-3')$	$^3J(2''-3')$	$^3J(3'-4')$
dT [b]	—— [c]	——	——	——	——	4.1
3'-dTMP [b]	10.2	7.2	6.5	6.8	3.7	4.0
5'-dTMP [d]	10.6	7.6	6.0	6.6	2.6	3.0
3',5'-dTDP [e]	10.5	8.2	6.0	6.1	2.3	2.3
3',5'-dTDP [f]	10.6	8.2	6.1	5.9	2.4	2.4
d(TpT)	10.4	6.9	6.5	7.0	3.8	3.5
d(TpT)	—— [c]	——	——	——	——	3.5
d(Tpm^{6}U)	11.2	7.0	6.8	7.1	3.6	4.2
	(10.6)	(7.1)	(6.8)	(7.3)	(3.7)	(3.6)
d(m^6UpT)	—— [c]	——	——	——	——	4.2
	—— [c]	——	——	——	——	(3.7)
m^6dU [g]	10.2	5.3	8.4	8.3	5.5	5.9
3'-m^6dUMP [g]	10.4	5.6	8.2	8.1	5.2	5.8
5'-m^6dUMP [g]	11.0	5.1	8.4	8.5	5.7	5.9
3',5'-m^6dUDP [e]	11.1	5.0	8.7	8.4	5.6	6.1
3',5'-m^6dUDP [f]	11.1	5.4	8.5	8.3	5.6	5.7
d(m^6Upm^{6}U)	12.3	7.5	6.4	6.1	4.9	4.8
d(m^6Upm^{6}U)	10.9	4.0	9.1	8.9	6.6	6.9
d(m^6UpT)	10.9	5.4	8.4	8.5	5.6	5.5
	(11.0)	(5.7)	(8.4)	(7.9)	(5.1)	(5.3)
d(Tpm^{6}U)	10.8	3.7	9.2	9.0	6.8	7.1
	(10.7)	(4.3)	(8.4)	(8.7)	(6.2)	(6.5)

FOOTNOTES FOR TABLE 5.6

a) In Hz at pH ∿6.5 and T = 293 K. Numbers in parenthesis at T = 333 K.

b) From Reference 29

c) Not available

d) From Reference 77a

e) At pH ∿3.5

f) At pH ∿7.4

g) From Reference 73

coupling is consistently larger than 5.7 Hz (except in the m^6dUp- part of d(m^6Upm^6U)). For the sake of a qualitative grasp of what is happening in solution in the m^6dU series, it is obvious that the ϕ(H3'-H4') torsion angle is, on the average, large in the m^6dU series, consistent with N-type conformers. An increase in ^{3}J(H3'-H4') implies an increase in the population of this state. The extent of the population changes is uncertain at present. Using this qualitative observation as a guide, it can be inferred that the N-type conformers are favored in the -pm^6dU fragments of d(m^6Upm^6U) and d(Tpm^6U) more than the corresponding 5'-nucleotide. On the other hand, the m^6dUp- parts of d(m^6Upm^6U) and d(m^6UpT) seem to have shifted their bias back towards the S-type conformer, relative to the 3'-nucleotide. In the case of the m^6dUp- part of d(m^6Upm^6U), the cis couplings ^{3}J(H1'-H2") and ^{3}J(H2"-H3') have decreased to values near those found in the dT series. This is accompanied by an increase in the sum (^{3}J(H1'-H2') + ^{3}J(H3'-H4')) to 12.3 Hz, at least 1 Hz larger than the sums observed in either the dT series or the other members of the m^6dU series. An explanation of the couplings in the 3'-nucleotidyl fragment in d(m^6Upm^6U) is not available, although it might be the result of the combined effects of decreased ring pucker and a return to the normal N- and S-type conformers.

An inspection of Table 5.6 reveals a relative consistency within the dT series. The ^{3}J(H3'-H4') values in the nucleoside, mononucleotides, and nucleotidyl fragments of the dinucleoside monophosphates in the dT series are between 3.0 and 4.2 Hz while ^{3}J(H3'-H4') in the

nucleoside diphosphate is 2.3 Hz and independent of pH. This indicates that there is little change in the conformational preference of the deoxy-sugars in the dT series, the molecules retaining their bias for the S-type conformer.

3. SUMMARY

The above discussion leaves some serious doubts concerning the nature of the deoxyribose ring conformational equilibrium, at least in the m^6dU series. It appears that the $N \rightleftharpoons S$ equilibrium in the dT series involves the ^3E and ^2E conformers found in the majority of ribo- and deoxyribonucleosides and nucleotides. The pseudorotational analysis also suggests that the S-type conformer in the m^6dU series is the $^2T_1$ form found in the crystal structure of m^6dU. Unfortunately, there is still some doubt as to the identity of the N-type conformer. As noted above, it could be either the $^3T_4$ or the normal ^3E pucker.

In the discussion that follows, the terms N-type and S-type pucker will be used when referring to the conformational bias of the deoxyribose ring. These labels will refer to the usual ^3E and ^2E conformations, respectively, when referring to the dT derivatives. In connection with the m^6dU series, however, there does not appear to be any justification, at this time, to applying specific conformers to these labels. It seems sufficient to emphasize that the conformational equilibrium in the m^6dU derivatives has been appreciably disrupted from the normal $N \rightleftharpoons S$ conformational blend.

C. BACKBONE CONFORMATION

1. THE $C_{5'}—C_{4'}$ BOND, Ψ

a. VICINAL PROTON-PROTON SPIN-SPIN COUPLING CONSTANTS

Table 5.7 contains the relevant vicinal proton-proton coupling constants for the dT and m^6dU series needed for the conformational analysis of the $C_{5'}—C_{4'}$ bond, ψ. Included in this table are the coupling constants for the dT [29] and m^6dU [73] nucleosides and nucleotides. The listed populations are calculated using Equations 2.13, 2.14, and 2.15 and the parameters discussed in Section II.B.3.a. Due to the support of the Remin-Shugar assignment[103] by the work of Ritchie and Perlin on (5'-^{2}H)adenosine[165], confirming the afore-mentioned assignment of $H_{5'}$ and $H_{5''}$, more confidence can be placed in the differentiation of the g_t and g_- conformations and the discussion of their populations.

i. Nucleosides and Mononucleotides

A summary of the work of Hruska and co-workers[29,73] on the dT and m^6dU nucleosides and mononucleotides is appropriate at this point. In the dT series, some general trends concerning the ψ populations are apparent. There is little change in ψ in the dT series upon 3'-phosphorylation. Formation of the 5'-nucleotide, however, stabilizes the ψ_+ conformer, as evidenced by the increase in $p(\psi_+)$. When moving from the dT to m^6dU series[23], a pronounced shift in populations occurs. In the dT to m^6dU transition, $p(\psi_+)$ is decreased in favor of $p(\psi_t)$.

TABLE 5.7

^3J(H4'-H5'), ^3J(H4'-H5"), AND THE Ψ ROTAMER POPULATIONS CALCULATED FROM THEM FOR A SERIES OF dT AND m^6dU DERIVATIVES[a]

	^3J(4'-5')	^3J(4'-5")	Σ [b]	$p(\Psi_+)$	$p(\Psi_t)$	$p(\Psi_-)$
dT [c]	3.6	5.0	8.6	0.44	0.35	0.21
3'-dTMP [c]	3.5	4.8	8.3	0.47	0.33	0.20
5'-dTMP [c]	—— d	—— d	7.6	0.54	—— d	—— d
3',5'-dTDP [e]	—— d	—— d	5.8	0.72	—— d	—— d
	—— d	—— d	(5.6)	(0.72)	—— d	—— d
d(TpT)	3.7	4.2	7.9	0.51	0.27	0.22
d(TpT)	2.3	3.7	6.0	0.70	0.22	0.18
d(Tpm^{6}U) [f]	2.8	4.7	7.5	0.55	0.32	0.13
	(3.4)	(4.7)	(8.1)	(0.49)	(0.32)	(0.19)
d(m^6UpT) [f]	2.9	4.4	7.3	0.51	0.29	0.14
	(3.1)	(4.8)	(7.9)	(0.51)	(0.33)	(0.16)
m^6dU [g]	3.4	6.5	9.9	0.31	0.50	0.14
3'-m^6dUMP [g]	3.9	6.1	10.0	0.30	0.46	0.24
5'-m^6dUMP [g]	4.3	6.3	10.6	0.24	0.48	0.28
3',5'-m^6dUDP [e]	3.4	7.5	10.9	0.21	0.60	0.19
	(3.3)	(7.9)	(11.2)	(0.18)	(0.64)	(0.18)
d(m^6Upm^{6}U)	3.6	6.6	10.2	0.28	0.51	0.21
d(m^6Upm^{6}U)	2.7	6.6	9.3	0.37	0.51	0.12
d(m^6UpT) [f]	3.2	6.8	10.0	0.30	0.53	0.17
	(3.5)	(6.5)	(10.0)	(0.30)	(0.50)	(0.20)
d(Tpm^{6}U) [f]	2.6	8.3	10.9	0.21	0.68	0.11
	(3.0)	(8.0)	(11.0)	(0.20)	(0.65)	(0.15)

FOOTNOTES FOR TABLE 5.7

a) Coupling constants in Hz recorded at 293 K and pH ≃ 6.5 unless otherwise noted.

b) $\Sigma = ({}^{3}J(H4'-H5') + {}^{3}J(H4'-H5''))$

c) From Reference 29

d) Not available

e) Sample at pH ≃ 3.6. Numbers in parenthesis at pH ≃ 7.5.

f) Numbers in parenthesis at T = 333 K

g) From Reference 73

This effect is mirrored in the 3'-dTMP to 3'-m^6dUMP transition. The consistency between dT to 3'-dTMP and m^6dU to 3'-m^6dUMP is reasonable, since the 3'-phosphate group is an exo substituent and is not expected to affect the ψ bond rotamer populations[73]. The m^6dU to 5'-m^6dUMP progression results in a decrease in $p(\psi_+)$ in excess of that observed in the dT to m^6dU change, and opposite to the trend in the dT to 5'-dTMP transition.

Hruska and co-workers[73] interpreted these observations by referring to the calculated charge distributions of a thymine base. These calculations indicated[166] that the 2-keto group of the thymine ring was a negative center while the 6-position was a positive center. In 5'-dTMP, the 6-position lies over the furanose ring in the anti conformer, and the positive character of the 6-position is expected to favor the closer approach of the negatively charged 5'-phosphate group. In 5'-m^6dUMP, the location of the 2-keto group over the furanose ring is expected to repel the negatively charged 5'-phosphate.

ii. Nucleoside Diphosphates

The data for both the di-monoanionic and di-dianionic forms of 3',5'-dTDP and 3',5'-m^6dUDP are included in Table 5.7. An analysis of the data shows an increased stabilization of the ψ_+ rotamer for both ionic forms of 3',5'-dTDP over that observed for 5'-dTMP. In the case of 3',5'-m^6dUDP, the $p(\psi_t)$ population is enhanced compared to 5'-m^6dUMP, primarily at the expense of ψ_-. These two trends can be rationalized by a consideration of molecular models, as follows. In the case of 3',5'-dTDP, rotation out of ψ_+ into ψ_- for a predominant S-type sugar

(see above) and ϕ_t bond rotamer (see below) will bring the 5'-phosphate into close proximity to the 3'-phosphate. Hence, in the diphosphate, an increase in ψ_+ will reduce the electrostatic repulsion between the two phosphates. From the models, it is clear that rotations into ψ_- are inhibited more than rotations into ψ_t, but the vicinal coupling data available for 3',5'-dTDP does not allow this to be verified.

In the case of 3',5'-m^6dUDP, the situation with respect to ψ rotamer redistribution is similar. Here, the change in sugar pucker (increase in N-type, decrease in S-type) further accents the electrostatic repulsion. As mentioned above, $p(\psi_t)$ increases, and $p(\psi_-)$ shows a corresponding decrease, while $p(\psi_+)$ remains essentially constant when compared with 5'-m^6dUMP. The N-type sugar pucker forces the 3'- and the 5'-phosphates even closer together for rotations into ψ_-. Space filling models indicate that for a predominant N sugar, and ϕ_t rotamer, rotation into ψ_- becomes very unlikely; hence the reduction of ψ_-. Upon further ionization to the di-dianionic form, the ψ populations are shifted slightly, but the changes are small.

iii. Dinucleoside Monophosphates

Turning now to the dinucleoside monophosphates, a comparison between the nucleotidyl fragments and the monomers is in order. Looking at the 3'-nucleotides first, little change is detected in $p(\psi_+)$ when progressing from 3'-dTMP to the dTp- fragments of d(TpT) and d(Tpm^{6}U). There is a slight decrease in $p(\psi_-)$ and a corresponding increase in $p(\psi_+)$ at 293 K for the dTp- part of d(Tpm^{6}U), but this shift in populations is reversed at 333 K. Generally, incorporation

of the 3'-nucleotide into a dimer has little effect on the ψ bond populations. The progression from 5'-dTMP to the -pdT fragment in d(TpT) increases the $p(\psi_+)$ population of -pdT in d(TpT), but there is little change in the ψ populations when comparing 5'-dTMP to the -pdT part in d(m^6UpT). The change in $p(\psi_+)$ for the 5'-dTMP to -pdT in d(TpT) transition is similar to the change in $p(\psi_+)$ for the 5'-dTMP to 3',5'-dTDP transition. Examination of the results for the m^6dU derivatives shows that there is little change in the ψ rotamers for the 3'-nucleotide fragment upon dimerization. The 5'-nucleotide fragments, on the other hand, show a substantial depopulation of the ψ_- rotamer with an increase in $p(\psi_+)$ for the -pm^6dU part of d(m^6Upm^6U) but an increase in $p(\psi_t)$ for the -pm^6dU part of d(Tpm^6U).

The apparent insensitivity of the ψ rotamer populations in the 3'-nucleotidyl fragments of dT and m^6dU upon dimerization is consistent with the analogous insensitivity of the nucleosides to 3'-phosphorylation. Little change in ψ rotamers would be expected since the exocyclic hydroxy methyl group and the 3'-phosphate (or the 5'-nucleotide attached to the 3'-position) are diametrically disposed across the deoxyribose ring.

The ψ bond rotamer populations for the 5'-nucleotidyl fragment of d(TpT) and d(m^6UpT) will be discussed first. The stabilization of the ψ_+ rotamer of -pdT in d(TpT) compared to 5'-dTMP and -pdT in d(m^6UpT) can be rationalized as follows. As noted in Section V.B.1., there is a slight shift in the N$\rightleftharpoons$S equilibrium in the -pdT part upon dimerization towards the N-state, but the change is experienced by the

5'-nucleotide fragments in both d(TpT) and d(m^6UpT). It is possible that additional stabilizing forces can arise from stacking between the thymine rings or from electrostatic attraction between the keto groups and the N-H groups of the two pyrimidine rings. The presence of these forces could, in turn, result in an increase in the $p(\psi_+)$ population. Ring current effects for pyrimidines are known to be small[16-18,166b], and Wood et al.[29] ruled out a stacking-type interaction because of the observed invariance of the base ring proton chemical shifts. This does not preclude the presence of intramolecular inter-base electrostatic interactions. If a hydrogen-bond type interaction is the case, a change in the N-glycosyl bond conformation of either base (i.e., from the preferred anti to syn) would remove the stabilization, resulting in the rotamer populations of ψ adopting values similar to those observed in 5'-dTMP, as is the case in d(m^6UpT).

Extending the series to the dinucleotide[36] or trinucleoside diphosphate level[38,167] does not change the $p(\psi_+)$ populations of the -pdTp- part of d(TpTp)[36], d(TpTpA)[38], and d(TpTpT) and d(TpTpC)[167]. An increase in $p(\psi_+)$ is also found in the terminal 5'-nucleotides of the trimers[38,167]. It appears that the stabilization of the ψ_+ rotamer is not affected by chain elongation. The crystal structure of d(TpT) has not been determined, but Camerman et al.[168] found no intramolecular hydrogen bonds or intramolecular stacking involving the bases in the crystal structure of the sodium salt of d(pTpT). For Na·d(pTpT), the dinucleotide was found in the "extended" form with $\omega',\omega = t,g_-$. It is interesting to note that the asymmetric unit of

the unit cell contains one molecule of sodium-d(pTpT) and 12 to 13 water molecules[168]. In addition, even though the molecule was crystallized at pH = 6.8, only two sodium ions were found per d(pTpT) molecule[168].

For a standard set of ψ, ϕ, and ϕ' angles (i.e., predominant $p(\psi_+)$, $p(\phi_t)$ populations and ϕ' in the range of ϕ'_t and ϕ'_-), it is the ω',ω angles of a dinucleoside monophosphate which determine the overall conformation of the molecule[169,170]. Kim et al.[170] have proposed seven basic conformations about ω',ω. One conformation, in which $\omega',\omega = g_-,g_-$, would bring the two bases of d(TpT) close enough to allow the formation of two hydrogen bonds. Wood et al.[29] and Cheng et al.[167] have proposed that d(TpT)[29], d(TpTpT)[167], and d(TpTpC)[167] exist predominantly in the extended t,g_- conformation about ω',ω based on the consistency of the base proton chemical shifts, and in light of the crystal structure of sodium-d(pTpT). Altona et al.[38], on the other hand, noted substantial upfield shifts for H_6,$H_{1'}$, $H_{2'}$, and $H_{2''}$ of the central fragment of d(TpTpA) compared to d(TpTp) and concluded that both ω',ω pairs were g_-,g_-; as implied from the circular dichroism spectra of dinucleoside monophosphates in solution, indicating some local order was present[171]. The minimum energy conformation determined from potential energy calculations of Broyde et al.[172] has indicated that the lowest energy conformer of d(TpT) is with ω',ω = g_-, g_- and the other bonds as above (i.e., ψ_+, ϕ_t, ^3E). This form is calculated to be 15.1 kJ $mole^{-1}$ more stable than the extended form ($\omega',\omega = t,g_-\psi = g_+{}^2T_3(\sim{}^3E)$) observed in the sodium-d(pTpT) and the

conformer proposed from the earlier NMR results[29,100,167]. The observed increase in $p(\psi_+)$ in -pdT of d(TpT) compared to 5'-dTMP, together with the similar values of $p(\psi_+)$ observed here for 5'-dTMP and -pdT of d(m^6UpT), indicates the existence of some stabilizing force which depends upon the orientation of the two bases. Whether this force involves base stacking or hydrogen bonding cannot be determined from the present data.

Returning now to the 5'-nucleotidyl fragments of d(Tpm^{6}U) and d(m^6Upm^{6}U), the observed trends in ψ are consistent, as noted above. Recall that in Section V.B.1. a substantial increase in the N-type sugar pucker population is detected when going from 5'-m^6dUMP to the -pm^{6}dU parts of either d(Tpm^{6}U) or d(m^6Upm^{6}U). For the ψ bond, $p(\psi_-)$ is decreased in both d(Tpm^{6}U) and d(m^6Upm^{6}U). This is consistent with the closer proximity of the 5'-phosphate and the 3'-hydroxyl of a 5'-nucleotide with a predominant N-type sugar. Rotations of ψ into g_- result in a closer approach of the 5'- and 3'-substituents. The similarities between d(Tpm^{6}U) and d(m^6Upm^{6}U) end here. As stated previously, the g_+ population increases with decreasing $p(\psi_-)$ in d(m^6Upm^{6}U), with $p(\psi_+)$ only slightly less than $p(\psi_t)$ (0.36 compared with 0.53, respectively). In contrast, the t conformer of ψ is supplemented by the decrease of $p(\psi_-)$ in d(Tpm^{6}U) ($p(\psi_t)$ = 0.68). Potential energy calculations show[172] that the low energy form of a dimer for a t conformation of ψ and an N-type sugar is coupled to ω',ω = g_-,t (fixed ϕ at t and ϕ' between t and g_-). Molecular models with these bond conformations may help in formulating a possible

interpretation. For a dinucleoside monophosphate with the 3'-pyrimidine anti and the 5'-pyrimidine syn, it appears that unfavorable interactions between the bases would occur for a g_+ conformation about ψ (and ω',ω = g_-,g_-) of the 5'-nucleotide. Thus, in d(Tpm^{6}U), it is possible that the g_+ conformer of ψ in the 5'-nucleotide is destabilized by repulsive interactions between the pyrimidine rings. On the other hand, if both bases were in the syn orientation, base-base interactions similar to those proposed for d(TpT) above could occur for a g_+ orientation of ψ in the 5'-nucleotide. In this conformation, the 5'-nucleotide base is near $C_{2'}$ and its substituents of the 3'-nucleotide fragment. An inspection of the chemical shifts of the m^{6}dUp- part of d(m^{6}Upm^{6}U) reveals that $H_{2'}$ and $H_{2''}$ are shifted 0.075 ppm upfield and 0.04 ppm downfield, respectively, when compared to 3'-m^{6}dUMP (the shifts between d(m^{6}UpT) and 3'-m^{6}dUMP for $H_{2'}$ and $H_{2''}$ are 0.045 and 0.016 ppm, respectively). The $C_{2'}$ carbon of the m^{6}dUp- part of d(m^{6}Upm^{6}U) is also affected, experiencing an upfield shift of 0.7 ppm compared to either 3'-m^{6}dUMP or the m^{6}dUp- part of d(m^{6}UpT). Further evidence that the increase in p(ψ_+) of the -pm^{6}dU part of d(m^{6}Upm^{6}U) is a result of interactions between the two pyrimidine rings can be obtained from photochemical studies in progress. A sample of d(m^{6}Upm^{6}U), irradiated with u.v. light under conditions similar to those used for the irradiation of d(TpT) has been found to yield photoproducts similar to those obtained from d(TpT) i.e., the products are of the internal cyclobutane type with the bases cyclized between C_5 and C_6 of the two pyrimidine rings (see Figure 3.4) as deduced from

preliminary ^{1}H and ^{13}C NMR studies. Irradiation of d(Tpm^{6}U), on the other hand, has not produced similar products under a variety of similar conditions. The evidence is not conclusive, however, since variations in the ω',ω bonds could also lead to unforseen stabilization of the g_+ conformer of ψ in the 5'-nucleotide of d(m^{6}Upm^{6}U).

b. CORRELATION BETWEEN THE SUGAR PUCKER AND THE $C_{5'}$—$C_{4'}$ BOND CONFORMATION

In an investigation of the possible correlation between the sugar pucker and the exocyclic bond conformation about $C_{5'}$—$C_{4'}$ suggested by X-ray studies[173], Hruska et al. reported the presence of a correlation in solution for a series of pyrimidine nucleosides[174]. Recently, Davies has extended this correlation to include purine nucleosides and purine and pyrimidine nucleotides[175]. The correlations indicate that the g_+ conformer of ψ is favored if the ribose, or deoxyribose, is predominantly in the N-state, and g_+ is less favored for a sugar pucker dominated by the S-state[174]. In the original study, Hruska et al.[174] noted that the correlation broke down for molecules in which there is a bulky keto group in close proximity to the ribose ring (e.g., orotidine and 1-(β-D-ribofuranosyl)cyanuric acid). A similar effect is observed here for the m^{6}dU derivatives. Figure 5.1 shows a plot of Σ (^{3}J(H4'-H5') + ^{3}J(H4'-H5")) vs ^{3}J(H3'-H4') from Hruska et al[174]. Included in this plot is the data for the dT and m^{6}dU series. As can be seen from Figure 5.1, the observations in the early study[174] are continued here. The original workers rationalized the deviations in terms of anomalous nonbonded interactions between the

FIGURE 5.1 is a plot of Σ (^3J(H4'-H5') + ^3J(H4'-H5")) vs ^3J(H3'-H4') (both in Hz). Symbols used are:

- ● for the data from Reference 174
- ○,⊙ for dT and m^6dU, respectively
- ×,⊗ for 3'-dTMP and 3'-m^6dUMP, respectively
- +,⊕ for 5'-dTMP and 5'-m^6dUMP, respectively
- ◆,◇ for 3',5'-dTDP and 3',5'-m^6dUDP, respectively
- ▽,▼ for the nucleotidyl fragments of d(Tpm^{6}U), respectively
- ■,□ for the nucleotidyl fragments of d(m^6UpT), respectively
- △,▲ for the nucleotidyl fragments of d(m^6Upm^{6}U), respectively

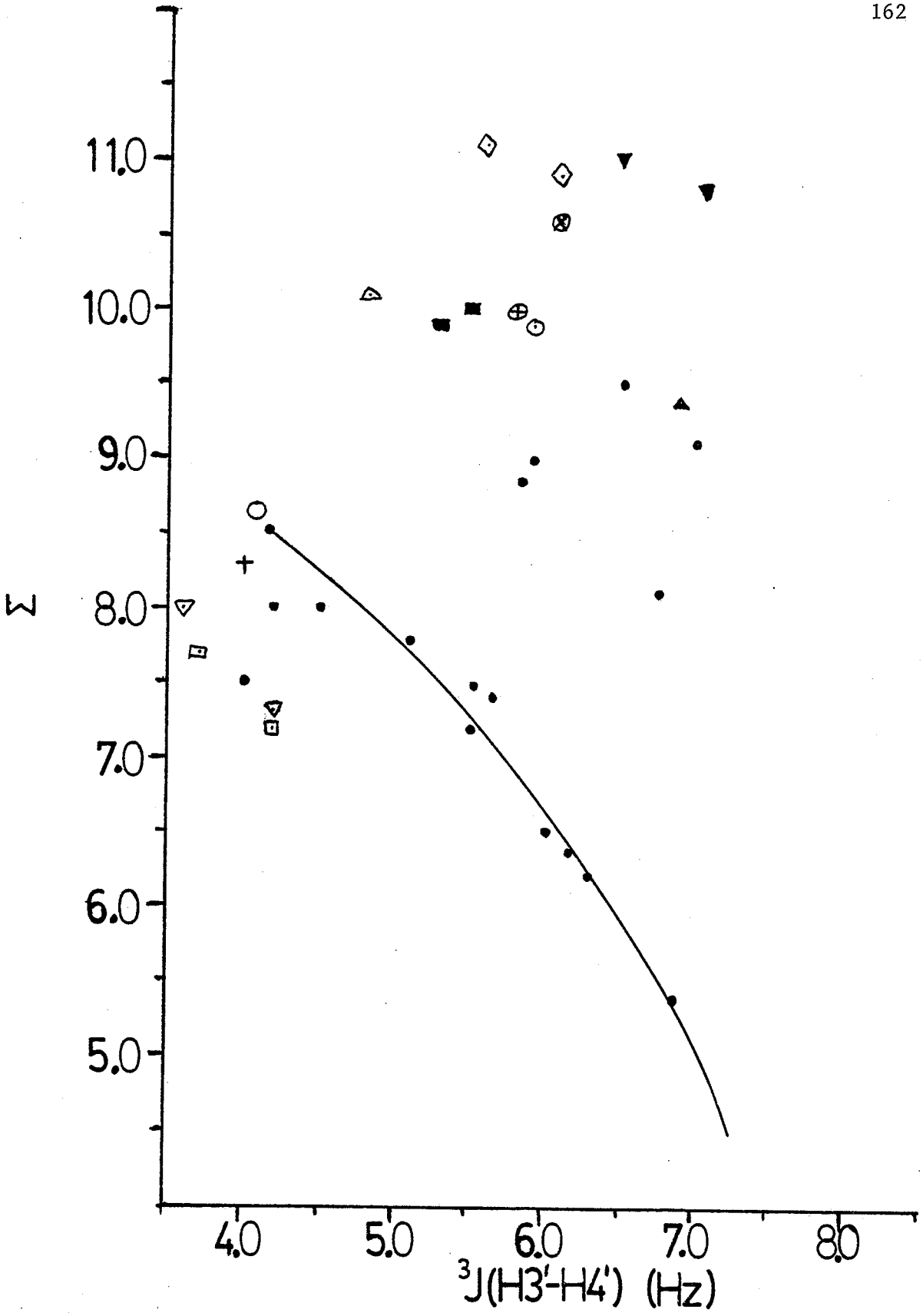
11.0
10.0
9.0
8.0
7.0
6.0
5.0
W
4.0
5.0
6.0
7.0
8.0
3J(H3'-H4') (Hz)

keto group and the sugar ring.

2. THE $O_{5'}$—$C_{5'}$ BOND, Φ

a. PROTON-PHOSPHORUS VICINAL SPIN-SPIN COUPLING CONSTANTS

The vicinal proton-phosphorus coupling constants for the 5'-nucleotides[29,73], the 3',5'-nucleoside diphosphates, and the 5'-nucleotidyl fragments of the dinucleoside monophosphates are presented in Table 5.8. Included in this table are the ϕ bond rotamer populations calculated from Equations 2.16, 2.17, and 2.18. As indicated by Hruska and co-workers[73], there is a slight reduction in $p(\phi_t)$ when going from the dT to m^6dU series. The authors[73] interpreted this as a result of the shift in the conformer preference of the ψ bond from g_+ to t. In the t state of ψ, the g_- and g_+ conformers of ϕ become more accessible due to a reduction in the steric interactions between the non-ester phosphate oxygens and the ribose ring substituents. This trend is continued in the nucleoside diphosphates. Comparison of 3',5'-dTDP with 3',5'm^6dUDP reveals that the t conformer in the latter molecule is slightly less populated. The difference is comparable to that observed for $p(\phi_t)$ between 5'-dTMP and 5'-m^6dUMP (a difference in $p(\phi_t)$ of 0.19 between the two 5'-nucleotides compared to a difference of 0.16 between the diphosphates). Secondary ionization of both molecules results in an increase of $p(\phi_t)$ for each, but the difference in populations (lower $p(\phi_t)$ in 3',5'-m^6dUDP) is preserved.

A comparison of the 5'-nucleotidyl fragments of the dimers shows that the trend is continued. The t conformer populations of ϕ in the

TABLE 5.8

^3J(H5'-P5') AND ^3J(H5''-P5') AND THE CALCULATED Φ ROTAMER POPULATIONS FOR A SERIES OF 5'-NUCLEOTIDES OF dT AND m^6dU [a]

	^3J(5'-5')	^3J(5''-5')	Σ' [b]	$p(\Phi_+)$	$p(\Phi_t)$	$p(\Phi_-)$
5'-dTMP [c]	—— d	—— d	7.6	—— d	0.83	—— d
3',5'-dTDP [e]	—— d	—— d	9.2	—— d	0.75	—— d
	—— d	—— d	(8.0)	—— d	(0.81)	—— d
d(TpT)	4.2	3.6	7.8	0.07	0.82	0.10
d(m^6UpT) [f]	3.9	4.0	7.9	0.09	0.81	0.09
	(4.5)	(5.0)	(9.5)	(0.09)	(0.74)	(0.11)
5'-m^6dUMP [g]	5.8	5.7	11.5	0.17	0.64	0.18
3',5'-m^6dUDP [e]	6.3	6.3	12.6	0.20	0.59	0.20
	(5.8)	(5.7)	(11.5)	(0.17)	(0.64)	(0.18)
d(m^6Upm^6U)	4.9	4.8	9.7	0.13	0.74	0.13
d(Tpm^6U) [f]	3.4	5.6	9.0	0.17	0.76	0.11
	(4.8)	(6.0)	(10.8)	(0.19)	(0.68)	(0.13)

a) Coupling constants in Hz recorded at 293 K and pH ∿ 6.5 unless otherwise noted.

b) $\Sigma' = (^3J(H5'-P5') + {}^3J(H5''-P5'))$

c) From Reference 29

d) Not available

e) Sample at pH ∿3.6. Numbers in parenthesis at pH ∿7.5.

f) Numbers in parenthesis for T = 333 K

g) From Reference 73

-pdT fragments are still higher than those observed for the -pm^{6}dU fragments, but the differences have decreased. For example, the difference in p(ϕ_t) between the 5'-nucleotide fragments in d(m^{6}UpT) and in d(TpT) and d(Tpm^{6}U) is only 0.08 compared to the 0.16 reduction above. This can be connected with the additional destabilization of the g_- state of ψ in the -pm^{6}dU series as a result of the increase in the N-type conformer of the deoxyribose ring. The increase in p(ϕ_t) in the -pm^{6}dU parts of d(Tpm^{6}U) and d(m^{6}Upm^{6}U) could be due to the increased steric interactions in the g_+ and g_- states of ϕ as a result of the ψ and sugar pucker conformational changes. The data at 293 and 333 K for both d(m^{6}UpT) and d(Tpm^{6}U) show a decrease in p(ϕ_t) at the higher temperature. These observations are consistent with the strong conformational bias of the t conformer of ϕ [101], as noted in Chapter II.

b. CORRELATION BETWEEN Ψ AND Φ

Correlations have been proposed relating the ψ_+ and ϕ_t rotamer populations of 5'-nucleotides[77a,108] and the 5'-nucleotidyl fragment of dinucleoside monophosphates[6,123]. An examination of the data presented here indicates that a similar correlation is not present. Apparently, this is due to the same reasons discussed above for the sugar pucker -ψ bond correlation, i.e., ψ has been displaced from its normal conformational preference and should not show a similar relationship to ϕ, as observed for other pyrimidine and purine nucleotides.

c. LONG-RANGE PROTON-PHOSPHORUS COUPLING CONSTANTS, ^{4}J(H4'-P5')

The reported ^{4}J(H4'-P5') coupling constants in Tables 4.1 to 4.8

are consistent with the calculated ψ and ϕ rotamer populations above. Using the correlation diagrams of Sarma et al.[107], the observed ^4J(H4'-P5') coupling constants in the dT series are consistent with a dominance of g_+ for ψ and t for ϕ. In addition, the absence of any detectable ^4J(H4'-P5') coupling in the m^6dU series is also consistent with the change of the ψ population bias to t and the reduction of t in ϕ. Both these observations for the dT and m^6dU series are consistent with the strong dependence of ^4J(H4'-P5') on both ψ and ϕ [107]. As either of these bonds rotate out of the g_+ and t conformers, respectively, the all-planar (all-trans) W coupling path needed to transmit this interaction is disrupted.

d. CARBON-PHOSPHORUS VICINAL SPIN-SPIN COUPLING CONSTANTS

i. Nucleotides and Nucleoside Diphosphates

Table 5.9 contains the carbon-phosphorus vicinal coupling constants at pH $\sim$7 for the 5'-nucleotides and 3',5'-nucleoside diphosphates in Tables 4.11 to 4.18. Included are the ϕ_t rotamer populations calculated from Equation 2.22. The agreement between ϕ_t populations calculated from proton-phosphorus coupling constants and carbon-phosphorus coupling constants is better for 5'-dTMP and 3',5'-dTDP than the analogous m^6dU derivatives.

The effect of pH on the vicinal ^3J(C4'-P5') couplings of 5'-dTMP, 3',5'-dTDP, 5'-m^6dUMP, and 3',5'-m^6dUDP is shown in Figure 5.2. The Alderfer-Ts'o data[56] for the ribose derivatives, 5'-UMP and 5'-AMP, are included. (Note that the ordinate of Figure 5.2 is given in Hz and in %t(ϕ) obtained from Equation 2.22.) Overall, the ^3J(C-P)

values span a range from 7.8 - 8.9 Hz, and thus are larger than the corresponding $^2J(C-P)$ values (see below). Weak sigmoidal behaviour can be discerned in the 5'-dTMP data, with $^3J(C-P)$ at pH > 8, on the average, 0.3 Hz less than at pH < 6.0. (Perhaps due to greater scatter of the points, this behaviour cannot be discerned in the data for 3',5'-dTDP, 5'-UMP, and 5'-AMP). Similarly, the data for the m^6dU derivatives define a sigmoidal curve, but here an increase of $\sim$0.3 Hz is seen in $^3J(C-P)$ as the solution becomes basic. If the ionization of the phosphate exerted only a direct (through-bond) effect on $^3J(C-P)$, this difference in behaviour for the dT and m^6dU derivatives would not be expected. Therefore, it is reasonable to conclude that these variations in $^3J(C-P)$ are in part due to the conformational consequences of phosphate ionization (see below).

In conformational terms, the $^3J(C-P)$ data (Figure 5.2) are in general agreement with previous ^1H NMR and X-ray diffraction studies. Thus, a distinct preference for ϕ_t is indicated, with $p(\phi_t) > 71\%$ in all instances. In the crystal state, all known 5'-nucleotidyl fragments are ϕ_t [101]. Furthermore, for 5'-dTMP, 3',5'-dTDP, 5'-UMP and 5'-AMP, the $^3J(C4'-P5')$ values are to within 0.5 Hz, identical at all pH values, with $p(\phi_t)$ in the range 78%-87%. Thus, for this collection of molecules, neither the nature of the base (purine or pyrimidine) nor of the sugar (ribose or deoxyribose), nor the presence of a 3'-phosphate influences $p(\phi_t)$. This is in good agreement with the work of Davies and Danyluk[77a] who found, for the purine and pyrimidine ribose and deoxyribose 5'-nucleotides, Σ' values in the narrow range 8.7 - 9.4 Hz, which

FIGURE 5.2 shows the variation of $^{3}J(C4'-P5')$ (in Hz) with pH. The symbols used are:

■,□ for 5'-dTMP and 5'-m^{6}dUMP, respectively

▲,Δ for 3',5'-dTDP and 3',5'-dUDP, respectively

×,+ for 5'-UMP and 5'-AMP, respectively from Reference 56

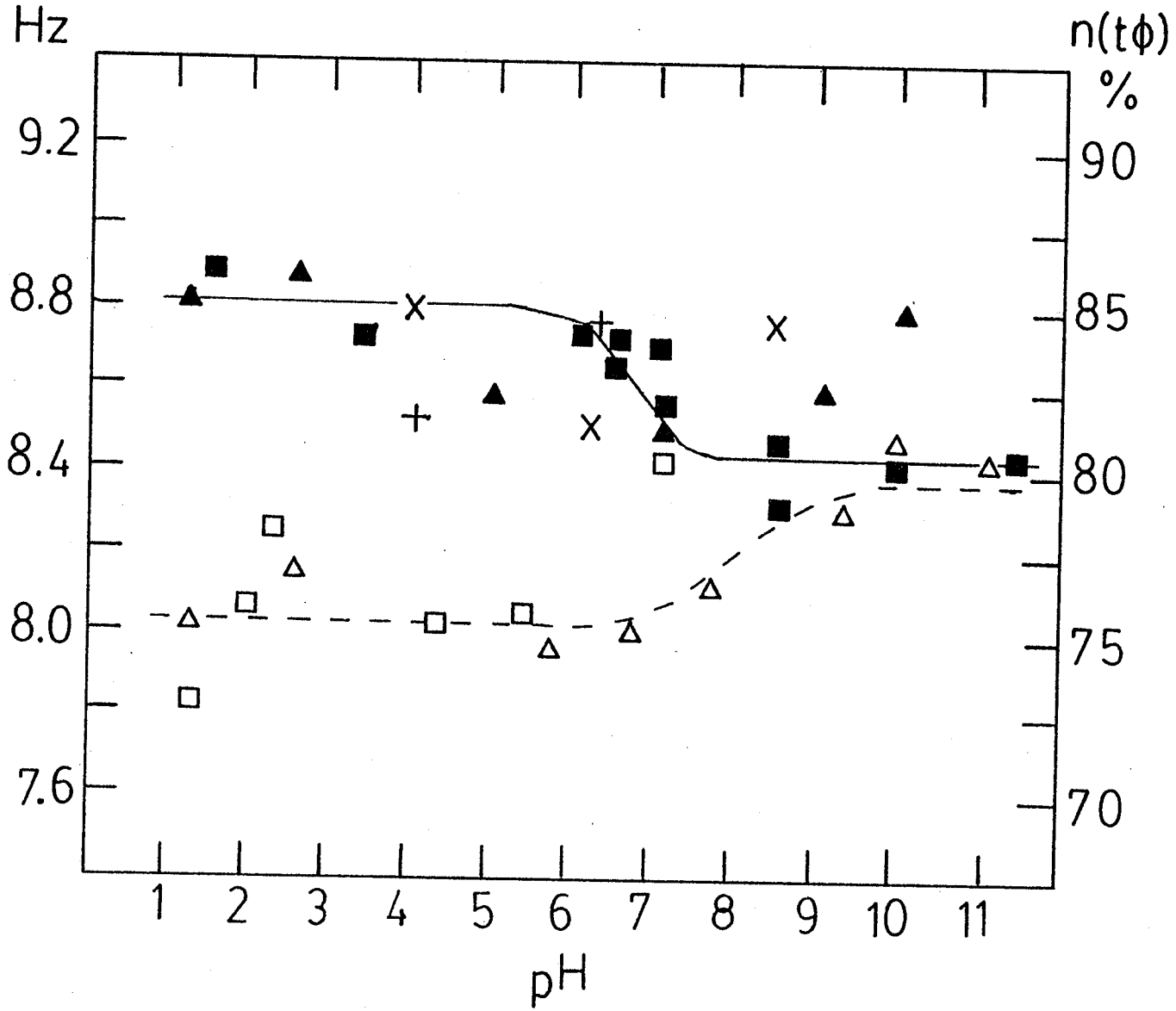
Hz
n(tϕ)
%
9.2
8.8
8.4
8.0
7.6
90
85
80
75
70
1
2
3
4
5
6
7
8
9
10
11
pH

correspond to $p(\phi_t)$ values in the range 75-78%.

It is interesting to note that at acid pH the $^3J(C4'-P5')$ values for the m^6dU molecules are on the average 0.7 Hz smaller than those for the dT derivatives. This apparent decrease in $p(\phi_t)$ for the 5'-m^6dUMP and 3',5'-m^6dUDP is in line with the understanding of syn nucleotides[73]. It is clear from space-filling models that for steric reasons the $C_{5'}—O_{5'}$ bond of a 5'-nucleotide must be ϕ_t (expected $^3J(C4'-P5')$ = 10 Hz) when the molecule is oriented ψ_+ about the $C_{4'}—C_{5'}$ bond (Figure 2.6). If the molecule rotates out of ψ_+ into ψ_t or ψ_-, then the ϕ_+ and ϕ_- orientations become more accessible (expected $^3J(C4'-P5')$ = 2 Hz). Thus, any perturbation which leads to a decrease in $p(\psi_+)$, the fractional population of ψ_+ conformer, should be manifest in a corresponding decrease in $p(\phi_t)$. This decrease in $p(\phi_t)$ should be manifest simultaneously in an increase in Σ' and a decrease in $^3J(C4'-P5')$ according to Equations 2.14 and 2.22. Earlier, George et al.[73] have shown from Σ' measurements that at pH = 6.0, replacement of dT by m^6dU at the 5'-nucleotide level leads to a reduction in $p(\phi_t)$ from 72% to 65%. The $^3J(C4'-P5')$ data parallel this trend by predicting for this replacement a reduction in $p(\phi_t)$ from 85% to 75% (Figure 5.2).

At basic pH, however, little difference is noted in the $^3J(C4'-P5')$ values for the dT and m^6dU molecules. Apparently, ionization of the phosphate has led to some ϕ bond changes in, particularly, the m^6dU molecules. Finally, it is interesting to note that $p(\phi_t)$ is not significantly (<10%) dependent at any pH upon the presence of a 3'-phosphate (compare 5'-dTMP with 3',5'-dTDP and 5'-m^6dUMP with 3',5'-m^6dUDP.

ii. Dinucleoside Monophosphates

An examination of the data for the 5'-nucleotidyl fragments of the dimers in Table 5.9 reveals an inconsistency in the t conformer populations of ϕ calculated from the proton-phosphorus and carbon-phosphorus vicinal coupling constants. Use of the parameters employed in the nucleotide analysis above yields abnormally large values of $p(\phi_t)$, especially for -pdT in d(TpT). The original parameterization[119] was derived on the basis of the observed couplings of 5'-nucleotides[54,153] and cyclic nucleotides[154,155,176]. It is possible that the magnitudes of ^3J(C-P) in a phosphodiester bond differ appreciably from those in a nucleotide or cyclic phosphate. An investigation of the dihedral angle dependence of phosphotriester model compounds shows that the vicinal coupling can be as large as 18 Hz for a dihedral angle of 180^o [178]. In preliminary studies mentioned above of the cyclobutane-type photodimers involving the m^6dU fragment, a ^3J(C4'-P5') value of 11.0 Hz has been observed. If this value is used for ^3J_t in Equation 2.22, along with a corresponding increase in ^3J_g, better agreement between the calculated $p(\phi_t)$ values from proton-phosphorus and carbon-phosphorus coupling constants is obtained. Whether or not these values for ^3J_g (3 Hz) and ^3J_t (11 Hz) for the 5'-fragment of dinucleoside monophosphates are generally applicable can only be determined through a comparison of the data for a series of dimers where both H-P and C-P couplings have been measured.

The observed ^3J(C4'-P5') values for the dimers can be discussed qualitatively. There is little temperature dependence of ^3J(C4'-P5')

TABLE 5.9

^3J(C4'-P5') AND THE CALCULATED t ROTAMER POPULATION OF Φ FOR A SERIES OF 5'-NUCLEOTIDES OF dT AND m^6dU [a]

	^3J(C4'-P5')	$p(\Phi_t)$ [b]	$p(\Phi_t)$ [c]	$p(\Phi_t)$ [d]
5'-dTMP	8.6	0.83	0.83	0.70
3',5'-dTDP	8.5	0.81	0.81	0.69
5'-m^6dUMP	8.4	0.80	0.64	0.68
3',5'-m^6dUDP	8.1	0.76	0.64	0.64
d(TpT)	10.3	1.04	0.82	0.91
d(m^6UpT)	8.5	0.81	0.81	0.69
d(Tpm^6U)	9.5	0.94	0.74	0.81
d(m^6Upm^6U)	8.7	0.84	0.76	0.71

a) Coupling constants in Hz at T = 300 K and pH ∿7.5 for the nucleotides and pH ∿6.5 for the dinucleoside monophosphates.

b) Calculated from Equation 2.22 using J_g = 2 Hz and J_t = 10 Hz.

c) Values from Table 5.8.

d) Calculated from Equation 2.22 using J_g = 3 Hz and J_t = 11 Hz.

for the d(Tpm^{6}U), d(m^{6}UpT), and d(m^{6}Upm^{6}U) dimers as shown in Tables 4.18, 4.19, and 4.20, respectively. The observed vicinal couplings for these molecules are ca 8.5 Hz between 310 and 340 K. In d(m^{6}UpT), ^{3}J(C4'-P5') increases from 7.6 to 8.0 Hz between 300 and 320 K, but the same coupling in d(Tpm^{6}U) decreases from 9.5 to 8.7 Hz in this same range. The observed ^{3}J(C4'-P5') in d(m^{6}Upm^{6}U) remains constant at 8.5 $\pm$ 0.2 Hz. In d(TpT), ^{3}J(C4'-P5') decreases monotonically from 10.3 to 7.9 Hz between 300 and 340 K. These observations are consistent with the minor reduction in p(ϕ_t) with increasing temperature as detected by proton-phosphorus vicinal coupling constants. In d(TpT), the carbon data indicate a more drastic reduction in p(ϕ_t) than do the corresponding proton-phosphorus coupling constants. It is not understood why the ^{3}J(C4'-P5') couplings in d(m^{6}UpT) indicate an increase in ϕ_t, contrary to the prediction from the proton data. It may be that some additional change is being reflected in this carbon-phosphorus coupling constant. Further work is needed to clarify this situation. Generally speaking, however, the two methods appear to complement each other.

e. CORRELATION OF Σ' WITH ^{3}J(C4'-P5')

Equations 2.16 and 2.22 suggest that the sum of the phosphorus couplings to $H_{5'}$ and $H_{5''}$ (Σ') should be correlated with the observed ^{3}J(C4'-P5'). Figure 5.3 is a plot of ^{3}J(C4'-P5') vs Σ'. Included in the plot are the Σ' values from 5'-AMP, 5'-UMP, ApA [35], and UpU [35] and the corresponding ^{3}J(C4'-P5') couplings[56] for the ribose series. As can be seen, a very rough correlation exists between Σ' and ^{3}J(C4'-P5').

FIGURE 5.3 is a plot of Σ' (^3J(H5'-P5') + ^3J(H5"-P5')) vs ^3J(C4'-P5'). Symbols used are:

● Ribonucleotide data, ^3J(C4'-P5') from Reference 56
Σ' from Reference 77 and 186

■,□ for 5'-dTMP and 5'-m^6dUMP, respectively

△,▲ for 3',5'-dTDP and 3',5'-m^6dUDP, respectively

⊙ for d(TpT)

⊕ for d(Tpm^6U)

⊗ for d(m^6UpT)

◈ for d(m^6Upm^6U)

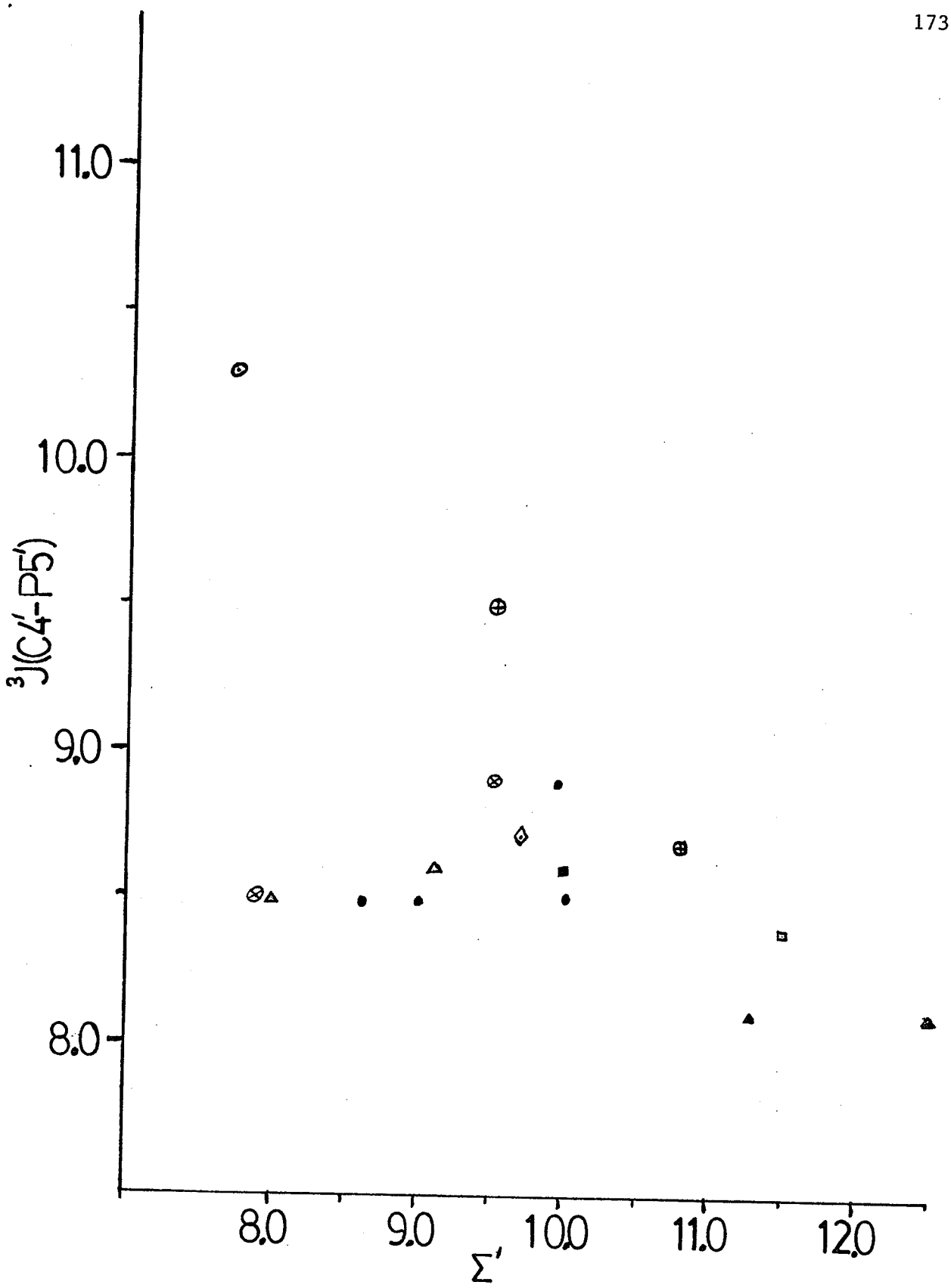
11.0
10.0
9.0
8.0
$^3J(C4'-P5')$
8.0
9.0
10.0
11.0
12.0
Σ'

It appears, however, that the nucleotide data are correlated differently than the 5'-nucleotidyl fragments of the dimers. In addition, the di-monoanionic forms of the nucleoside diphosphates are more in line with the dimers than the nucleotides. This may support the concept of different Karplus parameters for nucleotides and dinucleoside monophosphates. The limited data available, however, precludes any estimate in the differences in the two couplings.

3. THE $C_{3'}$—$O_{3'}$ BOND, Φ'

As mentioned in Chapter II, the rotamer analysis of the $C_{3'}$—$O_{3'}$ bond, ϕ', is not as straightforward as for the ψ and ϕ bonds. In the previous section, the results of the rotamer analysis of the ϕ bond obtained from proton-phosphorus and carbon-phosphorus coupling constants were discussed separately. In this section, it is useful to discuss the two methods together, not in a quantitative sense, but in a qualitative vein.

It seems appropriate to recap the problems concerning the ϕ' bond, outlined in Sections II.B.3.c. and II.C.2.b. In principle, three staggered conformers, g_+, t and g_- are accessible to the $C_{3'}$—$O_{3'}$ bond, ϕ' of a 3'-nucleotide (Figure 2.8). However, energy calculations[179-181] have indicated that the ϕ'_+ conformer can be excluded in any evaluation of the ϕ' conformer weightings. This conformer places the 3'-phosphate under the sugar ring in a gauche relation to both $C_{2'}$ and $C_{4'}$ and leads to severe crowding of the non-ester oxygens of the 3'-phosphate and the furanose substituents. Consideration of such

steric interactions led Olson and Flory[180] to conclude that ϕ' was restricted to two narrow ranges, one in each of the ϕ'_t and ϕ'_- domains. NMR spectroscopists have recently been interpreting their $^{13}C-^{31}P$ and $^{1}H-^{31}P$ coupling constant data in terms of a two-state $\phi'_t \rightleftharpoons \phi'_-$ model[29,56,77b,100].

However, because of a recent survey by Sundaralingam et al.[102] of the crystal structures of 3'-ribomononucleotides, the appropriateness of the two-state model for interpretation of solution coupling data must itself remain open to question. They have found that, for these ribose derivatives (eight in total), the ϕ' values define a single broad range from -91.5° to -164.9°. This range comprises adjoining segments of the ϕ'_- domain (centered at -60°) and the ϕ'_t domain (centered at -180°). In one instance, 3'-AMP·$2H_2O$, ϕ' is -123°, which means that the $H_{3'}$ and $P_{3'}$ are but 3° from the eclipsed situation. Thus, it seems that this eclipsed conformer does not present a particularly large barrier to interconversion between ϕ'_t and ϕ'_-. Energy calculations by Prusiner et al.[182] and Yathindra and Sundaralingam[183] also point to the absence of a major barrier to rotation about the $C_{3'}—O_{3'}$ bond. Given these studies by Sundaralingam and co-workers, translation of NMR data into ϕ'_t and ϕ'_- populations in a two-state model may be unjustified since the coupling constants could equally well be a reflection of averaging within a single broad range of conformer angles approximating that observed in the crystal state.

Because of this uncertainty, the coupling constants will be interpreted in a qualitative manner which does not imply a choice

between a two-state or a broad single-state model. The only assumption used in this section is that the vicinal H3'-P3' and the two vicinal C4'-P3' and C2'-P3' coupling constants vary in a Karplus manner with the ϕ' torsion angle. Thus, ^3J(H3'-P3') will be large in the molecules discussed, and ^3J(C2'-P3') and ^3J(C4'-P3') should be large in the g_- and t domains of ϕ', respectively, and relatively small in the t and g_- domains of ϕ', respectively (refer to Figure 2.8). If, in the future, strong evidence is provided for a two-state situation, then separate populations for t and g_- of ϕ' could be calculated quite simply from the data.

Table 5.10 contains the ^3J(H3'-P3'), ^3J(C2'-P3'), and ^3J(C4'-P3') vicinal coupling constants from Chapter IV. The proton data for the mononucleotides of dT [29] and m^6dU [73] are those from the literature. The reported ^3J(H3'-P3') values for 3',5'-m^6dUDP and the 3'-nucleotidyl fragments of d(m^6UpT) and d(m^6Upm^6U) were obtained from the ^{31}P spectra of the samples used to obtain the proton data reported above. These values are less accurate than those obtained from the proton iterative analysis, as discussed in Chapter IV.

Some trends are apparent from this table. All the ^3J(C2'-P3') and ^3J(C4'-P5') couplings are in the range of 0.5 to 4.3 and 5.3 to 8.3 Hz, respectively, indicating that ϕ' is predominantly in the t range. The ^3J(C4'-P3') values are consistently higher in the m^6dU derivatives than in the dT derivatives, as would be expected by the shift of the sugar pucker from the S-type to the N-type conformer (see below)[34]. In

TABLE 5.10

OBSERVED PROTON-PHOSPHORUS AND CARBON-PHOSPHORUS COUPLING CONSTANTS FOR 3'-NUCLEOTIDES AND 3'-NUCLEOTIDYL FRAGMENTS IN DINUCLEOSIDE MONOPHOSPHATES FOR A SERIES OF dT AND m^6dU DERIVATIVES[a]

	^3J(H3'-P3')	^3J(C2'-P3')	^3J(C4'-P3')
3'-dTMP [b]	7.8	2.9	5.8
3',5'-dTDP [c]	7.9	3.6	5.8
3',5'-dTDP [d]	8.3	3.0	5.9
d(TpT)	6.3	2.9	7.1
d(Tpm^6U) [e]	7.1 (7.6)	4.3 (4.3)	5.0 (5.3)
3'-m^6dUMP [f]	7.1	2.5	6.7
3',5'-m^6dUDP [c]	7.9	2.1	8.1
3',5'-m^6dUDP [d]	9.8	<0.7	8.3
d(m^6Upm^6U)	8.5 $\pm$ 1 [g]	2.3	7.4
d(m^6UpT) [e]	6.8 (7.4)	1.8 (2.8)	7.6 (8.2)

a) Value in Hz at pH ∿6.0 and T = 293 K unless otherwise noted

b) From Reference 29

c) At pH ∿3.6

d) At pH ∿7.4

e) Numbers in parenthesis at T ∿330 K

f) From Reference 73

g) Error larger due to nature of ^{31}P spectrum; see discussion in text.

addition, the ^3J(H3'-P3') couplings are in the range of 6.3 to 8.3 Hz, except for 3',5'-m^6dUDP at pH 7.4 and d(m^6Upm^6U). (The latter anomalies will be examined below.)

a. NUCLEOTIDE AND NUCLEOSIDE DIPHOSPHATES

Turning now to the titration data of the nucleotides and nucleoside diphosphates, Figure 5.4 shows the pH dependence of ^3J(C2'-P3') and ^3J(C4'-P3') couplings for 3'-dTMP, 3',5'-dTDT, 3'-m^6dUMP, and 3',5'-m^6dUDP; also included are the data for 3'-UMP (indicated by x) taken from Alderfer and Ts'o[56]. For our 2'-deoxyribose derivatives, as well as for 3'-UMP, the ^3J(C2'-P3') and ^3J(C4'-P3') couplings are confined to the ranges 0.5 - 3.9 and 5.9 - 8.5 Hz respectively. Thus, in all cases, a preference is indicated for the ϕ'_t domain in which $P_{3'}$ is trans to $C_{4'}$ and gauche to $C_{2'}$. There are, however, some important differences in the trends for the dT and m^6dU molecules.

The ^3J(C2'-P3') couplings on the one hand and ^3J(C4'-P3') couplings on the other are similar for 3'-dTMP and 3',5'-dTDP over the entire pH range. The presence of a 5'-phosphate, in either the monoanionic form (pH < 6.0) or dianionic form (pH > 8.0) appears to have little influence on the preferred orientation of the ϕ' bond in the dT series. The ^3J(C4'-P3') couplings are to within experimental error invariant over the pH range, while the ^3J(C2'-P3') couplings decrease by about 0.5 Hz in basic solution, reflecting, presumably, the secondary ionization of the 3'-phosphate. It would, however, be difficult to disentangle the contributions of the through-bond and the conformational effects of this ionization, but overall it seems that ϕ' for the dT

FIGURE 5.4 shows the variation of $^{3}J(C2'-P3')$ and $^{3}J(C4'-P3')$ (in Hz) with pH. The symbols used are:

●,○ for 3'-dTMP and 5'-m^{6}dUMP, respectively

▲,△ for 3',5'-dTDP and 3',5'-m^{6}dUDP, respectively

× for 3'-UMP from Reference 56

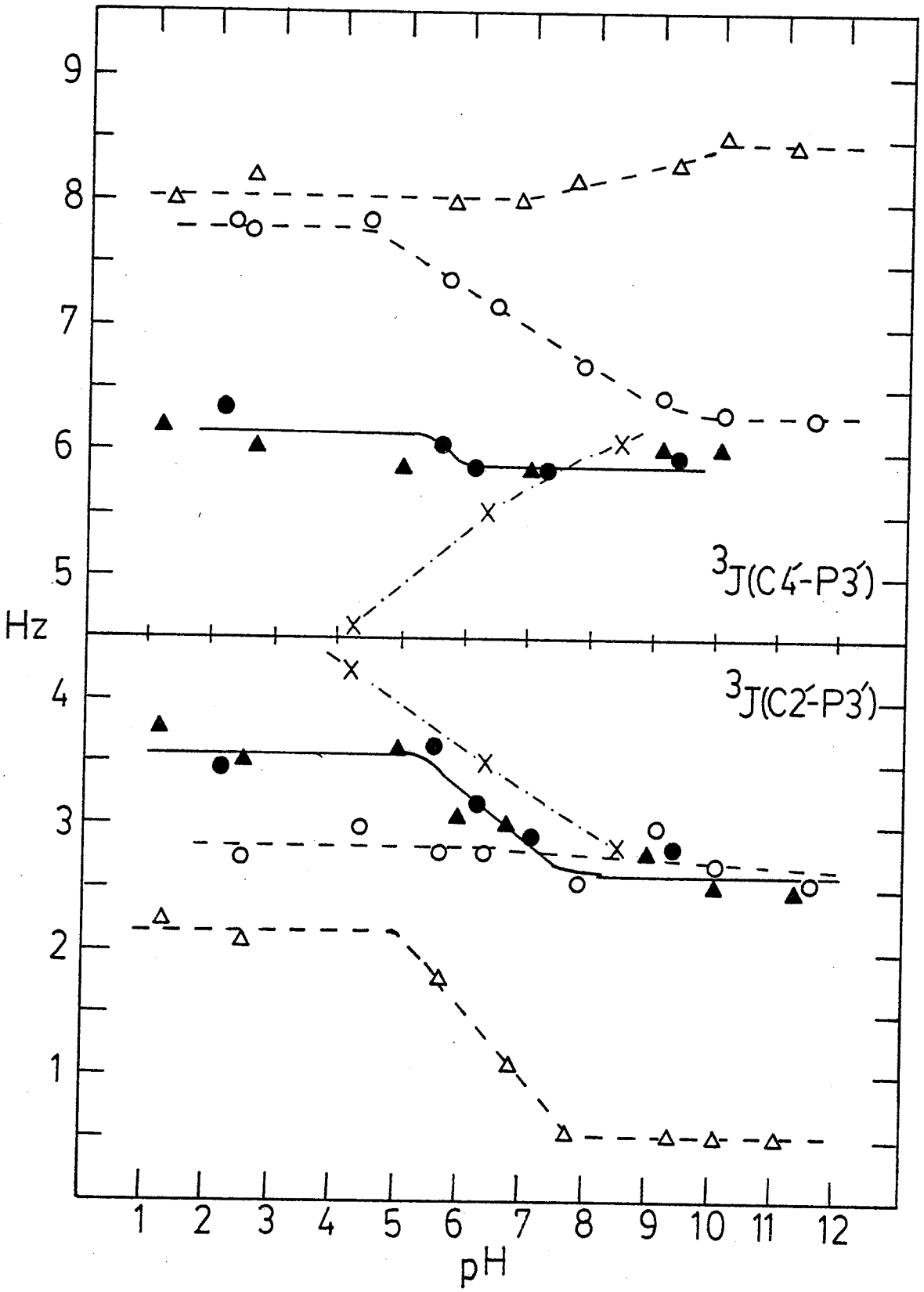
Hz
pH
^3J(C4'-P3')
^3J(C2'-P3')

derivatives is not affected by the changes in charge on the 3'- and 5'-phosphates.

It is interesting to note that in basic solution the corresponding couplings of 3'-UMP and 3'-dTMP are identical. In acid solution, however, ^{3}J(C4'-P3') in 3'-UMP is about 1.5 Hz smaller than its counterpart in 3'-dTMP while ^{3}J(C2'-P3') in 3'-UMP is about 0.5 Hz larger than its counterpart in 3'-dTMP. Thus, in basic solution, the 2'-hydroxyl has no influence on the ϕ' orientation which is apparent in the ^{13}C, ^{31}P couplings. However, in acid solution, when the phosphate groups are monoanionic, the 2'-hydroxyl appears to destabilize slightly the ϕ'_t domain - presumably the effect of the change in sugar conformations (predominant S-type in 3'-dTMP and near equal N-S conformers in 3'-UMP [77b]). The near equality of the ^{3}J(C2'-P3') (4.2 Hz) and ^{3}J(C4'-P3') (4.6 Hz) couplings of 3'-UMP in acid solution would indicate a near balance in time spent in the ϕ'_t and ϕ'_- domains.

For 3'-m^{6}dUMP and 3',5'-m^{6}dUDP at acid pH the ^{3}J(C4'-P3') couplings are about 1.5 - 2.0 Hz larger than those for the dT molecules. On the other hand, the ^{3}J(C2'-P3') couplings are smaller for the m^{6}dU molecules, by $\sim$0.5 Hz for 3'-m^{6}dUMP and by $\sim$1.5 Hz for 3',5'-m^{6}dUDP. Thus, the ϕ'_t domain appears to be stabilized by the syn m^{6}dU base, the effect being noticeably larger at the 3',5'-diphosphate level. This apparent dependence of the ϕ' orientation upon the conformation about the N-glycosyl link (χ) cannot be due to a direct effect since the base and 3'-phosphate lie on opposite sides of the sugar ring. It is more likely that this dependence of ϕ' on χ is mediated by the changes in

the sugar ring conformation elicted by the syn base (see below).

Some interesting changes (Figure 5.4) are seen in the m^6dU data as the solution enters the basic range in which the phosphates bear two negative charges. Thus, while $^3J(C4'-P3')$ for 3'-m^6dUMP shows a decrease from $\sim$7.8 Hz to 6.3 Hz, $^3J(C2'-P3')$ shows little dependence on pH. In basic solution, the couplings of 3'-m^6dUMP are to within experimental error identical to their counterparts in 3'-dTMP. Again, it would be difficult to disentangle direct effects from conformational effects of phosphate ionization. The data do indicate, however, that the syn base does not have large effects on the ϕ' torsion angle distribution of a 3'-nucleotide in basic solution.

More dramatic pH effects are noted for the 3',5'-diphosphate of m^6dU. Thus, in basic solution, $^3J(C2'-P3')$ decreases by 1.5 Hz to 0.5 Hz while $^3J(C4'-P3')$ increases by $\sim$0.5 Hz to 8.5 Hz. Thus, for 3'-m^6dUMP and 3',5'-m^6dUDP, the magnitudes of the corresponding couplings diverge as the phosphates undergo secondary ionization. Thus, in basic solution, large differences (2 Hz) are evident in the couplings for the pair of m^6dU derivatives. (In acid solution these differences are much smaller - about 0.7 Hz for $^3J(C2'-P3')$ and 0.2 Hz for $^3J(C2'-P3')$). These 2 Hz differences indicate that, for an m^6dU unit, the 5'-phosphate influences the conformation about the $C_{3'}—O_{3'}$ bond, particularly when the 3'- and 5'-phosphates bear two negative charges. This contrasts with the situation for 3'-dTMP and 3',5'-dTDP where no difference in the corresponding couplings is noted at any pH, no 5'-phosphate influence thus being apparent. The

magnitudes of the couplings for 3',5'-m^6dUDP in basic solution - 0.5 Hz for ^3J(C2'-P3') and ∿8.5 Hz for ^3J(C4'-P3') - indicate a very strong preference for the ϕ_t' conformer. The diminutive value of ^3J(C2'-P3') suggests further a strong tendency towards a 90° Karplus angle between the $C_{2'}$—$C_{3'}$ and $O_{3'}$—$P_{3'}$ bonds. The Govil-Smith equation[119] for ^{13}C-^{31}P couplings predicts that a 0.5 Hz coupling is expected for an 86° Karplus angle. This Karplus angle corresponds to a ϕ' value of -154° which falls near to the ϕ_t' extreme of the broad range defined by the ϕ' values of crystalline 3'-ribonucleotides (see above).

Also, given the diminutive value of ^3J(C2'-P3') (∿0.5 Hz) in 3',5'-m^6dUDP in basic solution, we may consider the magnitude of ^3J(C4'-P3') (8.5 Hz) as a lower-limit estimate for a trans (180° Karplus angle) ^3J(C-P) coupling for the $C_{4'}$—$C_{3'}$—$O_{3'}$—$P_{3'}$ and $C_{2'}$—$C_{3'}$—$O_{3'}$—$P_{3'}$ fragments for these molecules in basic solution.

Requiring some explanation are (a) the apparent stabilization of the ϕ_t' conformer by the syn m^6dU base and (b) the apparent influence of the 5'-phosphate on the ϕ' orientation in the m^6dU, but not the dT derivatives, and the strong, if not overwhelming, preference for ϕ_t' in 3',5'-m^6dUDP. The apparent dependence of the ϕ' orientation upon the conformation about the N-glycosyl linkage cannot be due to a direct interaction since the base and the 3'-phosphate lie on opposite sides of the sugar ring. The results of X-ray crystallographic and theoretical studies (discussed below) suggest that this dependence of ϕ' on χ is mediated by changes in the sugar ring pucker elicited by the change from the anti dT base to the syn m^6dU base.

Thus, of the eight known 3'-ribonucleotide crystal structures surveyed by Sundaralingam et al.[102], the two which are N-type have ϕ' in the t domain. Of the remaining six molecules - which are S-type - four are g_- and two are t. In their survey of the nucleotide units of crystalline yeast tRNA(phe), Jack et al.[184] have noted that the ϕ'_t range is preferred for N-type units while for the S-type units, ϕ'_- and ϕ'_t units are equally acceptable. In crystalline d(pTpT) [168], the internal $C_{3'}$—$O_{3'}$ bond is ϕ'_- and the linked 5'-terminal sugar is 2'endo. Thus, the available crystal data points to a correlation between the sugar pucker and the preferred ϕ' angle, namely, that ϕ'_- is likely only for S-type sugars and is destabilized by the N-type pucker. This trend is in line with predictions based on energy calculations by Sathyanarayana and Sasisekharan[185]. These theoreticians have suggested that ϕ'_- is destabilized in the N-type pucker by steric interactions between the phosphate oxygens and the $C_{5'}$ hydrogens. On the other hand, Jack et al.[185] suggested that the ϕ'_t is preferred when the unit is in the N-state because the 3'-phosphate oxygens and $O_{5'}$ are "rather close" in the N-type-ϕ'_- combination. Finally, Lee et al.[34] have interpreted their ^{1}H NMR data in terms of a correlation of the pucker-ϕ' conformations of dinucleoside monophosphates in aqueous solution analogous to that suggested by crystallographic and theoretical studies.

The trends in the ^3J(C-P) data of the dT and m^6dU derivatives can, for the most part, be understood in terms of this pucker-ϕ' correlation. Thus, 2'-deoxyribosides including 5'-dTMP [73] and

3',5'-dTDP are known to favor the S-type pucker in solution and in the crystal state[173,179]. However, the presence of the syn m^6dU base leads to a partial shift towards the N-type conformation[73]. The general shift towards ϕ_t' for the m^6dU derivatives is reasonable now if the ϕ_-' conformer is in fact unstable in a N-type sugar. Furthermore, the pronounced shift towards ϕ_t' in 3',5'-m^6dUDP upon secondary phosphate ionization suggests that the destabilization of the N-type-ϕ_-' combination is, at least in part, due to an electrostatic repulsion between the 3'- and 5'-phosphates. This repulsion would be particularly severe when the $C_{4'}$—$C_{5'}$ bond is g_- and less important for the g_+ and t conformers (see Figure 2.6).

Clearly then, rotation into ϕ_t' seems to be the mechanism to reduce the repulsion of the negatively charged phosphates. Apparently, when the 3'- and 5'-phosphates bear two negative charges (pH > 8.0) a preponderance of ϕ_t' is obtained. One notes, however, that no phosphate-phosphate interaction is apparent in 3',5'-dTDP since the ^{13}C-^{31}P couplings are identical at all pH values to the corresponding couplings in 5'-dTMP. This suggests that phosphate-phosphate interactions are important only in N-type sugars.

Undoubtedly of importance insofar as the difference in pH trends for the dT and m^6dU derivatives are concerned (Figure 5.3) is the conformation about the $C_{4'}$—$C_{5'}$ bond. The syn m^6dU base is known to cause rotation out of g_+ (Figure 2.6) which dominates in 5'-dTMP[29] and 3',5'-dTDP (see above).

b. DINUCLEOSIDE MONOPHOSPHATES

Turning now to the data concerning the ϕ' bond of the dinucleoside monophosphates, the trends observed for this bond can be discussed in the light of the observations made for the ψ bond in Section V.C.1.a.(ii). In order to explain the increase in the g_+ rotamer population of the ψ bond of the 5'-nucleotide fragment of d(TpT) compared to d(m^6UpT), the presence of stabilizing forces arising from interbase interactions was suggested. These interactions were consistent with a g_-,g_- conformation about ω',ω. Although the ϕ' conformation is not as critical for the presence of the interbase interactions as ω',ω, it follows from the examination of molecular models that ϕ'_t is more conducive to the proposed stabilization than ϕ'_-. As can be seen from an examination of the data in Table 5.10, there is a biasing of the ϕ'_t rotamer in d(TpT), reflected primarily by an increase in ^3J(C4'-P3') compared to this coupling in 3'-dTMP. Inspection of Table 4.17 shows that the two vicinal carbon-phosphorus couplings in the -pdT part of d(TpT) are independent of temperature, consistent with the independence of $p(\psi_+)$, as noted above (at 293 K $p(\psi_+)$ = 0.70 while at 338 K, $p(\psi_+)$ = 0.6 [29]). In the case of d(m^6UpT), the observed vicinal couplings, ^3J(C2'-P3') and ^3J(C4'-P3'), are similar to those observed for d(TpT). Also, there is a small temperature dependence of these couplings in d(m^6UpT). ^3J(C2'-P3') increases from 1.8 Hz at 300 K to 3.1 Hz at 340 K, while ^3J(C4'-P3') increases from 7.6 to $\sim$8 Hz over the same temperature range. This is consistent with the lack of any stabilization for the folded form in d(m^6UpT). As the temperature is

increased, the ϕ' bond can assume more flexibility, resulting in the change of the coupling constants. Another factor attributable to the change in the coupling constant is the decrease in the N-type nature of the deoxyribose ring.

Earlier, similar arguments concerning the lack or presence of intrabase interactions were discussed for d(Tpm^{6}U) and d(m^{6}Upm^{6}U), respectively. As indicated in Table 5.10, the ϕ' bond in these two molecules is also different. In Section V.C.2.a.(ii) above, the increase in ψ_t in the 5'-part of d(Tpm^{6}U), coupled with the decrease in ψ_+ and ψ_-, was taken as an indication that the molecule was predominantly in the extended form. The presence of a predominant S-type pucker in the dTp- fragment in d(Tpm^{6}U), coupled with the extended conformation, appears to have increased the flexibility of this bond. Indeed, the observed vicinal couplings, ^{3}J(H3'-P3') and ^{3}J(C4'-P3') in the dTp- of d(Tpm^{6}U), are similar to those observed in 3'-dTMP. In addition, the carbon-phosphorus coupling, ^{3}J(C2'-P3'), was increased to 4.3 Hz compared to 2.9 Hz in 3'-dTMP.

An inspection of Table 4.18 reveals that the two carbon-phosphorus coupling constants are insensitive to variations in temperature, varying by less than 0.5 Hz for either coupling. The near equality implies that ϕ' is sampling the whole range of conformers (whether they are of the two-state type or the single continuum type). The insensitivity of the couplings to temperature further supports this conclusion. This can be contrasted to the situation in d(m^{6}Upm^{6}U). As observed in d(TpT), the two carbon-phosphorus vicinal coupling constants, ^{3}J(C2'-P3') and

^3J(C4'-P3'), appear to be biased in favor of ϕ'_t.

In fact, the observed ^3J(C2'-P3') and ^3J(C4'-P3') couplings of the 3'-nucleotidyl fragments in d(TpT) and d(m^6Upm^6U) are nearly identical over the temperature range studied (Compare Tables 4.17 and 4.20). This is consistent with the proposed stabilization of the folded form in d(m^6Upm^6U), as discussed above. A comparison of the ^3J(H3'-P3') values in the two molecules, however, shows that the observed magnitude is ca 2 Hz larger in d(m^6Upm^6U) than in d(TpT). This should not be considered significant since the latter value was obtained from an iterative analysis of the proton spectrum while the former value was measured directly from the ^{31}P spectrum (The lines in the ^{31}P spectrum were too broad to assign, so in d(m^6Upm^6U), ^3J(H3'-P) is probably not accurate to more than $\pm$1 Hz.)

It is interesting to note that the conclusions concerning the nature of the ω',ω bond reached in the discussion of the ψ bond are consistent with the different behaviours noted in the ϕ' bonds of the corresponding molecules. The correlation between ψ and ϕ' behaviour in the molecules discussed above can be compared to the data for ApA. The reported magnitudes of ^3J(C2'-P3') of 3.7 and 4.6 Hz at 293 K and 343 K, respectively, and of ^3J(C4'-P3') of 5.5 and 4.3 Hz for the same temperatures[56], together with the ψ_+ rotamer populations (0.74 and 0.67 at 293 and 345 K, respectively), as well as the estimated extent of stacking of ca 38% and 20% for these two temperatures, are available for ApA [34,186]. In this molecule, increased temperature reduced the proportion of base stacked molecules in solution. As can be seen, the

two carbon-phosphorus vicinal couplings are similar at higher temperature, as observed in d(Tpm^{6}U). At low temperatures, the ϕ_t' conformer appears to be favored, as observed from the ^3J(C4'-P3') magnitude, and as the results of Kondo and Danyluk[186] indicate.

The presence of the overall folded conformation might be implied by a difference of the ^3J(C2'-P3') and ^3J(C4'-P3') magnitudes. If ^3J(C4'-P3') > ^3J(C2'-P3'), the possibility of folding is present. Near equality of these couplings, on the other hand, can be taken as an indication of the conformational flexibility of this bond, and possibly as the presence of an appreciable amount of the extended conformer in solution. This is only speculative, however, and additional correlations would have to be made for dimers by other techniques (ORD, sedimentation equilibrium, etc.) in order to verify this possible quantitative test.

c. THE SUM (^3J(C4'-P3') + ^3J(C2'-P3'))

A useful quantity to consider is the sum (^3J(C4'-P3') + ^3J(C2'-P3')). These sums for the 3'- and the 3',5'-phosphates of dT and m^{6}dU are plotted vs pH in Figure 5.5 along with the sum values for 3'-UMP and 3'-AMP from Alderfer and Ts'o[53]. The sums lie for the most part within the broad range from 8.3 Hz to 10.5 Hz. The data for the dT and m^{6}dU derivatives show a sigmoidal pH dependence, with the sums decreasing by ∿1 Hz as the solution becomes basic. That the inflection points occur in the pH 6-7 range suggests a dependence upon the ionization state of the phosphates. In both the acid and basic range, the m^{6}dU sums are typically larger than those of the dT derivatives by,

FIGURE 5.5 shows the variation of the sum, S, (^{3}J(C2'-P3') + ^{3}J(C4'-P3')) (in Hz) with pH. The symbols used are those in Figure 5.4.

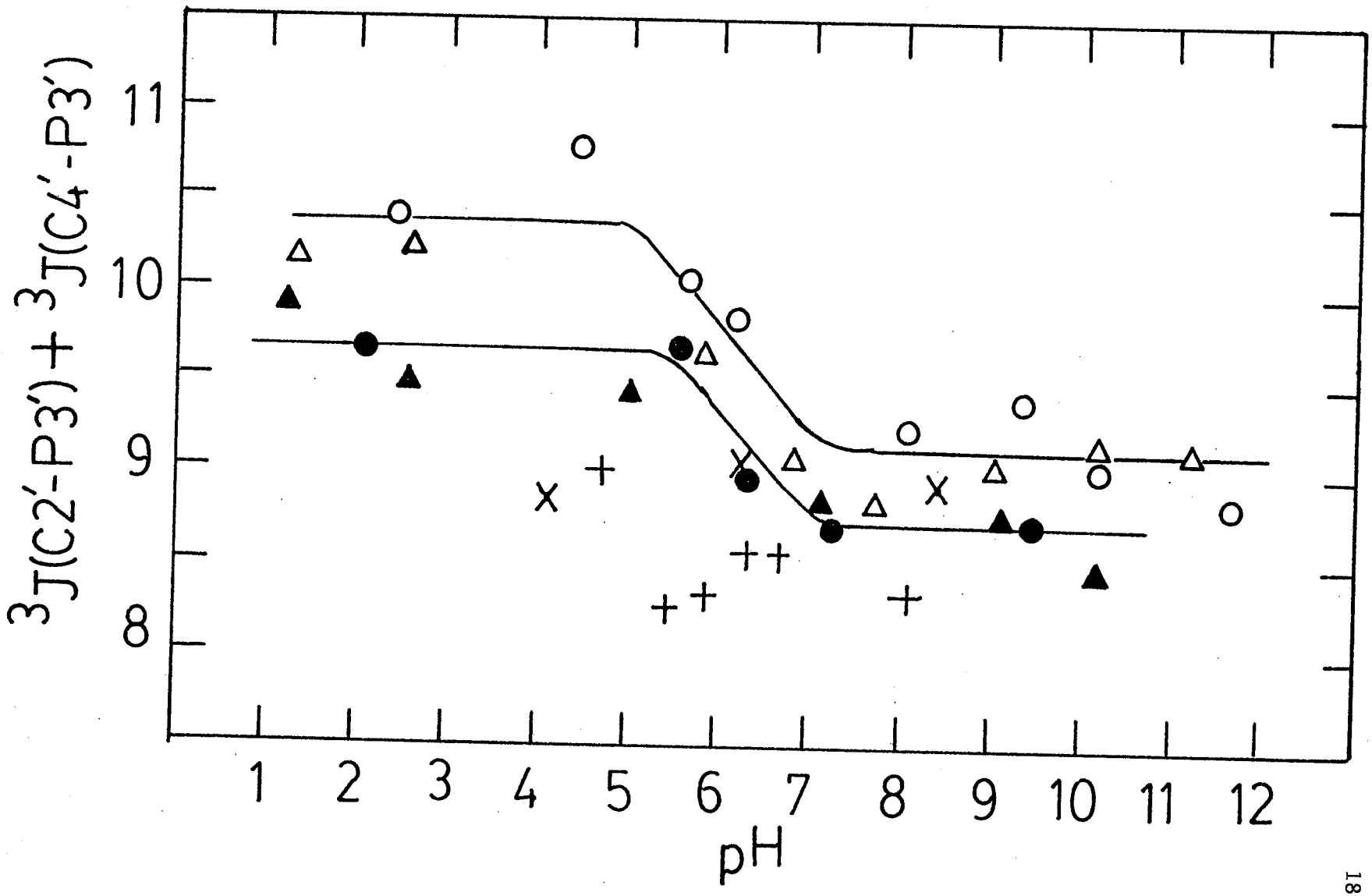

189

on the average, 0.5 Hz. The sum values are smaller for the ribose derivatives 3'-UMP (8.8 - 9.0 Hz) and 3'-AMP (8.3 - 9.0 Hz) and no inflection point is apparent in the pH range of phosphate ionization.

The variation in the sum (^3J(C2'-P3') + ^3J(C4'-P3')) is continued for the dinucleoside monophosphates. Table 5.11 shows the sum of the two vicinal carbon-phosphorus coupling constants vs temperature for the four dimers and the d(TpT) photodimer. The sum in d(TpT) remains constant at about 10 Hz over the temperature range. The data for the other three dimers, however, show a slight temperature dependence, with the sum in d(Tpm^{6}U), d(m^{6}UpT), and d(m^{6}Upm^{6}U) all increasing from about 9.5 Hz at 300 K to 10 Hz or larger at 340 K. In the photodimer of d(TpT), the sum is consistently larger than that observed in d(TpT) itself, starting at 1.6 Hz larger at 300 K and dropping to 0.8 Hz larger at 340 K.

The data in Figure 5.5 and Table 5.11 may serve to caution proponents of a two-state model for treatment of the $C_{3'}$—$O_{3'}$ bond who estimate ϕ_t' and ϕ_-' conformer populations from ^3J(C-P) couplings. In a two-state model with interconversion between "fixed" ϕ_t' and ϕ_-' conformers the sum values are expected to be constant[53]. However, it is clear from Figure 5.5 that the structure of the sugar and the phosphate ionization state have led to a spread about 20% in the sum values. Since the phosphate group is not protonated above pH $\geq$ 1, this ionization effect should not affect the sum of the couplings in the dinucleoside monophosphates. Hence, the variation in (^3J(C2'-P3') + ^3J(C4'-P3')) must be due to conformational changes about ϕ'. In a

TABLE 5.11

SUM OF THE OBSERVED VICINAL CARBON-PHOSPHORUS COUPLING CONSTANTS $^3J(C2'-P3')$ AND $^3J(C4'-P3')$ FOR A SERIES OF DINUCLEOSIDE MONOPHOSPHATES[a]

TEMP.	d(TpT)	d(Tpm^{6}U)	d(m^{6}UpT)	d(m^{6}Upm^{6}U)	d(T(p)T)
300	10.0	9.3	9.4	9.7	11.6
310	10.2	8.9	10.0	10.2	11.4
320	10.0	9.6	11.0	10.2	10.7
340	10.1	9.7	10.9	10.5	10.9

a) Values in Hz for pH ∿6.5 at T = 293 K

two-state model, the sum should remain constant[53]. For the dinucleoside monophosphates studied here, not only does the sum vary from molecule to molecule, but the sum for a given molecule is somewhat dependent on temperature, and the variations are well outside the estimated experimental error of better than $\pm$0.2 Hz. This variation is undoubtedly due in part to alterations in the angular characteristics of the "fixed" conformers as indicated by the temperature dependence of the dimers and, in the case of phosphate ionization, to direct effects on the individual ^3J(C-P) coupling. Some care must be taken then in comparisons of the measured data and calculated ϕ' populations.

D. GEMINAL CARBON-PHOSPHORUS COUPLING CONSTANTS

The following comments can be made about the geminal coupling constants ^2J(C3'-P3') and ^2J(C5'-P5') of the nucleotides, nucleoside diphosphates, and dinucleoside monophosphates of dT and m^6dU. Figure 5.6 shows the variations in ^3J(C3'-P3') and ^3J(C5'-P5') with pH. The magnitudes of these two couplings lie in the range of 4.1-5.1 Hz and 4.2-5.3 Hz, respectively and show little variation over the entire pH range. These are similar to the ^2J(C-P) values reported[53] as a function of pH for 3'-UMP, 3'-AMP, 5'-UMP, and 5'-AMP (4.3-5.0 Hz). The geminal couplings in the dinucleoside monophosphates fall into a slightly higher range (4.9-5.9 Hz) and do not show any pattern with variations in temperature. The couplings ^2J(C3'-P3') in d(Tpm^{6}U), d(m^6UpT), and d(m^6Upm^{6}U) and ^2J(C5'-P5') in d(m^6UpT) and d(m^6Upm^{6}U) are in the lower end of this range (4.9-5.5 Hz) while ^2J(C3'-P3') and ^2J(C5'-P5') in d(TpT) and d(Tpm^{6}U) are in the upper end of this range (5.6-5.9 Hz). Both geminal couplings in the photodimer of d(TpT) are larger than in the dinucleoside monophosphates (5.7-6.0 Hz).

Thus, the ^2J(C3'-P3') couplings appear to be relatively insensitive to the nature of the base (purine or pyrimidine), to the nature of the sugar (ribose or 2'-deoxyribose), to the position (3',5') and ionization state of the phosphate. Formation of the phosphodiester linkages of the dimers causes a slight increase in these couplings. Furthermore, since the dT and m^6dU derivatives favor the anti and syn conformations, respectively[72,73,76,135], insensitivity to the orientation of pyrimidine base about the N-glycosyl linkage is also indicated. It should be

FIGURE 5.6 shows the variation of $^{2}J(C5'-P5')$ and $^{2}J(C3'-P3')$ (in Hz) with pH. The symbols used are those in Figure 5.4 and 5.5.

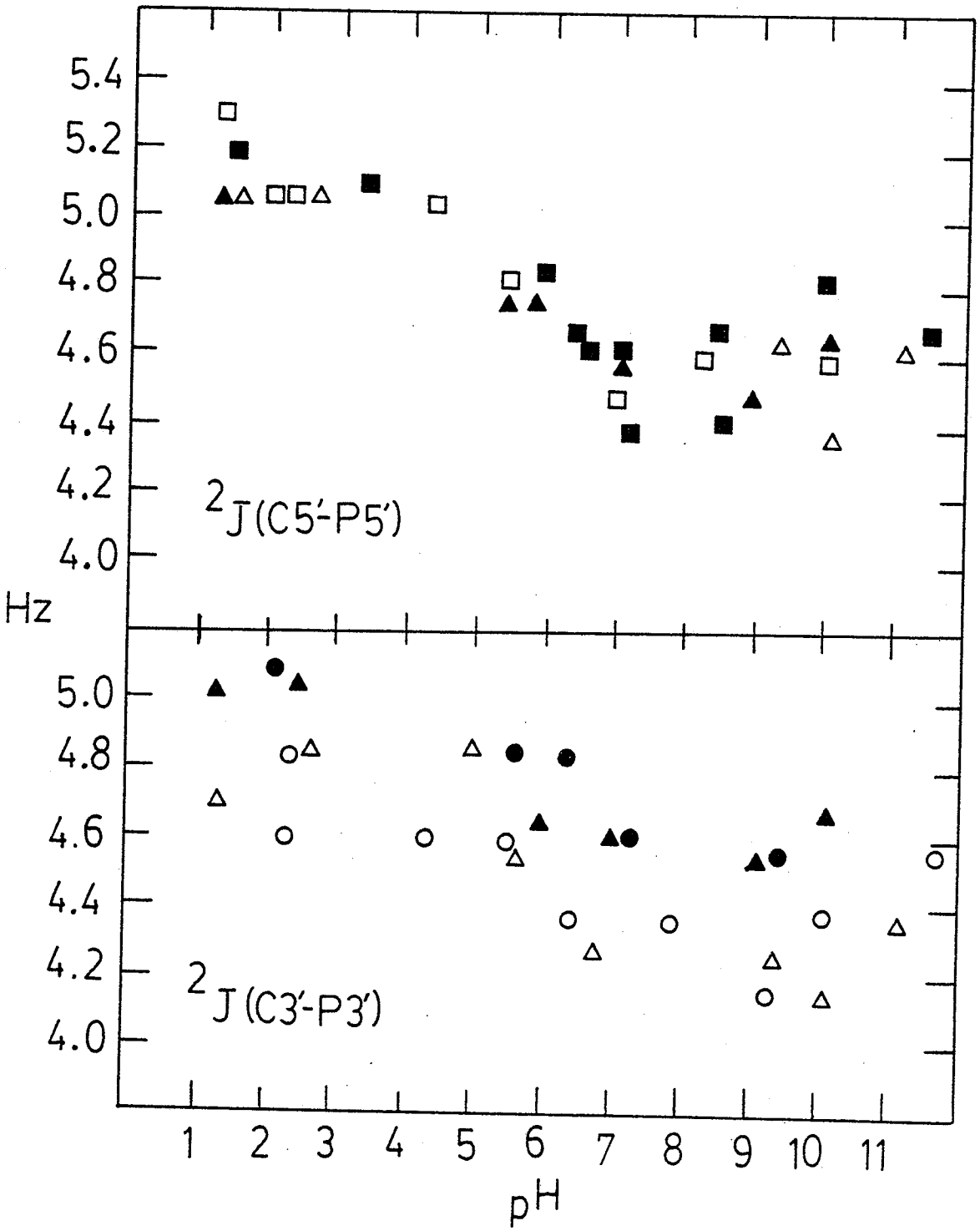
5.4
5.2
5.0
4.8
4.6
4.4
4.2
4.0
Hz
^2J(C5'-P5')
5.0
4.8
4.6
4.4
4.2
4.0
^2J(C3'-P3')
1 2 3 4 5 6 7 8 9 10 11
pH

stressed, however, that certain structural modifications can lead to large changes in ^2J(C-P) couplings. Thus, in the strained 3',5'-cyclic nucleotides, ^2J(C5'-P5') can be as large as 7.0 Hz[155], reflecting perhaps changes in the P—O—C bond angle and P—O torsion angle.

Though the ^2J(C-P) couplings vary little, a weak sigmoidal trend can be discerned in the pH titration curves (Figure 5.6). For both couplings, decreases of ∿0.5 Hz occur for the dT and m^6dU derivatives in the pH range 5-7 due presumably to the phosphate ionization. The plots are in reasonable agreement with the pKa values (∿6.3) reported for secondary phosphate ionization of 3'- and 5'-nucleotides in the 2'-deoxyribose series[60]. Note also that, on the average, the ^2J(C3'-P3') couplings are 0.3 Hz smaller for the m^6dU derivatives relative to the dT derivatives. This difference may be related to differences in the sugar pucker for the syn m^6dU and anti dT derivatives[73].

E. CARBON CHEMICAL SHIFTS

The effect of the N-glycosyl bond conformation on the ribose carbon chemical shifts was discussed in Section V.1.B. and will not be covered further. The carbon chemical shift differences between the nucleosides and mononucleotides, nucleotides and nucleoside diphosphates, and the nucleotides and dinucleoside monophosphates are shown in Tables 5.12 and 5.13 for the dT and m^6dU series, respectively. Phosphorylation effects will be discussed first, followed by dimerization effects.

1. NUCLEOTIDES AND NUCLEOSIDE DIPHOSPHATES

As can be seen in Tables 5.12 and 5.13, some characteristic chemical shift changes are observed in nucleosides upon phosphorylation. In the dT and m^6dU series, the carbon at the point of phosphorylation experiences a downfield shift of about 3.3 ppm. Additional phosphorylation of the nucleotides does not affect the magnitude of this shift in the dT series (i.e., $C_{3'}$ and $C_{5'}$ of 5'-dTMP and 3'-dTMP, respectively, are shifted downfield by 3 ppm in 3',5'-dTDP). In the m^6dU series, however, the effect of the second phosphate has been reduced by ca 0.5 ppm at the second site to about 2.7 ppm. The carbons adjacent to the point of phosphorylation are shifted upfield between 0.71 and 0.84 ppm in the 3'-nucleotides of both dT and m^6dU and between 0.87 and 1.42 ppm in the 5'-nucleotides of both series. Comparing the nucleotides with the nucleoside diphosphates, the upfield shift of the adjacent carbons is preserved, but the effects do not seem to be additive. The second carbon removed from the phosphate group is

TABLE 5.12

CARBON CHEMICAL SHIFT DIFFERENCES ($\Delta\delta$)
BETWEEN NUCLEOSIDES AND NUCLEOTIDES
AND NUCLEOTIDES AND DINUCLEOSIDE MONOPHOSPHATES
IN m^6dU DERIVATIVES[a]

	$\Delta\delta$(C1')	$\Delta\delta$(C2')	$\Delta\delta$(C3')	$\Delta\delta$(C4')	$\Delta\delta$(C5')
3'-m^6dUMP - m^6dU	-0.07	-0.72	+3.23	-0.84	-0.09
3',5'-m^6dUDP - 3'-m^6dUMP	-0.20	-0.06	-0.52	-1.39	+2.75
5'-m^6dUMP - m^6dU	-0.21	-0.20	-0.03	-1.42	+3.14
3',5'-m^6dUDP - 5'-m^6dUMP	+0.08	-0.58	+2.74	-0.81	-0.48
d($\underline{m^6U}$pm^{6}U) - 3'-m^6dUMP	+0.15	-0.70	+1.10	+0.21	-0.14
d($\underline{m^6U}$pT) - 3'-m^6dUMP	-0.27	+0.02	+0.85	-0.43	-0.09
d(m^6Up$\underline{m^6U}$) - 5'-m^6dUMP	-0.25	+0.19	-0.89	-0.49	+0.06
d(Tp$\underline{m^6U}$) - 5'-m^6dUMP	+0.06	+0.65	-0.18	+0.04	+0.63

a) Values are in ppm for samples at pH < 6.0 and T = 300 K. The difference is defined as the chemical shift of a carbon in the nucleotide minus the shift of the corresponding carbon in the nucleoside. A negative value indicates a shift to highfield.

TABLE 5.13

CARBON CHEMICAL SHIFT DIFFERENCES (Δδ)
BETWEEN NUCLEOSIDES AND NUCLEOTIDES
AND NUCLEOTIDES AND DINUCLEOSIDE MONOPHOSPHATES
IN dT DERIVATIVES[a]

	Δδ(C1')	Δδ(C2')	Δδ(C3')	Δδ(C4')	Δδ(C5')
3'-dTMP - dT	-0.03	-0.82	+3.46	-0.71	-0.01
3',5'-dTDP - 3'-dTMP	-0.02	+0.23	+0.42	-0.83	+3.22
5'-dTMP - dT	-0.06	+0.08	+0.66	-0.87	+3.23
3',5'-dTDP - 5'-dTMP	+0.01	-0.67	+3.28	-0.67	-0.02
d(TpT) - 3'-dTMP	+0.17	-0.21	+1.13	-0.27	-0.16
d(Tpm^{6}U) - 3'-dTMP	+0.38	-0.31	+0.66	-0.29	+0.19
d(TpT) - 5'-dTMP	-0.01	+0.09	-0.64	-0.68	+0.45
d(m^{6}UpT) - 5'-dTMP	-0.22	-0.06	-0.41	-0.34	+0.83

a) Values are in ppm for samples at pH < 6.0 and T = 300 K. The difference is defined as the chemical shift of a carbon in the nucleotide minus the shift of the corresponding carbon in the nucleoside. A negative value indicates a shift to highfield.

shifted downfield in the mononucleotides. In the nucleoside diphosphates, the situation is confused for this carbon by the countering effects of the two phosphates. In the pyrimidine ring, the C_5 and C_6 carbons show the characteristic downfield shift[51] associated with methylation, i.e., C_5 is 9 ppm downfield in dT compared to U [59], and C_6 is 15 ppm downfield in m^6dU compared to U [59]. The base carbons are insensitive to phosphorylation in the m^6dU series. In the dT series, the only carbon in the pyrimidine ring affected by phosphorylation is C_6, moving downfield by 2 ppm in 3'-dTMP, 5'-dTMP, and 3',5'-dTDP compared to dT. This could be evidence confirming the stabilization of the g_+ conformer in ψ for the 5'-nucleotides discussed in Section V.C.1.a.(ii), where it was argued[73] that the C_6-H position was a positive center and would favor the closer approach of the phosphate. It is unclear why the 3'-phosphate in 3'-dTMP and the 5'-phosphate in 5'-dTMP have an identical shift effect on C_6. It is doubtful that this effect is transmitted through the bonds since there is little change in the $C_{1'}$ shift in the dT or m^6dU series upon phosphorylation.

Figures 5.7, 5.8, and 5.9 show the variation of the chemical shifts with pH for the deoxyribose carbons in the mononucleotides and nucleoside diphosphates in the dT and m^6dU series. As can be seen from these graphs, all deoxyribose carbons reflect the ionization state of the phosphate(s), the point of phosphorylation experiencing the greatest change, with the effect diminishing upon increased separation from the phosphate group. The $C_{4'}$ carbons are also perturbed by the

FIGURE 5.7 is a plot of the carbon chemical shifts of $C_{2'}$ and $C_{5'}$ vs pH. Symbols used are

●, ○ for 3'-dTMP and 3'-m^6dUMP, respectively

■, □ for 5'-dTMP and 5'-m^6dUMP, respectively

▲, △ for 3',5'-dTDP and 3',5'-m^6dUDP, respectively

0.5 ppm has been added to the $C_{5'}$ chemical shifts in the m^6dU series in order to minimize the overlap of the titration curves.

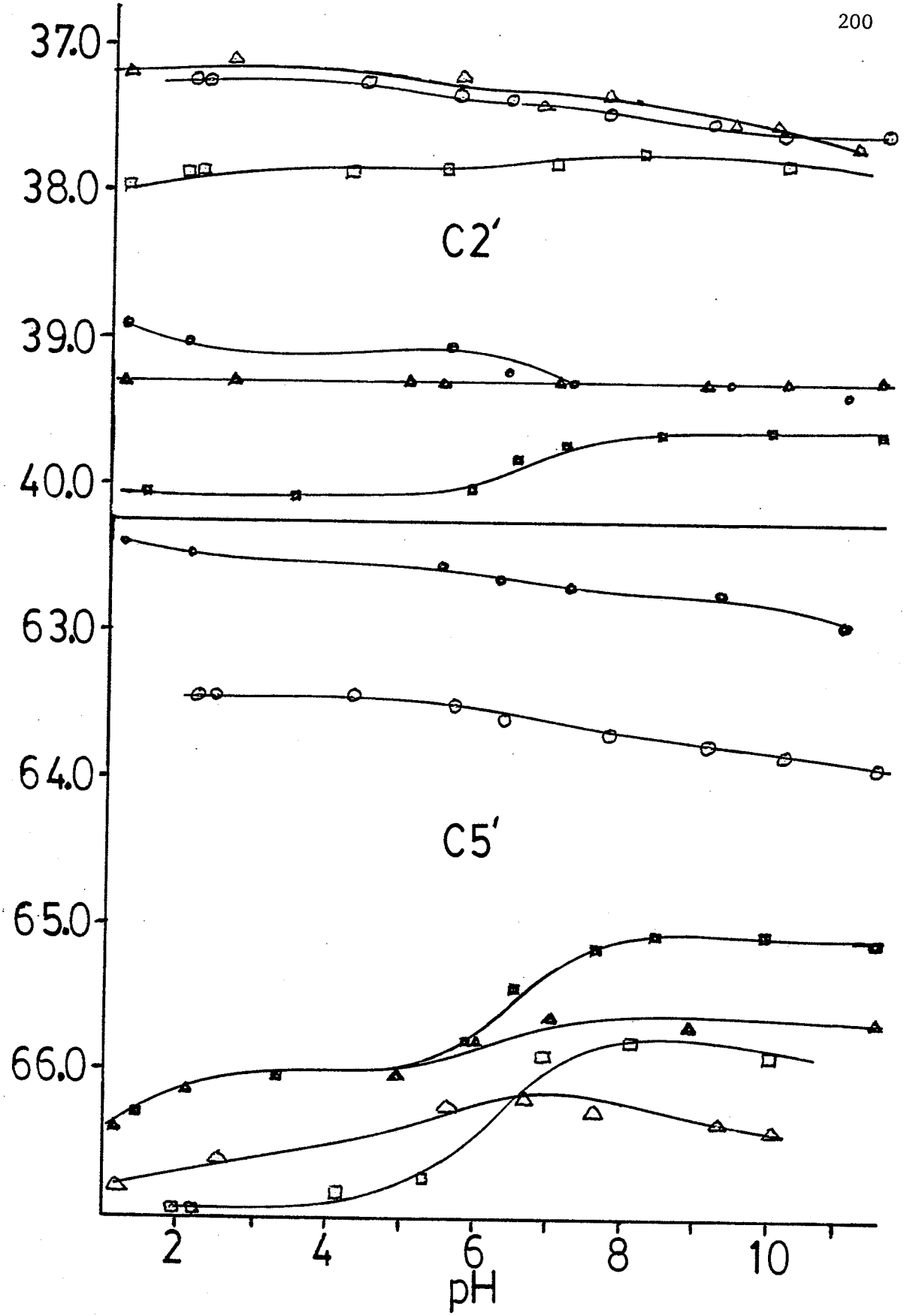
37.0
38.0
C2'
39.0
40.0
63.0
64.0
C5'
65.0
66.0
2
4
6
8
10
pH

FIGURE 5.8 is a plot of the carbon chemical shift of $C_{3'}$ vs pH. Symbols used are the same as those used in Figure 5.7. 1 ppm has been added to the $C_{3'}$ chemical shifts in the m^6dU series in order to minimize the overlap of the titration curves.

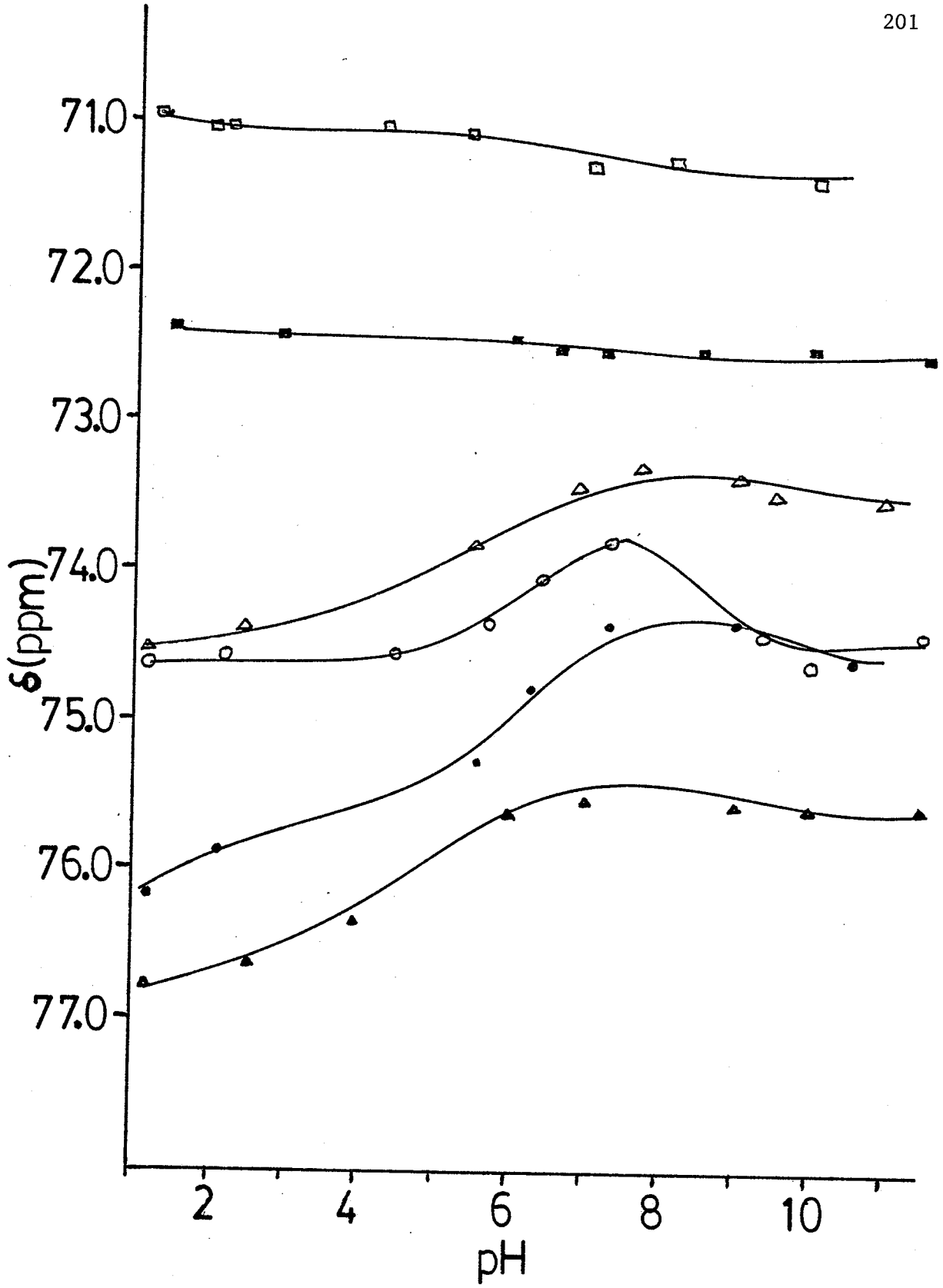
71.0
72.0
73.0
74.0
75.0
76.0
77.0
δ(ppm)
2
4
6
8
10
pH

FIGURE 5.9 is a plot of the carbon chemical shifts of $C_{1'}$ and $C_{4'}$ vs pH. Symbols used are the same as those in Figure 5.7. 1 ppm has been added to the $C_{4'}$ and 0.5 ppm has been added to the $C_{5'}$ chemical shifts in the m^6dU series in order to minimize the overlap of the titration curves.

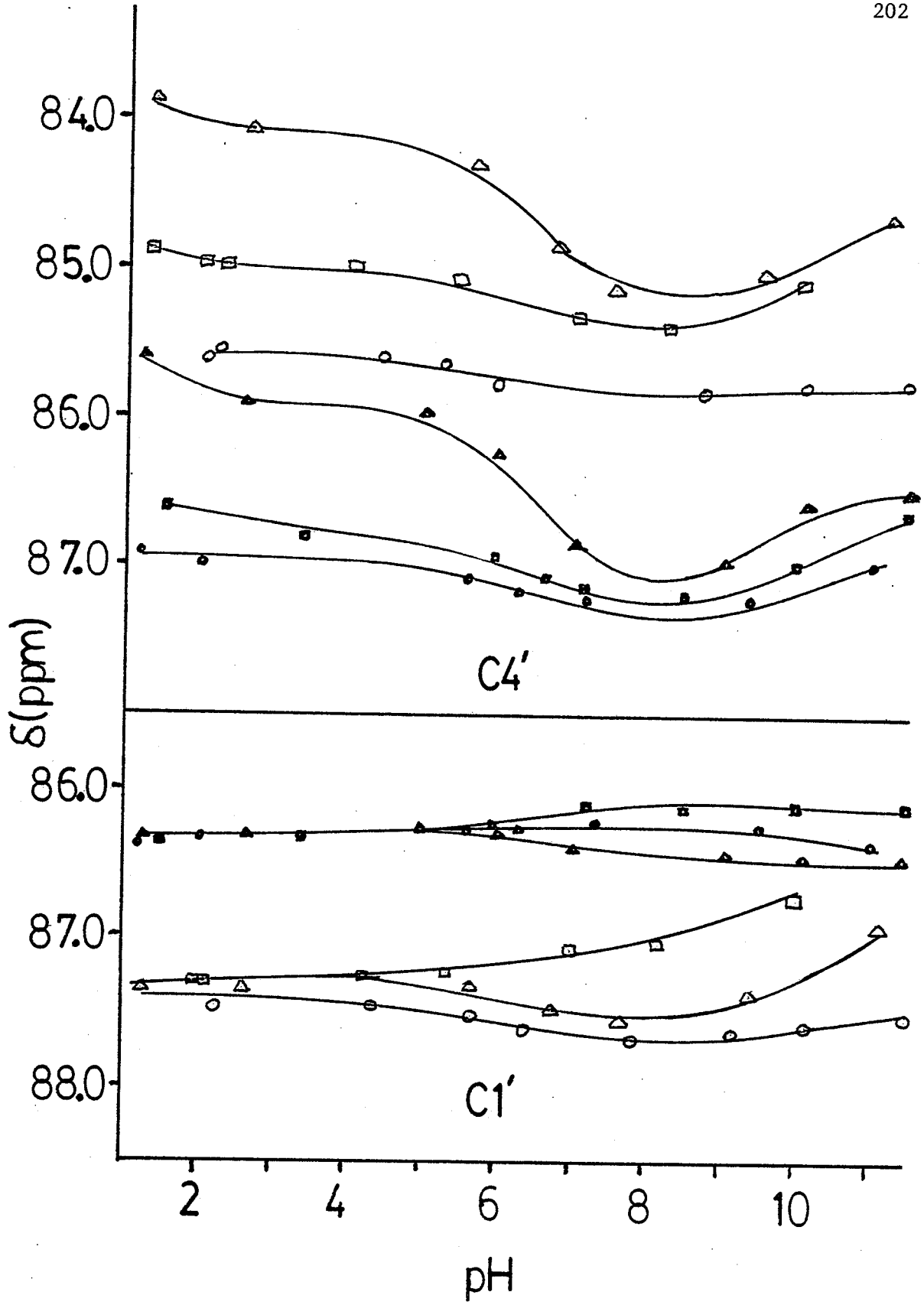
84.0
85.0
86.0
87.0
δ(ppm)
C4'
86.0
87.0
88.0
C1'
2
4
6
8
10
pH

base ionization, and this effect probably reflects small changes in the phosphate orientation due to electrostatic repulsion between the phosphate and the ionized pyrimidine ring. The $C_{3'}$ and $C_{5'}$ carbons are also affected by pyrimidine ionization, but to a lesser extent than $C_{4'}$. The effect of phosphorylation on $C_{3'}$ and $C_{5'}$ noted above for the deoxy sugars is larger than that observed in ribo pyrimidines[54,153] and ribo purines[187,188] (both about 2.5 ppm downfield) but about one half that observed in 2',3'- or 3',5'-cyclic nucleotides[154,155,187,188]. An alternating effect, although apparent in the work on the nucleotides[54,153,187,188] has not been specifically discussed.

2. DINUCLEOSIDE MONOPHOSPHATES

Tables 5.12 and 5.13 also contain the nucleotide to dinucleoside monophosphate chemical shift changes. The tables reveal that $C_{3'}$ and $C_{5'}$ are shifted further downfield by dimerization by 0.45 to 1.33 ppm for the 3'- and 5'-fragments in the dT series and by 0.06 to 1.10 ppm for these same carbons in the m^6dU series. The alternating effect is still apparent for some of the adjacent carbons, which would predict an upfield shift for the carbons next to the point of dimerization. Exceptions to this observation are $C_{4'}$ in the m^6dUp- part of d(m^6Upm^6U) (0.21 ppm downfield), $C_{2'}$ in the m^6dUP- part of d(m^6UpT) (0.02 ppm downfield), and $C_{4'}$ in the -pm^6dU part of d(Tpm^6U) (0.04 ppm downfield). Carbons further removed from the point of dimerization show no clear trend in chemical shift changes. These shift changes are consistent

with dimerization shifts observed for the ribose derivatives[54,153]. Tables 4.17 to 4.21 show that, aside from $C_{3'}$ and $C_{5'}$, there is little variation in carbon chemical shift with temperature for the dimers over the range studied. The temperature variation is similar to that observed in UpU and ApA [54,153].

The temperature invariance of the ^{13}C chemical shifts of the dinucleoside monophosphates is surprising in view of the conformational variabilities of these molecules. It is not clear why this is the case although it is possible that the conformational equilibria of the dimers are not appreciably perturbed within the temperature range studied (see proton data above).

F. A COMPARISON OF THE CARBON-13 RELAXATION TIMES (T_1's) OF d(TpT) AND THE INTERNAL CYCLOBUTANE PHOTODIMER, d(T(p)T)

In u.v. damaged DNA, the primary photoproduct has been found to be formed by thymines adjacent on the polynucleotide strand[189-194]. The major product has been identified as the internal cyclobutane type in the cis-syn form. (In this type of cyclobutane dimer, the two C_5's and the two C_6's are joined by a single bond, with the two methyl groups adjacent to each other and on the same side of the cyclobutane ring. See, for example, Reference 30 and Reference 195.) The minor product is also a cyclobutane type and denotes trans-syn. (The methyl groups are still adjacent, but on opposite sides of the cyclobutane ring.) In an examination of the photodimer production in model compounds, Jones et al.[196] have isolated two isomeric forms of the u.v. photoproduct of d(TpT) and have identified the major and minor product as the cis-syn and trans-syn forms, respectively. Recent studies by Liu and Yang[142] have shown that all three of the common pyrimidine nucleosides incorporated into dinucleoside monophosphates are capable of producing photodimers upon being irradiated with u.v. light. Studies in progress on the three dinucleoside monophosphates examined in this thesis (i.e., d(Tpm^{6}U), d(m^{6}UpT), and d(m^{6}Upm^{6}U)) have shown that d(Tpm^{6}U) does not produce u.v. products similar to d(TpT). The molecules d(m^{6}UpT) and d(m^{6}Upm^{6}U) do react upon u.v. irradiation, but the products from d(m^{6}UpT) have not been identified. There are two isomers of d(m^{6}Upm^{6}U) in nearly equal proportions (55:45), but they have not been separated. Preliminary results from the ^{1}H NMR and ^{13}C

NMR spectrum of the mixture indicate that the photoproducts are also of the internal cyclobutane type.

In light of the above information, it appears that the d(T(p)T) photodimer can be used as a model for the "pure" folded pyrimidine dinucleoside monophosphate. A comparison of the ^{13}C relaxation times for the protonated carbons in d(TpT) and d(T(p)T) might yield a qualitative estimate of the extent of folding in d(TpT).

Theoretical[121,122,197] and experimental[120,198] studies have demonstrated that the relaxation times of some protonated carbons in macromolecules are dominated by the direct, dipolar interaction between the carbon and the directly bound proton(s). In some cases (e.g., methyl groups) the presence of additional mobility will lengthen the relaxation time of the "free" functional group. In the case of the protonated carbons within the structural framework of a molecule, the observed T_1 gives an estimate of the overall correlation time for molecular reorientation[121]. Table 5.14 contains the observed NT_1 values for the ribose carbons, C_6, and the methyl group of the thymine ring in d(TpT) and the major product (i.e., cis-syn) of d(T(p)T). The first observation that can be made from the NT_1 values in Table 5.14 is that the methyl carbon's NT_1 value is about 10 times longer than the ribose carbons in d(TpT). In the photodimer, however, the methyl carbon's NT_1 value is only ca 4 times longer than the ribose carbons, consistent with the steric crowding that is expected in the cis-syn form of the cyclobutane ring. Turning now to an examination of the ribose carbons in the two molecules, only slightly different T_1's

TABLE 5.14

^{13}C RELAXATION TIMES FOR THE PROTONATED CARBONS IN d(TpT) AND d(T(p)T) [a]

	NT_1 [b] d(TpT)		NT_1 d(T(p)T)	
	dTp-	-pdT	dT(p)-	-(p)dT
CH_3	(1.92) [c]		(0.89) [c]	
$C_{2'}$	0.17	0.26	0.23	0.37
$C_{5'}$	0.19	0.14	0.21	0.26
$C_{3'}$	0.19	0.22	0.22	0.32
$C_{4'}$	0.19	0.17	0.24	0.24
$C_{1'}$	0.19	0.16	(0.33, 0.28) [c]	
C_6	(0.16, 0.16) [c]		(0.22, 0.21) [c]	

a) Both samples were 100 mgs/ml D_2O at pH 6.5 and 300 K.

b) NT_1 values are the observed ^{13}C T_1's multiplied by the number of directly bound protons.

c) These resonances cannot be assigned to a specific nucleotide residue.

are observed between d(TpT) and d(T(p)T). In d(TpT), the C_4, and C_1, carbons have (within experimental error) the same NT_1 values of 0.18 sec. while the same carbons in d(T(p)T) have NT_1 values of approximately 0.26 sec, slightly longer than those in d(TpT). Using the NT_1 values for the C_1, and C_4, carbons in d(TpT) and d(T(p)T), Equation 2.23 can be used to estimate the overall molecular reorientation correlation time, τ_c. Rearranging Equation 2.23 and substituting the values for the various constants, values for τ_c of 2×10^{-10} sec and 2.6×10^{-10} sec are obtained for d(T(p)T) and d(TpT), respectively. Using the procedure described by Edwards[123], a molecular volume, determined from the van der Waals increments of atoms of approximately 432 Å^3 is obtained. This value can be substituted into Equation 2.24, and using a value of 1.15 cP for the viscosity of the solution, an estimated correlation time of 1.2×10^{-10} sec is obtained. This value is in excellent agreement with the observed correlation times calculated above from the relaxation times. The factor of approximately two between the correlation times obtained from the relaxation measurements and molecular volumes is similar to the difference observed by Edwards[123] between the calculated molecular volumes and the volumes estimated from density measurements. The agreement between the correlation times for d(TpT) and d(T(p)T) and the calculated correlation time from molecular volumes indicates that there is little intermolecular association in solution at the sample concentration and temperature at which the measurements were made[199,200].

The difference in correlation times calculated for d(TpT) and d(T(p)T) from the observed T_1's is consistent with the presence of some of the extended conformation in solution for d(TpT). The τ_c calculated from the molecular volume assumes a spherical particle. If the molecule is actually an ellipsoid, the correlation time increases, resulting in a decrease in the observed T_1. The shorter T_1's for $C_{1'}$ and $C_{4'}$ in d(TpT) compared to $C_{1'}$ and $C_{4'}$ in d(T(p)T) indicate that there is some extended conformation for d(TpT) in solution. The accuracy of $\pm$10% in the observed ^{13}C T_1's precludes a quantitative estimate of the proportion of the extended conformation in solution for d(TpT).

Finally, it is interesting to note the difference in T_1's within a given molecule. In d(TpT), for example, the T_1's for $C_{2'}$ and $C_{3'}$ of the 5'-nucleotidyl fragment are significantly longer than the observed T_1's for the other ribose carbons, even $C_{2'}$ and $C_{3'}$ of the 3'-nucleotidyl fragment ($\sim$0.24 sec for $C_{2'}$ and $C_{3'}$ of the 5'-fragment compared to 0.18 sec for the other carbons). The situation in d(T(p)T) is identical, with T_1's for the $C_{2'}$ and $C_{3'}$ carbons of the 5'-fragment of 0.35 sec compared to a value of 0.22 sec for the other ribose carbons and C_6 of the pyrimidine rings. The longer T_1's for $C_{2'}$ and $C_{3'}$ or the 5'-nucleotidyl fragments of d(TpT) and d(T(p)T) are consistent with the flexibility about the $C_{2'}$—$C_{3'}$ bond which is involved in pseudorotation in these molecules. The data also suggests that the $C_{2'}$ and $C_{3'}$ carbons are less mobile in the 3'-fragment than in the 5'-fragment of a dinucleoside monophosphate.

It should be noted that the above comparison of T_1's is only qualitative. Accurate information concerning the overall and internal mobility of these molecules would require a careful and extensive study of the entire dT (and m^6dU) series. In addition, the relaxation studies should be correlated with other experimental techniques such as circular dichroism, dielectric relaxation, and other methods to get a more complete view of the dynamics of these molecules in solution.

CHAPTER VI

CONCLUSIONS

A number of conclusions can be drawn from the discussion of the data in the previous chapter.

First, the proton and carbon chemical shift data indicates that the N-glycosyl bond conformation of a dT or an m^6dU fragment is not affected by mono- or diphosphorylation of the nucleoside or by incorporation of a nucleotide into a dinucleoside monophosphate. Proton-carbon vicinal coupling constants for the nucleosides and mononucleotides of dT and m^6dU qualitatively agree with a predominant syn conformation in the m^6dU series and a predominant anti conformation in the dT series. An attempt at a quantitative determination of the syn-anti conformer populations for dT using the proton-carbon vicinal coupling constants between $H_{1'}$ and C_2 and/or C_6 was premature but informative. With proper parameterization, the proton-carbon vicinal coupling constants might be able to give quantitative information concerning the N-glycosyl bond conformers. The m^6dU fragment appears to be an ideal model to monitor the effect of the syn conformation of the N-glycosyl bond on the overall conformation of nucleotides, nucleoside diphosphates, and dinucleoside monophosphates.

Second, the presence of the syn pyrimidine in the m^6dU series has imposed changes in the conformational blend of the deoxyribose ring. Pseudorotational analysis of the proton-proton vicinal coupling constants of the deoxyribose ring indicates that the dT series follows the normal $N \rightleftharpoons S$ equilibrium observed for ribose and deoxyribose nucleosides and nucleotides. Pseudorotational analysis of the vicinal coupling constants observed in the m^6dU series indicates that the

phase angle of pseudorotation, P, and the amplitude of pucker, τ_m, are markedly different from the values observed in the dT series. The proposed S-state conformation of the m^6dU series in solutions agrees well with that observed for m^6dU in the crystal state. There is, however, some discrepancy in the conformer populations calculated by the pseudorotational method and empirical relationships. Also, it is uncertain what N-state conformer is coupled with the predicted S-state conformer. In general, the qualitative observations made for the nucleoside and mononucleotides of m^6dU are conserved in the nucleoside diphosphate and the m^6dU fragments of dinucleoside monophosphates.

Third, the conformational trends observed for the transition from the dT to m^6dU nucleosides and mononucleotides is continued in the nucleoside diphosphates and the dinucleoside monophosphates. Based on the observed trends in the $C_{5'}—C_{4'}$ and $C_{3'}—O_{3'}$ bond conformer preferences, it appears that there is an interaction between the two pyrimidine rings in a dinucleoside monophosphate when both bases have similar orientations about the N-glycosyl bond. That is, it appears as if d(TpT) and $d(m^6Upm^6U)$ favor an overall folded conformation while $d(Tpm^6U)$ favors an extended conformation. The situation in $d(m^6UpT)$ is uncertain, but the molecule might exist in the folded and extended forms to an equal extent. The observed carbon-phosphorus coupling constants provide additional information concerning the $O_{5'}—C_{5'}$ and $C_{3'}—O_{3'}$ bond conformers. In the case of the $O_{5'}—C_{5'}$ bond, ^3J(C4'-P5') complements the information obtained from the proton-

phosphorus vicinal coupling constants. In the case of the $C_{3'}—O_{3'}$ bond, $^{3}J(C2'-P3')$ and $^{3}J(C4'-P3')$ provide more information concerning the conformer preference about this bond than the single observed proton-phosphorus vicinal coupling constant. The observation concerning the carbon-phosphorus vicinal coupling constants applies to the nucleotides, nucleoside diphosphates and the dinucleoside monophosphates. It appears, however, that the parameterization of the carbon-phosphorus vicinal coupling constants might be different for nucleotides and dinucleoside monophosphates.

Fourth, the geminal carbon-phosphorus coupling constants appear to be less sensitive to conformational changes than the vicinal carbon-phosphorus coupling constants. The magnitude of the geminal coupling shows some dependence on the ionization state of the phosphate and the C—O—P bond angle. In general, the two bond carbon-phosphorus coupling constant is relatively insensitive to structural and conformational changes.

Finally, the carbon chemical shifts of the nucleotides and dinucleoside monophosphates show characteristic changes upon phosphorylation and dimerization. The electronic influence of the phosphate group appears to be present throughout the ribose ring as demonstrated by the titration curves for the nucleotides and nucleoside diphosphates. In addition, the carbon chemical shifts are sensitive to conformational changes such as the conformation of the N-glycosyl bond and, possibly, sugar pucker and the conformation about $O_{5'}—C_{5'}$ and $C_{3'}—O_{3'}$ in the nucleotides and nucleoside diphosphates. Unfortunately, there is

not enough ^{13}C chemical shift data available for nucleic acid derivatives to characterize the latter three conformational changes. In addition, the chemical shift changes for C_2, only give qualitative information about the N-glycosyl bond.

CHAPTER VII

RECOMMENDATIONS FOR FUTURE RESEARCH

The discussion of the data in the previous chapters has resulted in some important unanswered questions. There is a need for a parameterization of the proton-carbon vicinal coupling constants between H_1, and the pyrimidine carbons. The vicinal coupling constants in the m^6dU series might be a good estimate of the syn conformation proton-carbon vicinal coupling constants in pyrimidine derivatives. Still needed, however, are similar values for the anti conformation. Studies of the m^2dU series (i.e., the 2-methoxy derivative of dU), in which the pyrimidine is expected to be predominantly anti, might yield the desired values.

The problems concerning the deoxyribose ring pucker need to be investigated. Primarily, a concerted effort should be made to quantify the pseudorotational barrier in the deoxyribose ring. An accurate estimate of this barrier is needed to decide what type of averaging of the proton-proton vicinal coupling constants is appropriate. In addition, it would be interesting to find a crystal structure with an N-type conformation in the m^6dU series. This would clarify which N-type conformer is appropriate in the pseudorotational analysis of the m^6dU derivatives in solution. The desired N-type conformer might be present in the crystal structures of a 5'-protected nucleoside or the 5'-nucleotide. The N-type and S-type conformers in the solid state for these molecules might be generally applicable to nucleosides and nucleotides in the syn conformation.

It is apparent that an exhaustive study of the carbon-phosphorus

vicinal coupling constants is needed to better correlate the observed coupling constants with the conformational preferences of the ϕ and ϕ' bond. The parameterization is especially needed for ^3J(C2'-P3') and ^3J(C4'-P3') as these coupling constants are better indicators of the $C_{3'}$—$O_{3'}$ bond conformer preference than ^3J(H3'-P3').

It would also be interesting to see what effect a syn nucleoside has on the conformation of a trinucleoside diphosphate. The greatest perturbation is expected for a syn nucleoside in the central or 5'-terminal nucleotide. Studies along this line could be informative.

Finally, more information concerning the internal cyclobutane photodimers of pyrimidine nucleosides is needed. The carbon chemical shifts for d(T(p)T) are reported here but not discussed. This is due to the fact that there is not an unambiguous assignment of the most important carbons in the spectrum (i.e., $C_{1'}$, C_6, and C_5 from both fragments. Specific ^{13}C enrichment of $C_{1'}$ in one of the nucleotides should result in an unambiguous assignment of these carbons in both d(TpT) and d(T(p)T). A thorough investigation of the photodimers of the m^6dU series is also important. In addition, the trinucleoside diphosphate d(TpTpT) should be irradiated to determine if there is any preferred direction to photodimer formation.

BIBLIOGRAPHY

1. V. F. Bystrov, Prog. in NMR Spectroscopy 10, 41 (1976).

2. V. F. Brystov, A. S. Arseniev, and Yu. D. Gavilov, J. Mag. Res. 30, 151 (1978).

3. O. W. Howarth and D. M. J. Lilley, Prog. in NMR Spectroscopy 12, 1 (1978).

4.a. H. H. Mantsch, H. Saito, I. C. P. Smith, Prog. in NMR Spectroscopy 11, 211 (1977).

b. E. Oldfield, Prog. in NMR Spectroscopy 13, (1979).

5. T. D. Inch in "Annual Review of NMR Spectroscopy, Vol. 2" ed. by E. F. Mooney, Academic Press, New York, (1969).

6. D. B. Davies, Prog. in NMR Spectroscopy 12, 135 (1978).

7. D. R. Kearns, Ann. Rev. Biophys. Bioeng. 6, 477 (1977).

8. C. D. Jardetzky, J. Am. Chem. Soc. 82, 229 (1960).

9. C. D. Jardetzky, J. Am. Chem. Soc. 83, 2919 (1961).

10. C. D. Jardetzky, J. Am. Chem. Soc. 84, 62 (1962).

11. R. U. Lemieux, Can. J. Chem. 39, 116 (1961).

12. S. S. Danyluk and F. E. Hruska, Biochem. 7, 1038 (1968).

13. F. E. Hruska and S. S. Danyluk, J. Am. Chem. Soc. 90, 3266 (1968).

14. F. E. Hruska, C. L. Bell, T. A. Victor, and S. S. Danyluk, Biochem. 7, 3721 (1968).

15. F. E. Hruska and S. S. Danyluk, Biochim. Biophys. Acta. 157, 238 (1968).

16. M. P. Schweizer, A. D. Broom, P. O. P. Ts'o, and D. P. Hollis, J. Am. Chem. Soc. 90, 1042 (1968).

17 P. O. P. Ts'o, Ann. N. Y. Acad. Sci. 153, 785 (1969).

18. P. O. P. Ts'o, N. S. Kondo, M. P. Schweizer, and D. P. Hollis, Biochem 8, 997 (1969).

19. B. J. Blackburn, A. A. Gray, I. C. P. Smith, and F. E. Hruska, Can. J. Chem. 48, 2866 (1970).

20. F. E. Hruska, A. A. Grey, and I. C. P. Smith, J. Am. Chem. Soc. 92, 214 (1970).

21. F. E. Hruska, A. A. Grey, and I. C. P. Smith, J. Am. Chem. Soc. 92, 4088 (1970).

22 A. A. Grey, I. C. P. Smith, and F. E. Hruska, J. Am. Chem. Soc. 93, 1765 (1971).

23. D. J. Wood, F. E. Hruska, R. J. Mynott, and R. H. Sarma, Can. J. Chem. 51, 2571 (1973).

24. F. E. Evans and R. H. Sarma, J. Biol. Chem. 249, 4754 (1974).

25. C.-H. Lee, F. E. Evans, and R. H. Sarma, J. Biol. Chem. 250, 1290 (1975).

26. C. Altona, J. H. van Boom, J. R. de Jager, H. J. Koeners, and G. van Binst, Nature 247, 558 (1974).

27. C. Altona, H. J. Koeners, J. R. de Jager, J. H. van Boom and G. van Binst, Recl. Trav. Chim. 93, 169 (1974).

28. C. Altona in "Structure and Conformation of Nucleic Acids and Protein-Nucleic Acid Interactions" ed. by M. Sundaralingam and S. T. Rao, University Park Press, Balt., (1975), p. 613

29. D. J. Wood, F. E. Hruska, and K. K. Ogilvie, Can. J. Chem. 52, 3353 (1974).

30. F. E. Hruska, D. J. Wood, and K. K. Ogilvie in "Structure and Conformation of Nucleic Acids and Protein-Nucleic Acid Interactions" ed. by M. Sundaralingam and S. T. Rao, University Park Press, Balt., (1975), p. 339

31. C.-H. Lee, F. E. Evans, and R. H. Sarma, FEBS Lett. 51, 73 (1975).

32. F. E. Evans, C.-H. Lee, and R. H. Sarma, Biochem. Biophys. Res. Commun. 63, 106 (1975).

33. N. S. Kondo and S. S. Danyluk, Biochem. 15, 756 (1976).

34. C.-H. Lee, F. S. Ezra, N. S. Kondo, R. H. Sarma, and S. S. Danyluk, Biochem. 15, 3627 (1976).

35. F. S. Ezra, C.-H. Lee, N. S. Kondo, S. S. Danyluk, and R. H. Sarma, Biochem. 16, 1977 (1977).

36. D. J. Wood, K. K. Ogilvie, and F. E. Hruska, Can. J. Chem. 53, 2781 (1975).

37. F. E. Evans and R. H. Sarma, Nature 263, 567 (1976).

38. C. Altona, J. H. van Boom, and C. A. G. Haasnoot, Eur. J. Biochem. 71, 557 (1976).

39. D. M. Cheng, M. M. Dhingra, and R. H. Sarma, Nuc. Acid Res. 5, 4399 (1978).

40. G. P. Kreishman and S. I. Chan, Biopolymers 10, 159 (1971).

41. N. S. Kondo and S. S. Danyluk, J. Am. Chem. Soc. 94, 5121 (1972).

42. N. S. Kondo, A. Leung, and S. S. Danyluk, J. Labelled Comp. 9, 497 (1973).

43. K. Akasaka, S. Shibata, T. Imoto, and H. Hatano, J. Mag. Res. 17, 413 (1975).

44. J. H. Noggle and R. E. Schirmer, "Nuclear Overhauser Effect: Chemical Applications", Academic Press, New York (1971).

45. P. A. Hart and J. P. Davis in "Conformations of Biological Molecules and Polymers" ed. by E. D. Bergmann and B. Pullman, Academic Press, New York (1973), p. 279.

46. P. A. Hart, Biophys. J. 24, 833 (1979).

47. A. J. Jones, D. M. Grant, M. W. Winkley, and R. K. Robins, Proc. Nat. Acad. Sci., U.S.A. 65, 27 (1970).

48. A. J. Jones, D. M. Grant, M. W. Winkley, and R. K. Robins, J. Am. Chem. Soc. 92, 4079 (1970).

49. A. J. Jones, D. M. Grant, M. W. Winkley, and R. K. Robins, J. Phys. Chem. 74, 2684 (1970).

50. A. J. Jones, P. D. Gardner, D. M. Grant, W. M. Litchman, and V. Boekelhide, J. Am. Chem. Soc. 92, 2395 (1970).

51. D. E. Dorman and J. D. Roberts, Proc. Nat. Acad. Sci., U.S.A. 65, 19 (1970).

52. L. T. J. Delbaere, M. N. G. James, and R. U. Lemieux, J. Am. Chem. Soc. 95, 7866 (1973).

53. D. B. Davies, Studia Biophysica, Berlin Band 55, 29 (1976).

54. H. H. Mantsch and I. C. P. Smith, Biochem. Biophys. Res. Commun. 46, 808 (1972).

55. T. Schleich, B. P. Cross, B. J. Blackburn, and I. C. P. Smith in "Structure and Conformation of Nucleic Acids and Protein-Nucleic Acid Interactions) ed. by M. Sundaralingam and S. T. Rao, University Park Press, Balt. (1975), p. 223.

56. J. L. Alderfer and P. O. P. Ts'o, Biochem. 16, 2410 (1977).

57. A. Allerhand, D. Doddrell, and R. Komoroski, J. Chem. Phys. 55, 189 (1971).

58. O. Röder, H.-D. Lüdemann, and E. von Godammer, Eur. J. Biochem. 53, 517 (1975).

59. R. S. Norton and A. Allerhand, J. Am. Chem. Soc. 98, 1077 (1976).

60. P. J. Cozzone and O. Jardetzky, Biochem. 15, 4853 (1976).

61. P. J. Cozzone and O. Jardetzky, Biochem. 15, 4860 (1976).

62. R. Lichter and J. D. Roberts, J. Org. Chem. 35, 2806 (1970).

63. G. E. Hawkes, E. W. Randal, W. E. Holl, J. Chem. Soc. Perkin Trans II, 1268 (1977).

64. P. Buchner, W. Maurer, and H. Ruterjans, J. Mag. Res. 29, 45 (1978).

65. IUPAC-IUB Combined Commission on Biochemical Nomenclature:

a. J. Biol. Chem. 246, 4894 (1971).

b. Biochem. Biophys. Acta. 247, 1 (1971).

c. Biochem. 5, 1445 (1966).

d. J. Mol. Biol. 55, 299 (1971).

e. Eur. J. Biochem. 15, 203 (1970).

66. M. Sundaralingam, B. Pullman, W. Saenger, V. Sasisekharan, and H. R. Wilson in "Conformations of Biological Molecules and Polymers" ed. by E. D. Bergmann and B. Pullman, Academic Press, New York (1973), p. 815.

67. C. Altona and M. Sundaralingam, J. Am. Chem. Soc. 94, 8205 (1972).

68. W. Sanger, Angew. Chem. Internat. Edn. 12, 591 (1973).

69. S. Tran-Dinh and C. Chachaty, Biochem. Biophys. Acta. 335, 1 (1973).

70. F. E. Hruska, K. K. Ogilvie, A. A. Smith, and H. Wayborn, Can. J. Chem. 49, 2449 (1971).

71. R. Deslauriers and I. C. P. Smith, Can. J. Chem. 51, 833 (1973).

72. M. P. Schweizer, E. B. Banta, J. T. Witkowski, and R. K. Robins, J. Am. Chem. Soc. 95, 3770 (1973).

73. A. L. George, F. E. Hruska, K. K. Ogilvie, and A. Holy, Can. J. Chem. 56, 1170 (1978).

74. P. A. Hart and J. P. Davis, Biochem. Biophys. Res. Commun. 34, 733 (1969).

75. P. A. Hart and J. P. Davis, J. Am. Chem. Soc. 91, 512 (1969).

76. J. Cadet, R. Ducolomb, and C. Taieb, Tetrahedron Lett. 3455 (1975).

77.a. D. B. Davies and S. S. Danyluk, Biochem. 13, 4417 (1974).

b. D. B. Davies and S. S. Danyluk, Biochem. 14, 543 (1975).

78. C. Giessner-Prettre, and B. Pullman, J. Theor. Biol. 65, 171 (1977).

79. F. E. Hruska, Can. J. Chem. 49, 2111 (1971).

80. T. Schleich, T. R. Lusebrink, B. P. Cross, and N. P. Johnson, Nucleic Acid Res. 2, 459 (1975).

81. C. Giessner-Prettre and B. Pullman, J. Theor. Biol. 40, 441 (1973).

82. C. Giessner-Prettre and B. Pullman, Int. J. Quantum Chem. Symp. No. 7, 295 (1973).

83. R. K. Nanda, R. Tewari, G. Govil, and I. C. P. Smith, Can. J. Chem. 52, 371 (1974).

84. T. Imoto, K. Akasaka, and H. Hatano, Chem. Lett. 73 (1974).

85. K. Akaska, T. Imoto, S. Shibata, and H. Hatano, J. Mag. Reson. 18, 328 (1975).

86. M. Karplus, J. Chem. Phys. 33, 1842 (1969).

87. M. Karplus, J. Am. Chem. Soc. 85, 2870 (1963).

88. C.-H. Lee and R. H. Sarma, J. Am. Chem. Soc. 98, 3541 (1976).

89. M. Kainosho and K. Ajisaka, J. Am. Chem. Soc. 97, 6839 (1975).

90. B. P. Cross and T. Schleich, Biopolymers 12, 2381 (1973).

91. F. E. Hruska in "Conformations of Biological Molecules and Polymers" ed. by E. D. Bergmann and B. Pullman, Academic Press, New York (1973), p. 345.

92. J. B. Hendrikson, J. Am. Chem. Soc. 83, 4537 (1961).

93. A. Saran, D. Perahia, and B. Pullman, Theor. Chim. Acta. 30, 31 (1973).

94. H. Berthod and B. Pullman, Biochim. Biophys. Acta. 232, 595 (1971).

95. V. Sasisekharan in "Conformations of Biological Molecules and Polymers" ed. by E. D. Bergmann and B. Pullman, Academic Press, New York (1973), p. 247.

96. H. R. Wilson and A. Rahman, J. Mol. Biol. 56, 129 (1971).

97. M. Levitt and A. Warshel, J. Am. Chem. Soc. 100, 2607 (1978).

98. C. Altona and M. Sundaralingam, J. Am. Chem. Soc. 95, 2333 (1973).

99. W. Guschlbauer and T.-D. Son, Nucleic Acid Res. Spec. Pub. (1974), p. s85.

100. D. M. Cheng and R. H. Sarma, J. Am. Chem. Soc. 99, 7333 (1977).

101. M. Sundaralingam in "Conformations of Biological Molecules and Polymers" ed. by E. D. Bergmann and B. Pullman, Academic Press, New York (1973), p. 417.

102. M. Sundaralingam, private communication to F. E. Hruska.

103. M. Remin and D. Shugar, Biochem. Biophys. Res. Commun. 48, 636 (1972).

104. T. Schleich, B. J. Blackburn, R. D. Lapper, and I. C. P. Smith, Biochem. 11, 137 (1972).

105. D. Plochocka, A. Rabczenko, and D. B. Davies, Biochim. Biophys. Acta. 476, 1 (1977).

106. D. B. Davies and A. R. Rabczenko, J. Chem. Soc. Perkin Trans. 2, 1703 (1975).

107. R. H. Sarma, R. J. Mynott, D. J. Wood, and F. E. Hruska, J. Am. Chem. Soc. 95, 6457 (1973).

108. D. J. Wood, R. J. Mynott, F. E. Hruska, R. H. Sarma, FEBS Lett. 34, 323 (1973).

109. R. H. Sarma, C.-H. Lee, F. E. Hruska, and D. J. Wood, FEBS Lett. 31, 153 (1973).

110. L. D. Hall and R. B. Malcolm, Can. J. Chem. 50, 2092 (1972).

111. L. D. Hall and R. B. Malcolm, Can. J. Chem. 50, 2102 (1972).

112. B. Donaldson and L. D. Hall, Can. J. Chem. 50, 2111 (1972).

113. B. J. Blackburn, R. D. Lapper, and I. C. P. Smith, J. Am. Chem. Soc. 95, 2873 (1973).

114. D. K. LaVallee and C. L. Coulter, J. Am. Chem. Soc. 95, 576 (1973).

115. R. U. Lemieux, T. L. Nagabhushan, and B. Paul, Can. J. Chem. 773 (1972).

116. R. U. Lemieux, Ann. N. Y. Acad. Sci. 222, 915 (1973).

117. M. P. Schweizer and G. P. Kreishman, J. Magn. Reson. 9, 334 (1973).

118. T. Schleich, B. P. Cross, and I. C. P. Smith, Nucleic Acid Res. 3, 355 (1976).

119. G. Govil and I. C. P. Smith, Biopolymers 12, 2589 (1973).

120. R. S. Norton and A. Allerhand, J. Am. Chem. Soc. 98, 1007 (1976).

121. D. Doddrell, V. Glushko, and A. Allerhand, J. Chem. Phys. 56, 3683 (1972).

122. K. F. Kuhlmann, D. M. Grant, and R. K. Harris, J. Chem. Phys. 52, 3439 (1970).

123. J. T. Edwards, J. Chem. Ed. 47, 261 (1970).

124. D. G. Gorenstein and D. Kar, Biochem. Biophys. Res. Commun. 65, 1073 (1975).

125. D. G. Gorenstein, J. B. Findlay, R. K. Momii, B. A. Luxon, and D. Kar, Biochem. 15, 3796 (1976).

126. D. G. Gorenstein, J. Am. Chem. Soc. 97, 898 (1975).

127. J. H. Letcher and J. R. van Wazer in "Topics in Phosphorus Chemistry", ed. by M. Grayson and E. J. Griffith, Interscience, N. Y. (1967), vol. 5, chapters 2 and 3.

128. D. Purdela, J. Mag. Reson. 5, 23 (1971).

129. D. Purdela, Rev. Roumaine. Chim. 13, 1415 (1968).

130. F. R. Prado, C. Giessner-Prettre, B. Pullman, and J.-P. Daudley, J. Am. Chem. Soc. 101, 1737 (1979).

131. A. Holý, Collection Czechoslov. Chem. Commun. 38, 3912 (1973).

132. A. Holý, Tetrahedron Lett., 1147 (1973).

133. A. Holý, Collection Czechoslov. Chem. Commun. 39, 3374 (1974).

134. A. Holý, Collection Czechoslov. Chem. Commun. 39, 3177 (1974).

135. G. I. Birnbaum, F. E. Hruska, and W. P. Niemczura, J. Am. Chem. Soc. (submitted for publication).

136. V. Amarnath and A. D. Broom, Chem. Rev. 77, 183 (1977).

137. J. Stawinski, T. Hozumi, and S. A. Narang, Can. J. Chem. 54, 670 (1976).

138. J. Stawinski, T. Hozumi, S. A. Narang, C. P. Bahl, and R. Wu, Nucleic Acid Res. 4, 353 (1977).

139. K. L. Sadana and P. C. Loewen, Tetrahedron Letters No. 51, 5095 (1978).

140. J. H. van Boom, P. M. J. Burgers, P. H. van Deursen, and J. F. M. de Rooij, J. C. S. Chem. Commun. 167 (1976).

141. J. F. M. de Rooij, G. Wille-Hazeleger, P. M. J. Burgers, and J. H. van Boom, Nucleic Acid Res. 6, 2237 (1979).

142. F.-T. Liu and N. C. Yang, Biochem. 17, 4865 (1978).

143. R. L. Letsinger, K. K. Ogilvie, and P. S. Miller, J. Am. Chem. Soc. 91, 3360 (1969).

144. K. K. Ogilvie and L. A. Slotin, Can. J. Chem. 51, 2397 (1973).

145. J. Feeney, D. Shaw, and P. J. S. Pauwells, J. C. S. Chem. Commun. 554 (1970).

146. Derek Shaw, "Fourier Transform NMR Spectroscopy", Elsevier Scientific Publishing Co. (Amsterdam, 1976), p. 290.

147. F. W. Wehrli and T. Wirthlin, "Interpretation of Carbon-13 NMR Spectra", Heyden (London, 1976).

148. J. D. Cutnell, H. E. Bleich, and J. A. Glasel, J. Mag. Reson. 21, 43 (1976).

149. G. Levy and I. Peat, J. Mag. Reson. 18, 500 (1975).

150. M. Sass and D. Ziessow, J. Mag. Reson. 25, 263 (1977).

151. S. Castellano and A. A. Bothner-by, Melon Institute Publications (Pittsburgh, Pa., 1967).

152. C. W. Haigh and J. M. Williams, J. Mol. Spect. 32, 398 (1969).

153. I. C. P. Smith, H. H. Mantsch, R. D. Lapper, R. Deslauriers, and T. Schleich in "Conformation of Biological Molecules and Polymers" ed. by E. D. Burgman and B. Pullman, Academic Press, New York (1973), p. 381.

154. R. D. Lapper and I. C. P. Smith, J. Am. Chem. Soc. 95, 2878 (1973).

155. R. D. Lapper, H. H. Mantsch, and I. C. P. Smith, J. Am. Chem. Soc. 95, 2880 (1973).

156. D. J. Hunt and E. Subramanian, Acta. Cryst. B25, 2144 (1969).

157. A. E. V. Haschemeyer and A. Rich, J. Mol. Biol. 27, 369 (1967).

158.a. G. J. Karabatsos, C. E. Orzech, Jr., and N. Hsi, J. Am. Chem. Soc. 88, 1817 (1966).

158.b. A. S. Perlin and B. Casu, Tetrahedron Lett. 2921 (1969).

159. B. Pullman and A. Saran, Prog. in Nucleic Acid Res. Mol. Biol. 18, 216 (1976).

160. B. Pullman and H. Berthod in "Conformation of Biological Molecules and Polymers" ed. by E. B. Bergman and B. Pullman, Academic Press, N. Y. (1973), p. 209.

161. G. J. Karabatsos and C. F. Orzech, Jr., J. Am. Chem. Soc. 87, 560 (1965).

162. F. J. Weigert and J. D. Roberts, J. Am. Chem. Soc. 90, 3543 (1968).

163. G. I. Birnbaum, T.-S. Lin, G. T. Shiau, and W. H. Prusoff, J. Am. Chem. Soc. 101, 3353 (1979).

164. M. A. Viswamitra, O. Kennard, P. G. Jones, G. M. Sheldrick, S. Salisbury, L. Falvello, and Z. Shakked, Nature (London) 273, 687 (1978).

165. R. G. S. Ritchie and A. S. Perlin, Carbohydrate Res. 55, 121 (1977).

166.a. B. Pullman and A. Pullman, "Quantum Biochemistry", Interscience (New York, 1963).

b. C. Giessner-Prettre and B. Pullman, J. Theor. Biol. 27, 87 (1970).

167 D. M. Cheng M. M. Dhingra and R. H. Sarma, Nucleic Acid Res. 5, 4399 (1978).

168 N. Camerman, J. K. Fawcett, and A. Camerman, Science 182, 1142 (1973).

169 M. Sundaralingam, Biopolymers 7, 821 (1969).

170 S.-H. Kim, H. M. Berman, N. C. Seeman, and M. D. Newton, Acta. Cryst. B29, 703 (1973).

171 C. R. Cantor, M. M. Warshaw, and H. Shapiro, Biopolymers 9, 1059 (1970).

172 S. Broyde, R. M. Wartell, S. D. Stellman, and B. Hingerty, Biopolymers 17, 1485 (1978).

173 H. R. Wilson and A. Rahman, J. Mol. Biol. 56, 129 (1971).

174. F. E. Hruska, A. A. Smith, and J. G. Dalton, J. Am. Chem. Soc. 93, 4334 (1971).

175. D. B. Davies in "Nuclear Magnetic Resonance Spectroscopy in Molecular Biology", ed. by B. Pullman, Reidel Publishing Co., Dordrecht, Holland (1978), p. 71.

176. A. Saran, B. Pullman, and D. Perahia, Biochim., Biophys. Acta. 287, 211 (1972).

177. R. D. Lapper, H. H. Mantsch, and I. C. P. Smith, J. Am. Chem. Soc. 92, 6243 (1972).

178 G. W. Buchanan and C. Benezra, Can. J. Chem. 54, 231 (1976).

179. B. Pullman, D. Perahia, and A. Saran, Biochim. Biophys. Acta., 269, 1 (1972).

180. W. K. Olson and P. J. Flory, Biopolymers 11, 1 (1972).

181. N. Yathindra and M. Sundaralingam, Proc. Natl. Acad. Sci., U.S.A. 71, 3325 (1974).

182. P. Prusiner, N. Yathindra, and M. Sundaralingam, Biochim. Biophys. Acta. 366, 115 (1974).

183. N. Yathindra and M. Sundaralingam, Biochim. Biophys. Acta. 308, 17 (1973).

184. A. Jack, J. E. Ladner, and A. Klug, J. Mol. Biol. 108, 619 (1976).

185. B. K. Sathyanarayana and V. Sasisekharan in "Structure and Conformation of Nucleic Acids and Protein-Nucleic Acid Interactions", ed. by M. Sundaralingam and S. T. Rao, University Park Press, Baltimore (1975), p. 677.

186. N. S. Kondo and S. S. Danyluk, Biochem. 15, 756 (1976).

187. S. Uesugi and M. Ikehara, Chem. Pharm. Bull. 26, 3040 (1978).

188. S. Uesugi, S. Tanaka, and M. Ikehara, Eur. J. Biochem. 90, 205 (1978).

189. D. Weinblum and H. E. Johns, Biochim. Biophys. Acta, 114, 450 (1966).

190. G. M. Blackburn and R. J. H. Davies, J. Am. Chem. Soc. 89,

191. D. Weinblum, Biochem. Biophys. Res. Commun. 27, 384 (1967).

192. R. Anet, Tetrahedron Lett. 3713 (1965).

193. D. P. Hollis and S. Y. Wang, J. Org. Chem. 32, 1620 (1967).

194. N. Camerman and A. Camerman, J. Am. Chem. Soc. 92, 2523 (1970).

195. F. E. Hruska, D. J. Wood, K. K. Ogilvie, and J. L. Charlton, Can. J. Chem. 53, 1193 (1975).

196. H. E. Johns, M. L. Pearson, J. C. LeBlanc, and C. W. Helleiner, J. Mol. Biol. 9, 503 (1964).

197. E. Oldfield, R. S. Norton, and A. Allerhand, J. Biol. Chem. 250, 6368 (1975).

198. E. Oldfield, R. S. Norton, and A. Allerhand, J. Biol. Chem. 250, 6381 (1975).

199. W. D. Hamill, Jr., R. J. Pugmire, and D. M. Grant, J. Am. Chem. Soc. 96, 2885 (1974).

200. H.-D. Lüdemann and O. Röder, J. Am. Chem. Soc. 97, 4402 (1975).